DE GRUYTER

AQUEOUS MEDIATED HETEROGENEOUS CATALYSIS

Edited by Asit K. Chakraborti and Bubun Banerjee

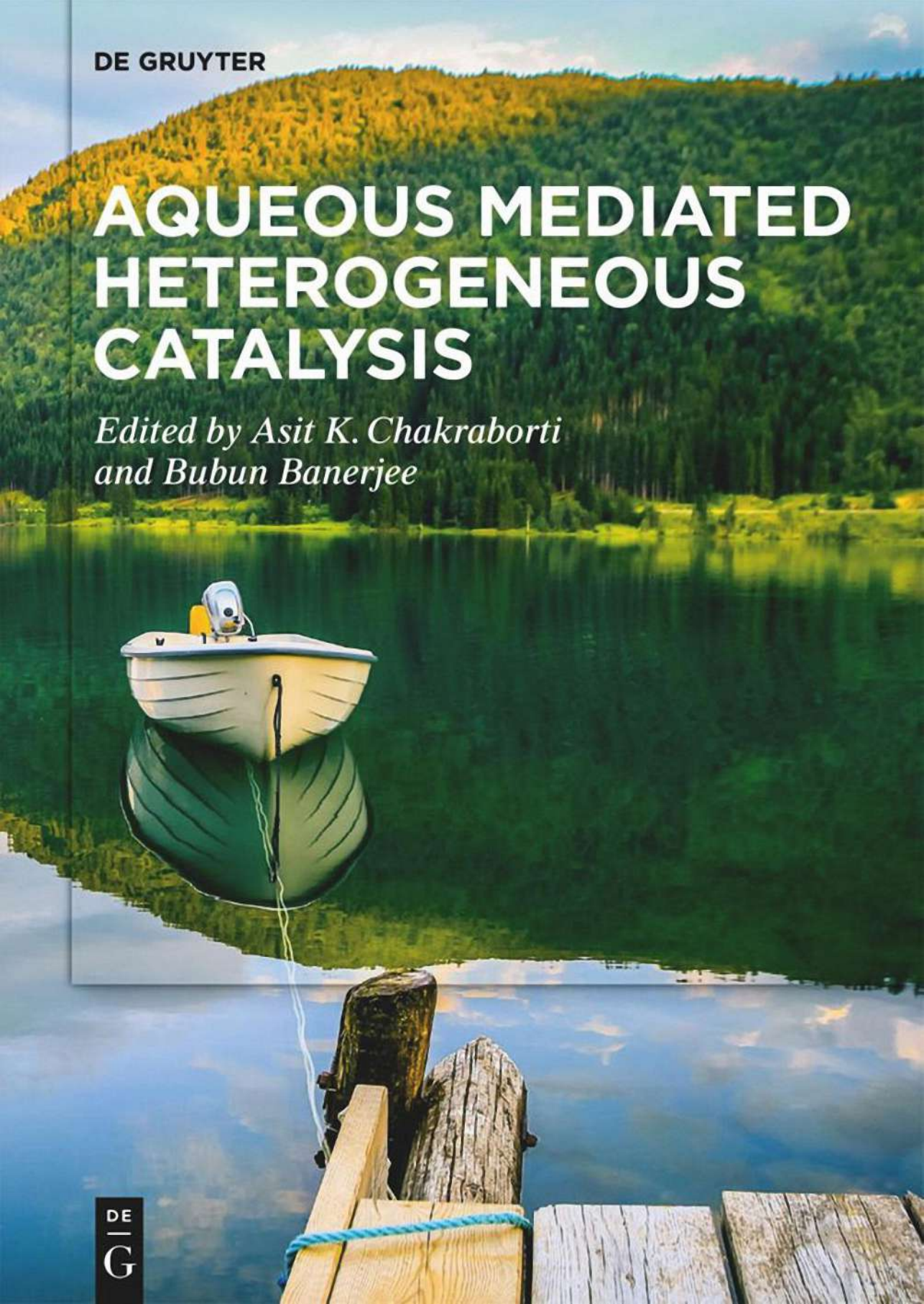

Asit K. Chakraborti and Bubun Banerjee (Eds.)
Aqueous Mediated Heterogeneous Catalysis

Also of Interest

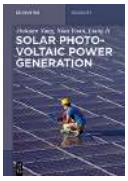

Solar Photovoltaic Power Generation
Jinhuan Yang, Xiao Yuan and Liang Ji, 2020
In Cooperation with: Publishing House of Electronics Industry
ISBN 978-3-11-053138-1, e-ISBN 978-3-11-052483-3

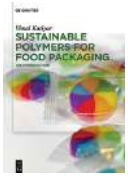

Sustainable Polymers for Food Packaging.
An Introduction
Vimal Katiyar, 2020
ISBN 978-3-11-064453-1, e-ISBN 978-3-11-064803-4

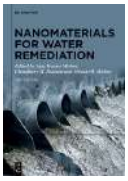

Nanomaterials for Water Remediation
Ajay Kumar Mishra, Chaudhery M. Hussain and Shivani B. Mishra (Eds.), 2020
ISBN 978-3-11-064336-7, e-ISBN 978-3-11-065060-0

Environmental Functional Nanomaterials
Qiang Wang and Ziyi Zhong (Eds.), 2020
ISBN 978-3-11-054405-3, e-ISBN 978-3-11-054418-3

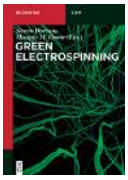

Green Electrospinning
Nesrin Horzum, Mustafa M. Demir, Rafael Muñoz-Espí and Daniel Crespy (Eds.), 2019
ISBN 978-3-11-056180-7, e-ISBN 978-3-11-058139-3

Aqueous Mediated Heterogeneous Catalysis

Edited by
Asit K. Chakraborti and Bubun Banerjee

DE GRUYTER

Editors
Prof. Asit K. Chakraborti
School of Chemical Sciences
Indian Association for the Cultivation of Science (IACS)
Jadavpur, Kolkata 700032
West Bengal
India
asitkumarchakraborti@gmail.com

Dr. Bubun Banerjee
Department of Chemistry
Akal University
Talwandi Sabo, Bathinda 151302
Punjab
India
banerjeebubun@gmail.com

ISBN 978-3-11-073845-2
e-ISBN (PDF) 978-3-11-073384-6
e-ISBN (EPUB) 978-3-11-073388-4

Library of Congress Control Number: 2022933192

Bibliographic information published by the Deutsche Nationalbibliothek
The Deutsche Nationalbibliothek lists this publication in the Deutsche Nationalbibliografie; detailed bibliographic data are available on the Internet at http://dnb.dnb.de.

Cover image: GCShutter/E+/gettyimages
Typesetting: Integra Software Services Pvt. Ltd.
Printing and binding: CPI books GmbH, Leck

www.degruyter.com

Contents

Foreword

Green or Sustainable Chemistry is concerned with the efficient utilization of raw materials, avoiding the toxic, obnoxious and hazardous reagents, use of green solvents in the chemical manufacturing processes and waste minimization. Green Engineering covers all aspects of sustainability. Enormous quantities of inflammable and toxic solvents are used in many transformations in the process industry. Notwithstanding organic solvents, like acetone, DMSO, DMF and aromatics like benzene, toluene and chlorinated solvents contribute to environmental pollution; they are yet used in huge amounts in many industries. The most important objective of green chemistry is to reduce the use of solvents or substituting them with less toxic ones. Environmentally benign and easily recyclable solvents requiring less energy input is the need of all industries. Sustainable solvents have caught the attention of researchers in academia and the practitioners in the chemical industry due to a growing awareness of the influence of solvents causing pollution, energy usage, and contributions to air quality and climate change. Solvent losses during processing and reuse represent a key segment of organic pollution, and thus solvent removal represents a larger percentage of process energy consumption, for instance, by distillation or membrane separation. A wide range of greener or more sustainable solvents have been proposed and developed over the last few years as reaction media. The global adverse impact on the environment of a chemical reaction/process depends on the selection of appropriate solvent. Several facets of the most prominent sustainable organic solvents that are favored include ionic liquids, deep eutectic solvents, supercritical fluids, switchable solvents, liquid polymers, and renewable solvents, aqueous blends, hydrotopes and above all, the ubiquitous water. In the perspective of the solvent selection guide of pharmaceutical industry, water is regarded as the best solvent for sustainable development because of its environmental friendliness, abundance, low cost, and non-flammability. In many water-based reactions, water increases the rate of reaction and enhances selectivity, as it activates the functional group by making hydrogen bonds with it. Due to the hydrophobic nature organic reactants in aqueous medium generally form aggregates to reduce the exposed organic surface area, thereby increasing the reaction rate.

Many homogeneous catalysts have been utilized that revealed significant catalytic activity but are hard to recover and reuse from the reaction mass. Consequently, during the last two decades, extensive attention has been provided to heterogeneous catalysts which can be recovered easily and reused several times in subsequent batches. Due to the large surface to volume ratio, various nano sized reusable heterogeneous catalysts are found to be more effective than the traditional homogeneous catalysts. Thus, aquatic organic reactions under heterogeneous catalysis are the most desirable and ideal towards development of sustainable chemistry.

https://doi.org/10.1515/9783110733846-203

This book titled 'Aqueous Mediated Heterogeneous Catalysis' co-edited by Asit K. Chakraborti and Bubun Banerjee will be a welcome addition to the literature devoted to this area. The first chapter covers the catalytic applications of various heterogeneous nanomaterials used in various organic transformations in water. Chapter 2 deals with the use of heterogeneous metal-organic frameworks (MOF) as catalysts for different organic transformations in aqueous media while chapter 3 demonstrates the utility of the organic-inorganic hybrid nanocatalysts for organic reactions in aqueous medium. Chapter 4 focuses on the aqueous mediated C-C coupling reactions using numerous metal-composites as efficient heterogeneous catalysts. The use of copper-based heterogeneous catalysts for the aqueous mediated synthesis of a wide range of organic molecules is discussed in Chapter 5. Chapter 6 provides elaborative literature related to gold nanoparticles catalyzed electrochemical CO2 reduction in water. Chapter 7 compiles the literature related to the reactions carried out by utilizing β-cyclodextrin based heterogeneous catalysts whereas water-mediated heterogeneous catalysis for a variety of functional group transformations is delineated in Chapter 8. The effect of ultrasound on aqueous mediated heterogeneous catalysis is discussed in Chapter 9. Chapter 10 provides updates on the scope and utilization of quantum dots as heterogeneous photocatalysts.

Overall, this book will find wide acceptance in academia and industry.

Professor (Dr.) Ganapati D. Yadav
D.Sc., D. Eng., USNAE, FTWAS, FNA, FASc, FNASc, FNAE, FRSC, FIE, FISTE, FIChemE, FIIChE, FICS, Padmashri Awardee (2016)
Emeritus Professor of Eminence
Former Vice Chancellor and R.T. Mody Distinguished Professor and
Tata Chemicals Darbari Seth Distinguished Professor of Innovation and Leadership
Institute of Chemical Technology, Mumbai, India
President, India Chemical Society, Kolkata, India

About Prof. Ganapati D. Yadav

Professor Ganapati D. Yadav is one of the topmost, highly prolific, and accomplished engineering-scientists in India. He is internationally recognized by many prestigious and rare awards as an academician, researcher and innovator, including his seminal contributions to education, research and innovation in Green Chemistry and Engineering, Catalysis, Chemical Engineering, Energy Engineering, Biotechnology, Nanotechnology, and Development of Clean and Green Technologies. For 10.5 years, he served as the Founding Vice Chancellor and R.T. Mody Distinguished Professor, and Tata Chemicals Darbari Seth Distinguished Professor of Leadership and Innovation at the Institute of Chemical Technology (ICT), Mumbai, which is a Deemed-to-be-University having Elite Status and Centre of Excellence given by the State Assembly on par with IITs/IISc/IISERs. He currently holds the titles of Emeritus Professor of Eminence and J.C. Bose National Fellow in ICT. He serves as the Adjunct Professor at University of Saskatchewan, Canada, RMIT University, Melbourne, Australia and Conjoint Professor, University of New Castle, Australia. He was conferred Padma Shri, the fourth highest civilian honour, by the President of India in 2016 for his outstanding contributions to Science and Engineering. He has been recipient of two honorary doctorates: D. Sc. (Hon. Causa, DYPU) and D. Eng. (Hon. Causa, NIT Agartala). As the Vice Chancellor he created many records.

In the November 2020 and 2021 surveys of Stanford University, where Indian scientists in top 2% of those in the World are honoured, Professor Yadav is number one in India in Physical Chemistry which is within 0.2% of the world scientists and is ranked at 66, for both years which is remarkable. He is a chemical engineer, but his research is in the field of catalysis science and engineering which is counted as part of physical chemistry.

His research productivity is phenomenal with supervision of 107 Doctoral and 135 Masters Theses, which is the first record in ICT and for any Engineering Professor in India. Besides, he has supervised 47 post-doctoral fellows, several summer fellows and research staff. He has published 503 original research papers, 115 granted national and PCT patents, 8 new patent applications; 3 books; h-index of 64, i10 index of 316; 15000+ citations in journals, patents, books, and monographs, and 850+ specials lectures/orations/seminars over the years. He is still actively involved in guiding 15 doctoral students, patenting, publishing, consulting, and transferring technologies to industry.

Under his dynamic leadership, ICT made phenomenal progress having been declared as Category I institute, started 23 new academic programmes, 5 new Departments and several Centres of Excellence, and establishment of two off-campuses in Bhubaneswar with total support of IOCL and Marathwada with total support of Govt. of Maharashtra, and collected phenomenal funds. The ICT is listed in top 100 institutes in the Developing World by Times Higher Education Ranking in 2019. The

https://doi.org/10.1515/9783110733846-204

Atal Innovation Ranking of MHRD has placed ICT as number 1 among Govt. funded Universities. He has personally won over 125 national and international honours, awards, fellowships, editorships, and several Life Time Achievement Awards by prestigious industrial organizations. He is an elected Fellow of Indian National Science Academy, Indian Academy of Sciences, National Academy of Sciences, India, Indian National Academy of Engineering as well as The World Academy of Sciences, Trieste (TWAS). He is a Fellow of Royal Society of Chemistry, UK, Institution of Chemical Engineers, UK, Indian Institute of Chemical Engineers, Indian Chemical Society, and Indian Society for Technical Education, among others. He was elected to the US National Academy of Engineering in 2022 and is among only 18 Indian nationals so far. He is currently the President of the Indian Chemical Society and Editor-in-Chief, Journal of the ICS being published by Elsevier.

The American Chemical Society (ACS) published a Festschrift (special issue) of Industrial and Engineering Chemistry Research (2014) in his honour with 65 original research papers from scientists from all over the world. He is the Founder President ACS India International Chapter. He has been in editorial boards of prestigious journals like: ACS Sustainable Chemistry & Engineering, Green Chemistry, Applied Catalysis A: Gen, Journal of Molecular Catalysis A: Chem., Catalysis Communications, International Journal of Chemical Reactor Engineering, Clean Technologies and Environmental Policy, Current Catalysis, etc. He is the Founding Editor-in-Chief of Catalysis in Green Chemistry & Engineering (2017, Begell House, USA). He has been a member or chaired several national and international committees of MHRD, DST, DBT, UGC, AICTE, CSIR, the PSA's on Green Chemistry, the Planning Commission's Pan India S&T Committee, and the Government of Maharashtra's Rajiv Gandhi S&T Commission Peers Group. He was Chairman, Research Council, CSIR-CSMCRI, member of RC of IICT Hyderabad and NIIST Trivandrum. He has served as a Chairman/member of Selection Committees of directors of many CSIR labs. He serves as Independent Director, on five renowned limited companies: Aarti Industries Ltd, Godrej Industries Ltd, Meghmani Organics Ltd, Bhageria Chemicals Ltd, and Clean Science and Technology Ltd.

He is also a member of Apex Council of Indian Oil R&D; Expert Advisory Committee, ONGC Energy Centre (OEC); Glexcon India Advisory Board on Process Safety and the Governing Council DBT-IndianOil Energy Centre, and member of the DBT-Pan IIT Centre for Bioenergy. He is Chairman of DST's National Expert Advisory Committee on Innovation, Incubation and Technology Enterprise, member of Advisory and Screening Committee of the Common Research and Technology Development Hubs of DSIR, Chairman, PAC of International Programmes in Chemical Sciences and Engineering, DST and Chairman, Expert Committee, Waste Management Technology, DST. He is a member of the Maharashtra Govt's Expert Committee on implementation of the National Education Policy(NEP 2020).

He had the honour of addressing 3 Convocations of renowned universities in India. He is fond of literature, etymology, and Sanskrit. The ICT's University song is written by him. There are over 60 video clips covering his biography (both English & Marathi), lectures, panel discussions, interviews on TV on YouTube.

https://www.youtube.com/playlist?list=PLclyJH91-TwvTScCVrcih3nrrPGgf8U8R

Author list

Arruje Hameed
Department of Biochemistry
Government College University Faisalabad
Faisalabad, Pakistan

Tanveer Hussain
Department of Applied Chemistry
Government College University Faisalabad
Faisalabad, Pakistan

Muhammad Fayyaz Farid
Department of Applied Chemistry
Government College University Faisalabad
Faisalabad, Pakistan

Tahir Farooq
Department of Applied Chemistry
Government College University Faisalabad
Faisalabad, Pakistan
e-mail: tahirfarooqfsd@gmail.com/
tfarooq@gcuf.edu.pk

Rakshit Ameta
Department of Chemistry
J. R. N. Rajasthan Vidyapeeth (Deemed to be University)
Udaipur 313001, Rajasthan
India

Jayesh Bhatt
Department of Chemistry
PAHER University
Udaipur 313003, Rajasthan
India

Priyanka Jhalora
Department of Chemistry
PAHER University
Udaipur 313003, Rajasthan
India

Suresh C. Ameta
Department of Chemistry
PAHER University
Udaipur 313003, Rajasthan
India

Anu Priya
Department of Chemistry
Akal University
Talwandi Sabo
Bathinda 151302, Punjab
India

Aditi Sharma
Department of Chemistry
Akal University
Talwandi Sabo
Bathinda 151302, Punjab
India

Manmeet Kaur
Department of Chemistry
Akal University
Talwandi Sabo
Bathinda 151302, Punjab
India

Arvind Singh
Department of Chemistry
Akal University
Talwandi Sabo
Bathinda 151302, Punjab
India

Bubun Banerjee
Department of Chemistry
Akal University
Talwandi Sabo
Bathinda 151302, Punjab
India
e-mail: banerjeebubun@gmail.com/
bubun_chm@auts.ac.in

https://doi.org/10.1515/9783110733846-205

Arruje Hameed
Department of Biochemistry
Government College University Faisalabad
38000 Faisalabad
Pakistan
e-mail: arrujeh@yahoo.com

Puja Basak
Department of Chemistry
University of North Bengal
Darjeeling
West Bengal
India

Pranab Ghosh
Department of Chemistry
University of North Bengal
Darjeeling
West Bengal
India
e-mail: pizy12@yahoo.com

Debashis Ghosh
Department of Chemistry
St. Joseph's College (Autonomous)
Bangalore 560027
Karnataka
India

Sumit Ghosh
Department of Chemistry
Visva-Bharati (A Central University)
Santiniketan 731235
India

Alakananda Hajra
Department of Chemistry
Visva-Bharati (A Central University)
Santiniketan 731235
India
e-mail: alakananda.hajra@visva-bharati.ac.in

Rajib Sarkar
Department of Chemistry
University of Calcutta
92 APC Road
Kolkata 700009
India
and
Department of Chemistry
Prabhu Jagatbandhu College
Jhorehat
Andul-Mouri
Howrah 711302
India

Chhanda Mukhopadhyay
Department of Chemistry
University of Calcutta
92 APC Road
Kolkata 700009
India
e-mail: cmukhop@yahoo.co.in

Yogesh A. Tayade
Department of Chemistry
Dhanaji Nana Mahavidyalaya
Faizpur 425503, Maharashtra
India

Dipak S. Dalal
School of Chemical Sciences
Kavayitri Bahinabai Chaidhari North
Maharashtra University
Jalgaon 425 001, Maharashtra
India
e-mail: dsdalal2007@gmail.com

Payal Malik
Department of Chemistry
Sant Longowal Institute of Engineering and
Technology
Longowal 148106, Sangrur, Punjab
India

Avtar Singh
Department of Chemistry
Sant Longowal Institute of Engineering and
Technology
Longowal 148106, Sangrur, Punjab
India

Anupama Parmar
PG Department of Chemistry
M M Modi College
Patiala 147001
Punjab, India

Harish Kumar Chopra
Department of Chemistry
Sant Longowal Institute of Engineering and Technology
Longowal 148106, Sangrur, Punjab
India
e-mail: hk67@rediffmail.com

Ashu Gupta
Department of Chemistry
Shyam Lal College
University of Delhi
New Delhi
India

Yukti Monga
Department of Chemistry
Shyam Lal College
University of Delhi
New Delhi
India
and
Green Chemistry Network Centre
Department of Chemistry
University of Delhi
New Delhi
India

Radhika Gupta
Department of Chemistry
Shyam Lal College
University of Delhi
New Delhi
India
and
Green Chemistry Network Centre
Department of Chemistry
University of Delhi
New Delhi
India

Rakesh Kumar Sharma
Green Chemistry Network Centre
Department of Chemistry
University of Delhi
New Delhi
India
e-mail: rksharmagreenchem@hotmail.com

Arruje Hameed, Tanveer Hussain, Muhammad Fayyaz Farid,
Tahir Farooq*

1 Recent developments about metal-organic frameworks as heterogeneous catalysts in aqueous media

1.1 Introduction

At the interface of coordination chemistry and material sciences, metal-organic frameworks (MOFs), a novel class of crystalline materials, have proved their value and worth as promising catalysts with unique structure and functionality. Their extraordinary surface area, ultrahigh porosity, and other topological attributes have made them attractive for applications in sensing, drug delivery, catalysis, and so on. They show a porous and periodic framework with self-assembled organic–inorganic hybrid units. The unique properties of MOFs are controlled by the structural chemistry of organic legends and metal ions. The MOFs can be designed and functionally tuned by adopting different approaches. The functional sites in MOFs could be developed by pre- and post-functionalized methodologies using organic legends, inorganic metals, and various guest functionalities. The MOFs could be functionalized using enzymes, metallic nanoparticles (NPs), and organometallic compounds [1].

In the perspective of catalysis, the MOFs are promising candidates due to adjustable framework and well-defined geometry, high porosity, and structural diversity of like metallic nodes and organic linkers [2]. The high structural tenability and uniform porous environment present them as advantageous catalytic materials compared to the traditionally used mesoporous silica, zeolite, and clays.

1.1.1 Synthesis and structural diversity of MOFs

The synthetic strategies and pre- and post-synthetic functionalization have put MOFs in three main categories. The structural nature of inorganic moieties and organic linkers represents the preparation of first-generation MOFs. Some chemical modifications allow the conversion of first-generation MOFs into second-generation MOFs with novel

*Corresponding author: Tahir Farooq, Department of Applied Chemistry, Government College University Faisalabad, Pakistan, e-mail: tahirfarooqfsd@gmail.com/tfarooq@gcuf.edu.pk
Arruje Hameed, Department of Biochemistry, Government College University Faisalabad, Pakistan
Tanveer Hussain, Muhammad Fayyaz Farid, Department of Applied Chemistry, Government College University Faisalabad, Pakistan

https://doi.org/10.1515/9783110733846-001

characters and properties. The applications of bioactive molecules, drugs, organic cations, and biomolecules allow the development of third-generation MOFs.

According to another classification, the MOFs could be rigid or flexible depending upon the structural nature of their framework. The MOFs could be crystalline or amorphous through coordination bonds; the metals are connected with organic linkers and the strength of the bond controls the crystalline nature, geometry, and symmetrical shape of the resulting MOF. The MOFs could be prepared by a range of synthetic methods including sonochemical, mechanochemical, solvothermal, and electrochemical methods (Figure 1.1). Various post-synthetic functionalizations are applied to modify the physiochemical properties of MOFs for their selective applications [3].

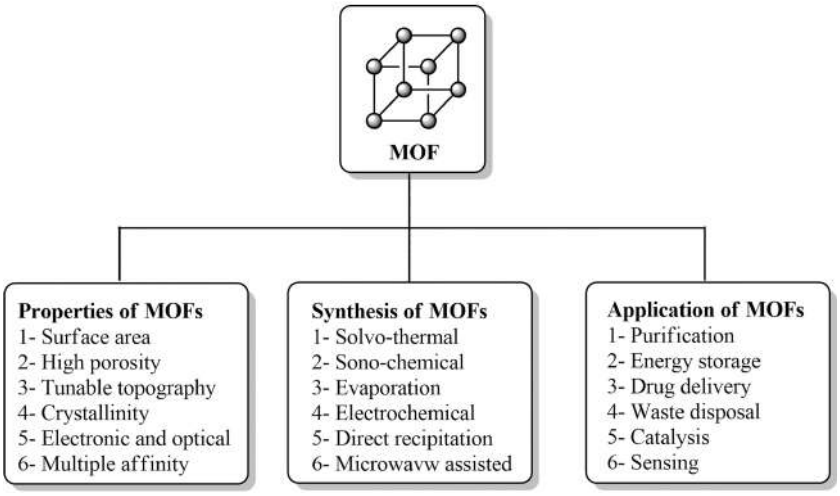

Figure 1.1: Synthesis and applications of MOFs.

In MOFs, the inorganic units (the metal ions) are also called secondary building units (SBUs) and the organic linkers could be heterocyclic compounds, carboxylates or anions like sulfonates or phosphonates (Figure 1.2). The chemistry of the functional groups, geometry, and coordination number of metal ions determine the final framework topology of MOFs. The nature of SBUs and unique characteristics of organic linkers confers highly critical attributes like specific recognition, chirality, and catalytic activity in the MOFs [4].

The MOFs represent promising feature of a heterogeneous catalyst. They could display linker-mediated as well as cluster-mediated catalytic activity. Therefore, the MOFs are considered the most promising heterogeneous catalyst for synthetic reactions and degradation studies [5, 6]. As described earlier, the MOFs could be tuned with desirable surface functionality and a porous environment. Thus, MOFs are attractive materials for effective decontamination of emerging contaminants (ECs) and environmental

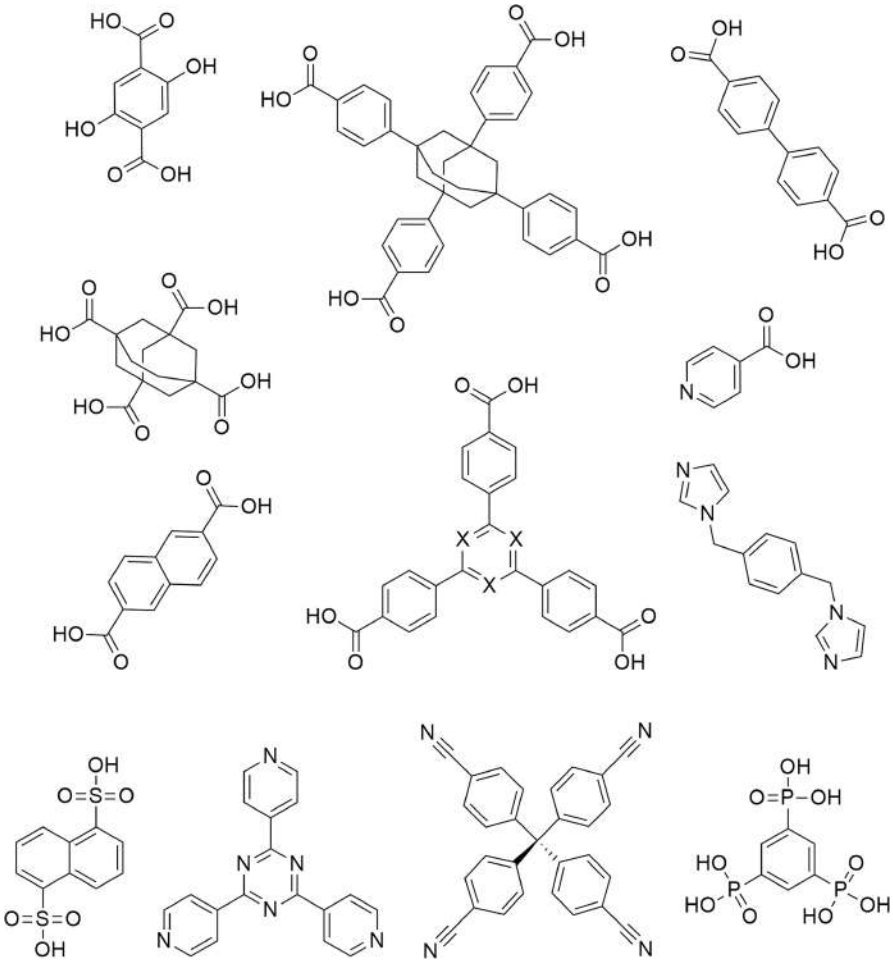

Figure 1.2: A few known organic linkers for MOF preparation.

remediations. Over the last few years, they have become the promising choice for organic pollutant management due to their wide applications in adsorption and catalysis. They develop hydrogen bonding, hydrophobic interactions, π–π stacking, and electrostatic interactions for the adsorption of different organic pollutants.

Over the last few decades, the photodegradation of ECs has received immense importance because it eliminates pollutants in a simple and practical way. The MOFs are also attractive for photocatalytic applications because they generate a charge-separated state with a wide adsorption spectrum due to the presence of organic linkers. In recent decades, heterogeneous photocatalytic degradation has received considerable attention because of the economical and facile applications of the catalyst with high reusability. In general, photocatalytic degradation proceeds through adsorption, surface reactions,

and desorption of the products. The MOFs have a highly porous structure, tunable surface functionalities, and wide adsorption spectrum and hence are capable of exhibiting high photocatalytic activity [7, 8].

1.1.2 The stability of MOFs in water

Despite great options for diverse applications of MOFs, there are some serious challenges in their scope of applications due to water stability issues. In an aqueous environment, they show structural destruction because water molecules could replace metal-coordinated linkers. Such stability issues limit their applications as heterogeneous catalysts in aqueous media. Great attempts have been made to prepare water-stable MOFs using suitable constituents. The water-mediated decomposition could be avoided using hydrophobic functionalities. The destruction of the MOF framework has been avoided using bulky alkyl groups.

As a part of post-synthetic strategies, the modification of functional groups has also been exploited to enhance the water stability of MOFs. Similarly, the reactivity of metal clusters could be controlled by post-synthetic methods. As a new strategy, MOFs are coated with protective layers to induce water and moisture stability. Very recently, Ding et al. [9] introduced one-step surface polymerization as a new post-synthetic modification strategy to increase the stability of MOFs in aqueous media. Advantageously, the post-synthetic functionalization of MOFs for water stability does not undermine their catalytic activity for various applications.

The subsequent sections of this chapter represent the applications of different MOFs as heterogeneous catalyst in aqueous media for,

I. Synthetic reactions/chemical transformations
II. Degradation of organic pollutant including dyes, pesticides, and antibiotic residuals

1.2 MOFs as heterogeneous catalysts in organic synthesis

In organic synthesis, the incorporation of N-containing groups into the target molecules is carried out through a promising methodology known as nitro-aldol condensation. This powerful set of reactions involves the reactions of aldehydes and nitroalkanes under acid/base-catalyzed conditions. Such C–C coupling reactions are named as Henry reactions showing some serious drawbacks such as the use of organic solvents, tedious work-up, non-recovery of base, and generation of salts in stoichiometric amounts. Therefore, the application of a suitable catalyst is required for efficient and eco-friendly Henry reactions. The MOFs are crystalline and porous

solids that show a highly stable structure and composition. They show exceptional catalytic applications owing to their high surface area and the possibility of the introduction of a variety of active sites. Various fine chemicals and pharmaceutical products are synthesized using MOFs as heterogeneous catalysts. They have also been used as an efficient heterogeneous catalyst in Henry reactions due to the presence of open metal sides and O- or N-containing groups [10]. Over the last few years, Henry's reactions have become a model reaction to verify the catalytic efficiency of MOFs. Different active sites such as basic functional groups and metal nodes like Lewis acids act as a catalyst in this model reaction [11].

MOFs carrying lanthanides exhibit several promising structural features due to flexible coordination geometries, high and variable coordination number, hard and oxophilic in nature. Usually, the lanthanide coordination networks carry more solvent molecules than d-block metal ions because lanthanides show a high coordination number [12]. Porous solid MOFs with coordinated, unsaturated, and Lewis-acidic lanthanides could be prepared by removing solvent molecules. In 2016, Karmakar et al. [13] used hydrothermal conditions to prepare a series of self-assembled lanthanide coordination polymers. Different lanthanide salts were reacted with H_2L_1 and H_2L_2 furnishing three-dimensional structures carrying trinuclear lanthanide nodes and L_1^{-2} ligands (Figures 1.3–1.5). The other isostructural coordination polymers develop H-bond interactions in 3D. In a variety of Henry reactions, different nitroalkanes and aldehydes were reacted using as prepared polymeric heterogeneous catalyst (Figure 1.6). The nitroaldol reaction was run in water and the catalyst was reused several times without any significant loss of its catalytic efficiency. In this study, the lanthanide-carrying MOFs were used as heterogeneous catalysts for the first time. The higher yields of the product were obtained with Sm MOF-3 among the five prepared MOFs.

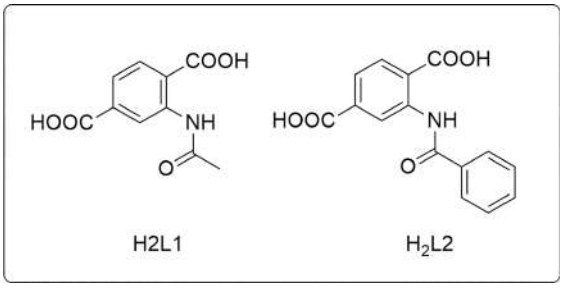

Figure 1.3: Structure of H_2L_1 and H_2L_2.

It has always been challenging to prepare novel MOFs as heterogeneous catalysts with high reusability and efficiency under milder conditions. In 2016, Karmakar et al. [14] used H_2L_1 linkers for the preparation of multidimensional MOFs. The prepared MOFs were employed as heterogeneous catalysts in Henry reactions and oxidation of alcohols

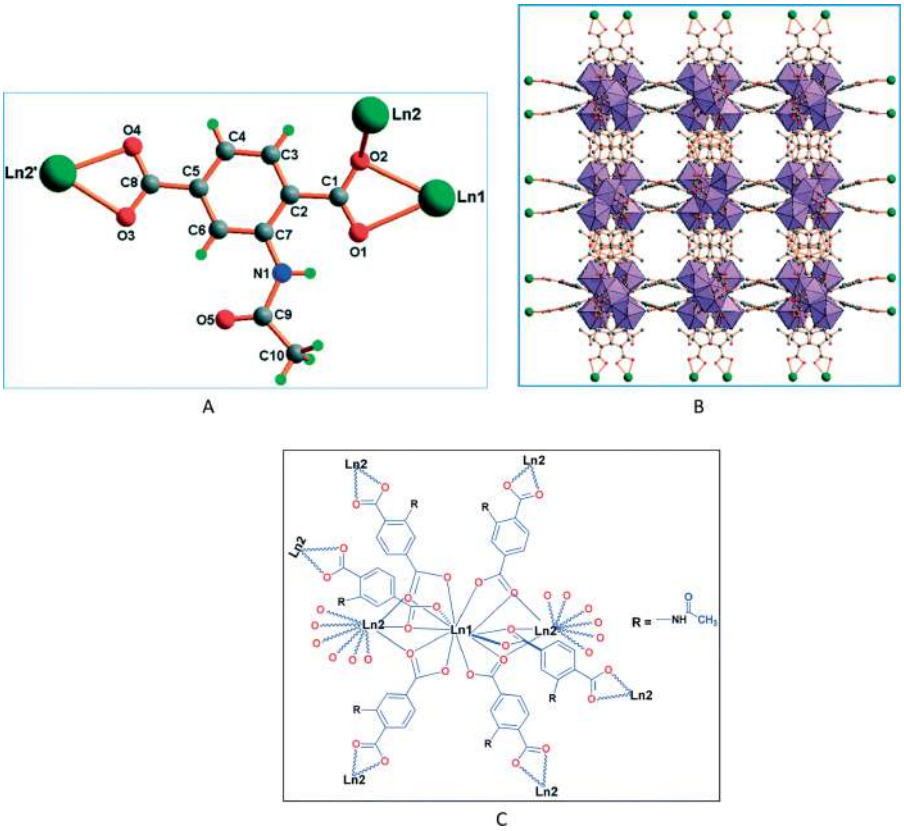

Figure 1.4: Lanthanide-based MOF (1–3) (reproduced with permission from [13] copyright 2016 Royal Society of Chemistry).

(Figure 1.7). They used H_2L_1 and Cd-, Zn-, and Cu- for the preparation of three different MOFs. The prepared Cu-MOF was found to be highly efficient in its catalytic activity in the Henry reaction performed in aqueous media (Figure 1.8). Thus, simple nitro-alcohols were prepared using green catalyst under non-toxic, environment-friendly, and economically viable conditions. The resulting 2D and 3D polymeric architectures acted as a solid catalyst and the dimetallic core acted as a SBU. The linker was chosen to control the protonation of acidic group, development of H-bonding sites, and introduction of various conformations.

Over the last few years, it has been highly desirable to develop monodispersed nanosized MOFs for biomedicine and selective heterogeneous catalysis. In 2019, Aryanejad et al. [15] used 4,4′-[benzene-1,4-diylbis (methylylidenenitrilo)] dibenzoic acid (H_2bdda) and cobalt acetate under ultrasound irradiation to prepare a novel nanostructures $Co_2(bdda)_{1.5}(OAc)_1.5H_2O$ (UoB-3) as Co-MOFs. The prepared UoB-3 was found as a highly stable and efficient heterogeneous nanocatalyst in Henry

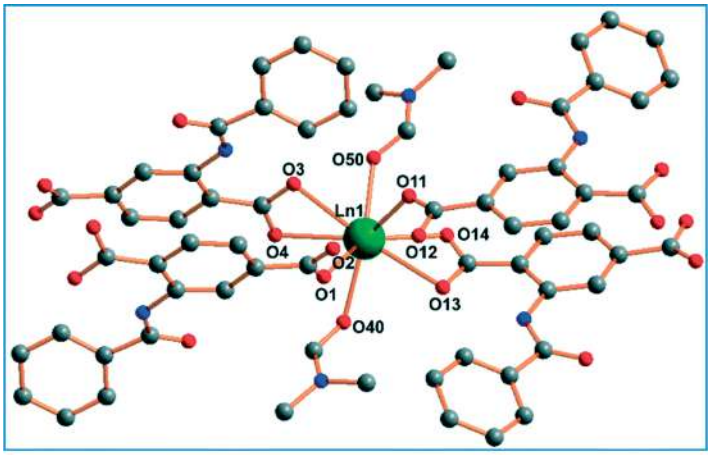

A

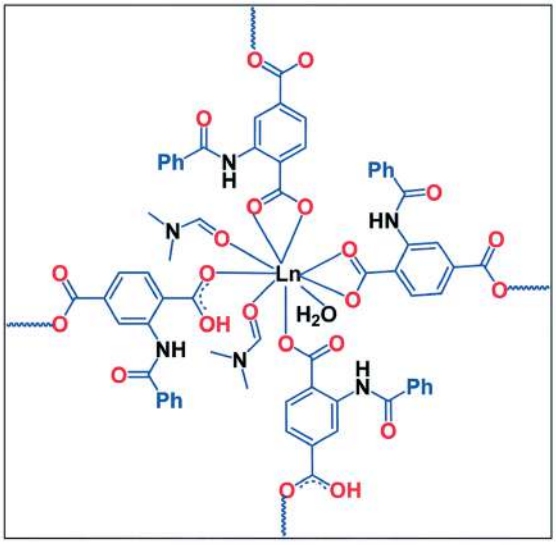

B

Figure 1.5: Lanthanide-based MOF (4 and 5) (reproduced with permission from [13] copyright 2016 Royal Society of Chemistry).

reactions in aqueous media (Figure 1.9). Further, the nanocatalyst exhibited higher reusability and good antibacterial nature.

The organic linkers could be functionalized to control adsorbate MOF interactions in advanced porous MOFs. Such tunable interactions are frequently used for the separation and adsorption of various pollutants. Recently, Patel et al. [16] prepared

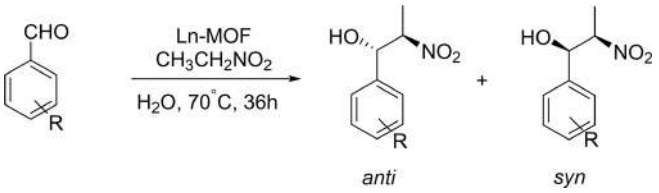

Figure 1.6: Ln-MOF catalyzed Henry reactions.

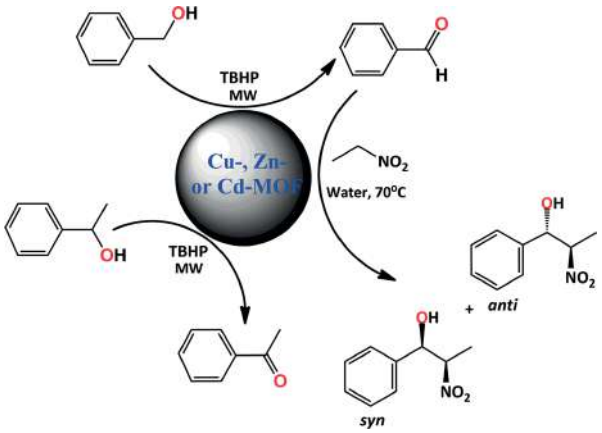

Figure 1.7: Cu-, Zn-, and Cd-MOF as heterogeneous catalysts in aqueous media (reproduced with permission from [14] Copyright 2016, American Chemical Society).

multifunctional MOFs as an efficient catalyst for Biginelli reactions and as adsorbents for hazardous organic dyes.

Over the years, the covalent organic frameworks (COFs) have become attractive functional materials with promising structural features like high chemical stability, tunability, and permanent porosity. They have been used for the preparation of heterogeneous composites catalysts (M@COFs) after loading metallic NPs [17]. However, most of the reported M@COFs-catalyzed C–C coupling reactions require harsh reaction conditions and toxic organic solvents. Therefore, it has been anticipated to develop novel M@COFs as green and eco-friendly catalysts with high efficiency under benign reaction conditions. Over the last few years, MOF-based phase transfer catalysts (PTC) have been developed with high catalytic efficiency for synthetic reactions in water [18].

Recently, Wang et al. [19] prepared COF decorated with Pd NPs Pd@COF-QA from *N*,*N*-dimethyldodecyl ammonium bromide. The as-prepared composite acted as an efficient PTC for Suzuki Miyaura coupling reaction in aqueous media (Figure 1.10). The Pd@COF-QA catalysis was found to be source-saving, green and economical in nature.

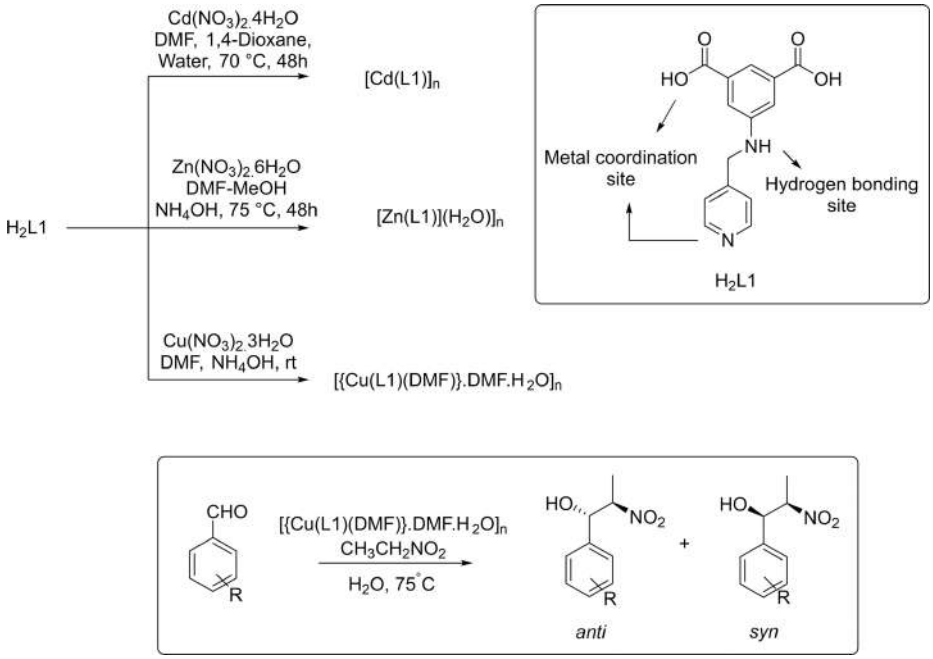

Figure 1.8: (a) Preparation of MOFs and (b) MOF-mediated Henry reaction.

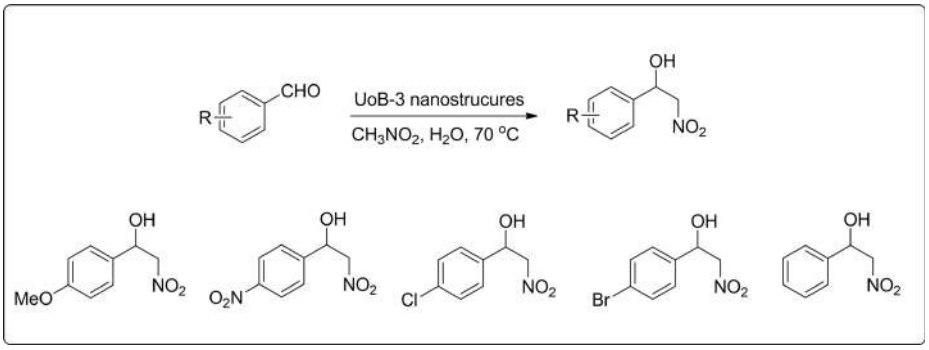

Figure 1.9: The Co-MOF-mediated Henry reaction in aqueous media.

The scope of Pd-based catalysis has been widened by the introduction of MOFs functionalized with Pd-NHC complexes. According to the post-synthetic approach, the MOFs are modified by incorporating NHCs through synthetic methods and then subsequent complexation with Pd. [20] The combination of metal ions with Pd-NHC-functionalized spacers helps to furnish modified MOFs as a second ligand pre-modification approach. In a recent effort, Niknam et al. [21] used MIL-101(Cr) for the preparation of novel Pd-NHC functionalized MOF and subsequently used it as a

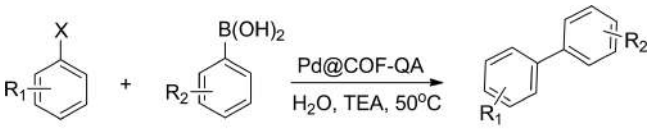

PhX	$PhB(OH)_2$	Yield
R_1=H, X=I	R_2= H	a: 99
R_1=2-OCH_3, X=I	R_2= H	b: 85
R_1=2-CF_3, X=I	R_2= H	c: 93
R_1=3-NO_2, X=I	R_2= H	d: 99
R_1=4-NO_2, X=I	R_2= H	e: 98

Figure 1.10: The Pd@COF-QA catalyzed Suzuki Miyaura reaction.

heterogeneous catalyst in C–C reactions (Figures 1.11 and 1.12). The as-prepared modified MOF acted as a highly efficient catalyst and provided good to excellent yield of products in short reaction time in aqueous media. The MOF-based catalyst exhibited the same catalytic efficiency on being reused after several runs.

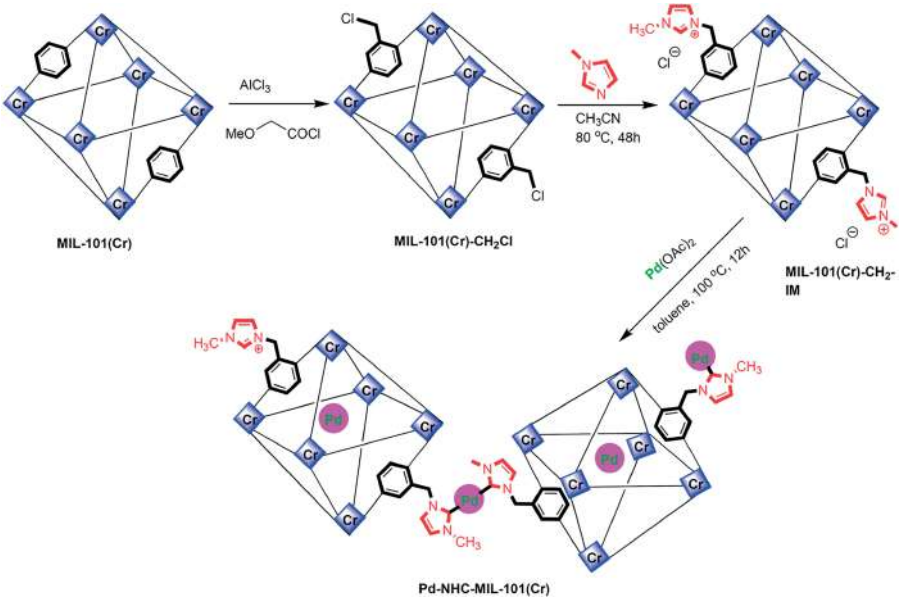

Figure 1.11: Synthesis of novel Pd-NHC functionalized MOF (reproduced with permission from [21] copyright 2020, John Wiley and Sons).

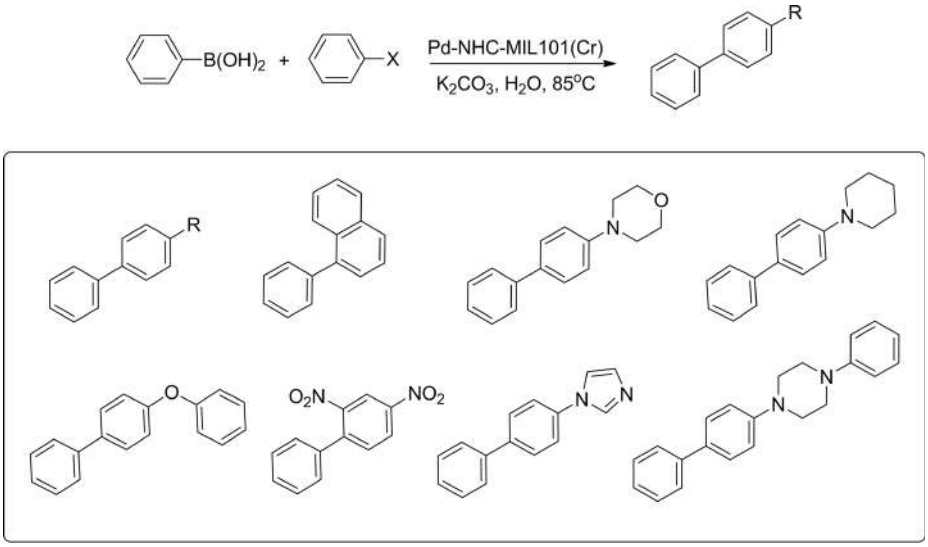

Figure 1.12: Pd-NHC functionalized MOF for cross coupling reactions.

Over the last few decades, the C–H oxidation has become an interesting choice for the preparation of various target molecules in synthetic chemistry. Various building blocks like amides, esters, and cyclic ketones have been prepared from the oxidation of benzylic methylene groups. The traditional C–H activation methodologies require multivalent transition metals and higher amounts of strong oxidants producing hazardous wastes at the end of the reaction. Therefore, MOFs were envisioned to act as highly selective and efficient heterogeneous catalysts for C–H activations under green and ecofriendly reactions. In 2018, Gao et al. [22] used hydrothermal conditions, ethyl diisopropylamine, and triethylamine as structure-directing agents for the preparation of two Cu^{I}-based MOFs 1 and 2 (Figures 1.13 and 1.14) [22]. Both of the prepared MOFs retain their crystallinity in acidic and basic aqueous solutions (pH 1–13) and a range of organic solvents. Further, the C–H oxidation of aryl cycloalkanes was carried out in an aqueous solution using Cu^{I} sites of prepared MOFs (Figure 1.15). The controlled experiments confirmed the excellent reusability, higher selectivity, and efficiency of the prepared MOFs.

In 2018, Sharma et al. [23] used surface-modified $CoFe_2O_4$ NPs as anchors to prepare magnetically retrievable Cu-iso-phthalate-based MOFs. The monodisperse and spherical $CoFe_2O_4$ NPs were prepared through a facile and one-pot solvothermal process and functionalized subsequently using 3-aminopropyltriethoxysilane. Then, covalent immobilization methodology was employed to decorate 3D Cu-iso-phthalate MOF with the prepared magnetic NPs. The $CoFe_2O_4@SiO_2@NH_2@Cu_{95}$-NIPA) hybrid MOF was employed as a heterogeneous catalyst in oxidative cross-coupling reaction for the

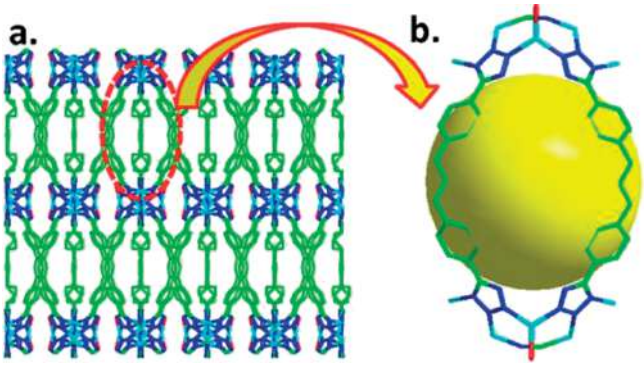

Figure 1.13: Crystal structure of MOF 1 (reproduced with permission from [22] copyright 2019, American Chemical Society).

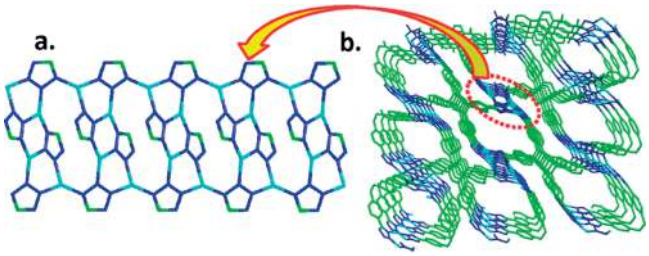

Figure 1.14: Crystal structure of MOF 2 (reproduced with permission from [22] copyright 2019, American Chemical Society).

preparation of a range of benzimidazoles (Figure 1.16). The prepared catalyst displayed a broad substrate scope, high efficiency, and reusability after several cycles.

The carbonyl compounds and compounds with active methylene are frequently reacted to produce a variety of synthetic, bioactive, and functional molecules under the approach called Knoevenagel condensation reaction. Accordingly, several catalysts including zeolites, organometallic compounds, and mesoporous materials have been employed to increase the reaction efficiency. However, most of the reported reactions required harsh reaction conditions including the use of toxic solvents, elevated temperature, and high loading of non-recoverable catalysts of heavy metals. Therefore, there is a great demand for the development of green and ecofriendly catalysts working under benign reaction conditions. To this end, various MOFs have been explored as heterogeneous catalysts in the Knoevenagel condensation reactions. However, the MOFs were found to be unstable in water and the reaction required higher temperature for a longer time. So, efforts are being made to develop highly stable and catalytically efficient MOFs for eco-friendly Knoevenagel condensation reactions [24, 25]. In the last few years, fluorinated-MOFs have been introduced as a novel class with higher

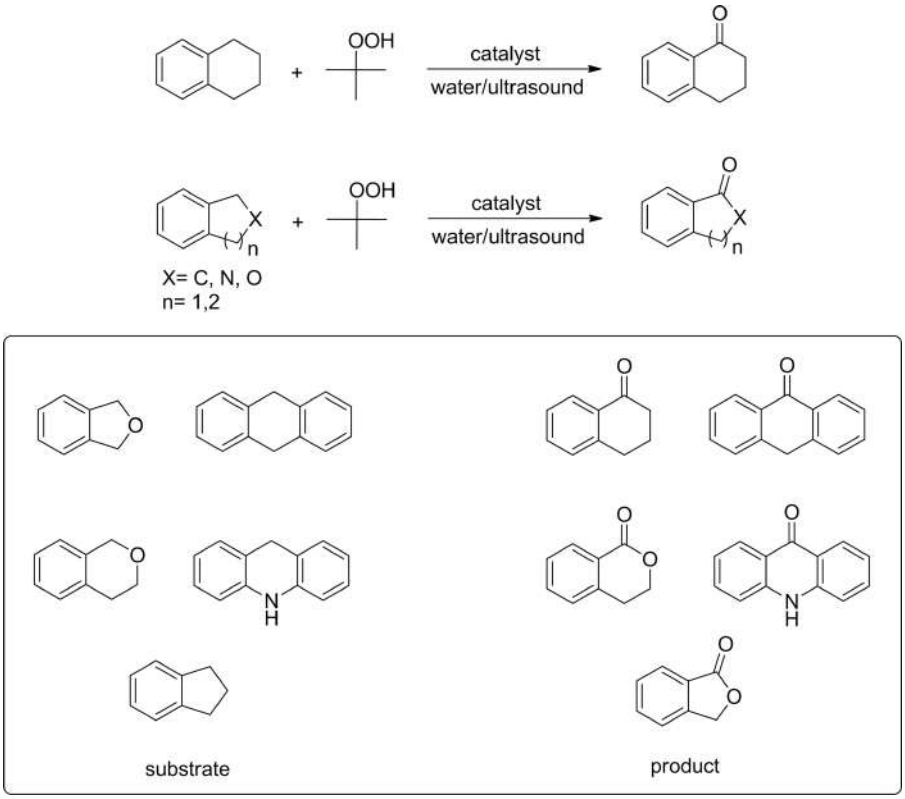

Figure 1.15: Cu[1]-based MOFs for C-H oxidation reaction.

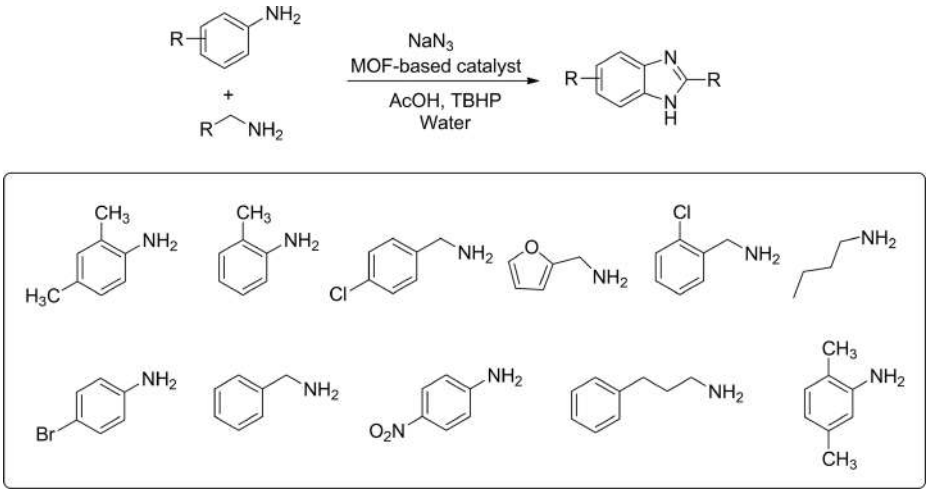

Figure 1.16: Hybrid-MOF mediated cross coupling.

selectivity, thermal stability, and catalytic efficiency. The fluorination bestowed MOFs with excellent optoelectronic properties, high acidity, and hydrophobicity [26, 27].

In 2018, Joharian et al. [28] used fluorinated dicarboxylate building block, diaza-butadiene, and diaza-hexadiene for the preparation of two pillared 3D F-MOFs as heterogeneous catalysts with high stability and efficiency. Both of the prepared catalysts, the TMU-55 and HTMU-55 were tested in Knoevenagel condensation reaction using water as green solvent (Figure 1.17). The fluoro groups enhanced the catalytic efficiency and stability, and both the catalysts did not lose their activity up to three repeated uses.

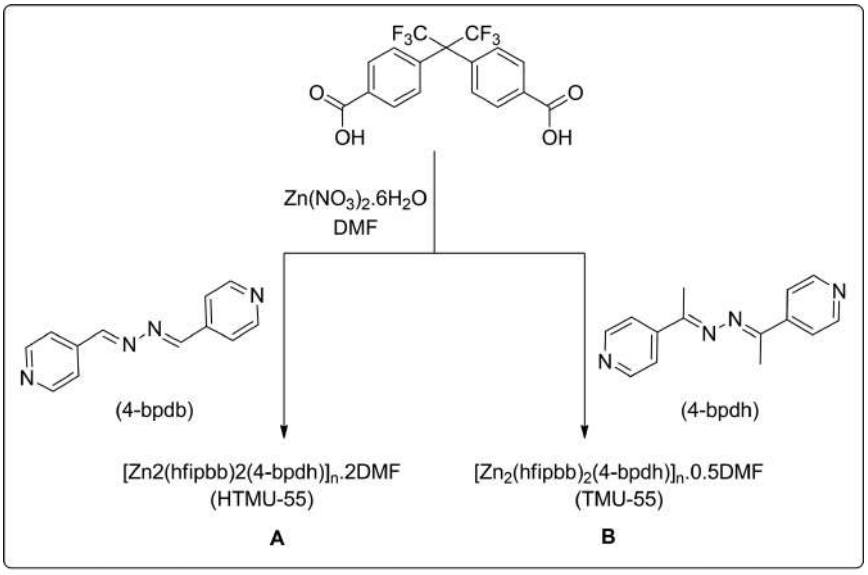

Figure 1.17: Novel 3D F-MOFs for Knoevenagel condensation reaction in water.

1.3 MOFs as heterogeneous catalysts for degradation of organic pollutants

Over the last decade, there has been an increasing public consciousness about the presence of emerging organic contaminants (EOCs) in the environment. Hundreds of EOCs make their way from industrial effluents and contaminate water resources and environment around us. The EOCs include a variety of structurally different compounds with a wide range of applications in industrial synthesis, veterinary drugs, pesticides, and pharmaceutical products.

Over the last decade, great attention has been given to the elimination of EOCs from water sources using several physio-chemical techniques including biodegradation, sonodegradation, chlorination, ozonization, and chemical degradation using heterogeneous catalysis. In recent times, MOFs have also been evaluated for the degradation of contaminants in water. The novel MOFs with a variety of organic linkers and inorganic nodes have been well-explored for the catalytic degradation of organic pollutants. The generally used chemical methods like chlorination produce hazardous by-products like haloacetamides, halomethane, chlorite, and chlorate. The sulfate radical-mediated oxidations, Fenton reactions, and photocatalysis have attracted great attention as advanced oxidation techniques for the degradation of EOCs over the last few decades. The MOFs are used in combination with sulfate radicals and H_2O_2 for the catalytic degradation of pollutants without generating secondary toxins. The MOFs catalyze the EOCs degradation due to its intrinsic catalytic activity or they are modified by post-synthetic methods for this purpose (Figure 1.18).

The MOFs do act as heterogeneous catalysts in water with high efficiency and reusability. The MOF-mediated photocatalysis have gained considerable attention for the catalytic degradation of EOCs due to advantages like easy tunability and high porosity. The adsorption of EOCs is enhanced due to availability of abundant active sites which subsequently increase substrate-catalyst interactions and lead to high catalytic degradations. The porosity and topological characters of MOFs are modulated by controlling the size of metal clusters and length of linkers.

1.3.1 MOFs as heterogeneous catalysts for degradation of organic dyes

Synthetic dyes in textile effluents have become major organic pollutants owing to their stable chemical nature and inertness toward oxidizing agents, heat, and light. Several physio-chemical methodologies like coagulation, chemical oxidation, and biodegradation have been developed for their degradation and removal from water. The highly efficient and facile dye removal is managed through the adsorption method. Accordingly, the MOFs with their ultrahigh porous nature have become

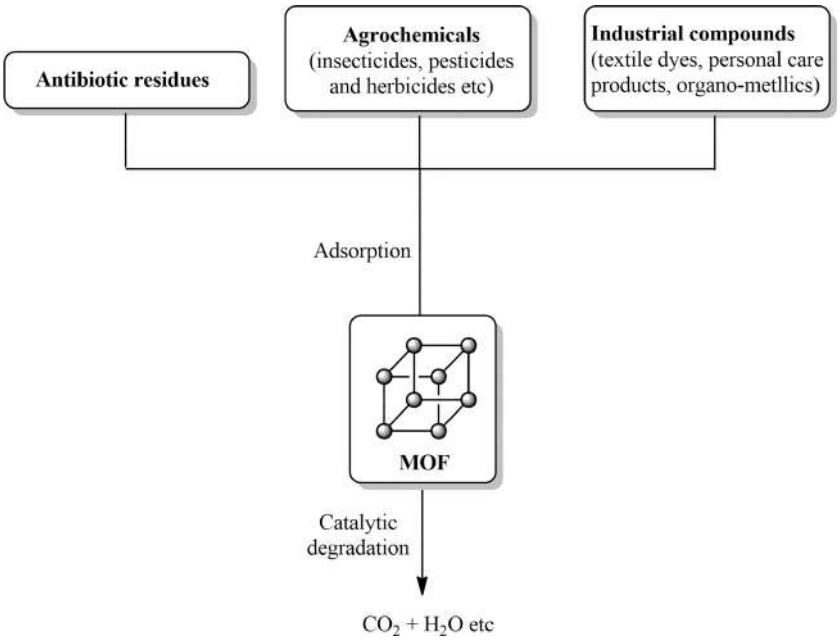

Figure 1.18: MOFs catalyzed degradation of organic contaminants.

attractive adsorbents for synthetic dyes and further catalytic degradation by the metal nodes or organic linkers. In recent years, they have gained attention for photocatalytic degradation of dyes in aqueous media.

Liu et al. [29] prepared Cu (1) 3,5-diphenyltriazolate (CuTz-1) as a novel MOF for photocatalytic degradation of organic dyes (Figures 1.19 and 1.20). The prepared heterogeneous catalyst was found chemically and thermally stable under acidic and basic conditions. The as-prepared MOF exhibited high efficiency and superior performance compared to other known composites and reported MOFs. During the catalytic activity, the Cu(II) produced from Cu(I) after the trapping of photogenerated holes behaved as photocatalyst for Fenton-like reactions. The CuTz-1 MOF efficiently decolorized the mixture of rhodamine B, methylene blue, methyl blue, and methyl orange under natural light. The study revealed the photocatalytic potential of CuTz-1 for the practical treatment of textile effluents containing a mixture of structurally different synthetic dyes.

The MOFs as photocatalysts with desirable topological features, morphology, and crystalline quality could be achieved through different MOF synthetic methodologies such as ultrasonication, vapor diffusion, and solvothermal strategies. They further allow the rational designing and fine-tuning of photocatalysis at the molecular level. The chemical nature of organic linkers helps to control the photocatalytic activity of

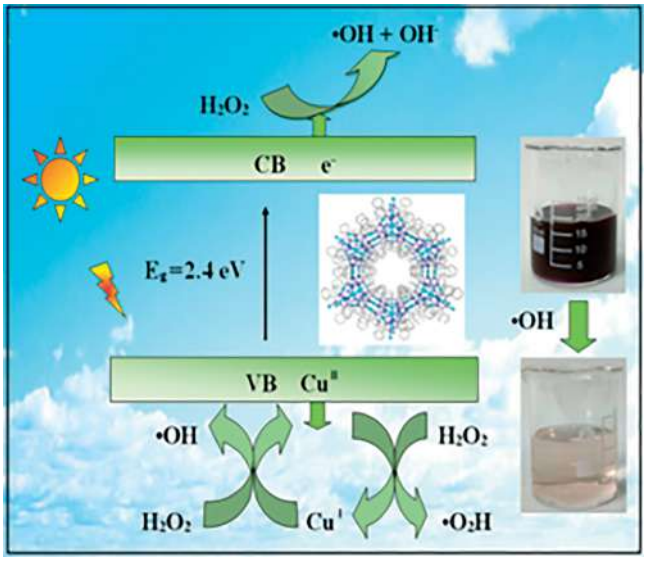

Figure 1.19: The CuTz-1 MOF-mediated photodegradation of dye [29] copyright Wiley-VCH Verlag GmbH & Co.

novel MOFs. The 4,4-bipyridine has become as an attractive linker with high electron transfer efficiency due to its conjugated and rigid structure. It has widely been used for the preparation of several MOFs. However, none of them have been studied for photocatalytic applications.

In 2018, Zhang et al. [30] used 4,4-bipyridine in the hydrothermal method for the preparation of $[Cu(4,4'\text{-bipy})Cl]_n$ (MOF-1), $[Co(4,4'\text{-bipy})\bullet(HCOO)_2]_n$ (MOF-2) as two 3D MOFs. In controlled experiments, the methylene blue was efficiently degraded by both of the prepared MOFs under visible light. The MOF-1 exhibited superior photocatalytic performance with the addition of H_2O_2. The photocatalysis proceeded through ligand to metal charge transfer mechanism and the catalytic efficiency remained unaffected even after four cycles. The prepared MOFs were suggested for applications on large-scale photodegradation of organic dyes in wastewater effluents.

The above mentioned studies have highlighted the potential of MOF for photocatalytic degradation of toxic synthetic dyes. However, in most of the cases, the photocatalytic efficiency of MOFs largely depends on the availability of cocatalyst like H_2O_2. The applications of such cocatalysts pose serious challenges for environment-friendly use of MOFs for the degradation of organic pollutants. So, it is of great interest to develop novel MOFs with high photocatalytic efficiency without using any cocatalyst or photosensitizer. Attempts have been made to prepare efficient MOFs with desirable structures using a mixed ligand strategy. The 1,2-bis-(4-pyridyl) ethylene has emerged as a

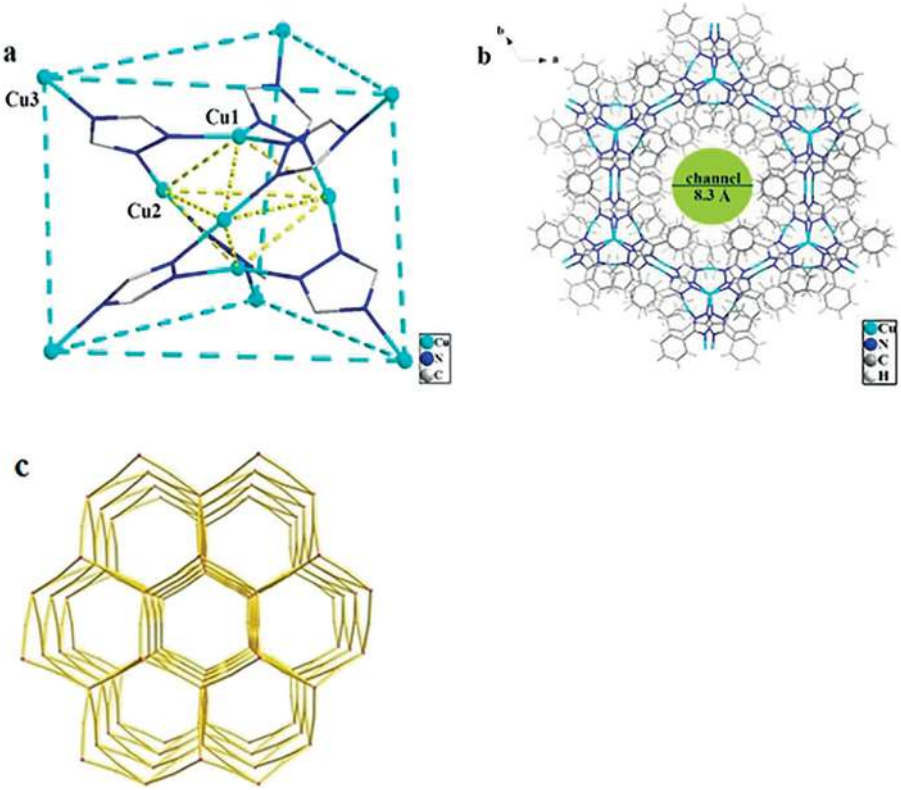

Figure 1.20: The 3D structure of prepared MOF (reproduced with permission from [29] copyright Wiley-VCH Verlag GmbH & Co.

promising ligand with high electron transfer efficiency due to its conjugated nature. It has been used for the preparation of different MOFs but no study revealed its photocatalytic applications.

Alamgir et al. [31] used solvothermal methods for the preparation of [Zn(bpe)(fdc)].2DMF for photodegradation of rhodamine B and crystal violet dyes (Figure 1.21). Under UV light, the prepared MOF acted as an efficient heterogeneous photocatalyst for the photodegradation of crystal violet in the absence of cocatalyst. In controlled experiments, the photocatalytic efficiency was examined by varying the dye concentration, amount of photocatalyst, and pH of the aqueous media. The prepared MOF was projected as a green catalyst for energy-efficient and eco-friendly photodegradation of organic pollutants.

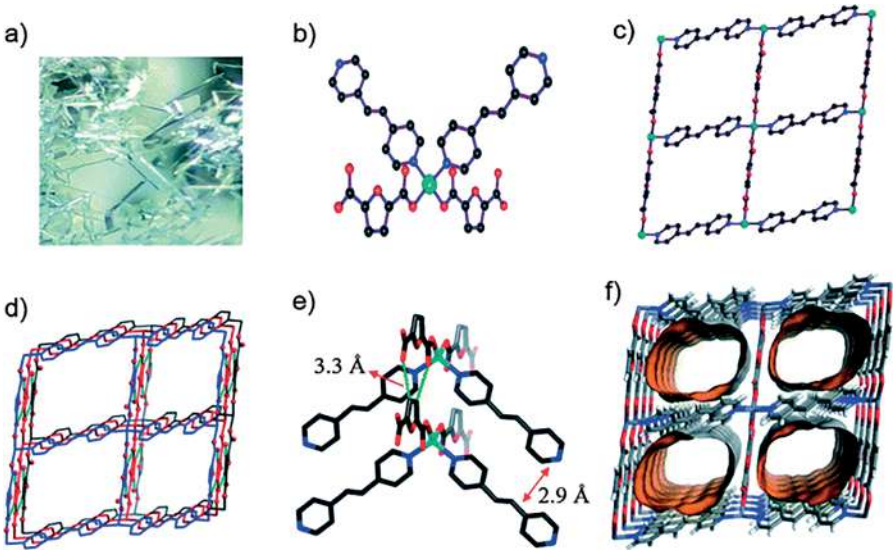

Figure 1.21: Crystal structure of mixed ligand MOF [31].

1.3.2 MOFs as heterogeneous catalysts for degradation of antibiotic residues

Around the globe, the natural environment has been threatened by the gradual accumulation of antibiotics over the last few decades. The ever-increasing consumption of antibiotics in humans, veterinary and aquaculture and have raised potential risks to the healthy environment. The high residues of undigested antibiotics are detected in water sources and waste effluents. The bacteria become resistant to such antibiotics and ultimately pose serious threats to living organisms and ecological components. There has been a huge success for the development of various adsorption techniques for the removal of residual antibiotics from water sources. Although most of the developed techniques are simple in operation, the disposal of adsorbed antibiotics and regeneration of most adsorbents raise serious issues and limit their efficiency. It is anticipated to develop novel multifunctional materials for the effective removal of antibiotics from water sources to maintain the best possible ecological standards.

As described earlier, the MOFs have become attractive materials for the adsorption and degradation of organic pollutants. However, some of the MOFs showed inefficient regeneration and poor water solubility. The preparation of MOFs using a variety of structurally different linkers has helped to develop MOFs with high water stability and catalytic efficiency. The porphyrin ligands have high stability and biocompatibility and the MOFs prepared from it like PCN-224 show high water

stability. Recently, Zong et al. [32] have used porphyrinic zirconium MOF, the PCN-224 for photocatalytic degradation of ciprofloxacin and tetracycline. The MOFs were prepared with different particle sizes. The best adsorption capacity and photocatalytic was exhibited by the prepared PCN-224 MOF with 300 nm particle size. The adsorbates were adsorbed on MOF through electrostatic, π–π, and hydrogen bonding interactions. The photocatalysis helped in the regeneration of MOF under visible light. Further, it did not lose its photocatalytic activity significantly even after several usages. The prepared MOFs were anticipated to have the potential for application in the removal of residual antibiotics in water sources.

Over the last few decades, the Fe-based MILs have become promising MOFs due to their economical availability in wide applications. They show high water and chemical stabilities and are used as a catalyst. The presence of Fe–O clusters makes such MOFs visible-light responsive. In 2016, Li et al. [33] used four different kinds of Fe-based MILs for the degradation of acid orange dye. In another study, the rhodamine B was photodegraded efficiently using Fe_3O_4-MIL-101 as a heterogeneous catalyst. Such studies represent Fe-based MILs as an efficient catalyst for the degradation of organic pollutants. However, they have not been employed for the removal of antibiotics from aqueous media.

In a recent study, Wang et al. [34] used Fe-based MOFs for the degradation of tetracycline. They used Fe-MIL-53, Fe-MIL-100, and Fe-MIL-101 for the photocatalytic degradation of tetracycline. The controlled experiments were performed to evaluate process efficiency by varying concentrations of tetracycline, adsorption time, and MOF concentration. The comparative study revealed Fe-MIL-101 as the best heterogeneous catalyst for the degradation of tetracycline. Its photocatalytic efficiency increased with the increase of time in the optimization study. Its economical synthesis and high catalytic efficiency suggested it as a promising candidate for the photodegradation of residual antibiotics in water sources (Figure 1.22).

Paula et al. [35] reported photodegradation of amoxicillin residuals using Zn-containing two MOFs namely Zn (1,4-benzenedicarboxylate) (Zn-BDC) and zeoliticimidazolate framework-8 (ZIF-8) (Figure 1.23). Both MOFs provided Zn as platforms for the photocatalytic degradation of antibiotics. The photocatalytic degradation proceeded through the cleavage of the β-lactam ring.

In 2020, Sohrabnezhad et al. [36] synthesized NH_2-MIL-53(Al) on the Fe_3O_4@SiO_2 NPs for the preparation of core@shell structure as Fe_3O_4@SiO_2@MIL-53-NH_2 (Al) nanocomposite (FeSi@MN NC). The preparation method used a salt linker and the product was used for photocatalytic degradation of ampicillin in water. The prepared heterogeneous catalyst was activated by visible light. The catalytic activity was supported by superparamagnetism and large surface area of MIL-53(Al). Such materials generally show high thermal stability and simple structural morphology. The FeSi@M-core@shell exhibited low photocatalytic efficiency compared to FeSi@MN core–shell. In a recent report, Ren et al. [37] introduced a green and economical microwave-assisted ball milling method for the economical preparation of Zn-MOF. They used

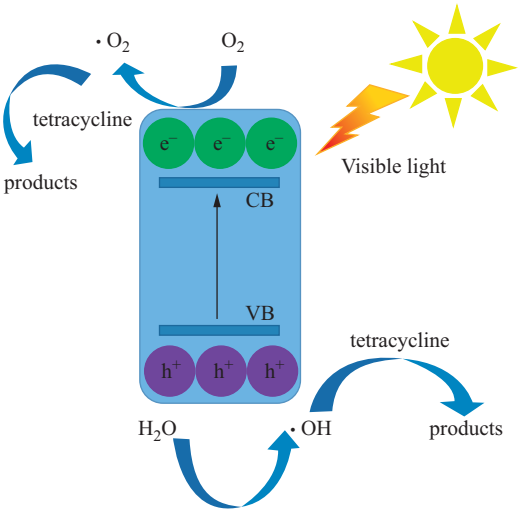

Figure 1.22: Photocatalytic degradation of tetracycline (reproduced with permission from [34] copyright 2018 Elsevier).

1,3,5-benzenetricarboxylic acid and Zn-acetate monohydrate in this novel preparation method. The prepared Zn-MOF was employed as a heterogeneous photocatalyst for the degradation of organic pollutants including Congo red and tetracycline in aqueous media. The photocatalytic efficiency of the Zn-MOF increases significantly with the addition of H_2O_2. This novel method for the preparation of MOFs was proved to be fast, facile, and economical for the removal of organic pollutants from wastewater effluents.

1.3.3 MOFs as heterogeneous catalysts for degradation of pesticides

The fungicides, insecticides, and herbicides are the most commonly used pesticides in croplands and their usage has increased to three million tons in a year. Over the last few years, they have been recognized as EOCs due to their persistent nature. They produced serious ecological concerns due to their toxic nature with highly stable chemical structures. The biotic and abiotic degradation of pesticides does not meet full success and produces even more toxic intermediates. The removal and degradation of pesticides are highly important for environmental safety and public health because of their negative impacts on health that include damages to the endocrine and nervous system.

The generally used traditional wastewater treatments are unable to degrade such pollutants. Over the last two decades, attention has been diverted to reduce the toxicity of such agriculturally derived pollutants. The photocatalysis, Fenton-

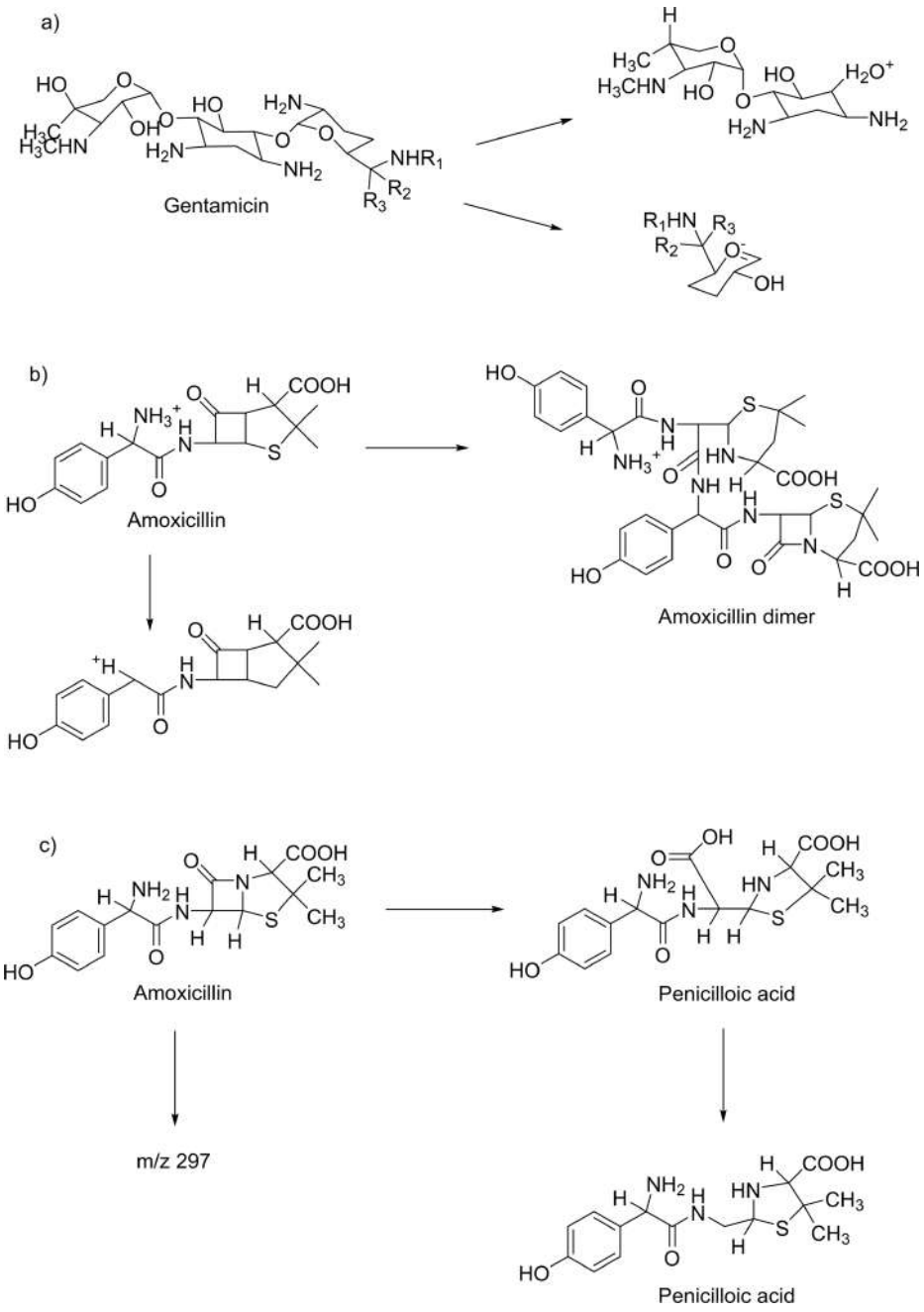

Figure 1.23: Photocatalytic degradation of antibiotic residues using Zn-containing two MOFs.

like reaction, and ozonation have emerged as advanced oxidation techniques for the degradation and removal of pesticides. Among these, photocatalysis is regarded as a green, energy-efficient, and cost-effective method for the degradation of organic pollutants including pesticides. As described earlier, the traditional photocatalyst shows low photodegradation efficiency due to solubility and dispersion issues. The MOFs have emerged as alternative photocatalyst due to high surface area and ultrahigh porous nature. The MOFs are associated with abundant active sites for enhanced adsorption of pollutants. An increased substrate–catalyst interaction results in higher photocatalytic degradation. The size of the metal clusters and the length of the organic linkers have been used to modulate the porosity, topology, and morphology of MOFs for the desired catalytic efficiency.

Organophosphates are a major class of pesticides, widely used for pest control around the globe. They are of serious ecological concern as they show their presence in water sources due to their persistent nature. Advanced oxidation processes have been widely explored for the removal of organophosphates from wastewater effluents. However, these techniques generally rely on inorganic minerals like Fe-exchanged zeolites and clay-based Fe nanocomposites. The MOFs have become an attractive class of photocatalyst with tunable functionality due to the selection of a wide range of organic ligands. Li et al. [38] studied the degradation of organophosphates using a newly developed MOF-based heterogeneous photo-Fenton catalyst (Figure 1.24). The degradation mechanism involved the hydroxylation and hydrolysis and subsequent oxidation that results in complete mineralization of the substrate producing NO_3^-, PO_4^{-3}, and CO_2 (Figure 1.25). The reported heterogeneous catalyst displayed high stability, efficiency, and reusability in optimization studies. In recent times, the Zr-based MOFs have emerged as a special class with ultrahigh structural stabilities and applications as heterogeneous catalysts for the degradation of organic pollutants, chemical warfare agents (CWAs), and organophosphates

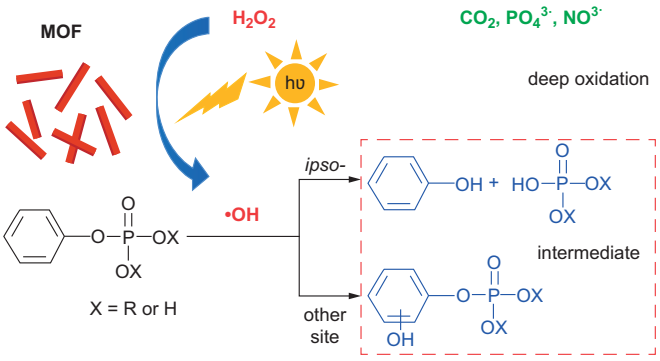

Figure 1.24: MOF as heterogeneous photo-Fenton catalyst (reproduced with permission from [38] copyright 2017 Royal Society of Chemistry).

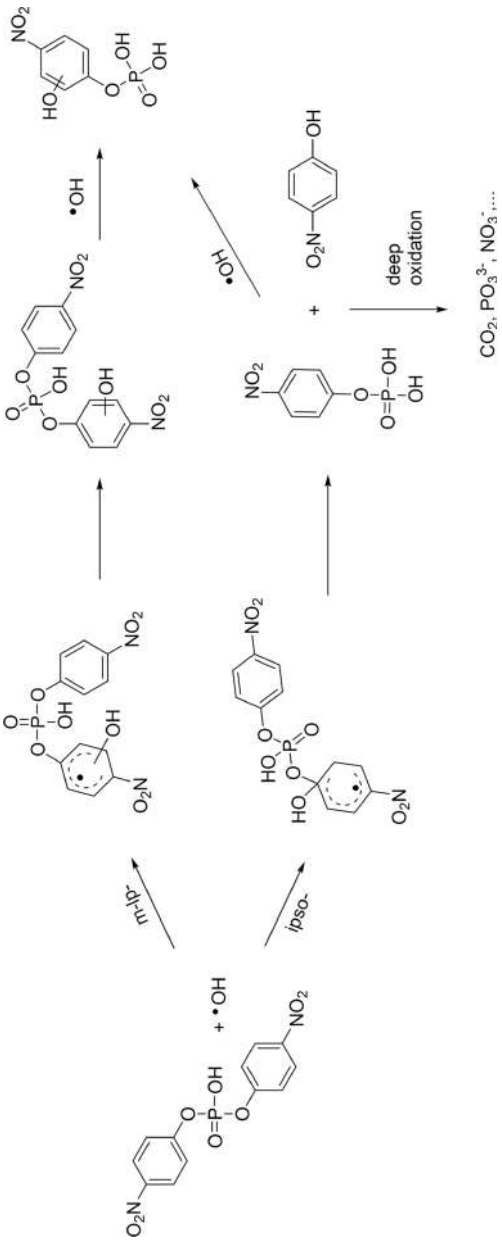

Figure 1.25: MOF-mediated degradation of organophosphates.

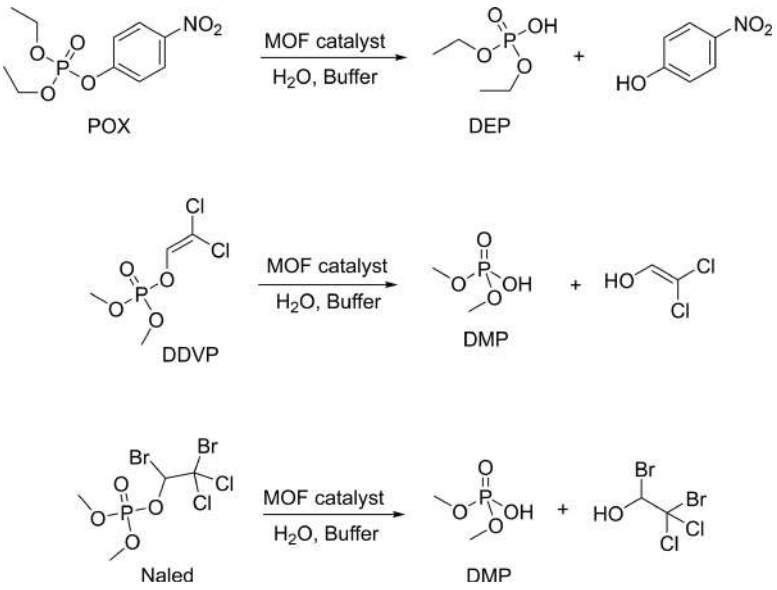

Figure 1.26: Zr-MOF catalyzed degradation of organophosphate.

[39, 40]. In 2021, Nam et al. [41] used PCN-224 as a Zr-based MOF for catalytic degradation of organophosphates like papaoxone, dichlorvos, and naled (Figure 1.26). The PCN-224 with six connected Zr nodes did not lose its catalytic efficiency in a continuous flow system even after several cycles. The Zr node connectivity and geometry were found to be vital for the catalytic efficiency of the Zr-based MOFs during the degradation process of organophosphates.

The herbicides are usually sensitive to photodegradation because they could generate hydroxyl radicals with high energy and reactivity. Over the past few years, great attention has been given for the development of new photocatalysts with high efficiency to avoid the generation of toxic by-products [42]. The conventional photocatalysts are inefficient in aqueous media due to the broad bandgap and low surface area. However, the Ag(I)-based photocatalysts fully utilize the energy of UV-light, visible light, and sunlight due to the presence of an appropriate bandgap. The structural diversity, morphological attributes, and wide range of applications of MOFs have made them attractive as novel photocatalysts for the degradation of herbicides. Accordingly, low-cost Ag-MOF has been explored as highly efficient heterogeneous catalyst for photodegradation studies of organic pollutants [43, 44]. Hayati et al. [45] used sonochemical and laying methods for an environmental-friendly preparation of $[Ag(p\text{-}OH\text{-}C_6H_4CO_2)_2(NO_3)]_n$ as Ag-MOF. The prepared compound performed a simultaneous photocatalytic degradation of widely used herbicides namely 2,4-dichlorophenoxyacetic acid and 2-methyl-4-chlorophenoxyacetic acid in aqueous media. The excellent photocatalytic efficiency of the Ag-MOF was over 96% under natural light. Various controlled

experiments were performed for the optimization of reaction time, pH, temperature, and reactant concentrations.

Owing to severe toxic nature, the CWAs pose severe threats to military personnel and civilian populations. Therefore, a proper detoxification of CWAs is of high importance for the safety of precious lives. Over the last few decades, several new high-tech materials have been explored for the catalytic degradation of CWAs. Among those, the MOFs have become attractive choice due to highly porous nature and large surface area. However, the powder form of MOFs is not recommended for protective clothing and gas filters due to issues related to particle aggregation. In 2016, Zhao et al. [46] came up with an idea of MOF-nanofiber kebab as novel catalysts for degradation of CWAs (Figure 1.27). The electrospun nanofibers exhibit high mechanical strength and extremely large surface area. The polyamide-6 nanofibers coated with TiO_2 were used for the preparation of Zr-MOF thin films UiO-66, UiO-67, and UiO-66-NH_2. The prepared MOF-functionalized nanofibers acted as highly active catalysts for ultrafast degradation of CWAs (Figure 1.28).

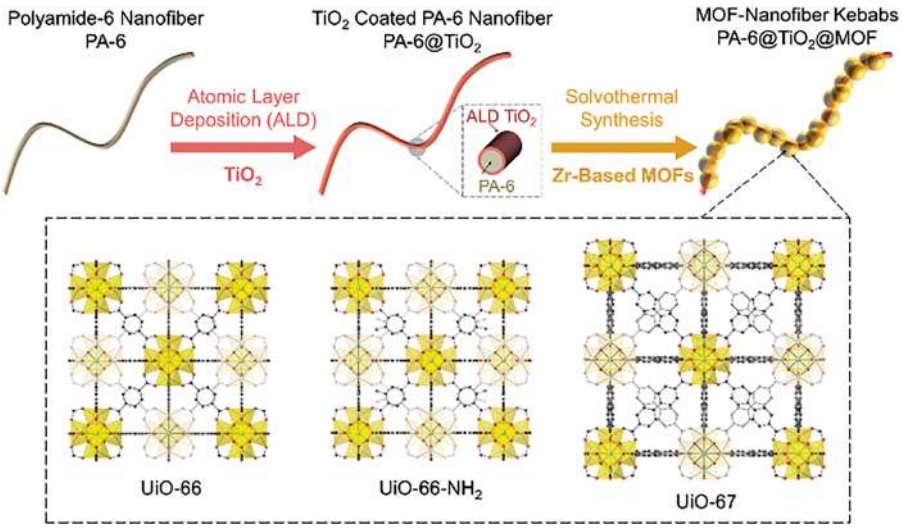

Figure 1.27: Preparation of Zr-based MOF nanofibers (reproduced with permission from [46] copyright 2016 Wiley-VCH).

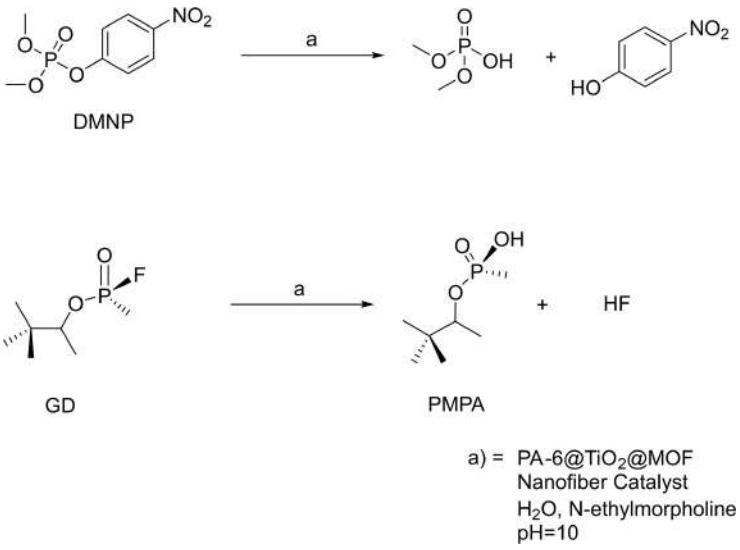

Figure 1.28: Catalytic degradation of chemical warfare using MOF-based nanofibers.

1.4 Conclusions

Over the past decade, the MOFs have offered great opportunities for rational designing of highly stable and efficient heterogeneous catalysts. The water stability of MOFs has remained a challenge for their wide range of applications. However, several pre- and post-functionalization methodologies have been developed that ensure their stability and unprecedented catalytic efficiency in aqueous media. Herein, we have highlighted the MOFs as efficient and reusable heterogeneous catalysts for organic synthesis or detoxification of organic pollutants in aqueous media. They present superiority in catalysis owing to the availability of metal centers as well as organic linker as catalytic sites. They have emerged as promising catalysts because of their highly tunable surface, structural diversity, and uniform porous environment.

References

[1] Bavykina, A, Kolobov, N, Khan, IS, Bau, JA, Ramirez, A, Gascon, JJCR. Metal–organic frameworks in heterogeneous catalysis: Recent progress, new trends, and future perspectives. Chem Rev, 2020, 120, 8468–8535.

[2] Kitagawa, SJCSR. Metal–organic frameworks (MOFs). Chem Soc Rev, 2014, 43, 5415–5418.

[3] He, H, Li, R, Yang, Z, Chai, L, Jin, L, Alhassan, SI. et al., Preparation of MOFs and MOFs derived materials and their catalytic application in air pollution: A review. Catalysis Today, 2021, 375, 10–29.
[4] Sharmin, E, Zafar, F Introductory chapter: Metal organic frameworks (MOFs). Metal-organic frameworks IntechOpen, 2016.
[5] Yang, S, Peng, L, Bulut, S, Queen, WLJCAEJ. Recent Advances of MOFs and MOF-Derived Materials in Thermally Driven Organic Transformations. Chem Eur J, 2019, 25, 2161–2178.
[6] Patial, S, Raizada, P, Hasija, V, Singh, P, Thakur, VK, Nguyen, V-HJMTE Recent advances in photocatalytic multivariate metal organic framework (MOFs) based nanostructures toward renewable energy and the removal of environmental pollutants. Materials Today Energy 2020, 100589.
[7] Qiu, J, Zhang, X, Feng, Y, Zhang, X, Wang, H, Yao, JJACBE. Modified metal-organic frameworks as photocatalysts. Appl Catal B, 2018, 231, 317–342.
[8] Russo, V, Hmoudah, M, Broccoli, F, Iesce, M, Jung, O, DiSerio, MJCE. Applications of Metal Organic Frameworks in Wastewater Treatment: A Review on Adsorption and Photodegradation. Front Chem Eng, 2020, 2, 581487.
[9] Ding, M, Jiang, H-LJCC. Improving water stability of metal–organic frameworks by a general surface hydrophobic polymerization. CCS Chem, 2021, 3, 2740–2748.
[10] Cirujano, FG, Luque, R, Dhakshinamoorthy, A. Metal-Organic Frameworks as Versatile Heterogeneous Solid Catalysts for Henry Reactions. Molecules, 2021, 26, 1445.
[11] Cirujano, FG, Luque, R, Dhakshinamoorthy, AJM. Metal-Organic Frameworks as Versatile Heterogeneous Solid Catalysts for Henry Reactions. Molecules, 2021, 26, 1445.
[12] Cheng, P, Bosch, M. Lanthanide metal-organic frameworks. Springer, Berlin, Heidelberg, 2015.
[13] Karmakar, A, Hazra, S, da Silva, MFCG, Paul, A, Pombeiro, AJ. Nanoporous lanthanide metal–organic frameworks as efficient heterogeneous catalysts for the Henry reaction. CrystEngComm, 2016, 18, 1337–1349.
[14] Karmakar, A, Martins, LM, Hazra, S, Guedes, DSMFC, Pombeiro, AJ. Metal–organic frameworks with pyridyl-based isophthalic acid and their catalytic applications in microwave assisted peroxidative oxidation of alcohols and henry reaction. Cryst Growth Des, 2016, 16, 1837–1849.
[15] Aryanejad, S, Bagherzade, G, Moudi, M. Design and development of novel Co-MOF nanostructures as an excellent catalyst for alcohol oxidation and Henry reaction, with a potential antibacterial activity. Appl Organomet Chem, 2019, 33, e4820.
[16] Patel, U, Parmar, B, Patel, P, Dadhania, A, Suresh, E. The synthesis and characterization of Zn (II)/Cd (II) based MOFs by a mixed ligand strategy: A Zn (II) MOF as a dual functional material for reversible dye adsorption and as a heterogeneous catalyst for the Biginelli reaction. Mater Chem Front, 2021, 5, 304–314.
[17] Ma, HC, Zhao, CC, Chen, GJ, Dong, YB. Photothermal conversion triggered thermal asymmetric catalysis within metal nanoparticles loaded homochiral covalent organic framework. Nat Commun, 2019, 10, 1–9.
[18] Hu, YH, Wang, JC, Yang, S, Li, YA, Dong, YB. CuI@ UiO-67-IM: A MOF-Based Bifunctional Composite Triphase-Transfer Catalyst for Sequential One-Pot Azide–Alkyne Cycloaddition in Water. Inorg Chem, 2017, 56, 8341–8347.
[19] Wang, JC, Liu, CX, Kan, X, Wu, XW, Kan, JL, Dong, YB, Cof-qa:, P. a phase transfer composite catalyst for aqueous Suzuki–Miyaura coupling reaction. Green Chem, 2020, 22, 1150–1155.
[20] Tanabe, KK, Cohen, SM. Postsynthetic modification of metal–organic frameworks – A progress report. Chem Soc Rev, 2011, 40, 498–519.

[21] Niknam, E, Panahi, F, Khalafi-Nezhad, A. Immobilized Pd on a NHC functionalized metal–organic framework MIL-101 (Cr): An efficient heterogeneous catalyst in Suzuki–Miyaura coupling reaction in water. Appl Organomet Chem, 2020, 34, e5470.
[22] Gao, K, Huang, C, Yang, Y, Li, H, Wu, J, Hou, H. Cu (I)-based metal–organic frameworks as efficient and recyclable heterogeneous catalysts for aqueous-medium C–H oxidation. Cryst Growth Des, 2018, 19, 976–982.
[23] Sharma, RK, Yadav, S, Sharma, S, Dutta, S, Sharma, A. Expanding the horizon of multicomponent oxidative coupling reaction via the design of a unique, 3D copper isophthalate MOF-based catalyst decorated with mixed spinel CoFe2O4 nanoparticles. ACS Omega, 2018, 3, 15100–15111.
[24] Opanasenko, M, Dhakshinamoorthy, A, Shamzhy, M, Nachtigall, P, Horáček, M, Garcia, H. et al., Comparison of the catalytic activity of MOFs and zeolites in Knoevenagel condensation. Catal Sci Technol, 2013, 3, 500–507.
[25] Panchenko, VN, Matrosova, MM, Jeon, J, Jun, JW, Timofeeva, MN, Jhung, SH. Catalytic behavior of metal–organic frameworks in the Knoevenagel condensation reaction. J Catal, 2014, 316, 251–259.
[26] Curran, DP, Gladysz, JA. Handbook of Fluorous Chemistry. Wiley-VCH, Weinheim, 2004.
[27] Stavila, V, Talin, AA, Allendorf, MD. MOF-based electronic and opto-electronic devices. Chem Soc Rev, 2014, 43, 5994–6010.
[28] Joharian, M, Morsali, A, Tehrani, AA, Carlucci, L, Proserpio, DM. Water-stable fluorinated metal–organic frameworks (F-MOFs) with hydrophobic properties as efficient and highly active heterogeneous catalysts in aqueous solution. Green Chem, 2018, 20, 5336–5345.
[29] Liu, CX, Zhang, WH, Wang, N, Guo, P, Muhler, M, Wang, Y. et al., Highly efficient photocatalytic degradation of dyes by a copper–triazolate metal–organic framework. Chem Eur J, 2018, 24, 16804–16813.
[30] Zhang, M, Wang, L, Zeng, T, Shang, Q, Zhou, H, Pan, Z. et al., Two pure MOF-photocatalysts readily prepared for the degradation of methylene blue dye under visible light. Dalton Trans, 2018, 47, 4251–4258.
[31] Talha, K, Wang, YJ, Ullah, R, Wang, B, Wang, L, Wu, W. et al., Construction of a mixed ligand MOF as “green catalyst” for the photocatalytic degradation of organic dye in aqueous media. RSC Adv, 2021, 11, 23838–23845.
[32] Zong, Y, Ma, S, Gao, J, Xu, M, Xue, J, Wang, M. Synthesis of Porphyrin Zr-MOFs for the Adsorption and Photodegradation of Antibiotics under Visible Light. ACS Omega, 2021, 6, 17228–17238.
[33] Li, X, Guo, W, Liu, Z, Wang, R, Liu, H. Fe-based MOFs for efficient adsorption and degradation of acid orange 7 in aqueous solution via persulfate activation. Appl Surf Sci, 2016, 369, 130–136.
[34] Wang, D, Jia, F, Wang, H, Chen, F, Fang, Y, Dong, W. et al., Simultaneously efficient adsorption and photocatalytic degradation of tetracycline by Fe-based MOFs. J Colloid Interface Sci, 2018, 519, 273–284.
[35] Paula, MV, Barros, AL, Wanderley, KA, GFd, S, Eberlin, M, Soares, TA. et al, Metal organic frameworks for selective degradation of amoxicillin in biomedical wastes. J Braz Chem Soc, 2018, 29, 2127–2136.
[36] Sohrabnezhad, S, Pourahmad, A, Karimi, MF. Magnetite-metal organic framework core@ shell for degradation of ampicillin antibiotic in aqueous solution. J Solid State Chem, 2020, 288, 121420.
[37] Ren, Q, Wei, F, Chen, H, Chen, D, Ding, B. Preparation of Zn-MOFs by microwave-assisted ball milling for removal of tetracycline hydrochloride and Congo red from wastewater. Green Process Synth, 2021, 10, 125–133.

[38] Li, WJ, Li, Y, Ning, D, Liu, Q, Chang, L, Ruan, WJ. An Fe(ii) metal–organic framework as a visible responsive photo-Fenton catalyst for the degradation of organophosphates. New J Chem, 2018, 42, 29–33.
[39] Bai, Y, Dou, Y, Xie, LH, Rutledge, W, Li, JR, Zhou, HC. Zr-based metal–organic frameworks: Design, synthesis, structure, and applications. Chem Soc Rev, 2016, 45, 2327–2367.
[40] Kirlikovali, KO, Chen, Z, Islamoglu, T, Hupp, JT, Farha, OK. Zirconium-based metal–organic frameworks for the catalytic hydrolysis of organophosphorus nerve agents. ACS Appl Mater Interfaces, 2020, 12, 14702–14720.
[41] Nam, D, Kim, Y, Kim, M, Nam, J, Kim, S, Jin, E. et al., Role of Zr6 Metal Nodes in Zr-Based Metal–Organic Frameworks for Catalytic Detoxification of Pesticides. Inorg Chem, 2021, 60, 14, 10249–10256.
[42] Amorisco, A, Losito, I, Carbonara, T, Palmisano, F, Zambonin, P. Photocatalytic degradation of phenyl-urea herbicides chlortoluron and chloroxuron: Characterization of the by-products by liquid chromatography coupled to electrospray ionization tandem mass spectrometry. Rapid Communications in Mass Spectrometry: An International Journal Devoted to the Rapid Dissemination of Up-to-the-Minute Research in Mass Spectrometry, 2006, 20, 1569–1576.
[43] Surib, NA, Sim, LC, Leong, KH, Kuila, A, Saravanan, P, Lo, KM. et al., Ag+, Fe 3+ and Zn 2+-intercalated cadmium (ii)-metal–organic frameworks for enhanced daylight photocatalysis. RSC Adv, 2017, 7, 51272–51280.
[44] Song, H, Wang, N, Shi, X, Meng, H, Han, Y, Wu, J. et al., Photocatalytic active silver organic framework: Ag(I)-MOF and its hybrids with silver cyanamide. Appl Organomet Chem, 2020, 34, e5972.
[45] Hayati, P, Mehrabadi, Z, Karimi, M, Janczak, J, Mohammadi, K, Mahmoudi, G. et al., Photocatalytic activity of new nanostructures of an Ag (i) metal–organic framework (Ag-MOF) for the efficient degradation of MCPA and 2, 4-D herbicides under sunlight irradiation. New J Chem, 2021, 45, 3408–3417.
[46] Zhao, J, Lee, DT, Yaga, RW, Hall, MG, Barton, HF, Woodward, IR. et al., Ultra-Fast Degradation of Chemical Warfare Agents Using MOF–Nanofiber Kebabs. Angewandte Chemie, 2016, 128, 13418–13422.

Rakshit Ameta, Jayesh Bhatt, Priyanka Jhalora, Suresh C. Ameta*

2 Quantum dots as heterogeneous photocatalysts

2.1 Introduction

Quantum dots (QDs) are semiconductor particles with small nanometric size. These have distinct optical, chemical, mechanical, physical, and electronic properties which are different from macroparticles. When QDs are illuminated by UV light, an electron in the semiconducting QD can be excited to a state from the lower energy (valence band) to higher energy (conductance band). The excited electron can come back into the valence band and sidewise, releasing its energy in the form of light emission. The color of emitted light depends on the energy difference (band gap) between the conductance band and the valence band [1].

Uses of QDs are quite versatile such as photocatalyst, solar cells, laser, LEDs, memory, photodetectors, photovoltaics, and quantum computers. It is anticipated that QDs will occupy a prominent position in these fields in years to come.

Carbon, graphene, and other QDs can be prepared by both the top-down and bottom-up methods. Synthesis of QDs has numerous advantages like simple operations, low-cost, non-toxic raw materials, renewable resources, and expeditious reactions.

Photocatalysis deals with chemical reactions taking place in the presence of light and a semiconductor (photocatalyst). Photocatalysis has a wide range of applications such as deodorizing, air purifying, antifogging, antibacterial, self-cleaning, and water purification. Photocatalysis is a green chemical pathway and is the need of the day.

When a photocatalyst is in a different phase from its reactants, it is called heterogeneous photocatalysis. It includes a variety of reactions: oxidations (partial or total), hydrogen transfer, dehydrogenation, deposition of metal, removal of contaminants of water, removal of gaseous pollutants from air, and so on.

Transition metal chalcogenides are commonly used heterogeneous photocatalysts. These are semiconductors having unique characteristics. Semiconductors normally possess a void region of energy and there are no energy levels in this region as compared to metals having a continuum of electronic states. There is no chance to promote recombination of an electron and hole, which are produced by photoactivation in the solid. Such a void region is termed as band gap and it extends from the

*Corresponding author: **Suresh C. Ameta**, Department of Chemistry, PAHER University, Udaipur, 313003, (Raj.) India
Rakshit Ameta, Department of Chemistry, J. R. N. Rajasthan Vidyapeeth (deemed to be university), Udaipur, 313001, (Raj.), India
Jayesh Bhatt, Priyanka Jhalora, Department of Chemistry, PAHER University, Udaipur, 313003, (Raj.) India

https://doi.org/10.1515/9783110733846-002

top of the highest occupied molecular orbital (valence band) to the bottom of the unoccupied molecular orbitals (conduction band). When a photon with energy equal to or greater than band gap of semiconductor is absorbed by any such material, then an electron jumps from the valence band to the conduction band, which creates a positive hole in the valence band. This photogenerated pair of electron and hole is called an exciton. Thus, any oxidation–reduction reaction can take place at the surface of photocatalyst due to this electron–hole pair (Figure 2.1).

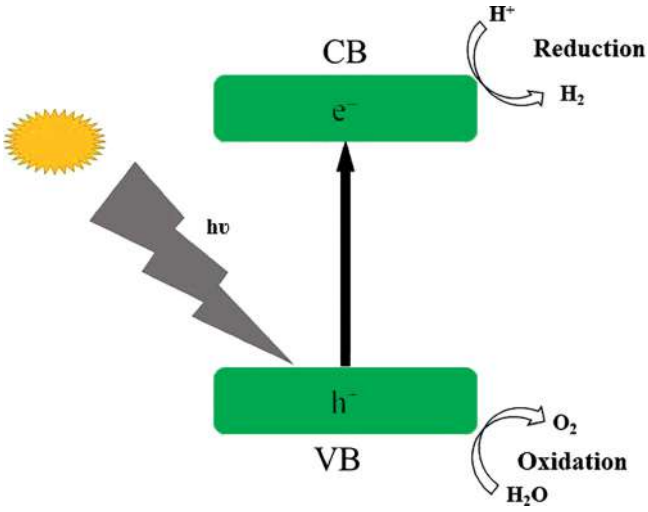

Figure 2.1: Principle of photocatalysis.

These excited electrons and holes recombine by releasing the energy in the form of heat, which was gained in the form of light in the process of excitation of an electron. This type of exciton recombination is not desired. The presence of higher levels leads to a photocatalyst, which is inefficient. Therefore, efforts are made to develop photocatalysts with extended exciton lifetime, improved electron–hole separation, sensitization, use of cocatalyst, metal or non-metal doping, and so on. Thus, photocatalysts are designed to assist reactions between oxidants and excited electrons to give reduced products. The second reaction possibility is between the reductants and holes to give oxidized products. The positive holes may react with the water/hydroxyl ions present on the surface to produce a hydroxyl radical (active oxidizing species). The first step in the reaction is the generation of exciton (electron–hole pair) by photoinduced excitation in semiconducting (SC) as:

$$SC + h\nu \rightarrow SC(h^+ + e^-)$$

Oxidation reactions may proceeds as;

$$h^+ + OH^- \rightarrow {}^{\bullet}OH$$

$$h^+ + H_2O \rightarrow H^+ + {}^{\bullet}OH$$

$$2H_2O + 2h^+ \rightarrow H_2O_2 + 2H^+$$

$$H_2O_2 \rightarrow 2{}^{\bullet}OH$$

Reduction reactions may proceed as;

$$e^- + O_2 \rightarrow {O_2}^{-\bullet}$$

$$H_2O + {O_2}^{-\bullet} + H^+ \rightarrow O_2 + H_2O_2$$

$$H_2O_2 \rightarrow 2{}^{\bullet}OH$$

As a result, hydroxyl radicals are generated through oxidation or reduction reactions. These hydroxyl radicals are the strongest oxidizing agent next to fluorine and are also non-selective in nature.

2.2 Wastewater treatment

Water is the basic necessity of plants, animals, and human beings. Demand for pure water is increasing regularly due to increase in population. There is an urgent need to develop alternate treatment technology to purify water. A number of processes have been tried for this purpose, but photocatalysis is commonly used in wastewater treatment [2].

QDs are zero dimensional in nature and these are much smaller in size, and therefore, they have unique properties. The QDs can find different applications as compared to their bulk counterparts due to size, composition, shape, and so on. These semiconducting nanoparticles (NPs) are emerging as promising fluorescent materials, environmental remediation, light emitting diodes, sensors, targeted drug delivery system/vehicles, and so on. It is an attractive method to treat wastewater through heterogeneous photocatalysis using QDs.

2.2.1 Degradation of dyes

Miao et al. [3] prepared carbon quantum dots (CQDs) (visible light responsive) embedded in mesoporous TiO_2 materials via sol–gel method. It was reported that NPs were randomly packed in mesopores and inverse surfactant micelles were formed by interconnected intraparticles. The CQDs were introduced to make full utilization of sunlight (>400 nm) without disturbing the mesopores. The photocatalytic activity

of the CQDs/meso-Ti-450 was studied in degradation of methylene blue (MB). The photocatalytic activity of the composite material was enhanced to a great extent in the presence of visible light. It was reported that highest photocatalytic performance could be achieved by 5% CQDs/meso-Ti-450 in 60 min. It was claimed that MB was almost completely (98%) removed by 5% CQDs/meso-Ti-450, while commercial P25 can remove only 10% dye under visible light conditions.

Nanophotocatalysts ZnS QDs were prepared by Mansur et al. [4] which were functionalized with chitosan (ZnS–CHI) by an ecofriendly colloidal chemical method. It was reported that chitosan can be used as an effective capping ligand for fabrication of water-soluble ZnS QDs. The average nanocrystal size was found to be 3.8 nm. The dyes MB and methyl orange were effectively degraded/oxidized by ZnS/chitosan nanostructured photocatalyst under UV irradiation.

A facile method of preparation of SnO_2 QDs was reported by Yousaf et al. [5], which was decorated on 2D material g-C_3N_4. The photocatalytic performance of as-prepared SnO_2/g-C_3N_4 nanohybrids was used for degrading rhodamine-B. It was suggested that enhanced activity may be due to synergetic effect between exfoliated g-C_3N_4 layers and SnO_2 QDs. However, it was reported that the ratio of g-C_3N_4 to SnO_2 significantly affect the photocatalytic activity. When the ratio was kept 1:2, the highest performance was exhibited.

Sood et al. [6] reported use of simple sol–gel, template free method for the synthesis of TiO_2 QDs. It was revealed that as-synthesized TiO_2 QDs possess well-crystalline pure anatase phase and it exhibited good photoluminescent properties. They also investigated the catalytic behavior of these QDs by photocatalytic degradation of the dye indigo carmine under UV-light. The optimum dose of the catalyst was found to be 0.75 g L^{-1}. It was reported that low concentrations of dye and acidic pH range favored this degradation.

Green aqueous based synthesis routes were selected by Rajabi and Farsi [7] for synthesizing pure and transition metal ions doped ZnS QDs at room temperature. These ZnS QDs were doped with three transition metal ions (Mn^{2+}, Co^{2+}, and Ni^{2+} ions). The average particle size of the QDs was found to be in the range of 1–3 nm. They investigated photocatalytic activities of ZnS QDs in the removal of methyl violet, a cationic dye. Effect of the different operational parameters on decolorization efficiency was also studied such as dopant, amount of QDs, pH, irradiation time, ionic strength, and dye concentration.

Palanisamy et al. [8] synthesized ZnS QDs, Bi/β-Bi_2O_4, and ZnS/Bi/β-Bi_2O_4 nanocomposites by precipitation, solvothermal, as well as wet impregnation method. It was reported that combination of bare ZnS QDs with Bi/β-Bi_2O_4 nanocomposite exhibited very good photocatalytic activity against toxic pollutants such as MB and rhodamine B. This nanocomposite was found to be three times more efficient as compared to pristine ZnS QDs. The as-prepared composite exhibited good stability and there was no significant loss of activity even after five cycles.

Synthesis of iron oxide (Fe_3O_4) metal NPs (MNPs) and functionalized zinc sulfide QDs was carried out by Rajabi et al. [9] through a simple chemical precipitation method. They used sodium dodecyl sulfate and 2-mercaptoethanol for surface modification and capping of ZnS QDs and Fe_3O_4 MNPs, respectively. It was observed that the mean particle size of ZnS QDs and Fe_3O_4 MNPs were approximately 1–3 and 50–80 nm, respectively. Although, both of these methods can be considered as simple, green, and efficient strategies for the removal of organic dyes, but efficiency of the QDs-based photodegradation for the removal of Victoria blue R (VBR) was found to be higher than MNPs. It was reported that the maximum decolorization of 95% and 65% could be achieved for 30 mg L^{-1} of VBR in 20 and 45 min at optimum pH 10 and 7.5 in the presence of 8 and 10 mg of QDs and MNPs, respectively.

The ZnS QDs were biosynthesized from Zn tolerant *Penicillium* sp. by Jacob et al. [10] under ambient reaction conditions. It was revealed that these ZnS QDs are spherical particles with an average diameter of 11.08 nm. These biogenic ZnS QDs were then used for the photodegradation of the MB dye, and good photocatalytic activity was observed. The dye degradation efficiency was found to be enhanced on increasing ZnS nanocatalyst/dye ratio and it reached to equilibrium in 6 h. These ZnS nanohybrids have practical applicability in the removal of pollutants in textile, paper, and dyeing industries.

Cui et al. [11] reported a photocatalyst that consists of Cu_2O QDs, which were incorporated into flower-like BiOBr. These were synthesized using reduction chemistry and then used for decontaminating the waste water containing organic dyes and phenol. It was reported that 3 wt% of the as-prepared QDs-Cu_2O/BiOBr composites showed much higher activity for degrading MB in the presence of visible light. This activity was about 1.4 times higher as compared to BiOBr, which indicated that this composite has a great potential for application in the removal/degradation of hazardous organic contaminants.

Sharma et al. [12] prepared monometallic Fe@CQDs, iron NPs (Fe NPs), and nanocomposite of Fe/Ag@CQDs through by simple reduction/coprecipitation method. Monometallic nanocomposite photocatalytic activity of NPs, FeOCQs, and Fe/Ag@CQDs was utilized for degradation of fast green dye from aqueous solution. The catalytic nature was also evaluated for the esterification of acetic acid and oxidation of benzyl alcohol. The Fe NPs gave maximum yield (87%) for oxidation of benzyl alcohol at 80 °C in presence of hydrogen peroxide. It was also reported that esterification of acetic acid with different alcohols (ethyl, isopropyl, and butyl alcohol). It was observed that butyl alcohol gave maximum esterification, that is, 82%, 80%, and 84% with Fe NPs, Fe@CQDs, and Fe/Ag@CQDs, respectively.

An environment friendly synthesis of SnO_2 QDs was investigated by Bhattacharjee and Ahmaruzzaman [13] via a microwave heating method. They used two amino acids for this purpose, that is, aspartic and glutamic acids. It was reported that the average diameter of SnO_2 QDs was ~1.6 nm when glutamic acid was used. It was with smaller diameter (~2.6 nm) as compared to the QDs prepared using aspartic

acid. The as-synthesized SnO_2 QDs were found to be effective photocatalyst in the removal of eosin Y and rose Bengal in the presence of direct sunlight.

Stieve et al. [14] developed a method to increase photocatalytic activity of bismuth oxyhalides (BiOX), which involves canon QDs sensitization. They prepared different sizes of carbon dots (CDs) using microwave-promoted synthesis under the influence of citric acid with urea as the precursor. Then, a specific wt% of CDs were introduced into different BiOX nanosheets using a surfactant in hydrothermal method. The photocatalytic activity of BiOBr, BiOCl, and BiOI were compared with their CD-integrated composite for degradation of rhodamine B. They followed this activity order:

$$BiOI < BiOBr < BiOCl$$

It was revealed that BiOX nanosheets had enhanced photocatalytic activity on integrating CDs.

Jat et al. [15] studied photocatalytic degradation of fast green in presence of visible light using SnO_2 TiO_2 QDs. They prepared this composite by hydrothermal method using stannic chloride (hydrate) as precursor for SnO_2 QDs. It was reported that the as-prepared composite had more photocatalytic activity than titania nanopowder for degradation of fast green.

2.2.2 Degradation/reduction of nitro compounds

Liu et al. [16] prepared CQDs@Pd nanoclusters CQDs@Pd-SnS_2 with Pd NPs (<5 nm) via in situ where CQDs reduced Pd(II). This composite is efficient in reducing aromatic nitro compounds in the presence of visible-light, $NaBH_4$, and H_2O (Figure 2.2). It was observed that the conversion rate of 4-nitrophenol (4-NP) could attain 99.7% on this composite in the presence of visible light within 40 min. It was reported that degradation was 586.5, 31.9, and 202.4 times faster than that observed in using the SnS_2, Pd-SnS_2, and CQDs-SnS_2.

Mahto et al. [17] synthesized N, S co-doped CDs (NS CDs). Subsequantly they prepared N, S-doped CDs-Au nanocomposites via solution method using these as reducing and stabilizing agents. The catalytic activity of the as-synthesized nanocomposites was observed for reduction of, 4-nitroaniline (4-NA), nitrobenzene (NB), and 4-NP. The apparent rate constants (k_{app}) of reduction was determined as 5.35×10^{-2} s^{-1}, 8.9×10^{-2}, and 1.37×10^{-1} for NB, 4-NA, and 4-NP, respectively. It was obtained that the rate of reduction of 4-NP by $NaBH_4$ with these NS CDs-Au NCs was the highest.

The SnO_2 QDs decorated on TiO_2 nanospheres have been synthesized by Bhatt et al. [18]. They used these as photocatalyst in photodegradation of 2-nitrophenol (2-NP). It was reported that the as-synthesized photocatalyst exhibited a more effective degradation of 2-NP as compared to pure TiO_2 nanospheres.

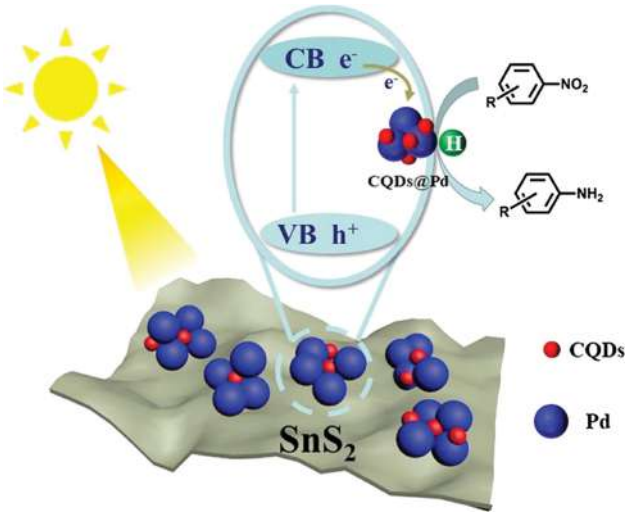

Figure 2.2: The use of CQDs@Pd-SnS_2IV ps for degradation of aromatic nitro compounds (adapted from Liu et al., J. Colloid Interface Sci. 2019, 555, 423–430.).

Lv et al. [19] developed simple and green in-situ method for the preparation of Au NPs on nitrogen-doped graphene QDs (NGQDs). They mixed NGQDs and $HAuCl_4 \cdot 4H_2O$ without using any surfactant and reductant for this purpose. The as-obtained Au NPs-NGQDs showed high catalytic performance in degradation of 4-NP. These Au NPs provided high catalytic activity because of its free catalytic surface, which has no surfactant capping. Its turnover frequency was also determined to be 12 h^{-1} reflecting its high catalytic efficiency.

2.2.3 Degradation of phenols

Liang et al. [20] reported the preparation of CQDs-sensitized ZnO composites. They also used these for photocatalytic degradation of phenol in the presence of visible light. It was observed that this sensitization extended spectral response range of this composite to the visible region that will enhance the utilization of sunlight. It was also revealed that the photocatalytic activity of this composite sensitized by CQDs was about 60% higher as compared to ZnO and that too with good reusability (up to 10 cycles) and stability.

A one-pot solvothermal route was used by Kumar et al. [21] to prepare graphitic carbon nitride QDs which were O and S co-doped (OSCNQDs). It was then hybridized with Bi_2MoO_6 (BMO) photocatalyst. These were utilized to degrade aqueous solution of phenol from wastewater in the presence of visible light. It was observed that 98% photodegradation of phenol was achieved in the presence of (OSCNQDs/BMO) nanohybrid

under visible light. It was attributed to the effective formation and coupling of Z-scheme heterostructure. Therefore, this nanohybrid exhibited prominent absorption in visible region, superior photoactivity, and enhanced space charge isolation.

The reactivity of biopolymer-based nanocarbon dots (NCDs) was investigated by Pirsaheb et al. [22]. They carried out the synthesis of NCDs via a simple hydrothermal carbonization method in the removal of phenol. They could achieve phenol degradation (>99%) in the presence of 12 mmol H_2O_2 in 20 min. The NCDs catalyst exhibited good recyclability.

Martínez et al. [23] synthesized $AgInS_2$ (AIS) QDs (size 4.0 ± 1.6 nm) and then loaded these onto ZnO nanopyramids (ZnONPy). It was revealed that the 1%AIS@ZnO NPy composite exhibited the highest degradation of phenol in aqueous media (92% in 1 h under light ($\lambda > 350$ nm). It was found to be 4 and 68 times than for bare ZnONPy and AIS QDs, respectively.

Guo et al. [24] prepared carbon nitride QDs (CNQDs)/TiO_2 NP heterojunctions. They mixed the as-prepared CNQDs and TiO_2 by mechanical stirring for this purpose. The photocatalytic degradation of bisphenol A was observed under stimulated sunlight (Figure 2.3). It was reported that the TiO_2 NP with CNQDs had an optical band gap of 3.02 eV making it useful in visible light region. It was revealed that all

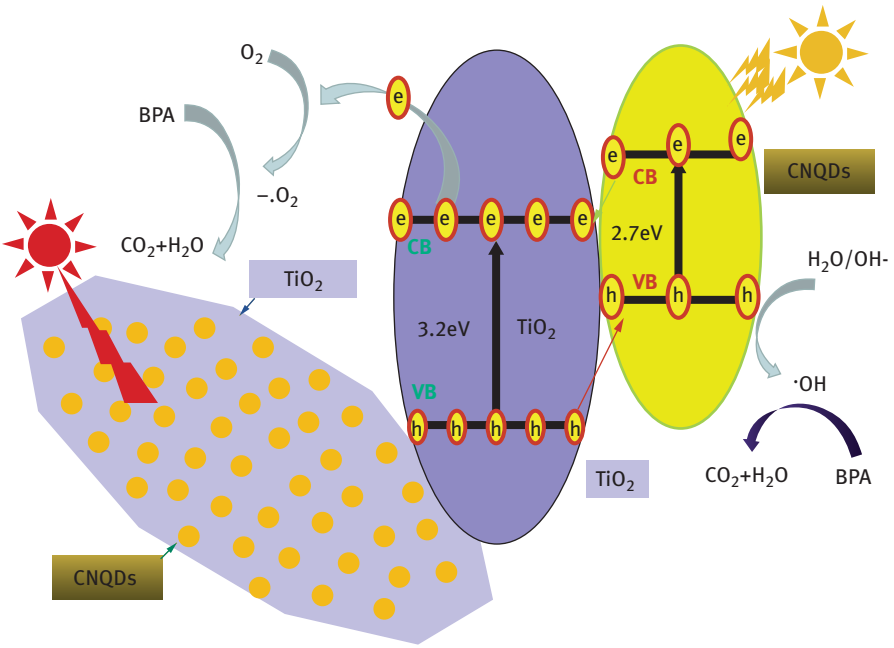

Figure 2.3: The use of CNQDs/TiO_2 for degradation of bisphenol A (adapted from Guo et al., Int J Hydrogen Energy 2020, 45(43), 22,534–22,544.).

the CNQDs-x/TiO_2 composites exhibited higher photocatalytic activities than that of the pure TiO_2 and it was about 25 times higher.

Bajorowicz et al. [25] decorated $KNbO_3$ with CdS QD to form a composite photocatalysts and thereafter comodified it with Bi_2S_3 QDs. A combination of two methods was used for this purpose, hydrothermal a linker-assisted route of adsorption thioglycolic acid and starch were used as capping agents. It was observed that QDs were deposited on surface of the perovskite-type $KNbO_3$. A stable heterostructure was obtained with good dispersion. The as-obtained $KNbO_3$-based composites exhibited enhanced photocatalytic performance for the degrading phenol in the presence of visible light in aqueous solution. Ternary 30% CdS–5%Bi_2S_3 QD-decorated $KNbO_3$ composite exhibited highest photocatalytic activity with enhanced stability. The catechol, benzoquinone, hydroquinone, and 1,2,4-benzenetriol were detected as oxidation intermediates, which ultimately formed non-cyclic organic acids.

Hasija et al. [26] employed a green synthetic approach to prepare CQDs using naturally occurring bamboo leaves. They used hydrothermal method for this purpose. The as-prepared CQDs were used for fabrication of Z-scheme P-doped g-C_3N_4/AgI/ZnO/CQDs (PGCN) heterojunction. The AgI/ZnO/CQD was immobilized on graphitic carbon nitride (g-C_3N_4). It was used for degradation of 2,4-dinitrophenol (DNP) in wastewater. Complete mineralization of DNP into CO_2, H_2O, and inorganic ions was observed. An improvement in photocatalytic performance was due to the electron sink behavior of CQDs, which was the result of integration of g-C_3N_4 to AgI/ZnO with CQDs. This photocatalyst exhibited significant recyclability (up to 10 cycles) and stability.

Ortega-Liebana et al. [27] studied the role of carbon nanodots (CNDs) in sensitizing TiO_2 so as to make a photocatalyst, which is active in visible-light and not only using solar energy efficiently, but is also durable, inexpensive, and environmentally friendly. Stevia plant and Argentinean yerba mate were used as source of carbon to produce a series of CNDs with varied levels of P and N doping. These CNDs were assembled with TiO_2 to get heterogeneous photocatalysts and used for photodegradation of 2,4-dichlorophenol in the presence of NIR and visible-light.

2.2.4 Degradation of drugs

Liu et al. [28] synthesized CQDs, which were modified with porous graphitic carbon nitride (g-C_3N_4) via polymerization method. This CQDs modified g-C_3N_4 exhibited almost 15 times higher degradation of diclofenac (DCF) as compared to graphite carbon nitride. It was found that CQDs were anchored to g-C_3N_4 surface forming C–O bond, which provided channels for easy transfer of photoexcited electrons on DCF to the conduction band of graphitic carbon nitride. It was revealed that superoxide radical ($O_2^{\bullet}-$) was the main oxidizing species in degrading of DCF. This degradation

involves ring closure, ring hydroxylation, and C–N bond cleavage. Such a hybrid photocatalysts exhibited appreciable reusability in five cycles.

Kumar et al. [29] reported synthesis of self-assembled CQDs (metal free) and RGO layers modified S@g-C_3N_4/B@g-C_3N_4 (CRSB) photocatalyst. They used it for the degradation of chloramphenicol (CMP) (10 mg L^{-1}) in the presence of visible radiation and sunlight. It was observed that visible light absorption could be achieved on modified reduced graphene oxide (rGO) with CQDs composite sample CRSB that photodegraded 99.1% CMP in 90 min under visible light and retained its activity in natural solar light (92.4% in 120 min). They also designed a stable heterojunction using boron and sulfur doped g-C_3N_4. They observed that degradation rate using CRSB (0.0810 min^{-1}) was ten times than that observed with g-C_3N_4 (0.00802 min^{-1}).

A graphitic carbon nitride (g-C_3N_4) (tubular) was modified with CQDs by Zhao et al. [30] and was used for the removal of carbamazepine (CBZ) in the presence of visible light. It was reported that surface bonded CQDs did not affect the band gap of g-C_3N_4, but it highly inhibited the recombination of charge and as a result, CBZ degradation was increased more than fivefold on incorporating CQDs in g-C_3N_4.

Zhao et al. [31] prepared decorated phosphorus-doped g-C_3N_4nanosheets with Co_3O_4 QDs via thermal polymerization. They used vitamin B_{12} (VB12) as the source of cobalt and phosphorus mixed with melamine. It was found that a particular amount of VB12 improved the photocatalytic activities, but an inhibition was observed with higher amount of VB12. Sample containing weight ratio of VB12 (1%) displayed maximum photocatalytic activity during degradation of metronidazole, which was almost double than that observed with pure g-C_3N_4.

Liu et al. [32] prepared a CQD oxygen-rich titanium dioxide nanosheets composite via a modified two-step hydrothermal method. It was then used for photodegradation of tetracycline (TC). It was reported that the as-prepared composite could enhance the degradation of TC to 94.1% in 2 h under visible light. This rate of degradation was found to be almost 2.3 times higher than that of titanium dioxide nanosheets. The hole (h^+) played a major role in the degradation of TC, but superoxide radical ($O_2^{\bullet-}$) and Hydroxyl radical ($^{\bullet}OH$) also played some role in the catalytic reaction. It was interesting to note that the toxicity of TC solution first increased in 10 min; thereafter decreased slowly to that of pure water.

Wei et al. [33] prepared ZnS QD nanomaterials using a hydrothermal method. The photocatalytic properties of ZnS QDs were observed for degradation of antibiotic ciprofloxacin (CIP). It was revealed that the as-prepared ZnS QD exhibited good photocatalytic property under UV irradiation and effectively degraded CIP, but its activity is not high enough and its degradation efficiency was only 45.75% under visible light.

2.2.5 Degradation of other organics

The CD@Fe_3O_4 photocatalysts were synthesized by Rong et al. [34] through a hydrothermal route. The Fe_3O_4 was used as the core material to synthesize CD@Fe_3O_4particles. The ethylene diamine and citric acid were used as a raw material. These were observed as uniform, hemisphere and monodispersed particles with size of almost 3 nm as evident from High-resolution transmission electron microscopy (HRTEM). It was revealed that the half-life of hexaconazole (an herbicide) in CD@Fe_3O_4 photocatalysts was almost 4 days with daylight lamp, which is much lower than that without CD@Fe_3O_4 photocatalysts (over 100 days).

Das and Dhar [35] synthesized tin dioxide QDs using *Camellia sinensis* shoots as reducing agent and stabilizer. Crystalline nature of tin dioxide QDs and the size of the particle was determined as 4.3 nm. These were having flake-like morphology, which was capped by phenolic compounds of *C. sinensis*. These QDs were used for the photocatalytic degradation of thiamethoxam and it was reported that 57% degradation was achieved within 45 min.

Some chalcogenide CdX (X = chalcogens) QDs/TiO_2 hybrids were prepared by Hua et al. [36]. These were used for degradation of benzene in presence of visible light. It was reported that the photocatalytic degradation of benzene was about 95%, 90%, and 86% on using CdS-TiO_2, CdSe-TiO_2, and CdTe-TiO_2, respectively. Hydroxyl radical and h^+ were proposed as active oxidizing species in the photocatalytic degrading benzene over CdX-TiO_2.

Tin oxide QDs were prepared by Liu et al. [37] through oxidation and simple hydrolysis. It was reported that the as-prepared QDs had an average particle size of 2.23 nm. The fluorescence properties of these QDs were used in detection of heavy metal ions such as Ni^{2+}, Fe^{3+}, Cd^{2+}, and Pb^{2+}, which quenched photoluminescence. These QDs responded to the presence of ions in the range of 2.48 to 100 ppm Ni^{2+}. These SnO_2 QDs can be used to detect these heavy metal ions in all real samples, the contaminated water, reclaimed water, as well as sea water. A linear correlation was found between Ni^{2+} concentration (log) against fluorescence emission intensity.

2.3 Photogeneration of hydrogen

QDs have a number of parameters that may be adjusted to get the desired band gap in photocatalyst. The enlargement of the band gap is a significant driving force for the charge transfer and as a result, photocatalytic reactions were promoted. A strong quantum-confinement effect was observed, which makes the transfer of these charge carriers outside the boundary of QDs conveniently. In addition, more photons (multiple) could be absorbed, generating multiple excitons per QDs [38].

Li et al. [39] prepared monolayer MoS_2 QDs through laser ablation of bulk MoS_2-material in water. It was reported that the as-prepared MoS_2 QDs exhibited excellent electrocatalytic activity for evolution of hydrogen, which was attributed to abundant active edge sites, high specific surface area, and excellent electrical conductivity.

The MoS_2 QDs were obtained by Baldovi et al. [40] in colloidal suspensions by laser ablation (532 nm) of commercial MoS_2 particles in acetonitrile. These MoS_2 QDs obtained by laser ablation were constituted by 3–6 MoS_2 layers (1.8–4 nm thickness). It was reported that these QDs' photocatalytic activity under UV-Vis irradiation could be used for generation of H_2. The CH_3OH was used as sacrificial electron donor, may be due to electron transfer kinetics and an increase in the reduction potential of electrons in conduction band.

Chen et al. [41] fabricated ZnCdS QDs without carbon support by controlled annealing and ion-exchange procedure and sequential sulfidation. It was reported that photocatalytic activity of these QDs for generation of hydrogen can be enhanced through adjustment of quantum sizes. An optimal production rate (3.70 mmol h^{-1} g^{-1}) of H_2-could be achieved in the presence of visible light. The rate was found to be higher than that with bulk ZnCdS.

Cao et al. [42] prepared CdS QDs grown in situ on graphitic carbon nitride nanosheets, which were well dispersed. It was observed that the resultant CdS–C_3N_4-nanocomposites exhibited excellent photocatalytic evolution of hydrogen in the presence of visible light in comparison to pure g-C_3N_4. Such an enhanced photocatalytic activity may be due to interfacial transfer of holes photogenerated and electrons between CdS and g-C_3N_4.

Metallic Cu/Ag QDs were decorated on TiO_2 nanotubes (Cu/Ag@TNT) by Reddy et al. [43] via photo deposition method. They observed generation of hydrogen in the presence of Cu/Ag@TNT catalyst in aqueous glycerol suspension using natural sun light. An enhanced photocatalytic evolution rate of H_2 was obtained with Cu/Ag@TNT (CAT-2.0) as compared to TiO_2 nanotubes (TNT), monometallic Ag@TNT (AT-2.0), and Cu@TNT (CT-2.0). This better photocatalytic H_2 evolution rate was attributed to localized surface plasmon resonance (LSPR) effect due to Ag-injected charge carriers into the TiO_2 catalyst (conduction band). The Cu cocatalyst also acts as an electron acceptor from TiO_2 to reduce H^+ ions into H_2 gas.

The TiO_2 NPs were prepared modified as the cobalt sulfide QDs (CoSx QDs) by Yu et al. [44] using precipitation–deposition method. They utilized TiO_2, sodium sulfide, and cobalt acetate as the precursors. These QDs act as effective cocatalyst, facilitating the transfer of photogenerated electrons. They also served as the active site for the reaction between water and electrons; as a result, separation of the e^-/h^+ pairs and the photocatalytic H_2 generation was also enhanced. It was reported that the amount of CoSx exhibited an optimum value at about 5% TiO_2, where production rates of H_2 could achieve 838 μmol h^{-1} g^{-1}, which was 35 times more than that of pure TiO_2.

Wang et al. [45] reported the fabrication of CuO/TiO_2 heterojunction as advanced photocatalysts for water splitting. It was revealed that 5% content CuO modified TiO_2 nanosheets exhibited much higher activity for H_2 evolution (~0.04 mmol h^{-1}). It was also observed that its stability was good even after five cycles of 15 h.

Ma et al. [46] synthesized $CdSe\ QDs/CeO_2$ (111) heterostructures via a wet chemistry method. They observed higher photocatalytic H_2 evolution (283.32 μmol $g^{-1}h^{-1}$) and it was due to the enhanced higher separation, light absorbance intensity and edge, and lower recombination, and relatively longer lifetime of the photogenerated carriers.

Du et al. [47] fabricated $BiVO_4@ZnIn_2S_4/Ti_3C_2$ MXene QDs (QDs) photocatalyst via in-situ growth, which was combined with solvothermal method. They reported that Ti_3C_2 MXene QDs can be used as cocatalysts for water splitting photo catalytically. These QDs could achieve effective splitting of water into H_2 and O_2 under visible light with rates of evolution up to 102.67 and 50.83 μmol g^{-1} h^{-1} (~1:2). These QDs also exhibited higher photocatalytic degradation efficiency for bisphenol A ~ 96.4%.

A zero-dimensional/two-dimensional heterostructure binary ZnO-SnO_2 QDs, was deposited on the surface of g-C_3N_4 nanosheets by Vattikuti et al. [48]. The SnO_2–ZnO QDs/g-C_3N_4 hybrid was prepared through an in-situ copyrolysis. This hybrid showed a higher rate of hydrogen production (13 673.61 μmol g^{-1}). The production rate is almost 2.27 and 1.06 times more than that with binary pristine g-C_3N_4 photocatalyst and ZnO/g–C_3N_4 hybrid. An enhanced visible absorption and reduced recombination was considered responsible for increased performance of the as-synthesized zinc oxide-modified g-C_3N_4 and tin oxide.

Xiao et al. [49] developed a dual-functional $Ag_2O\ QD/ZnIn_2S_4$ nanosheet (AO/ZIS) composite photocatalyst via an in-situ deposition process. It was reported that these AO/ZIS hybrids exhibited higher photocatalytic performance for generation of hydrogen. They revealed that highest photocatalytic H_2 production rate (2334.19 μmol g^{-1}) was observed with AO/ZIS-2 which was 3.38 times more than that of $ZnIn_2S_4$. It was suggested that an enhanced spectral absorption, increased surface area, and the formation of p–n heterojunction were considered responsible for superior photocatalytic activities.

2.4 Reduction of carbon dioxide

Carbon dioxide concentrations in the atmosphere are regularly increasing due to combustion of fossil fuel resulting in global warming. The major barrier to this process is the availability of an efficient and robust catalyst for reduction of CO_2, particularly catalysts achieving products such as methanol, ethanol, or butanol [50].

Photocatalytic reduction of carbon dioxide to hydrocarbons is one of the most sustainable and promising solutions for conversion of solar energy (light) to chemical

energy in the form of high value-added products or chemicals and also decreasing an ever-increasing environmental pollution.

QDs are promising candidates for harvesting visible light, but they normally exhibited selectivity and low activity for photocatalytic reduction of carbon dioxide. Metal complexes QDs may exhibit improved catalytic activity if these are functionalized but it was observed that such fabricated QDs still suffer from low stability and selectivity in reducing CO_2. There is an increasing demand to overcome these problems.

The $CsPbBr_3$ QDs are potential candidates for reduction of CO_2 due to their high molar extinction coefficient, excellent photoelectric properties, defect tolerance, and low exciton binding energy. But the pristine $CsPbBr_3$ QDs exhibited poor photocatalytic performance because of rapid recombination of charge and less efficient catalytic sites for adsorption/activation of CO_2.

Halide perovskite QDs (HP QDs) are widely used in the field of photocatalysis due to their excellent performance, but there are certain limitations such as lead toxicity and instability.

The $CsPbBr_3$ QDs/Bi_2WO_6 nanosheet (CPB/BWO) (heterojunction) photocatalysts was fabricated by Wang et al. [51] and it was used for photocatalytic CO_2 reduction. It was revealed that this photocatalyst achieved an excellent photocatalytic performance with CH_4/CO as 503 μmol g^{-1}, which is almost 9.5 times more than that with pristine $CsPbBr_3$. This heterojunction also exhibited an improved stability in photocatalytic reactions.

Guzman et al. [52] fabricated assemblies with polycations poly-(2-trimethylammonium) ethyl methacrylate (PM), poly-diallyl dimethylammonium, and CdTe nanocrystals. It was revealed that the modified surfaces were active in CO_2 reduction, with a better activity from dark and irradiation conditions. They reported that major product of reduction of CO_2 was CH_3OH; however, some traces of HCOOH and CO were also observed. It was suggested that PM modified electrodes with QDs (2.77 nm size) exhibited a selective production of CH_3OH.

Qin et al. [53] prepared g-C_3N_4 photocatalyst, which was modified by NiS_2 QDs (cocatalyst) through hydrothermal process. The as-prepared composite showed stability as well as superior activity in photocatalytic CO_2 reduction. They could obtain highest CO evolution rate on NSQD/CN-25 catalyst (10.68 μmol h^{-1} g^{-1}) and it was almost 3.88 times higher as compared to g-C_3N_4. The apparent quantum efficiency (AQE) was found to be 2.03%. It was indicated that some intermediate products were also obtained (such as COO^-, CO_3^{2-}, and HCO_3^-) in this process.

Wang et al. [54] reported a photocatalytic system, involving $CsPbBr_3$ QDs coupled with covalent triazine frameworks (CTFs) and it can be used for reduction of CO_2 under visible light. Here, the periodical pore structures of CTFs and triazine rings helped in separation of charge in $CsPbBr_3$ and making these more effective with strong CO_2 adsorption/activation capacity.

The Bi_2MoO_6 QDs (BM QDs) with the size of 5 nm in diameter were in situ grown by Dai et al. [55] on reduced graphene oxide (rGO) layers. This sensitized graphene for better visible light response and provides more activity for sun light-driven reduction of CO_2. It was reported that small-sized BM QDs will generate some active electrons and donate these electrons to the rGO layers on irradiation. About 84.8 methanol and 57.5 μmol g^{-1} of ethanol were obtained on BM QDs/rGO in 4 h due to transport and higher electron extraction over the BM QDs/rGO interface. This total yield of alcohols over BM/rGO (142.3 μmol g^{-1}) was found to be 4.4 and 2.2 times than with flower-like Bi_2MoO_6 (32.2 μmol g^{-1}), and unmodified Bi_2MoO_6 QDs (64.0 μmol g^{-1}), respectively.

Dai et al. [56] prepared WS_2 QDs (WS_2 QDs), which were doped with Bi_2S_3-nanotubes. They utilized WS_2 QDs as seeds for this purpose. It was reported that the perfect junction interface was there between WS_2 and Bi_2S_3, which provides lower resistance for rapid electron transfer on the interface efficient by separated electron–hole pairs. The WS_2@Bi_2S_3 nanotubes exhibited more photocatalytic activity in reduction of CO_2 as compared to pristine Bi_2S_3 nanotubes. The 38.2 and 27.8 μmol g^{-1} of methanol and ethanol could be produced using WS_2 (4 wt% loading) in presence of Vis-NIR light in 4 h. A low-resistance interface in heterojunction and electron pathway through Bi_2S_3 nanotubes were responsible for its higher photocatalytic activity.

The lead-free $Cs_2AgInCl_6$ perovskite QDs (CAIC QDs) were prepared by Chen et al. [57] via the hot-injection method. Then, CAIC QDs@Ag composites were synthesized with different Ag loading and adjustment of the Cl source. It was found that the CAIC QDs@Ag composite has better carrier separation efficiency and fast electron transport, which are very important for the improvement in reduction of CO_2. It was reported that CAIC QDs@Ag-2 composite could achieve the highest yield of 26.4 and 28.9 μmol g^{-1} for CO and CH_4, respectively. It was also observed that there is no significant decrease in photoreduction performance even after recycling test for 9 h, which indicated that the CAIC QDs@Ag composite was stable during photocatalysis process.

The $CsPbBr_3$ QDs/UiO-66(NH_2) nanocomposites were fabricated by Wan et al. [58] by combining the advantages of UiO-66(NH_2) and $CsPbBr_3$ QDs. It was reported that these nanocomposites exhibited significantly enhanced photocatalytic activity for CO_2 reduction. When $CsPbBr_3$ QDs content was kept 15 wt%, then 98.57 μmol · g^{-1} CO was produced. The increased photocatalytic performance was attributed to large accessible specific surface area improvement in electron extraction as well as transfer between $CsPbBr_3$ QDs and UiO-66(NH_2) and higher absorption capacity of visible light.

Li et al. [59] synthesized CQDs/Cu_2O heterostructure, and these can be used for efficient photocatalytic reduction of CO_2 to methanol in presence of solar light. It was revealed that CQDs/Cu_2O photocatalyst exhibited significant stability in this process, and it was all due to the photoinduced electron-transfer properties of these CQDs.

Wang et al. [60] reported that doping of CdS QDs with transition-metals sites can be helpful to overcome the limitations of low stability and selectivity. These doped QDs gave highly selective photocatalytic reaction of CO_2 with H_2O (almost 100 % selectivity to CH_4 and CO was there). They reported that doping Ni sites into the CdS lattice could be effective by trapping these photoexcited electrons on surface catalytic sites, which suppresses H_2 evolution to a greater extent.

Shu et al. [61] fabricated a multiwalled carbon nanotube (MWCNT)/$CsPbBr_3$-perovskite QDs (QDs) nanocomposite. Here, the highly conducting MWCNT acts as an electron acceptor, which can inhibit recombination of charge carrier in $CsPbBr_3$-QDs. It was reported that $CsPbBr_3$/MWCNT exhibited the highest photocatalytic performance, when the MWCNT content was kept at 4.0 wt%. The yields of CO and CH_4 were found to be 3.14 and 2.13 times than that with pristine $CsPbBr_3$ QDs, respectively. It was reported that a fast electron extraction and transfer to MWCNT from $CsPbBr_3$ QDs, and better ability for visible light harvesting may be responsible for the better photocatalytic performance.

2.5 Application in solar cells

Photoelectrochemical (PEC) cells have a potential for developing a solar energy conversion system, which can resolve ever-increasing problems of energy crisis and deterioration of environment. However, the non-availability of stable and eco-friendly electrodes limits their practical uses. QDs are one among promising materials, which are considered for the development of third-generation photovoltaics. The QDs have certain advantages such as tunable band gap of multiple exciton, easy synthesis, generation, low cost, and high absorption coefficient. One of the potential solutions for increasing photoconversion efficiencies is to extend the absorption range of QDs.

Zinc oxide can be used as electron-transporting layers (ETLs) in organic solar cells. But it needs light-soaking process to achieve a high device performance in these cells, because of mismatched energy bands and surface defects with the photoactive layer.

$CsPbI_3$ all-inorganic perovskite QDs are effective as light absorbers in solar cells. This is because of their thermal stability and suitable optical band gap. But their phase transition from cubic to yellow orthorhombic is quite easy and it hinders their further applications in stable photovoltaic devices. The $CsPbBr_3$ QDs is a potential material for stable solar cells with ultrahigh voltage.

Wang et al. [62] carried out synthesis of N, S-doped CQDs (N,S-CQDs) via hydrothermal process. They used ammonium persulfate and ascorbic acid as reagents. The as-synthesized CQDs were found to be 2–7 nm in size with a graphite-structured core and amorphous carbon on the shell. It was confirmed that these CQDs are highly

sulfur- and nitrogen-doped leading to a quantum yield of 33%. It was reported that the improvement in performance and the elimination of light-soaking effect for ZnO:N, S-CQDs cells were due to the ZnO surface defect passivation by N,S-CQDs. The cells with N,S-CQDs-modified ZnO ETL exhibited a high power conversion efficiency (9.31%), which is higher as compared to reference ZnO cells.

Kim et al. [63] reported the preparation of colloidal $CuInTe_2$, and $CuInTe_{2-x}Se_x$-alloyed QDs. They used a simple hot injection method. It was confirmed that the as-synthesized QDs were cationic rich phase of $CuIn_{1.5}Te_{2.5}$ and $Cu_{0.23}In_{0.36}Te_{0.19}Se_{0.22}$. It was also revealed that the gradient alloyed $Cu_{0.23}In_{0.36}Te_{0.19}Se_{0.22}$ QDs show much enhanced stability over $CuIn_{1.5}Te_{2.5}$ QDs. It was observed that such solar cell exhibited 17.4 mA cm^{-2} 0.40 V of open circuit voltage (V_{oc}), short circuit current density (J_{sc}), at 100 mWcm^{-2} under AM 1.5 G illumination.

Nong et al. [64] fabricated an eco-friendly photoanode with higher PEC cells performance, where $AgInS_2$ QDs (QDs) were embedded into three-dimensional (3D) graphene nanowalls (GNWs). These $AgInS_2$ QDs were synthesized through hydrothermal method and then these were deposited on GNWs by a method which is catalyst-free. Here, electron acceptor is GNWs, which can transport the photogenerated carriers of $AgInS_2$ QDs due to its interconnected 3D conductive network. The $AgInS_2$/GNWs photoanodes exhibited fast photoresponse upon excitation by light with short decay-time and rise-time of 0.41 and 0.23 s, respectively. They reported that a photocurrent density of 145 μA cm^{-2} could be achieved.

Three-dimensional ZnO spheres were prepared by Lin et al. [65] through a hydrothermal method. Later, they used these QDs in dye-sensitized solar cells (DSSCs). It was reported that ZnS layer was deposited on the surface of CdS/ZnO photoanodes when the desired thickness was obtained of sensitized CdS QDs for ZnO spheres. It can improve the photoelectric properties further. They deposited CdS QDs and ZnS over layer by successive ionic layer adsorption and reaction (SILAR) method. It was also revealed that the power conversion efficiency was increased from 0.60% to 1.43% on treatment of CdS/ZnO photoanodes by ZnS overlayer.

Zhang et al. [66] developed a simple and efficient post-treatment approach using guanidinium thiocyanate (GASCN). It can exchange the capping ligands of $CsPbBr_3$ QDs, which can improve the carrier transport properties through increased electrical coupling between QDs. These QD-based solar cells exhibited highest efficiency of more than 5% along with an ultrahigh V_{oc} of 1.65 V.

Kumar et al. [67] obtained SnSe QDs on theTiO_2 mesoporous layers. They used SILAR method for this purpose. The major advantages of this method include high loading rate as well as better coverage of the surface of TiO_2 matrix by the QDs. The as-prepared device shows a photoconversion efficiency of 0.78%, which is the more than other SnSe QD-based solar cells.

The SnS QDs (8 nm) were synthesized by Li et al. [68] via in situ reaction at room temperature. They used stannous chloride as precursor of Sn and it was coated on the TiO_2 photoanodes to form a solid precursor film. Then, $(NH_4)_2S$ was dissolved in

ethanol. The SnS QDs were generated by immersing this Sn-coated TiO_2photoanode into this solution. It was found that the SnS/TiO_2 solar cell exhibited the best photovoltaic performance after 20 deposition cycles. It had open-circuit voltage V_{oc} of 510 mV, a short-circuit current density J_{sc} of 2.41 mA cm^{-2}, and a fill factor FF of 0.49 with a power conversion efficiency of 0.61% on AM 1.5 illumination. The performance was doped on further deposition due to agglomeration of QDs increased by charge transfer resistance.

Shen et al. [69] introduced CdS/Cu_xS QDs as sensitizers in QD sensitized solar cells (QDSSCs). Here, CdS photoanode was immersed in cupric chloride methanol solution to replace cadmium ion by copper ions. They used p-type Cu_xS layer as hole-transport material on the surface of the CdS QDs. As a result, light harvesting of photoanode was increased apart from charge separation on photoexcitation. It was revealed that power conversion efficiency and electron collection efficiency of this solar cell were improved from 1.21% to 2.78% and from 80% to 92%, respectively.

Li et al. [70] reported that dye-sensitized ZnO solar cells performed better with a facile surface-treatment approach via chemical-bath deposition onto surface of ZnO NPs decorated with QDs of Zn_2SnO_4. It was observed that open-circuit photovoltage was increased, may be due to increased conduction-band edge of ZnO and inhibition of interfacial charge recombination. A decrease in adsorption amounts of N719 dye was observed on deposition of Zn_2SnO_4 but aggregates of Zn_2SnO_4 acted as light-scattering layer in a better way. It resulted in an enhanced short-circuit photocurrent. It was revealed that a higher efficiency of 4.38 % could be achieved under AM 1.5 illumination, when it is cosensitized by 10 μm-thick ZnO film with D131 and N719 dyes.

Peng et al. [71] used simultaneous nucleation and growth approach for the synthesis of Cu–In–Ga–Se (CIGSe) QDs, which can harvest light in range around 1,000 nm. These were used as sensitizers to construct QDSSCs. It was revealed that intrinsic recombination in CIGSe QDSSCs was suppressed well as compared to that in CISeQDSSCS. It was reported that CIGSe based QDsSSCSCs using titanium mesh supported mesoporous carbon counter electrode exhibited greater efficiency of 11.49% J_{sc} = 25.01 mA cm^{-2}, V_{oc} = 0.740 V, and FF = 0.621) under the irradiation of AM 1.5 as compared to 9.46% for CISeQDsCs.

AlGhamdi et al. [72] fabricated DSSCs, where TiO_2 photoanode was cosensitized by CdSe-QDs and N719 organic dye. It was reported that photovoltaic performance of cosensitized cell with an optimum concentration of CdSe-QDs was much better than the cell sensitized by N719 dye. It was attributed to selective transfer of photogenerated electrons from energy state of N719 dye to its conduction band, and better absorbance in the visible range. It was observed that photovoltaic conversion efficiency of this cell was 7.09%, which was cosensitized by CdSe-QDs at ethanol concentration (1 mg 15 mL^{-1}) and N719 dye. It indicated 37% increase in photovoltaic efficiency as compared to the cell, which was sensitized by N719 dye only.

Yu and Li [73] fabricated $Zn_xCd_{1-x}Se$@ZnO hollow spheres (HS) based on ZnO HS using ion-exchange process and used in QDSSCs. It was reported that sizes of the $Zn_xCd_{1-x}Se$@ZnO HS could be easily tuned from ~300 to ~800 nm using ZnO HS. It was observed that a better performance was achieved with $Zn_xCd_{1-x}Se$@ZnO HS with an average size ~500 nm as-compared to QDSSCs based on other sizes of $Zn_xCd_{1-x}Se$@ZnO HS. The power conversion efficiency can be improved further by using the mixture of $Zn_xCd_{1-x}Se$@ZnO HS with various sizes. This was attributed to light-scattering effect of size hollow spheres and also gradient structure composition of $Zn_xCd_{1-x}Se$@ZnO HS.

2.6 Conclusion

Photocatalysis has emerged as a promising field of research these days, which includes waste water treatment, generation of hydrogen, reduction of carbon dioxide, solar cells, and so on. Recently, QDs have found numerous applications in these fields with higher efficiency in some cases as compared to their micro- and macro-counterparts. It is all due to their size, morphology, quantum confinement effect, unique optical and electrical properties, and so on. Apart from it, QDs are now commonly used in biomedical imaging, targeted drug delivery, and cancer diagnosis and therapy to quote some interesting examples. This chapter presents a review of the subject and it is anticipated that QDs will occupy a prominent position in solving some of these problems in years to come.

References

[1] Bakirhan, NK, Kaya, SI, Ozkan, SA. Basics of electroanalytical methods and their applications with quantum dot sensors. In: Electroanalytical Applications of Quantum Dot-Based Biosensors, Uslu, B Ed., Netherlands: Elsevier, 2021, 37–80.

[2] Ameta, R, Solanki, MS, Benjamin, S, Ameta, SC. Photocatalysis. In: Advanced Oxidation Processes for Waste Water Treatment, Ameta, S, Ameta, R Ed., CRC Press Taylor and Francis: New York, 2018, 135–175.

[3] Miao, R, Luo, Z, Zhong, W, Chen, SY, Jiang, T, Dutta, B, Nasr, Y, Zhang, Y, Suib, SL. Mesoporous TiO_2 modified with carbon quantum dots as a high-performance visible light photocatalyst. Appl Catal B: Environ, 2016, 189, 26–38.

[4] Mansur, AA, Mansur, HS, Ramanery, FP, Oliveira, LC, Souza, PP. “Green” colloidal ZnS quantum dots/chitosan nano-photocatalysts for advanced oxidation processes: Study of the photodegradation of organic dye pollutants. Appl Catal B: Environ, 2014, 158, 269–279.

[5] Yousaf, MU, Pervaiz, E, Minallah, S, Afzal, MJ, Honghong, L, Yang, M Tin oxide quantum dots decorated graphitic carbon nitride for enhanced removal of organic components from water: Green process. Res Phy 2019, 14, 10.1016/j.rinp.2019.102455.

[6] Sood, S, Kumar, S, Umar, A, Kaur, A, Mehta, SK, Kansal, SK. TiO_2 quantum dots for the photocatalytic degradation of indigo carmine dye. J Alloys Compd, 2015, 650, 193–198.
[7] Rajabi, HR, Farsi, M. Effect of transition metal ion doping on the photocatalytic activity of ZnS quantum dots: Synthesis, characterization, and application for dye decolorization. J Mol Catal A: Chem, 2015, 399, 53–61.
[8] Palanisamy, G, Bhuvaneswari, K, Pazhanivel, T, Shankar, R, Katubi, KM, Alsaiari, NS, Ouladsmane, M ZnS quantum dots and Bi metals embedded with two dimensional β-Bi_2O_4 nanosheets for efficient UV-visible light driven photocatalysis. Mater Res Bull 2021, 142, 10.1016/j.materresbull.2021.111387.
[9] Rajabi, HR, Arjmand, H, Kazemdehdashti, H, Farsi, M. A comparison investigation on photocatalytic activity performance and adsorption efficiency for the removal of cationic dye: Quantum dots vs. magnetic nanoparticles. J Environ Chem Eng, 2016, 4, 2830–2840.
[10] Jacob, JM, Rajan, R, Aji, M, Kurup, GG, Pugazhendhi, A. Bio-inspired ZnS quantum dots as efficient photo catalysts for the degradation of methylene blue in aqueous phase. Cer Int, 2019, 45, 4857–4862.
[11] Cui, W, An, W, Liu, L, Hu, J, Liang, Y. Novel Cu_2O quantum dots coupled flower-like BiOBr for enhanced photocatalytic degradation of organic contaminant. J Hazard Mater, 2014, 280, 417–427.
[12] Sharma, G, Kumar, A, Naushad, M, Kumar, A, Ala'a, H, Dhiman, P, Ghfar, AA, Stadler, FJ, Khan, MR. Photoremediation of toxic dye from aqueous environment using monometallic and bimetallic quantum dots based nanocomposites. J Clean Prod, 2018, 172, 2919–2930.
[13] Bhattacharjee, A, Ahmaruzzaman, M. A novel and green process for the production of tin oxide quantum dots and its application as a photocatalyst for the degradation of dyes from aqueous phase. J Colloid Interface Sci, 2015, 448, 130–139.
[14] Stieve, B A novel bismuth oxyhalide/carbon quantum dot photocatalyst for the degradation of trichloroethane. Presented in University of Illinois, United State, Emerging Contaminants in the Environment Conference, 27–28 April 2021.
[15] Jat, KK, Bhatt, J, Ameta, SC. Photodegradation of Fast Green by Using SnO_2 Quantum Dots/ TiO_2 Nanoparticles Composite. J Applicable Chem, 2019, 8, 139–145.
[16] Liu, M, Wang, R, Liu, B, Guo, F, Tian, L. Carbon quantum dots@ Pd-SnS_2 nanocomposite: The role of CQDs@ Pd nanoclusters in enhancing photocatalytic reduction of aromatic nitro compounds. J Colloid Interface Sci, 2019, 555, 423–430.
[17] Mahto, MK, Samanta, D, Konar, S, Kalita, H, Pathak, AN. S doped carbon dots – Plasmonic Au nanocomposites for visible-light photocatalytic reduction of nitroaromatics. J Mater Res, 2018, 33, 3906–3916.
[18] Bhatt, J, Jat, KK, Rai, AK, Ameta, R, Ameta, SC. Photodegradation of 2-Nitrophenol, an Endocrine Disruptor, Using TiO_2 Nanospheres/SnO_2 Quantum Dots 2. In: Green Chemistry and Biodiversity, Aguilar, CN, Ameta, SC, Hagji, AK Eds., Apple Academisc Press: Canada, 2019, 1–21.
[19] Lv, W, Ju, Y, Chen, Y, Chen, X. *In situ* synthesis of gold nanoparticles on N-doped graphene quantum dots for highly efficient catalytic degradation of nitrophenol. Int J Hydrogen Energy, 2018, 43, 10334–10340.
[20] Liang, H, Tai, X, Du, Z, Yin, Y Enhanced photocatalytic activity of ZnO sensitized by carbon quantum dots and application in phenol wastewater. Optical Mater 2020, 100, 10.1016/j. optmat.2020.109674.
[21] Kumar, A, Raizada, P, Singh, P, Hosseini-Bandegharaei, A, Thakur, VK Facile synthesis and extended visible light activity of oxygen and sulphur co-doped carbon nitride quantum dots modified Bi_2MoO_6 for phenol degradation. J PhotochemPhotobio A: Chem 2020, 397, 10.1016/j.jphotochem.2020.112588.

[22] Pirsaheb, M, Moradi, S, Shahlaei, M, Farhadian, N. Application of carbon dots as efficient catalyst for the green oxidation of phenol: Kinetic study of the degradation and optimization using response surface methodology. J Hazard Mater, 2018, 353, 444–453.
[23] Martínez, MCN, Bajorowicz, B, Klimczuk, T, Żak, A, Łuczak, J, Lisowski, W, Zaleska-Medynska, A. Synergy between $AgInS_2$ quantum dots and ZnO nanopyramids for photocatalytic hydrogen evolution and phenol degradation. J Hazard Mater, 2020, 398, 123250.
[24] Guo, R, Zeng, D, Xie, Y, Ling, Y, Zhou, D, Jiang, L, Jiao, W, Zhao, J, Li, S. Carbon nitride quantum dots (CNQDs)/TiO_2 nanoparticle heterojunction photocatalysts for enhanced ultraviolet-visible-light-driven bisphenol a degradation and H_2 production. Int J Hydrogen Energy, 2020, 45, 22534–22544.
[25] Bajorowicz, B, Kowalska, E, Nadolna, J, Wei, Z, Endo, M, Ohtani, B, Zaleska-Medynska, A. Preparation of CdS and Bi_2S_3 quantum dots co-decorated perovskite-type $KNbO_3$ ternary heterostructure with improved visible light photocatalytic activity and stability for phenol degradation. Dalton Trans, 2018, 47, 15232–15245.
[26] Hasija, V, Sudhaik, A, Raizada, P, Hosseini-Bandegharaei, A, Singh, P Carbon quantum dots supported AgI/ZnO/phosphorus doped graphitic carbon nitride as Z-scheme photocatalyst for efficient photodegradation of 2,4-dinitrophenol. J Environ Chem Eng 2019, 7, 10.1016/j.jece.2019.103272.
[27] Ortega-Liebana, MC, Hueso, JL, Ferdousi, S, Arenal, R, Irusta, S, Yeung, KL, Santamaria, J. Extraordinary sensitizing effect of co-doped carbon nanodots derived from mate herb: Application to enhanced photocatalytic degradation of chlorinated wastewater compounds under visible light. Appl Catal B: Environ, 2017, 218, 68–79.
[28] Liu, W, Li, Y, Liu, F, Jiang, W, Zhang, D, Liang, J. Visible-light-driven photocatalytic degradation of diclofenac by carbon quantum dots modified porous g-C_3N_4: Mechanisms, degradation pathway and DFT calculation. Water Res, 2019, 151, 8–19.
[29] Kumar, A, Kumari, A, Sharma, G, Du, B, Naushad, M, Stadler, FJ Carbon quantum dots and reduced graphene oxide modified self-assembled S@C_3N_4/B@ C_3N_4 metal-free nano-photocatalyst for high performance degradation of chloramphenicol.J Mol Liq 2020, 300, 10.1016/j.molliq.2019.112356.
[30] Zhao, C, Liao, Z, Liu, W, Liu, F, Ye, J, Liang, J, Li, Y Carbon quantum dots modified tubular g-C_3N_4 with enhanced photocatalytic activity for carbamazepine elimination: Mechanisms, degradation pathway and DFT calculation. J Hazard Mater 2020, 381, 10.1016/j.jhazmat.2019.120957.
[31] Zhao, Z, Fan, J, Deng, X, Liu, J. One-step synthesis of phosphorus-doped g-C_3N_4/Co_3O_4 quantum dots from vitamin B_{12} with enhanced visible-light photocatalytic activity for metronidazole degradation. Chem Eng J, 2019, 360, 1517–1529.
[32] Liu, X, Yang, Y, Li, H, Yang, Z, Fang, Y Visible light degradation of tetracycline using oxygen-rich titanium dioxide nanosheets decorated by carbon quantum dots. Chem Eng J 2021, 408, 10.1016/j.cej.2020.127259.
[33] Wei, M, Yang, L, Yan, Y, Ni, L. Preparation of ZnS quantum dot photocatalyst and study on photocatalytic degradation of antibiotics. Mater Exp, 2019, 9, 413–418.
[34] Rong, S, Tang, X, Liu, H, Xu, J, Yuan, Z, Peng, X, Niu, J, Wu, Y, He, L, Qian, K Synthesis of carbon dots@Fe_3O_4 and their photocatalytic degradation properties to hexaconazole. NanoImpact 2021, 22, 10.1016/j.impact.2021.100304.
[35] Das, J, Dhar, SS. Synthesis of SnO_2 quantum dots mediated by *Camellia sinensis* shoots for degradation of thiamethoxam. Toxicol Environ Chem, 2020, 102, 186–196.
[36] Hua, J, Wang, M, Jiao, Y, Li, H, Yang, Y. Strongly coupled CdX (X = S, Se and Te) quantum dots/TiO_2 nanocomposites for photocatalytic degradation of benzene under visible light irradiation. Optik, 2018, 171, 95–106.

[37] Liu, J, Zhang, Q, Xue, W, Zhang, H, Bai, Y, Wu, L, Zhai, Z, Jin, G Fluorescence characteristics of aqueous synthesized tin oxide quantum dots for the detection of heavy metal ions in contaminated water. Nanomaterials 2019, 9, 10.3390/nano9091294.
[38] Fan, XB, Yu, S, Hou, B, Kim, JM. Quantum dots based photocatalytic hydrogen evolution. Isr J Chem, 2019, 59, 762–773.
[39] Li, B, Jiang, L, Li, X, Ran, P, Zuo, P, Wang, A, Qu, L, Zhao, Y, Cheng, Z, Lu, Y. Preparation of monolayer MoS_2 quantum dots using temporally shaped femtosecond laser ablation of bulk MoS_2 targets in water. Sci Rep, 2017, 7, 1–12.
[40] Baldovi, HG, Latorre-Sánchez, M, Esteve-Adell, I, Khan, A, Asiri, AM, Kosa, SA, Garcia, H. Generation of MoS_2 quantum dots by laser ablation of MoS_2 particles in suspension and their photocatalytic activity for H_2 generation. J Nanoparticle Res, 2016, 18, 1–8.
[41] Chen, J, Lv, S, Shen, Z, Tian, P, Chen, J, Li, Y. Novel ZnCdS quantum dots engineering for enhanced visible-light-driven hydrogen evolution. ACS Sustain Chem Eng, 2019, 7, 13805–13814.
[42] Cao, SW, Yuan, YP, Fang, J, Shahjamali, MM, Boey, FY, Barber, J, Loo, SCJ, Xue, C. *Insitu* growth of CdS quantum dots on g-C_3N_4 nanosheets for highly efficient photocatalytic hydrogen generation under visible light irradiation. Int J Hydrogen Energy, 2013, 38, 1258–1266.
[43] Reddy, NL, Kumar, S, Krishnan, V, Sathish, M, Shankar, MV. Multifunctional Cu/Ag quantum dots on TiO_2 nanotubes as highly efficient photocatalystsfor enhanced solar hydrogen evolution. J Catal, 2017, 350, 226–239.
[44] Yu, Z, Meng, J, Xiao, J, Li, Y, Li, Y. Cobalt sulfide quantum dots modified TiO2 nanoparticles for efficient photocatalytic hydrogen evolution. Int J Hydrogen Energy, 2014, 39, 15387–15393.
[45] Wang, Y, Zhou, M, He, Y, Zhou, Z, Sun, Z *In situ* loading CuO quantum dots on TiO_2 nanosheets as cocatalyst for improved photocatalytic water splitting. J Alloys Compd 2020, 813, 10.1016/j.jallcom.2019.152184.
[46] Ma, Y, Ou, P, Wang, Z, Zhu, A, Lu, L, Zhang, Y, Zeng, W, Song, J, Pan, J. Interface engineering in CeO_2 (111) facets decorated with CdSe quantum dots for photocatalytic hydrogen evolution. J Colloid Interface Sci, 2020, 579, 707–713.
[47] Du, X, Zhao, T, Xiu, Z, Xing, Z, Li, Z, Pan, K, Yang, S, Zhou, W $BiVO_4$@ $ZnIn_2S_4$/Ti_3C_2MXene quantum dots assembly all-solid-state direct Z-Scheme photocatalysts for efficient visible-light-driven overall water splitting. Appl Mater Today 2020, 20, 10.1016/j.apmt.2020.100719.
[48] Vattikuti, SP, Reddy, PAK, Shim, J, Byon, C. Visible-light-drivenphotocatalyticactivityof SnO_2–ZnO quantum dots anchored on g-C_3N_4 nanosheets for photocatalytic pollutant degradation and H_2 production. ACS Omega, 2018, 3, 7587–7602.
[49] Xiao, Y, Peng, Z, Zhang, W, Jiang, Y, Ni, L. Self-assembly of Ag_2O quantum dots on the surface of $ZnIn_2S_4$ nanosheets to fabricate pn heterojunctions with wonderful bifunctional photocatalytic performance. Appl Surface Sci, 2019, 494, 519–531.
[50] Wu, HL, Li, XB, Tung, CH, Wu, LZ Semiconductor quantum dots: An emerging candidate for CO_2 photoreduction. Adv Mater 2019, 31, 10.1002/adma.201900709.
[51] Wang, J, Wang, J, Li, N, Du, X, Ma, J, He, C, Li, Z. Direct Z-scheme 0D/2D heterojunction of $CsPbBr_3$ quantum dots/Bi_2WO_6 nanosheets for efficient photocatalytic CO_2 reduction. ACS Appl Mater Interfaces, 2020, 12, 31477–31485.
[52] Guzmán, D, Isaacs, M, Tsukuda, T, Yamazoe, S, Takahata, R, Schrebler, R, Burgos, A, Osorio-Román, I, Castillo, F CdTe quantum dots modified electrodes ITO-(Polycation/QDs) for carbon dioxide reduction to methanol. Appl Surface Sci 2020, 509, 10.1016/j.apsusc.2020.145386.

[53] Qin, H, Guo, RT, Liu, XY, Shi, X, Wang, ZY, Tang, JY, Pan, WG 0D NiS_2 quantum dots modified 2D g-C_3N_4 for efficient photocatalytic CO_2 reduction. Colloids Surf A: PhysicochemEng Aspects 2020, 600, 10.1016/j.colsurfa.2020.124912.
[54] Wang, Q, Wang, J, Wang, JC, Hu, X, Bai, Y, Zhong, X, Li, Z. Coupling $CsPbBr_3$ quantum dots with covalent triazine frameworks for visible-light-driven CO_2reduction. ChemSusChem, 2021, 14, 1131–1139.
[55] Dai, W, Xiong, W, Yu, J, Zhang, S, Li, B, Yang, L, Wang, T, Luo, X, Zou, J, Luo, S. Bi_2MoO_6 quantum dots *in situ* grown on reduced graphene oxide layers: A novel electron-rich interface for efficient CO_2 reduction. ACS Appl Mater Interfaces, 2020, 12, 25861–25874.
[56] Dai, W, Yu, J, Luo, S, Hu, X, Yang, L, Zhang, S, Li, B, Luo, X, Zou, J WS_2 quantum dots seeding in Bi_2S_3 nanotubes: A novel Vis-NIR light sensitive photocatalyst with low-resistance junction interface for CO_2 reduction. Chem Eng J 2020, 389, 10.1016/j.cej.2019.123430.
[57] Chen, T, Zhou, M, Chen, W, Zhang, Y, Ou, S, Liu, Y. $Cs_2AgInCl_6$ double perovskite quantum dots decorated with Ag nanoparticles for photocatalytic CO_2 Reduction. Sustain Energy Fuels, 2021, 5, 3598–3605. 10.1039/D1SE00754H.
[58] Wan, S, Ou, M, Zhong, Q, Wang, X. Perovskite-type $CsPbBr_3$ quantum dots/UiO-66 (NH_2) nanojunction as efficient visible-light-driven photocatalyst for CO_2 reduction. Chem Eng J, 2019, 358, 1287–1295.
[59] Li, H, Zhang, X, MacFarlane, DR Carbon quantum dots/Cu_2O heterostructures for solar-light-driven conversion of CO_2 to methanol. Adv Energy Mater 2015, 5, 10.1002/aenm.201401077.
[60] Wang, J, Xia, T, Wang, L, Zheng, X, Qi, Z, Gao, C, Zhu, J, Li, Z, Xu, H, Xiong, Y. Enabling visible-light-driven selective CO_2 reduction by doping quantum dots: Trapping electrons and suppressing H_2evolution. AngewChemie Int Ed, 2018, 57, 16447–16451.
[61] Shu, M, Zhang, Z, Dong, Z, Xu, J. $CsPbBr_3$ perovskite quantum dots anchored on multiwalled carbon nanotube for efficient CO_2 photoreduction. Carbon, 2021, 182, 454–462.
[62] Wang, Y, Yan, L, Ji, G, Wang, C, Gu, H, Luo, Q, Chen, Q, Chen, L, Yang, Y, Ma, CQ, Liu, X. Synthesis of N, S-doped carbon quantum dots for use in organic solar cells as the ZnO modifier to eliminate the light-soaking effect. ACS Appl Mater Interfaces, 2018, 11, 2243–2253.
[63] Kim, S, Kang, M, Kim, S, Heo, JH, Noh, JH, Im, SH, Seok, SI, Kim, SW. Fabrication of $CuInTe_2$ and $CuInTe_{2-x}Se_x$ ternary gradient quantum dots and their application to solar cells. ACS Nano, 2013, 7, 4756–4763.
[64] Nong, J, Lan, G, Jin, W, Luo, P, Guo, C, Tang, X, Zang, Z, Wei, W. Eco-friendly and high-performance photoelectrochemical anode based on $AgInS_2$ quantum dots embedded in 3D graphene nanowalls. J Mater Chem C, 2019, 7, 9830–9839.
[65] Lin, Y, Lin, Y, Meng, Y, Wang, Y. CdS quantum dots sensitized ZnO spheres via ZnS overlayer to improve efficiency for quantum dots sensitized solar cells. Cer Int, 2014, 40, 8157–8163.
[66] Zhang, X, Qian, Y, Ling, X, Wang, Y, Zhang, Y, Shi, J, Shi, Y, Yuan, J, Ma, W. α-$CsPbBr_3$ perovskite quantum dots for application in semitransparent photovoltaics. ACS Appl Mater Interfaces, 2020, 12, 27307–27315.
[67] Kumar, DK, Loskot, J, Kříž, J, Bennett, N, Upadhyaya, HM, Sadhu, V, Reddy, CV, Reddy, KR. Synthesis of SnSe quantum dots by successive ionic layer adsorption and reaction (SILAR) method for efficient solar cells applications. Solar Energy, 2020, 199, 570–574.
[68] Li, H, Ji, J, Zheng, X, Ma, Y, Jin, Z, Ji, H. Preparation of SnS quantum dots for solar cells application by an *insitu* solution chemical reaction process. Mater Sci Semicond Process, 2015, 36, 65–70.
[69] Shen, T, Bian, L, Li, B, Zheng, K, Pullerits, T, Tian, J A structure of CdS/CuxS quantum dots sensitized solar cells. Appl Phylett 2016, 108, 10.1063/1.4952435.

[70] Li, Y, Wang, Y, Chen, C, Pang, A, Wei, M. Incorporating Zn_2SnO_4 quantum dots and aggregates for enhanced performance in dye-sensitized ZnOsolar cells. Chemistry–A Europ J, 2012, 18, 11716–11722.
[71] Peng, W, Du, J, Pan, Z, Nakazawa, N, Sun, J, Du, Z, Shen, G, Yu, J, Hu, JS, Shen, Q, Zhong, X. Alloying strategy in Cu–In–Ga–Se quantum dots for high efficiency quantum dot sensitized solar cells. ACS Appl Mater Interfaces, 2017, 9, 5328–5336.
[72] AlGhamdi, JM, AlOmar, S, Gondal, MA, Moqbel, R, Dastageer, MA. Enhanced efficiency of dye co-sensitized solar cells based on pulsed-laser-synthesized cadmium-selenide quantum dots. Solar Energy, 2020, 209, 108–117.
[73] Yu, L, Li, Z. Synthesis of $Z_{nx}Cd_{1-x}Se$@ ZnO hollow spheres in different sizes for quantum dots sensitized solar cells application. Nanomaterials, 2019, 9(2), 132.

Anu Priya, Aditi Sharma, Manmeet Kaur, Arvind Singh,
Bubun Banerjee*

3 Ultrasound-assisted heterogeneous catalysis in aqueous medium

3.1 Introduction

To protect *Mother Nature* from ever-increasing chemical pollution, sustainable organic transformations are in high demand to produce various organic scaffolds, especially fine chemicals, agrochemicals, pharmaceutically promising agents, paints, agrochemicals, and many others [1–4]. The scientists of the twenty-first century are constantly trying to make their protocols eco-friendly by using mild reaction conditions, safer chemicals, non-toxic or less toxic solvents, reusable catalysts, and so on [5–8]. Along with many other modifications, the involvement of ultrasonic wave has a huge impact on sustainable developments. In our recent reviews, we have compiled a vast literature establishing the fact that ultrasound-assisted protocols are much more advantageous over conventional stirring methods in terms of reaction rates and product yields [9–15]. In many occasions, organic transformations were carried out in the absence of any catalyst under the influence of ultrasonic irradiation [9]. Under ultrasonic-irradiated conditions, many organic reactions were accomplished in water [12]. It was proposed that under ultrasonic irradiated conditions, a large number of cavitation bubbles grow up rapidly in the reaction mixture and subsequent collapse of these bubbles result in the formation of microjets that can produce fine emulsions between the reactants and can increase the local temperature within the reaction mixture, which eventually helps to cross the activation energy barrier [16–20].

Under these environmental conscious days, catalysts play a significant role in designing sustainable procedures [21]. During the last two decades, scientists focused much on heterogeneous catalysts as it can be recovered easily and reused several times for further reactions. Various nanosized reusable heterogeneous catalysts are also found efficient, economical, and much more effective than the traditional commercially available homogeneous catalysts due to their high absorbing ability and most

Acknowledgments: Authors are thankful to Prof. Gurmail Singh, Vice-Chancellor, Akal University for his wholehearted encouragement and support. BB is grateful to Akal University and Kalgidhar Trust, Baru Sahib, India, for the financial assistance.

***Corresponding author: Bubun Banerjee,** Department of Chemistry, Akal University, Talwandi Sabo, Bathinda, Punjab-151302, India, E-mail: banerjeebubun@gmail.com/ bubun_chm@auts.ac.in
Anu Priya, Aditi Sharma, Manmeet Kaur, Arvind Singh, Department of Chemistry, Akal University, Talwandi Sabo, Bathinda, Punjab-151302, India.

https://doi.org/10.1515/9783110733846-003

importantly large surface to volume ratio [22–26]. By applying an external magnet, magnetic nanocatalysts are usually separated/recovered easily which provides an extra advantage by reducing the cost of the protocol [27–35].

On the other hand, undoubtedly, water is regarded as the best solvent for sustainable developments because of its plentiful availability, cheapness, environmental friendliness, and non-flammability [36, 37]. On many occasions, water as a solvent activates the functional groups by making hydrogen bonds with them. Due to the hydrophobic nature organic reactants in aqueous medium generally form aggregates to reduce the exposed organic surface area, thereby increasing the reaction rate [38–40].

Thus, after realizing the individual advantages in terms of sustainability, scientists are trying to design improved protocols by employing heterogeneous catalysts under ultrasonic irradiated conditions in water. As a result, in the recent past, there were immense applications of heterogeneous catalysts under ultrasound irradiated conditions in water for the synthesis of diverse organic scaffolds. The present chapter summarizes the literature related to the latest developments on ultrasound-assisted heterogeneous catalysis in water.

3.2 Ultrasound-assisted organic transformations by using heterogeneous catalysts in water

3.2.1 Ultrasound-assisted synthesis of N-heterocycles by using heterogeneous catalyst in water

3.2.1.1 Synthesis of 2-aryl-benzimidazoles

Benzimidazole skeleton is common in many marketed drugs (Figure 3.1) [41]. 2-Aryl-substituted benzimidazoles showed significant biological efficacies including antibacterial [42], antiviral [43], antiprotozoal [44], antimalarial [45], anti-inflammatory [46], and anticancer [47] activities. Because of these significant bioactivities, a number of homogeneous as well as heterogeneous catalysts such as $Fe(HSO_4)_3$ [48], $MgCl_2.6H_2O$ [49], camphor sulfonic acid [41], nano-In_2O_3 [50], nano-$MnFe_2O_4$ [51], Zn^{2+}-K10-clay [52], $TiCl_3$.OTf [53], and NaY–zeolite [54] were used for the synthesis of 2-arylbenzimidazoles under various reaction conditions. Chakraborti et al. addressed the potential issue on selectivity of the formation of 2-substitute versus 1,2-disubstituted benzimidazoles using solid supported catalysts [55] and hydrogen-bond assisted catalytic influence of fluorinated alcohols [56]. Chakraborti et al. further addressed the selectivity issue in developing novel “all water” chemistries for tandem *N*-alkylation-reduction-condensation routes to access *N*-arylmethyl-2-

substituted benzimidazoles [57] and *N*-aryl-2-substituted benzimidazoles [56] in regiospecific manner.

In view of the importance of benzimidazoles, efforts in developing new catalytic procedures remained unabated and the use of alternative source of energy drew the attention. In this regard, the use of visible light has been found to be useful for developing a new tandem dehydrogenation-deaminative cyclocondensation route to 2-aryl benzimidazole by Chakraborti et al. [58]. In the quest for utilizing the advantages of the alternative source of energy in the preparation of this important class of heterocycles, the use of heterogeneous catalyst in aqueous medium under ultrasound irradiation gained popularity. Sapkal et al. [59] synthesized a series of 2-aryl-1*H*-benzimidazoles (**3**) from the reactions of various aromatic aldehydes (**1**) and *o*-phenylenediamines (**2**) in the presence of a catalytic amount of nano-BiOCl in water under ultrasonic irradiation at ambient temperature (Figure 3.2). In the absence of ultrasound, the same catalyst afforded lower yield. After the reaction, the heterogeneous nanocatalyst was recovered and reused further for seven successive runs with almost equal efficiency. Under these developed conditions, aldehydes having electron donating or withdrawing

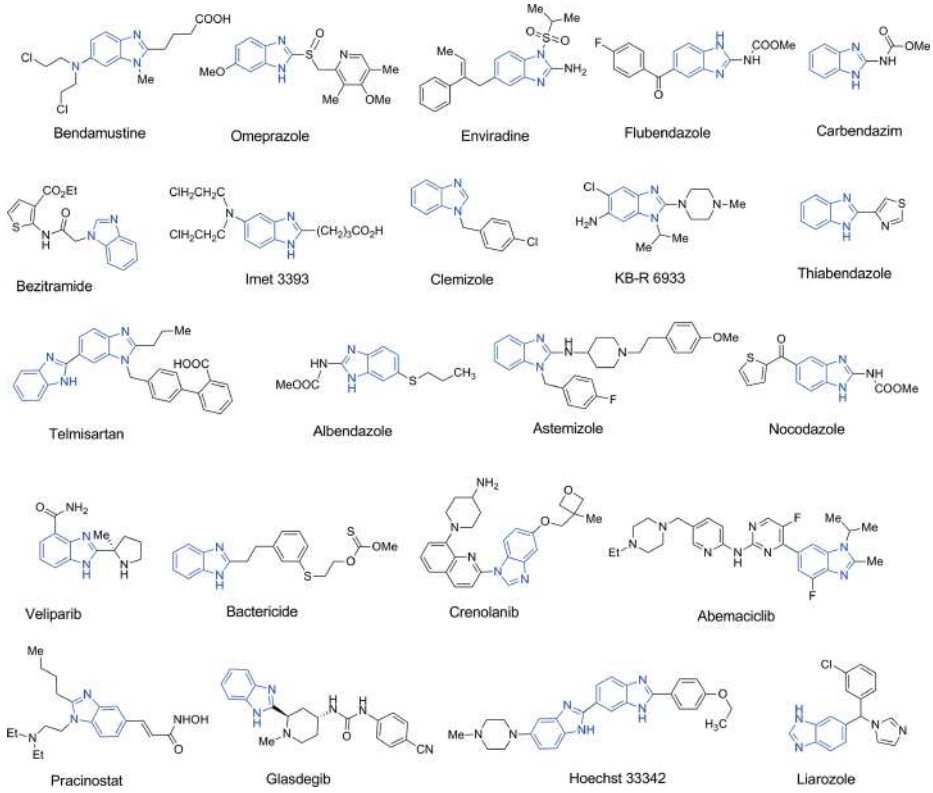

Figure 3.1: Commercially available drug molecules containing benzimidazole skeleton.

substituents afforded the desired products with excellent yields. However, heteroaryl aldehydes produced the products in moderate yields. Mild reaction conditions, short reaction times, use of water as solvent, and environmental friendliness are some of the notable advantages of this protocol.

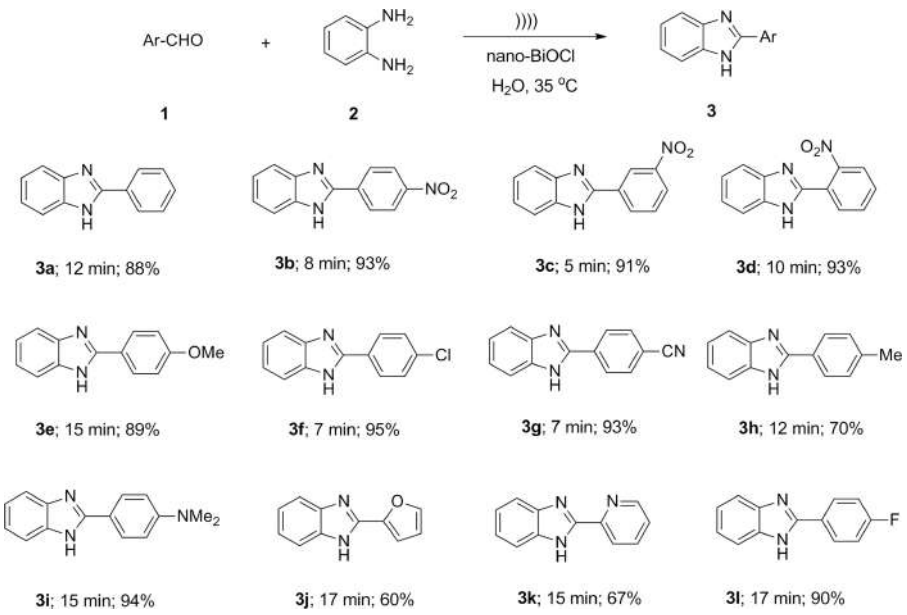

Figure 3.2: Ultrasound-assisted synthesis of 2-aryl-1*H*-benzimidazoles using nano-BiOCl as an efficient heterogeneous catalyst.

3.2.1.2 Synthesis of quinoxaline and related scaffolds

Many commercially available drug molecules such as the quinox, sulfaquinoxaline, chloroquinoxaline sulfonamide, quinacilin, and olaquindox possess quinoxaline as the main structural unit (Figure 3.3) [60]. Moreover, quinoxaline skeleton is also very common in naturally occurring bioactive compounds such as echinomycin and triostin A [61]. Recently, fused heterocycles particularly dibenzo[*a*,*c*]phenazines and acenaphtho[1,2-*b*]quinoxalines have gained considerable attention. Synthesis of dibenzo[*a*,*c*]phenazines was carried out from the reactions of *o*-phenylenediamines (**2**) and phenanthrene-9,10-dione (**4**) under various reaction conditions using a number of metal containing homogeneous or heterogeneous catalysts such as $MgSO_4.7H_2O$ [62], $PbCl_2$ [63], silica-bonded *S*-sulfonic acid [64], tungstate sulfuric acid [65], molybdate sulfuric acid [66], and nano-TiO_2 [67]. All these reported protocols suffer from a common demerit, that is, longer reaction time. The application of surfactant micelles as microreactors has been demonstrated by Chakraborti et al. during the

synthesis of quinoxalines in aqueous medium in the presence several neutral, cationic, and anionic surfactants [68]. Further, they adopted the "all water" chemistry of "tandem-alkylation-reduction-cyclocondensation" to develop a regiocontrolled synthesis of 2-aryl quinoxalines [69]. The potential of quinoxalines for various therapeutic applications led synthetic organic/medicinal chemists to continue to delve into the development of newer protocols for quinoxaline synthesis integrating the advantages of aqueous medium, heterogeneous catalysis and ultrasound energy.

Toward this objectives, Dandia et al. [70] synthesized dibenzo[*a*,*c*]phenazine (**6**) in 95% yield within 20 min under ultrasound-assisted conditions using nano-$CuFe_2O_4$ as a magnetically separable heterogeneous catalyst in aqueous medium at ambient temperature (Figure 3.4). Other catalysts such as *L*-proline, sulfamic acid and *p*-toluenesulfonic acid afforded lower yields of **6** even after 1 h of sonication. Organic solvents such as ethanol, methanol, toluene, and acetonitrile generated moderate yields (74–82%) of **6**. Synthesis of dibenzo[*f*,*h*]pyrido[2,3-*b*]quinoxaline (**7**) was accomplished in excellent yield from the reactions of pyridine-2,3-diamine (**5**) and phenanthrene-9,10-dione (**4**). They were also able to synthesize a series of structurally diverse quinoxaline analogs (**10**,**11**,**12**) under the same optimized reactions conditions from the reactions of benzil (**8**) and various 1,2-diamine derivatives (**2**,**5**,**9**) (Figure 3.5). A 10 mol% nano-$CuFe_2O_4$ was able to catalyze the reaction of acenaphthylene-1,2-dione (**13**) and *o*-phenylenediamines (**2**) which afforded the corresponding acenaphtho[1,2-*b*]quinoxaline in excellent yield (Figure 3.6).

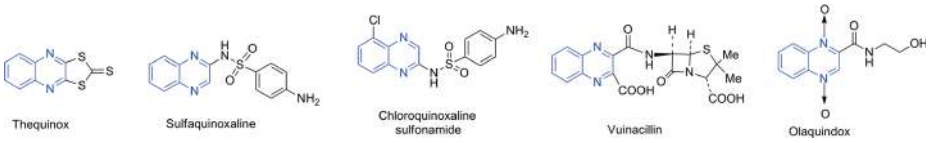

Figure 3.3: Commercially available drug molecules containing quinoxaline skeleton.

3.2.1.3 Synthesis of spiropolyhydroquinoline derivatives

Dandia et al. [71] developed another ultrasound-assisted facile protocol for the synthesis of biologically promising spiropolyhydroquinoline derivatives (**21**) via one-pot four component reactions of various cyclic ketones (**15**,**16**,**17**), dimedone (**18**), meldrum's acid (**19**), and aryl or aliphatic amines (**20**) in the presence of a catalytic amount of nano-ZnS in water (Figure 3.7). Plausible mechanism of this transformation is depicted in Figure 3.8. When the other conditions remained same, solvents like acetonitrile, toluene, methanol, and ethanol were found to be less effective for this transformation compared to water. During optimizations, it was found that under ultrasonic irradiated conditions, the other catalysts such as ceric ammonium nitrate, *p*-TSA, sulfamic acid, and *L*-proline afforded lower yield of the product

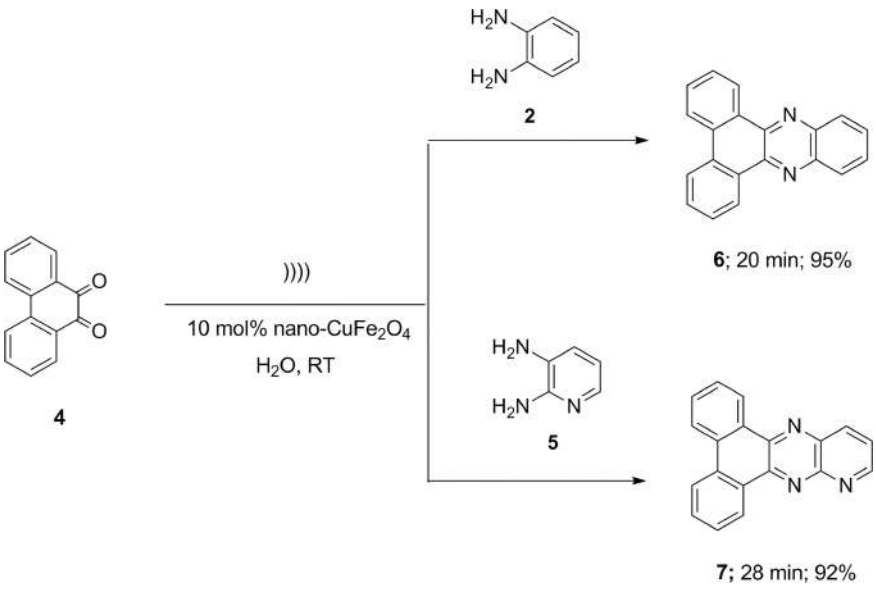

Figure 3.4: Ultrasound-assisted nano-$CuFe_2O_4$ catalyzed synthesis of quinoxalines in water.

(**21e**) in water. Under refluxed condition, the same catalyst produced only 64% yield of the product **21e** even after 4 h of sonication. In the absence of any catalyst, moderate yield was obtained by using only ultrasound. After completion of the reaction, the products were extracted with ethyl acetate and the catalyst containing aqueous part was recycled for three successive runs.

3.2.1.4 Synthesis of triazolo[1,2-a] indazoletriones

Because of its wide biological applicability, triazolo[1,2-*a*]indazoletriones were synthesized by using a number of homogeneous as well as heterogeneous catalysts such as sulfamic acid [72], sulfonated polyethylene glycol [73], *p*-toluene sulfonic acid [74], camphor-10-sulfonic acid [75], glycerol [76], $ZrOCl_2.8H_2O$ [77], silica nanoparticles using rice husk [78], melamine trisulfonic acid [79], quinuclidine-stabilized $FeNi_3$ nanoparticles [80], and tungstosilicic acid [81] as catalysts. These reported methods definitely have some merits but majority of them were carried out for prolonged heating under solvent-free conditions. Therefore, tedious work-up procedure was required to isolate the synthesized products. Non-reusability of the catalyst, longer reaction times, and the use of sulfonated catalysts are the common drawbacks of some of these reported methods. In 2017, Verma et al. [82] developed a simple ultrasound-assisted water-mediated environmentally benign protocol for the synthesis of triazolo[1,2-*a*]indazoletriones (**23**) from one-pot three-component reactions of substituted benzaldehydes (**1**),

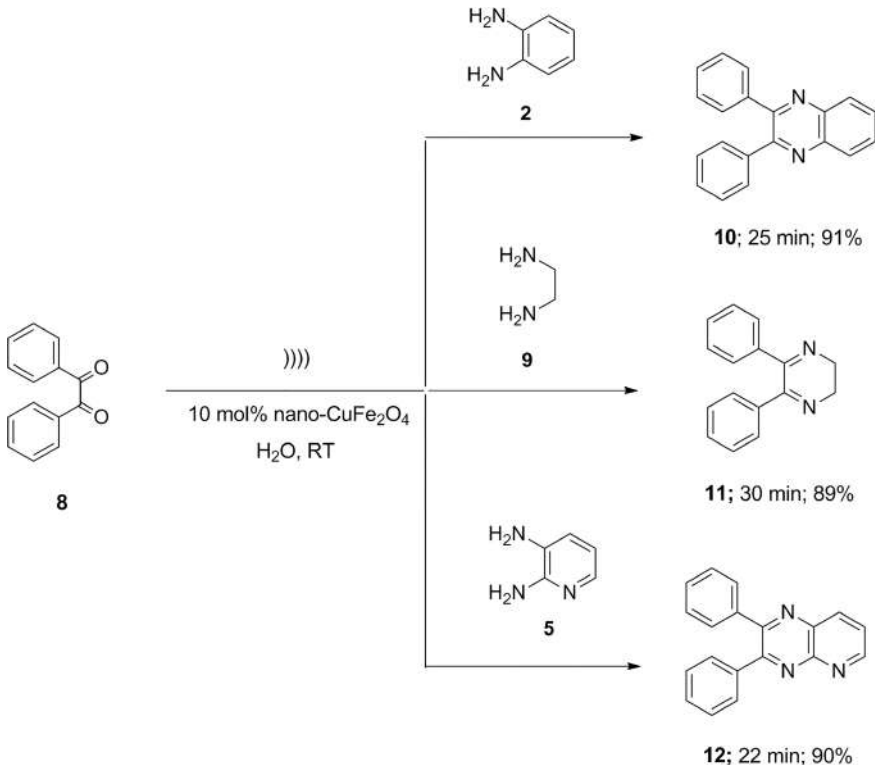

Figure 3.5: Ultrasound-assisted nano-$CuFe_2O_4$ catalyzed synthesis of quinoxaline analogs in water.

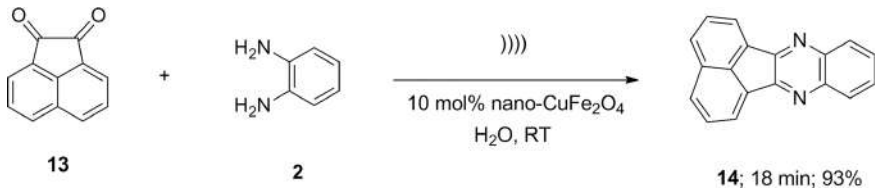

Figure 3.6: Ultrasound-assisted nano-$CuFe_2O_4$ catalyzed synthesis of acenaphtho[1,2-*b*] quinoxaline in water.

dimedone (**18**), 4-phenylurazole (**22**) using SiO_2-coated ZnO nanoparticles (ZnO@SiO_2 NPs) as an efficient heterogeneous nanocatalyst at 60 °C (Figure 3.9). After first run, the nanocatalyst was recovered and recycled for further six successive runs without any significant loss in its catalytic activity. All the products were isolated in good to excellent yields by just simple filtration. Reusability of the catalyst, simple work-up procedure, short reaction times, and aqueous medium are some of the notable advantages of this protocol.

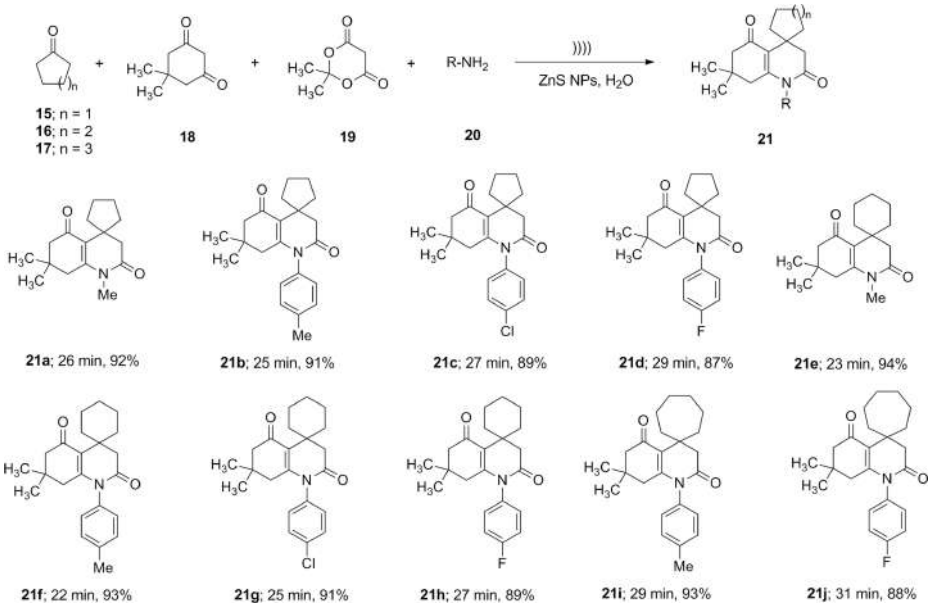

Figure 3.7: Ultrasound-assisted nano-ZnS catalyzed synthesis of spiropolyhydroquinolines.

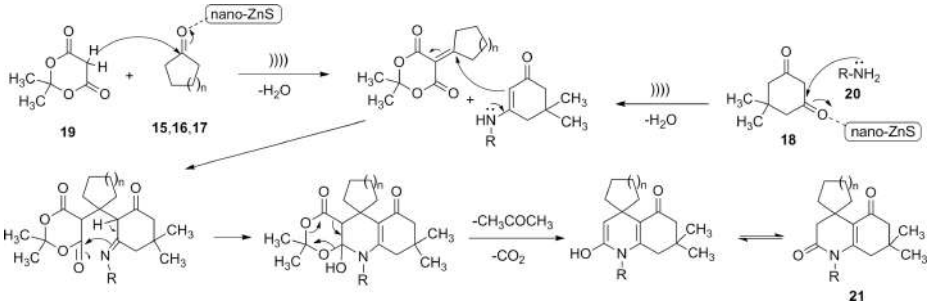

Figure 3.8: Plausible mechanism for the synthesis of spiropolyhydroquinolines.

3.2.1.5 Synthesis of pyrido[2,3-d:6,5-d]dipyrimidines

Naeimi and Didar [83] prepared $CuFe_2O_4$ via coprecipitation of $Cu(NO_3)_2$ and $FeCl_3$ in basic solution, 95 °C. The nanoparticles synthesized were characterized by using field-emission scanning electron microscope and X-ray diffraction studies. By using this synthesized nanomaterial as an efficient reusable heterogeneous catalyst, they were able to prepare a series of pyrido[2,3-*d*:6,5-*d*]dipyrimidines (**26**) in excellent yields by using one-pot reaction protocol between substituted benzaldehydes (**1**), 2-thiobarbituric acid (**24**) and ammonium acetate (**25**) in water at ambient temperature

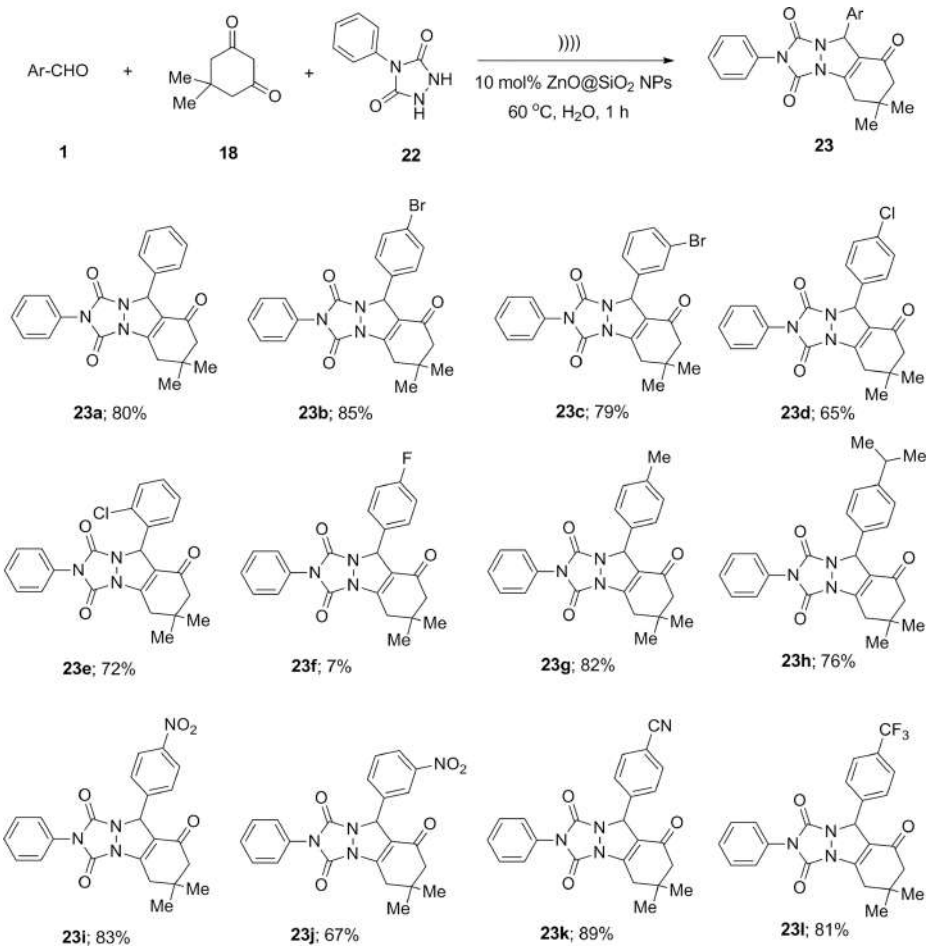

Figure 3.9: Ultrasound-assisted synthesis of triazolo[1,2-*a*] indazoletriones using a catalytic amount of silica supported nano-ZnO as catalyst in water.

under ultrasound-assisted conditions (Figure 3.10). All the reactions were completed within a few minutes. It was reported that, under conventional stirring conditions, the formation of the compound **26a** required longer time. The nanocatalyst was recovered easily by applying an external magnet and recycled four times without any significant loss in the product formation. Under the same optimized conditions, synthesis of 5,5′-(1,4-phenylene)*bis*(2,8-dithioxo-2,3,7,8,9,10-hexahydropyrido[2,3-*d*:6,5-*d*']dipyrimidine-4,6 (1*H*,5*H*)-dione) (**26g**) was also accomplished by using terephthaldehyde instead of monoaldehydes whereas 2-hydroxybenzaldehyde and 4-(*N*, *N*-dimethylamino)benzaldehyde were unable to form the desired products (**26h**,**26i**). Uses of water as solvent, easily separable and reusable nanocatalyst, and short reaction times are some of the major advantages of this protocol.

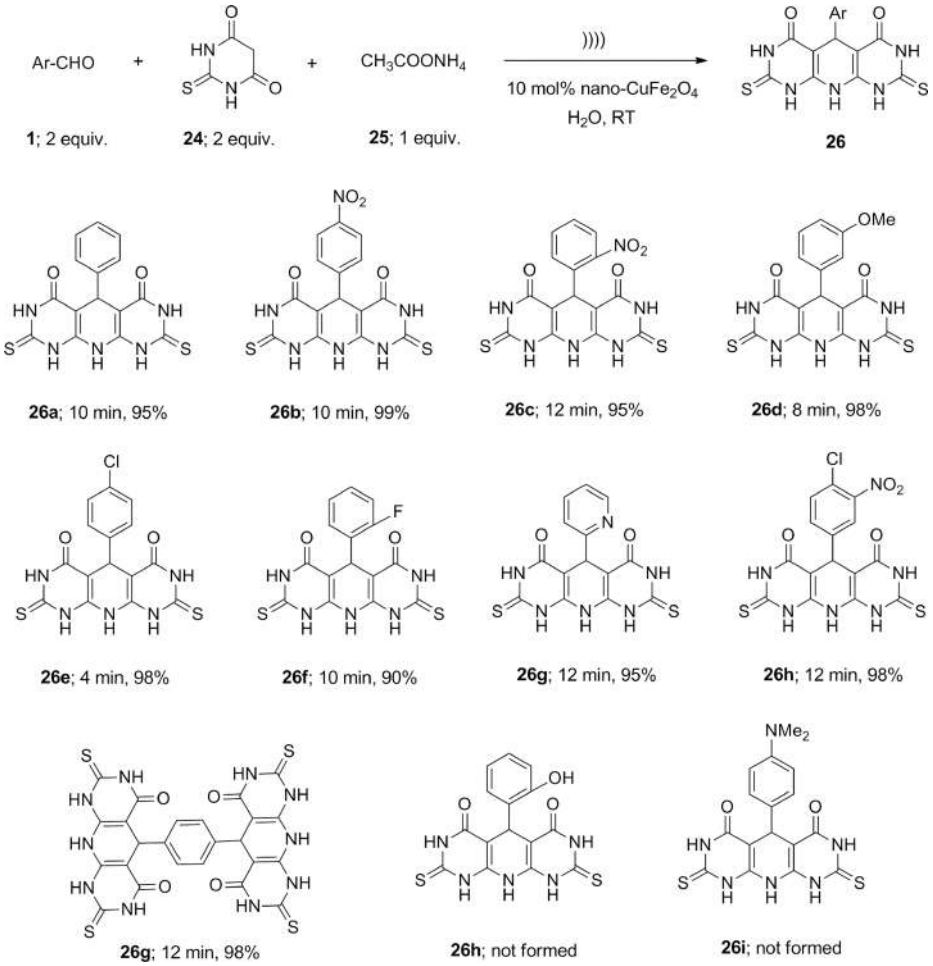

Figure 3.10: Ultrasound-assisted synthesis of pyrido[2,3-*d*:6,5-*d*']dipyrimidine derivatives using nano-$CuFe_2O_4$ as catalyst in water.

3.2.2 Ultrasound-assisted synthesis of O-heterocycles by using heterogeneous catalyst in water

3.2.2.1 Synthesis of 2-amino-3-cyano-pyran and pyran-annulated heterocycles

Pyran and related compounds generally possess a wide range of biological activities [84–86]. Recently, various synthetic 2-amino-3-cyano-pyran-annulated heterocyclic scaffolds have also been evaluated to for various biological activities such as anti-cancer, antibacterial, and antirheumatic, antifungal (Figure 3.11) [87–94].

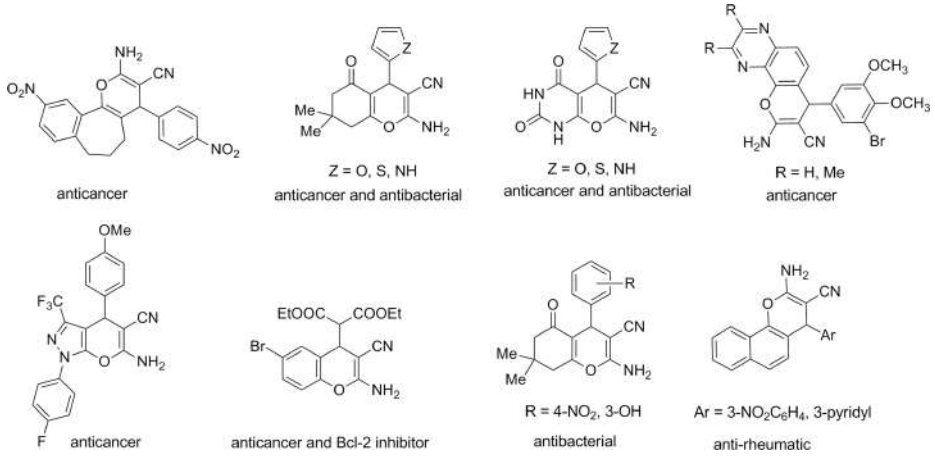

Figure 3.11: Synthetic 2-amino-3-cyano-pyran-annulated heterocyclic scaffolds with potent biological activities.

Esmaeilpour et al. [95] prepared magnetically separable iron oxide functionalized silica immobilized per molybdic acid nanoparticles (Fe_3O_4@SiO_2-imid-$H_3PMo_{12}O_{40}$ nanoparticles). They characterized the synthesized materials by using various techniques such as scanning electron microscopy (SEM), transmission electron microscopy (TEM), Fourier transform infrared (FT-IR), dynamic light scattering, and vibrating sample magnetometer. Using these well-characterized magnetically separable nanomaterials as catalyst, a series of 2-amino-3-cyano-tetrahydro-4*H*-benzo[*b*] pyrans (**28**) were synthesized by one-pot three-component reactions of substituted benzaldehydes (**1**), malononitrile (**27**), and dimedone (**18**) under ultrasonic irradiation in water at room temperature (Figure 3.12). Aldehydes having either electron donating or withdrawing substituent afforded the desired products in excellent yields. All the reactions were also carried out under conventional heating (refluxed) conditions in water. It was observed that under conventional heating, the reactions required longer times and afforded lower yields. After completion of the reaction, the catalyst was recovered easily and reused for further eight successive runs without any notable loss in product yield. Under the same optimized reactions conditions, 2-amino-3-cyano-3,4-dihydropyrano[*c*]chromenes (**30**) were also synthesized in excellent yields from the reactions of various aromatic aldehydes (**1**), malononitrile (**27**), and 4-hydroxycoumarin (**29**) (Figure 3.13). Uses of magnetically separable/reusable catalyst, aqueous medium, short reaction times, excellent yields, and easy work-up procedure are some of the major advantages of this developed protocol. Under ultrasound-assisted conditions, Saha et al. [96] also synthesized another series of 2-amino-3-cyano-tetrahydro-4*H*-benzo[*b*]pyran (**28**) as well as 2-amino-3-cyano -3,4-dihydropyrano[*c*]chromenes (**30**) by using nickel nanoparticles as an efficient reusable heterogeneous catalyst in water at room temperature (Figure 3.14). By

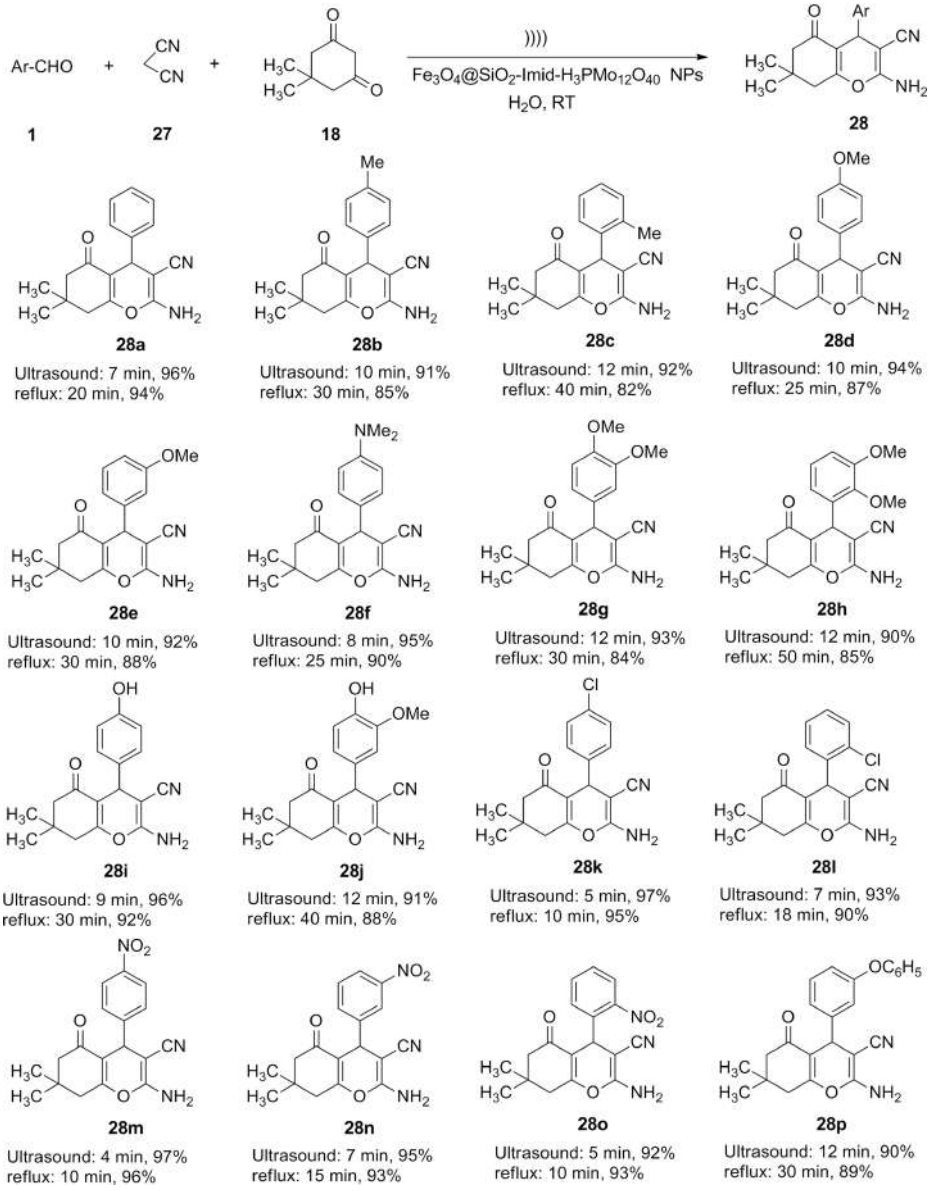

Figure 3.12: Ultrasound-assisted Fe_3O_4@SiO_2-imid-$H_3PMo_{12}O_{40}$ nanoparticles catalyzed synthesis of 2-amino-3-cyano-tetrahydro-4*H*-benzo[*b*]pyran in water.

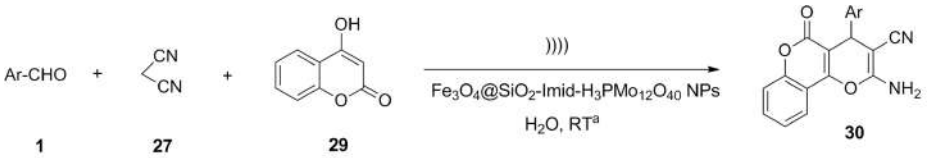

1 27 29 30

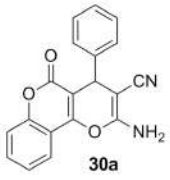

30a

Ultrasound: 6 min, 97%
reflux: 15 min, 95%

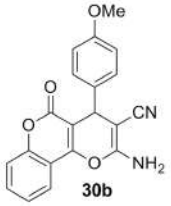

30b

Ultrasound: 8 min, 93%
reflux: 25 min, 88%

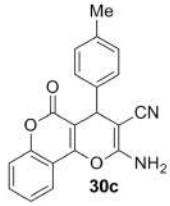

30c

Ultrasound: 8 min, 95%
reflux: 25 min, 90%

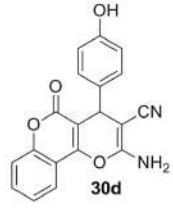

30d

Ultrasound: 10 min, 96%
reflux: 25 min, 93%

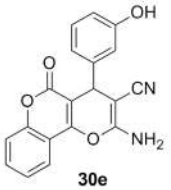

30e

Ultrasound: 7 min, 95%
reflux: 30 min, 95%

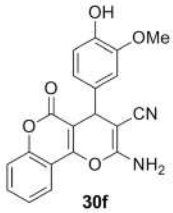

30f

Ultrasound: 12 min, 92%
reflux: 30 min, 86%

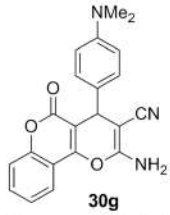

30g

Ultrasound: 10 min, 94%
reflux: 20 min, 91%

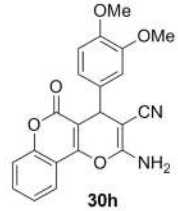

30h

Ultrasound: 10 min, 90%
reflux: 30 min, 86%

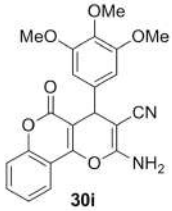

30i

Ultrasound: 12 min, 88%
reflux: 40 min, 89%

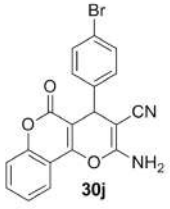

30j

Ultrasound: 6 min, 96%
reflux: 15 min, 92%

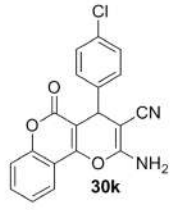

30k

Ultrasound: 5 min, 96%
reflux: 12 min, 95%

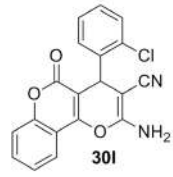

30l

Ultrasound: 8 min, 90%
reflux: 15 min, 88%

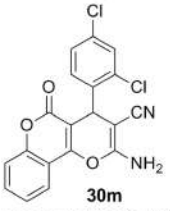

30m

Ultrasound: 5 min, 97%
reflux: 8 min, 93%

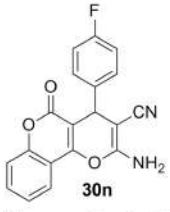

30n

Ultrasound: 6 min, 91%
reflux: 10 min, 93%

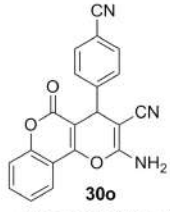

30o

Ultrasound: 6 min, 95%
reflux: 12 min, 96%

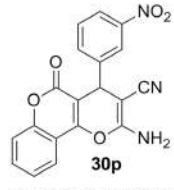

30p

Ultrasound: 6 min, 93%
reflux: 10 min, 91%

Figure 3.13: Ultrasound-assisted Fe_3O_4@SiO_2-imid-$H_3PMo_{12}O_{40}$ catalyzed synthesis of 2-amino-3-cyano-3,4-dihydropyrano[*c*]chromenes in water.

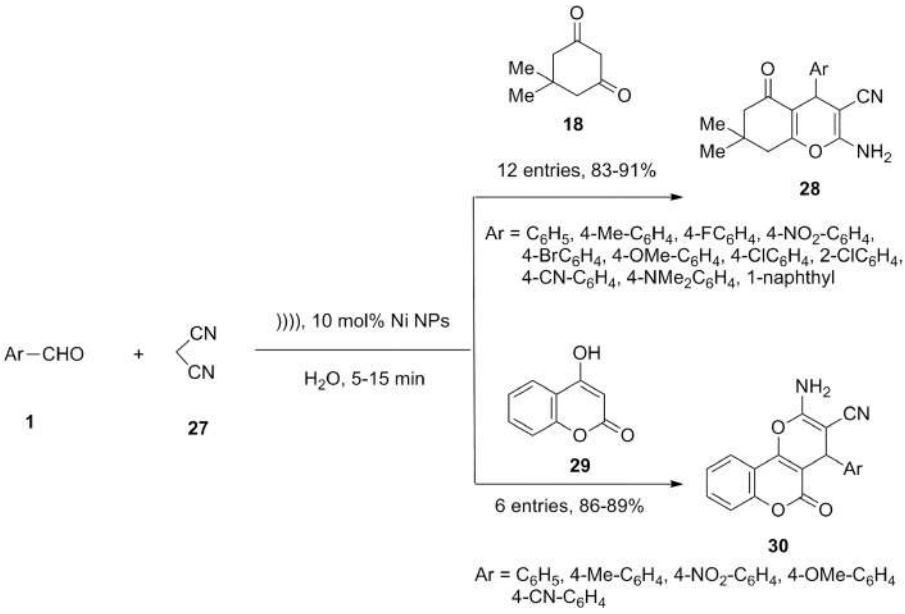

Figure 3.14: Ultrasound-assisted synthesis of 2-amino-3-cyano-pyran annulated heterocycles using nickel nanoparticles as catalyst in water.

following a reported microemulsion method, they prepared nickel nanoparticles by the reduction of $NiCl_2.6H_2O$ with hydrazine hydride [97]. After reaction, the nickel nanoparticles were recovered quantitatively and reused further for four successive runs. In 2015, Safari and Javadian [98] successfully immobilized chitosan on Fe_3O_4 nanoparticles. They employed this heterogeneous magnetically separable catalyst for the synthesis of 2-amino-3-cyano-4*H*-chromenes (**32**) via three-component reactions of various aldehydes (**1**), malononitrile (**27**), and resorcinol (**31**) under ultrasound-assisted conditions in water at 50 °C (Figure 3.15). All the reactions were completed within 25 min. Along with various substituted benzaldehydes, a number of aliphatic aldehydes also underwent reaction smoothly and afforded the desired products with

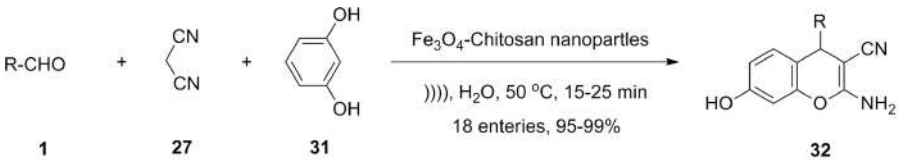

R = C_6H_5, 4-Me-C_6H_4, 4-OMe-C_6H_4, 3-ClC_6H_4, 3-OHC_6H_4, 2-FC_6H_4, 2-OMe-C_6H_4, 2,4-diCl-C_6H_3, 2,6-diCl-C_6H_3, 3,5-diOMe-C_6H_3, 2-naphthyl, 2-furyl, 2-thienyl, 5-Me-2-furyl, Et, Pr, hepthyl, 4-CHOC_6H_4

Figure 3.15: Ultrasound-assisted synthesis of 2-amino-3-cyano-4*H*-chromenes using chitosan immobilized Fe_3O_4 nanoparticles as catalyst in water.

good yields. The magnetic catalyst was recovered easily by using a bar magnet and recycled for four successive runs without any significant loss in its catalytic efficiency. In the absence of ultrasound, the same reaction required longer times.

3.2.2.2 Synthesis of 1,8-dioxo-octahydroxanthenes

Recent studies revealed the promising anticancer activity of some synthetic 1,8-dioxo-octahydroxanthenes (Figure 3.16) [99]. Several methods were reported for efficient synthesis of 1,8-dioxo-octahydroxanthene derivatives (**33**) using various homogeneous as well as heterogeneous catalysts such as $FeCl_3.6H_2O$ [100], NH_4Cl [101], $InCl_3.4H_2O$ [102], $BiCl_3$ [103], and amberlyst-15 [104]. Longer reaction times and high heating are some of the common demerits of these reported protocols. In 2010, Rostamizadeh et al. [105] developed a simple, efficient, and ultrasound-assisted protocol for the rapid synthesis of 1,8-dioxo-octahydroxanthenes (**33**) via pseudo three-component reactions between one equivalent of aromatic aldehydes (**1**) and two equivalents of dimedone (**18**) using nanosized MCM-41-SO_3H as an efficient mesoporous heterogeneous catalyst in water at 60 °C (Figure 3.17). The same amount of catalyst afforded lower yields under conventional heating conditions at 90 °C. Stirring at 60 °C, the same failed to synthesize the desired products. Some other homogeneous catalysts such as $ZrOCl_2$, $ZrOCl_2$/K10, $NaHSO_4$, and $NaHSO_4$/SiO_2 were also afforded very poor yields of the desired products.

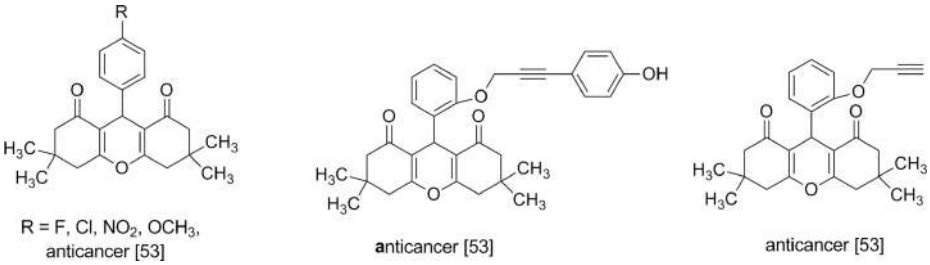

Figure 3.16: A few 1,8-dioxo-octahydroxanthenes having anticancer activity.

3.2.2.3 Synthesis of aryl-14H-dibenzo[a,j]xanthenes

Mahdavinia et al. [106] synthesized a series of aryl-14*H*-dibenzo[*a*,*j*]xanthenes (**35**) via one-pot pseudo three-component reactions between one equivalent of aldehydes (**1**) and two equivalents of β-naphthol (**34**) in the presence of a catalytic amount of silica supported ammonium dihydrogen phosphate ($NH_4H_2PO_4/SiO_2$) as a heterogeneous reusable catalyst under ultrasound-assisted conditions in aqueous

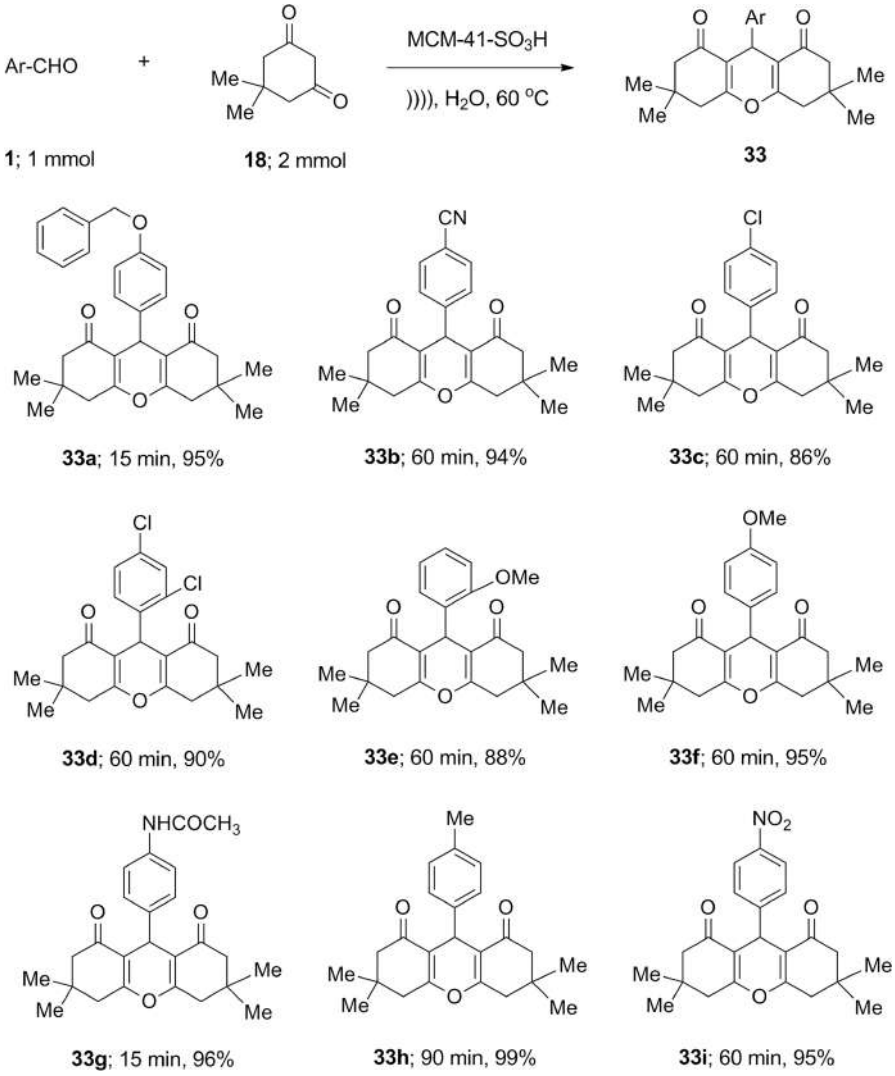

Figure 3.17: Ultrasound-assisted MCM-41-SO_3H catalyzed synthesis of 1,8-dioxo-octahydroxanthenes in water.

medium at 40 °C (Figure 3.18). The heterogeneous catalyst was recovered and reused for five successive runs with almost equal efficiency. Without catalyst, the reaction did not occur. Under conventional stirring conditions, 100 mg of this catalyst afforded only 20% yield of the 14-(4-bromophenyl)-14*H*-dibenzo[*a*,*j*]xanthenes after 2h.

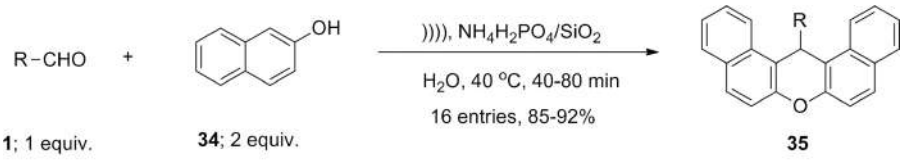

R = C_6H_5, 4-Br-C_6H_4, 3-Br-C_6H_4, 4-OMe-C_6H_4, 2-OMe-C_6H_4, 4-Me-C_6H_4, 4-Cl-C_6H_4, 2-Cl-C_6H_4, 3-Cl-C_6H_4, 2,4-diCl-C_6H_3, 4-NO_2-C_6H_4, 3-NO_2-C_6H_4, 2-NO_2-C_6H_4, 4-F-C_6H_4, 4-OH-C_6H_4, $C_6H_5CH_2$

Figure 3.18: Ultrasound-assisted $NH_4H_2PO_4/SiO_2$ catalyzed synthesis of aryl-14*H*-dibenzo[*a*,*j*] xanthenes in water.

3.2.3 Ultrasound-assisted synthesis of N,O-heterocycles by using heterogeneous catalyst in water

3.2.3.1 Synthesis of pyranopyrazoles

In 2015, Dam et al. [107] prepared dopamine functionalized magnetic nanoparticles supported *L*-proline catalyst (nano-FDP). The synthesized nanomaterials were characterized by using FT-IR, EDX, TEM, and SEM analysis. Using catalytic amount of this synthesized nanomaterial, a series of pyrano-pyrazole derivatives (**38a-h**) were also synthesized via one-pot four component reactions of ethyl acetoacetate (**36**), phenyl hydrazine (**37**), aromatic aldehydes (**1**), and malononitrile (**27**) in water at room temperature (Figure 3.19). Under ultrasound-assisted conditions, a catalytic amount of nickel nanoparticles (10 mol%) was also capable of promoting the formation of another series of pyrano-pyrazole derivatives (**38**) in excellent yields via one-pot three-component reactions between substituted benzaldehydes (**1**), malononitrile (**27**), and 3-methyl-1-phenyl-1*H*-pyrazol-5(4*H*)-one (**39**) in aqueous medium (Figure 3.20) [90].

3.2.3.2 Synthesis of spiro[indoline-3,4′-pyrano[2,3-c]pyrazoles]

Under ultrasound-assisted conditions, Dandia et al. [108] synthesized a series of structurally diverse spiro[indoline-3,4′-pyrano[2,3-c]pyrazoles] (**41a-l**) via one-pot three-component reactions of isatins (**40**), malononitrile (**27**) or ethyl-2-cynoacetate (**27a**), and 3-methyl-1-phenyl-2-pyrazolin-5-one (**39**) using a catalytic amount of zinc sulfide nanoparticles in water at room temperature (Figure 3.21). All the reactions were completed within 15 min and afforded the desired products in excellent yields. The catalyst containing aqueous medium was reused for three further runs without any significant loss in product yields.

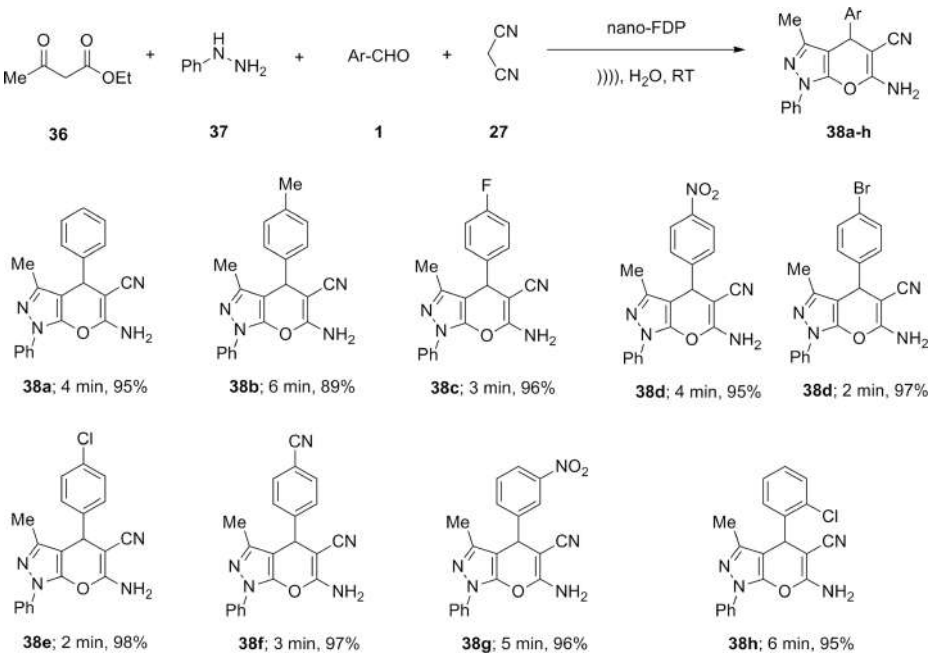

Figure 3.19: Ultrasound-assisted four component synthesis of pyrano-pyrazoles using dopamine functionalized magnetic nanoparticles supported *L*-proline as catalyst in water.

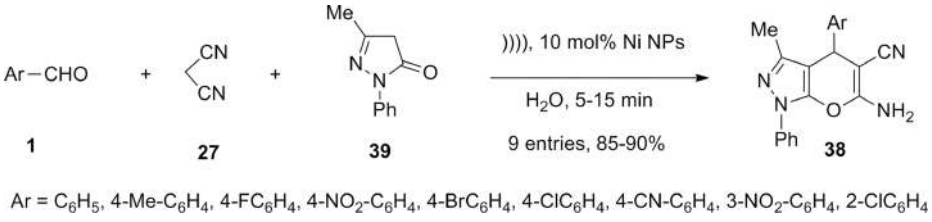

Figure 3.20: Ultrasound-assisted three-component synthesis of pyrano-pyrazoles using nickel nanoparticles as catalyst in water.

3.2.3.3 Synthesis of spiro[chromene-4,3′-indolines]

Under ultrasound-assisted conditions, a series of spiro[chromene-4,3′-indolines] (**42a-l**) was also synthesized by using zinc sulfide nanoparticles as catalyst from the reactions of isatins (**40**), malononitrile (**27**) or ethyl-2-cynoacetate (**27a**), and dimedone (**18**) in water at ambient temperature (Figure 3.22) [108]. Under ultrasound-irradiated conditions, a catalytic amount (10 mol%) of nickel nanoparticles in water was also able to promote the synthesis of the compound **42a** in 89% yield within 10 min [96].

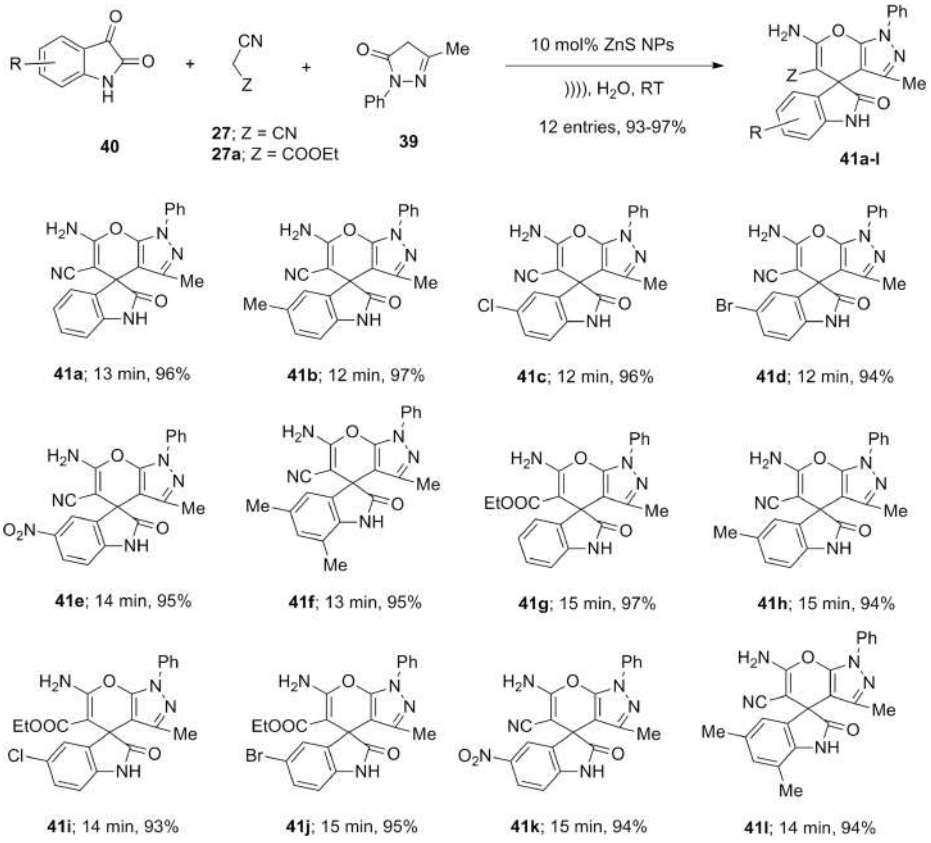

Figure 3.21: Ultrasound-assisted three-component synthesis of spiro[indoline-3,4′-pyrano[2,3-*c*] pyrazoles] using ZnS nanoparticles as catalyst in water.

3.2.3.4 Synthesis of spiro[indoline-3,4′-pyrano[3,2-c]chromene]

Under ultrasound-assisted conditions, synthesis of 2′-amino-2,5′-dioxo-5′*H*-spiro[indoline-3,4′-pyrano[3,2-*c*]chromene]-3′-carbonitrile (**43**) was achieved via one-pot three-component reactions of isatin (**40**), malononitrile (**27**), and 4-hydroxycoumarin (**29**) in the presence of a catalytic amount of nickel nanoparticles in water (Figure 3.23) [96]. Under this condition, the compound **43** was obtained in 88% within 10 min.

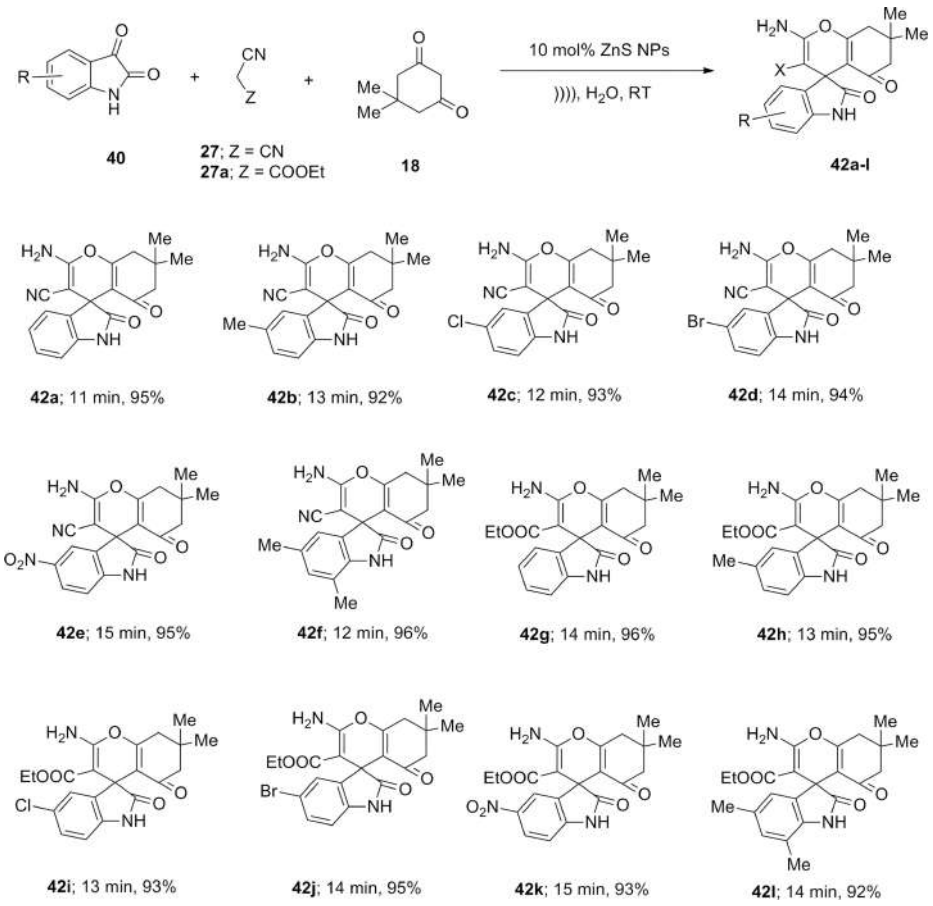

Figure 3.22: Ultrasound-assisted three-component synthesis of spiro[chromene-4,3′-indolines] using ZnS nanoparticles as catalyst in water.

3.2.4 Ultrasound assisted synthesis of N,S-heterocycles by using heterogeneous catalyst in water

3.2.4.1 Synthesis of spiro[indole-pyrido[3,2-e]thiazine]

Arya et al. [109] successfully immobilized Brønsted acidic ionic liquids in the mesoporous channels of a porous ZSM-5 zeolite. By employing this synthesized materials as catalyst, they prepared a series of structurally diverse spiro[indole-pyrido[3,2-*e*] thiazine] derivatives (**45**) from the reactions of isatins (**40**), substituted anilines (**20**), and 2-mercaptonicotinic acid (**44**) under ultrasound-assisted conditions in water at 95 °C (Figure 3.24). Using the same amount of catalyst, they also carried

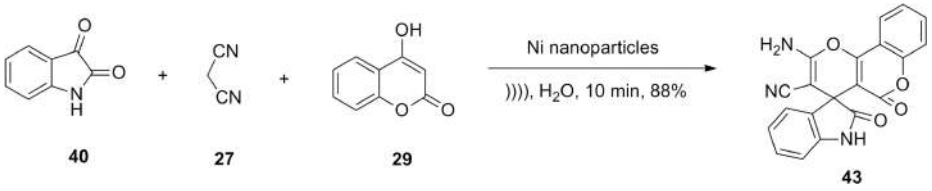

Figure 3.23: Ultrasound-assisted three-component synthesis of spiro[indoline-3,4′-pyrano[3,2-c] chromene] using nickel nanoparticles as catalyst in water.

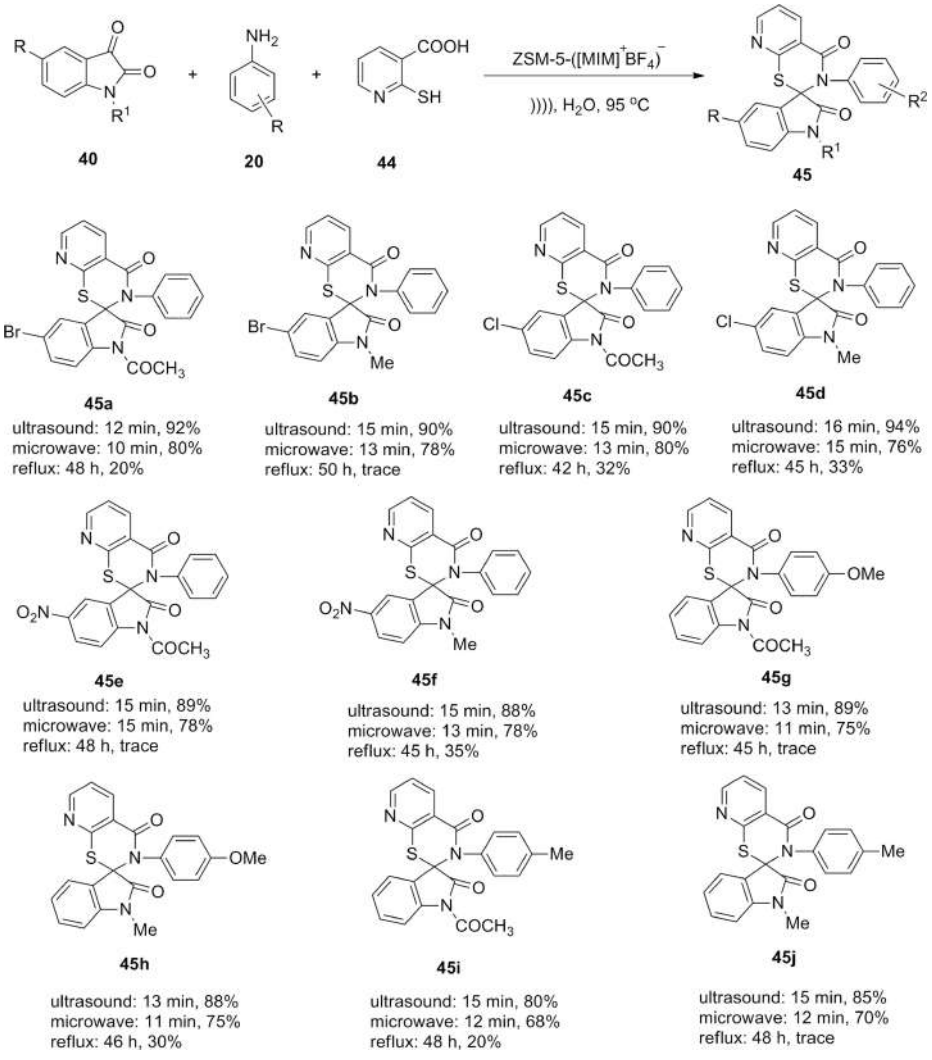

Figure 3.24: Ultrasound-assisted three-component synthesis of spiro[indole-pyrido[3,2-e]thiazine] using zeolite supported Brønsted-acid ionic liquid as catalyst in water.

out the reaction under microwave-irradiated and under refluxed conditions. Interestingly, little bit of lower yields was obtained under microwave-assisted conditions. Very poor yields were recorded under conventional refluxed conditions. The catalyst was recycled five times with almost equal efficiency.

3.2.5 Ultrasound assisted Knoevenagel condensation by using heterogeneous catalyst in water

Amine functionalized silica-coated Fe_3O_4 nanoparticles (SiO_2@ Fe_3O_4@NH_2) were synthesized by Ying et al. [110] (Figure 3.25). After characterization of the prepared materials, they employed the same as an efficient, heterogeneous, magnetically separable nanocatalyst for the reactions of substituted benzaldehydes (**1**) and 2-(benzo[*d*]thiazol-2-yl)acetonitrile (**46**) in water under ultrasound-assisted conditions at ambient temperature. The reactions afforded the corresponding Knoevenagel condensed products (**47**) in good to excellent yields (Figure 3.26). In absence of the catalyst, the reaction could not produce the desired product even under ultrasonic irradiated conditions. By using conventional stirring method, the same reactions required longer times and afforded lower yields at 60 °C. The nanocatalyst was recovered easily and reused for eight successive runs with almost equal efficiency.

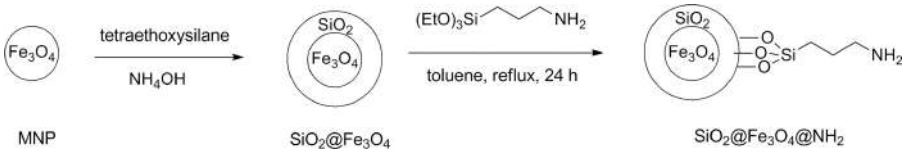

Figure 3.25: Functionalization of amine on silica coated Fe_3O_4 nanoparticles.

3.2.6 Ultrasound-assisted Heck reaction by using heterogeneous catalyst in water

Ultrasound-assisted Heck reaction between phenyl iodides (**48**) and methyl acrylate (**49**) was carried out in the presence of a catalytic amount of in-situ generated Pd(0) nanoparticles in water at 25 °C (Figure 3.27) [111]. Addition of tetrabutylammonium bromide (TBAB) as a phase transfer catalyst in basic medium improved the yield of the desired products (**50**). It was assumed that methyl acrylate (**49**) may have acted as a reducing agent to form the in-situ generated Pd(0) nanoparticles from palladium chloride. On the other hand, it was proposed that the acoustic cavitation formed by sonication may also accelerate the formation of Pd(0) nanoparticles in-situ. The phenyl iodides having electron-donating substituent at *para* position showed excellent regioselectivity.

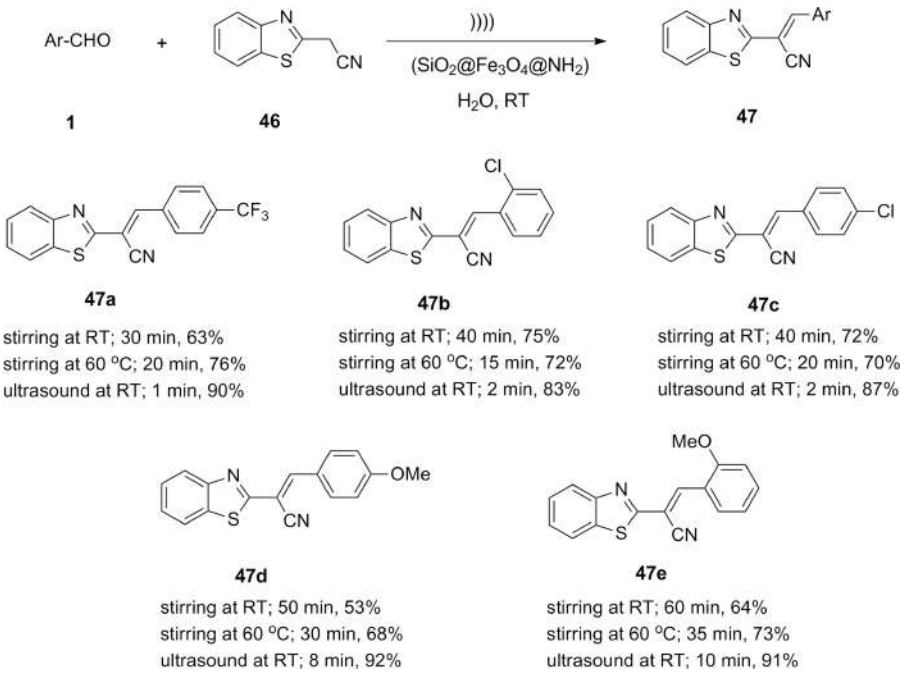

Figure 3.26: Ultrasound-assisted $SiO_2@Fe_3O_4@NH_2$ catalyzed Knoevenagel condensation in water.

3.2.7 Ultrasound-assisted Suzuki reaction by using heterogeneous catalyst in water

Zhang et al. [112] demonstrated a simple and efficient ultrasound accelerated Suzuki coupling reaction of phenylboronic acid (**51**) with phenyl iodide (**48**) in the presence of TBAB and cyclopalladated ferrocenylimines as an efficient heterogeneous catalyst in water (Figure 3.28). It was found that ultrasonic irradiation accelerated the reaction drastically compared to the conventional heating conditions.

3.2.8 Ultrasound-assisted miscellaneous reactions by using heterogeneous catalyst in water

3.2.8.1 Synthesis of 2-aryl-2,3-dihydro-1H-3-pyrazolones

Ziarati et al. [113] developed a facile and ultrasound-assisted one-pot four-component reaction protocol for efficient synthesis of 2-aryl-2,3-dihydro-1*H*-3-pyrazolones (**53**)

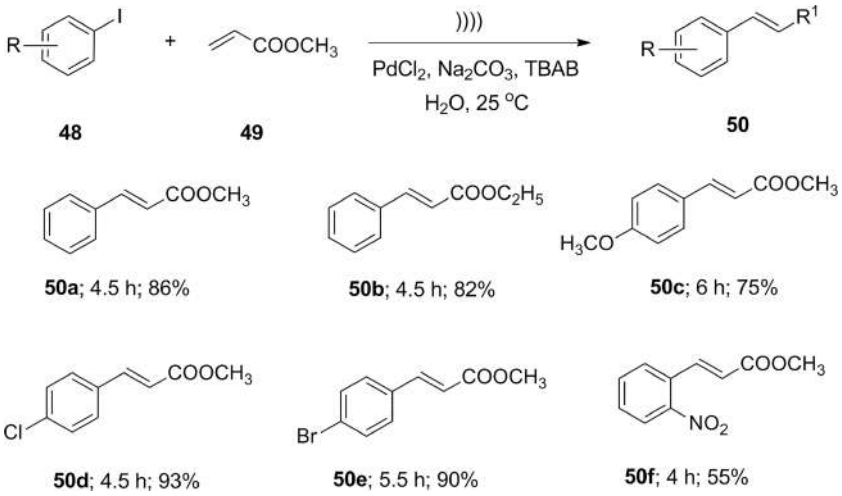

Figure 3.27: Ultrasound-assisted aqueous-mediated Heck reaction by using in-situ generated Pd(0) nanoparticles.

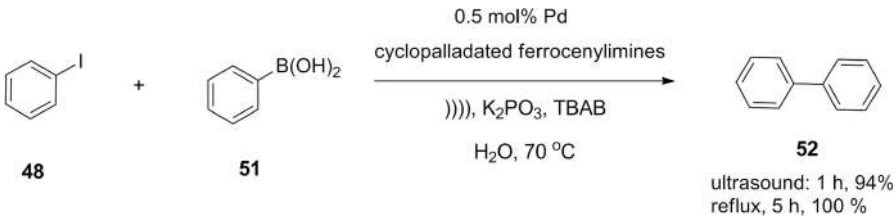

Figure 3.28: Ultrasound-assisted Suzuki reaction using cyclopalladated ferrocenylimines as catalyst in water.

starting from phenyl hydrazine (**37**), ethyl acetoacetate (**36**), substituted benzaldehydes (**1**), and β-naphthol (**34**) using nanocopper iodide as a heterogeneous catalyst in water at room temperature (Figure 3.29). All the reactions were completed within 45 min and afforded excellent yields. The same reaction when carried out under reflux conditions using conventional heating produced lesser yields even after a few hours. The used catalyst was recovered and recycled for five successive runs with almost equal efficiency. Short reaction times, simple purification procedure, high product yields, reusability of the catalyst, and use of water as solvent are the salient features of this protocol.

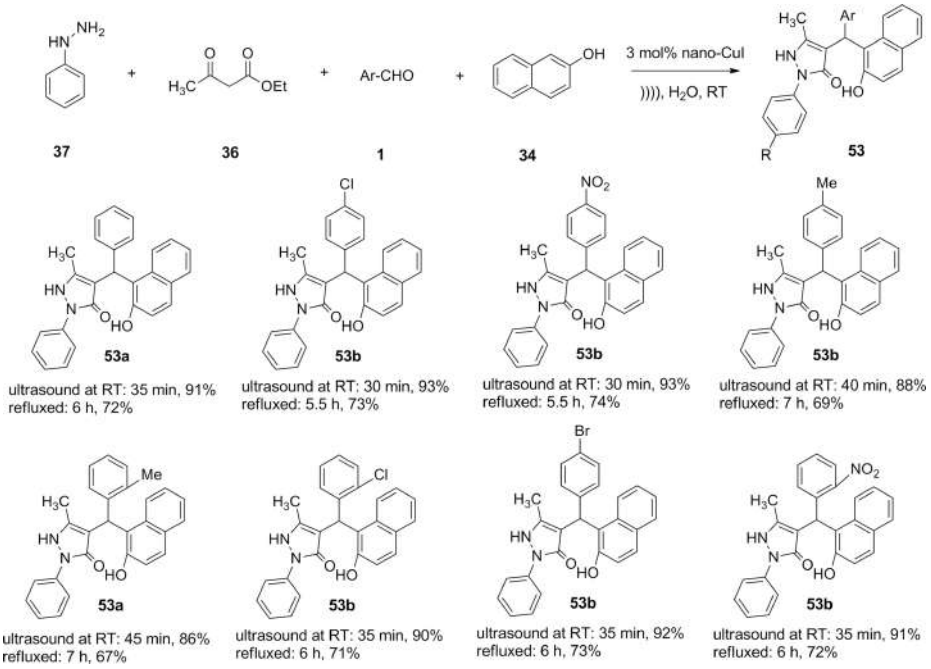

Figure 3.29: Ultrasound-assisted aqueous-mediated nano-CuI-catalyzed synthesis of 2-aryl-2,3-dihydro-1*H*-3-pyrazolones.

3.2.8.2 Synthesis of 2,2′-arylmethylene bis(3-hydroxy-5,5-dimethyl-2-cyclohexene-1-ones)

A series of 2,2′-arylmethylene *bis*-(3-hydroxy-5,5-dimethyl-2-cyclohexene-1-one) derivatives (**54**) were synthesized via pseudo-three component reactions of one equivalent of substituted benzaldehydes (**1**) and two equivalents of dimedone (**18**) under

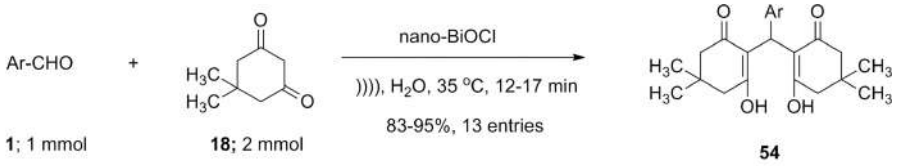

Ar = C_6H_5, 4-OCH_3-C_6H_4, 4-NO_2-C_6H_4, 3-NO_2-C_6H_4, 2-NO_2-C_6H_4, 4-Cl-C_6H_4, 3-Cl-C_6H_4, 2-Cl-C_6H_4, 4-OH-C_6H_4, 4-OH,3-CH_3-C_6H_3, 3-Br-C_6H_4, 4-CH_3-C_6H_4

Figure 3.30: Ultrasound-assisted BiOCl nanoparticles-catalyzed synthesis of 2,2′-arylmethylene *bis*(3-hydroxy-5,5-dimethyl-2-cyclohexene-1-ones) in water.

ultrasound-assisted conditions using a catalytic amount of nano-BiOCl in water at 35 °C (Figure 3.30) [59].

3.3 Conclusions

Ultrasound-assisted reactions were found to be much more advantageous than the conventional stirring at room temperature. Moreover, heterogeneous catalysts are becoming more attractive due to their ease of recovery and reusable nature. On the other hand, there will be no doubt to accept that water is the safest solvent to carry out organic transformation. The present chapter deals with the literature related to the latest developments on ultrasound-assisted heterogeneous catalysis in water.

References

[1] Davies, HM, Lian, Y. The combined C–H functionalization/cope rearrangement: Discovery and applications in organic synthesis. Acc Chem Res, 2012, 45, 923–935.
[2] Shen, ZL, Wang, SY, Chok, YK, Xu, YH, Loh, TP. Organoindium reagents: The preparation and application in organic synthesis. Chem Rev, 2013, 113, 271–401.
[3] Kotha, S, Khedkar, PR. A useful green reagent in organic synthesis. Chem Rev, 2012, 112, 1650–1680.
[4] Nugent, WA. "Black Swan Events" in organic synthesis. Angew Chem Int Ed, 2012, 51, 8936–8949.
[5] Kaneda, K, Mizugaki, T. Development of concerto metal catalysts using apatite compounds for green organic syntheses. Energy Environ Sci, 2009, 2, 655–673.
[6] Trost, BM. On inventing reactions for atom economy. Acc Chem Res, 2002, 35, 695–705.
[7] Brahmachari, G, Banerjee, B. Catalyst-free organic synthesis at room temperature in aqueous and non-aqueous media: An emerging field of green chemistry practice and sustainability. Curr Green Chem, 2015, 2, 274–305.
[8] Sankar, M, Dimitratos, N, Miedziak, PJ, Wells, PP, Kiely, CJ, Hutchings, GJ. Designing bimetallic catalysts for a green and sustainable future. Chem Soc Rev, 2012, 41, 8099–8139.
[9] Banerjee, B. Recent developments on ultrasound assisted catalyst-free organic synthesis. Ultrason Sonochem, 2017, 35, 1–14.
[10] Banerjee, B. Recent developments on ultrasound assisted one-pot multi-component synthesis of biologically relevant heterocycles. Ultrason Sonochem, 2017, 35, 15–35.
[11] Banerjee, B. Recent developments on ultrasound-assisted synthesis of bioactive *N*-heterocycles at ambient temperature. Aust J Chem, 2017, 70, 872–888.
[12] Banerjee, B. Recent developments on ultrasound-assisted organic synthesis in aqueous medium. J Serb Chem Soc, 2017, 82, 755–790.
[13] Banerjee, B. Ultrasound and Nano-Catalysts: An ideal and sustainable combination to carry out diverse organic transformations. ChemistrySelect, 2019, 4, 2484–2500.
[14] Kaur, G, Sharma, A, Banerjee, B. Ultrasound and ionic liquid: An ideal combination for organic transformations. ChemistrySelect, 2018, 3, 5283–5295.

[15] Banerjee, B, Tajti, A, Keglevich, G. Ultrasound-assisted synthesis of organophosphorus compounds. 2018, 248–263. https://doi.org/10.1515/9783110535839-013.
[16] Mason, TJ. Ultrasound in synthetic organic chemistry. Chem Soc Rev, 1997, 26, 443–451.
[17] Flint, EB, Suslick, KS. The temperature of cavitation. Science, 1991, 253, 1397–1399.
[18] Suslick, KS Ed., Ultrasound: Its chemical, physical, and biological effects, VCH Publishers: New York, 1988, 336.
[19] Suslick, KS, Crum, LA. Sonochemistry and Sonoluminescence. In: Encyclopedia of Acoustics, Crocker, MJ Ed, Wiley-Interscience: New York, 1997, Vol. 1, 271–282.
[20] Suslick, KS, Grinstaff, MW. Protein microencapsulation of nonaqueous liquids. J Am Chem Soc, 1990, 112, 7807–7809.
[21] Brahmachari, G, Banerjee, B. Catalyst-Free organic synthesis at room temperature in aqueous and non-aqueous media: An emerging field of green chemistry practice and sustainability. Curr Green Chem, 2015, 2, 274–305.
[22] Sharma, RK, Dutta, S, Sharma, S, Zboril, R, Varma, RS, Gawande, MB. Fe_3O_4 (iron oxide)-supported nanocatalysts: Synthesis, characterization and applications in coupling reactions. Green Chem, 2016, 18, 3184.
[23] Polshettiwar, V, Varma, RS. Green chemistry by nano-catalysis. Green Chem, 2010, 12, 743–754.
[24] Gawande, MB, Branco, PS, Varma, RS. Nano-magnetite (Fe_3O_4) as a support for recyclable catalysts in the development of sustainable methodologies. Chem Soc Rev, 2013, 42, 3371–3393.
[25] Gawande, MB, Bonifácio, VDB, Varma, RS, Nogueira, ID, Bundaleski, N, Ghumman, CAA, Teodoro, OMND, Branco, PS. Magnetically recyclable magnetite–ceria (Nanocat-Fe-Ce) nanocatalyst-applications in multicomponent reactions under benign conditions. Green Chem, 2013, 15, 1226–1231.
[26] Banerjee, B. Recent developments on nano-ZnO catalyzed synthesis of bioactive heterocyclic. J Nanostruct Chem, 2017, 7, 389–413.
[27] Baig, RBN, Varma, RS. Magnetically retrievable catalysts for organic synthesis. Chem Commun, 2013, 49, 752–770.
[28] Baig, RBN, Varma, RS. Organic synthesis via magnetic attraction: Benign and sustainable protocols using magnetic nanoferrites. Green Chem, 2013, 15, 398–417.
[29] Baruwati, B, Polshettiwar, V, Varma, RS. Magnetically recoverable supported ruthenium catalyst for hydrogenation of alkynes and transfer hydrogenation of carbonyl compounds. Tetrahedron Lett, 2009, 50, 1215–1218.
[30] Baig, RBN, Varma, RS. Magnetic silica-supported ruthenium nanoparticles: An efficient catalyst for transfer hydrogenation of carbonyl compounds. ACS Sustainable Chem Eng, 2013, 1, 805–809.
[31] Polshettiwar, V, Varma, RS. Nano-organocatalyst: Magnetically retrievable ferrite-anchored glutathione for microwave-assisted Paal–Knorr reaction, aza-Michael addition, and pyrazole synthesis. Tetrahedron, 2010, 66, 1091–1097.
[32] Polshettiwar, V, Baruwati, B, Varma, RS. Nanoparticle-supported and magnetically recoverable nickel catalyst: A robust and economic hydrogenation and transfer hydrogenation protocol. Green Chem, 2009, 11, 127–131.
[33] Polshettiwar, V, Varma, RS. Nanoparticle-supported and magnetically recoverable ruthenium hydroxide catalyst: Efficient hydration of nitriles to amides in aqueous medium. Chem Eur J, 2009, 15, 1582–1586.
[34] Polshettiwar, V, Varma, RS. Nanoparticle-supported and magnetically recoverable palladium (Pd) catalyst: A selective and sustainable oxidation protocol with high turnover number. Org Biomol Chem, 2009, 7, 37–40.

[35] Polshettiwar, V, Baruwati, B, Varma, RS. Magnetic nanoparticle-supported glutathione: A conceptually sustainable organocatalyst. Chem Commun, 2009, 1837–1839.
[36] Simon, M-O, Li, C-J. Green chemistry oriented organic synthesis in water. Chem Soc Rev, 2012, 41, 1415–1427.
[37] Chanda, A, Fokin, VV. Organic Synthesis "On Water". Chem Rev, 2009, 109, 725–748.
[38] Gawande, MB, Bonifácio, VD, Luque, R, Branco, PS, Varma, RS. Benign by design: Catalyst-free in-water, on-water green chemical methodologies in organic synthesis. Chem Soc Rev, 2013, 42, 5522–5551.
[39] Breslow, R. Hydrophobic effects on simple organic reactions in water. Acc Chem Res, 1991, 24, 159–164.
[40] Butler, RN, Coyne, AG. Water: Nature's reaction enforcer-comparative effects for organic synthesis "In-Water" and "On-Water". Chem Rev, 2012, 110, 6302–6337.
[41] Kaur, G, Moudgil, R, Shamim, M, Gupta, VK, Banerjee, B. Camphor sulfonic acid catalyzed a simple, facile, and general method for the synthesis of 2-arylbenzothiazoles, 2-arylbenzimidazoles, and 3*H*-spiro[benzo[*d*]thiazole-2,3′-indolin]-2′-ones at room temperature. Synth Commun, 2021, 51, 1100–1120.
[42] Sharma, S, Gangal, S, Rauf, A. Convenient one-pot synthesis of novel 2-substituted benzimidazoles, tetrahydrobenzimidazoles and imidazoles and evaluation of their in vitro antibacterial and antifungal activities. Eur J Med Chem, 2009, 44, 1751–1757.
[43] Budow, S, Kozlowska, M, Gorska, A, Kazimierczuk, Z, Eickmeier, H, Colla, PL, Gosselin, G, Seela, F. Substituted benzimidazoles: Antiviral activity and synthesis of nucleosides. Arkivoc, 2009, 3, 225–250.
[44] Navarrete-Vázquez, G, Cedilla, R, Hernandez-Campos, A, Yepez, L, Hernandez-Luis, F, Valdez, J, Morales, R, Cortes, R, Hernandez, M, Castillo, R. Synthesis and antiparasitic activity of 2-(Trifluoromethyl)benzimidazole derivatives. Bioorg Med Chem, 2001, 11, 187–190.
[45] Toro, P, Klahn, AH, Pradines, B, Lahoz, F, Pascual, A, Biot, C, Arancibia, R. Organometallic benzimidazoles: Synthesis, characterization and antimalarial activity. Inorg Chem Commun, 2013, 35, 126–129.
[46] Pedini, M, Alunni, BG, Ricci, A, Bastianini, L, Lepri, E. New heterocyclic derivatives of benzimidazole with germicidal activity–XII–Synthesis of N1-glycosyl-2-furyl benzimidazoles. Farmaco Societa Chimica Italiana, 1989, 1994, 49, 823–827.
[47] Kim, JS, Gatto, B, Yu, C, Liu, A, Liu, LF, LaVoie, EJ. Substituted 2,5'-Bi-1H-benzimidazoles: Topoisomerase I inhibition and cytotoxicity. J Med Chem, 1996, 39, 992–998.
[48] Eshghi, H, Rahimizadeh, M, Shiri, A, Sedaghat, P. One-pot synthesis of benzimidazoles and benzothiazoles in the presence of $Fe(HSO_4)_3$ as a new and efficient oxidant. Bull Korean Chem Soc, 2012, 33, 515–518.
[49] Ghosh, P, Subba, R. $MgCl_2.6H_2O$ catalyzed highly efficient synthesis of 2-substituted-1*H*-benzimidazoles. Tetrahedron Lett, 2015, 21, 2691–2694.
[50] Santra, S, Majee, A, Hajra, A. Nano indium oxide: An efficient catalyst for the synthesis of 1,2-disubstituted benzimidazoles in aqueous media. Tetrahedron Lett, 2012, 53, 1974–1977.
[51] Brahmachari, G, Laskar, S, Barik, P. Magnetically separable $MnFe_2O_4$ nano-material: An efficient and reusable heterogeneous catalyst for the synthesis of 2-substituted benzimidazoles and the extended synthesis of quinoxalines at room temperature under aerobic conditions. RSC Adv, 2013, 3, 14245–14253.
[52] Dhakshinamoorthy, A, Kanagaraj, K, Pitchumani, K. Zn^{2+}-K10-clay (clayzic) as an efficient water-tolerant, solid acid catalyst for the synthesis of benzimidazoles and quinoxalines at room temperature. Tetrahedron Lett, 2011, 52, 69–73.
[53] Azizian, J, Torabi, P, Noei, J. Synthesis of benzimidazoles and benzoxazoles using $TiCl_3OTf$ in ethanol at room temperature. Tetrahedron Lett, 2016, 57, 185–188.

[54] Mobinikhaledi, A, Forughifar, N, Zendehdel, M, Jabbarpour, M. Conversion of aldehydes to benzimidazoles using NaY zeolite. Synth React Inorg Met Org Nano-Metal Chem, 2008, 38, 390–393.
[55] Kumar, D, Kommi, DN, Chebolu, R, Garg, SK, Kumar, R, Chakraborti, AK. Selectivity control during the solid supported protic acid catalyzed synthesis of 1,2-disubstituted benzimidazoles and mechanistic insight to rationalize selectivity. RSC Adv, 2013, 3, 91–98.
[56] Kommi, DN, Jadhavar, PS, Kumar, D, Chakraborti, AK. "All water" one-pot diverse synthesis of 1,2-disubstituted benzimidazoles: Hydrogen bond driven 'synergistic electrophile-nucleophile dual activation' by water. Green Chem, 2013, 15, 798–810.
[57] Kommi, DN, Kumar, D, Bansal, R, Chebolu, R, Chakraborti, AK. "All-water" chemistry of tandem *N*-alkylation-reduction-condensation for synthesis of *N*-arylmethyl-2-substituted benzimidazoles. Green Chem, 2012, 14, 3329–3335.
[58] Sofi, FA, Sharma, R, Rawat, R, Chakraborti, AK, Bharatam, PV. Visible light promoted tandem dehydrogenation-deaminative cyclocondensation under aerobic condition for the synthesis of 2-aryl benzimidazoles/quinoxalines from ortho-phenylenediamines and arylmethyl/ethyl amines. New J Chem, 2021, 45, 4569–4573.
[59] Sapkal, BM, Labhane, PK, Satam, JR. In water–ultrasound-promoted synthesis of tetraketones and 2-substituted-1*H*-benzimidazoles catalyzed by BiOCl nanoparticles. Res Chem Intermed, 2017, 43, 4967–4979.
[60] Kaur, G, Singh, A, Kaur, N, Banerjee, B. A general method for the synthesis of structurally diverse quinoxalines and pyrido-pyrazine derivatives using camphor sulfonic acid as an efficient organo-catalyst at room temperature. Synth Commun, 2021, 51, 1121–1131.
[61] Watanabe, K. Exploring the biosynthesis of natural products and their inherent suitability for the rational design of desirable compounds through genetic engineering. Biosci Biotechnol Biochem, 2008, 72, 2491–2506.
[62] Karami, B, Khodabakhshi, S. A facile synthesis of phenazine and quinoxaline derivatives using magnesium sulfate heptahydrate as a catalyst. J Serb Chem Soc, 2011, 76, 1191–1198.
[63] Karami, B. Khodabakhshi, S. A novel and simple synthesis of some new and known dibenzo phenazine and quinoxaline derivatives using lead dichloride. J Chil Chem Soc, 2013, 58, 1655–1658.
[64] Niknam, K, Saberi, D, Mohagheghnejad, M. Silica bonded S-sulfonic acid: A recyclable catalyst for the synthesis of quinoxalines at room temperature. Molecules, 2009, 14, 1915–1926.
[65] Karami, B, Khodabakhshi, S, Nikrooz, M. A modified synthesis of some novel polycyclic aromatic phenazines and quinoxalines by using the tungstate sulfuric acid (TSA) as a reusable catalyst under solvent-free conditions. J Chin Chem Soc, 2012, 59, 187–192.
[66] Karami, B, Khodabakhshi, S, Nikrooz, M. Synthesis of aza-polycyclic compounds: Novel phenazines and quinoxalines using molybdate sulfuric acid (MSA). Polycycl Aromat Compd, 2011, 31, 97–109.
[67] Alinezhad, H, Tajbakhsh, M, Salehian, F, Biparva, P. Synthesis of quinoxaline derivatives using TiO_2 nanoparticles as an efficient and recyclable catalyst. Bull Korean Chem Soc, 2011, 32, 3720–3725.
[68] Kumar, D, Seth, K, Kommi, DN, Bhagat, S, Chakraborti, AK. Surfactant micelles as microreactors for the synthesis of quinoxalines in water: Scope and limitations of surfactant catalysis. RSC Adv, 2013, 3, 15157–15168.
[69] Tanwar, B, Purohit, P, Raju, BN, Kumar, D, Kommi, DN, Chakraborti, AK. An "all-water" strategy for regiocontrolled synthesis of 2-aryl quinoxalines. RSC Adv, 2015, 5, 11873–11883.

[70] Dandia, A, Singh, R, Joshi, J, Maheshwari, S. Magnetically separable $CuFe_2O_4$ nanoparticles: An efficient catalyst for the synthesis of quinoxaline derivatives in tap-water under sonication. Eur Chem Bull, 2013, 2, 825–829.
[71] Dandia, A, Singh, R, Gupta, SL, Rathore, KS. ZnS nanoparticle catalysed four component syntheses of novel spiropolyhydroquinoline derivatives in aqueous medium under ultrasonic irradiation. Proc Natl Acad Sci India Sect A Phys Sci, 2014, 85, 19–27.
[72] Kidwai, M, Chauhan, R. Sulfamic acid: An efficient, cost-effective and recyclable catalyst for the synthesis of triazole[1,2-a]indazole-trione derivatives. RSC Adv, 2012, 2, 7660–7665.
[73] Hasaninejad, A, Zare, A, Shekouhy, M. Highly efficient synthesis of triazolo[1,2-a]indazole-triones and novel spiro triazolo[1,2-a]indazole-tetraones under solvent-free conditions. Tetrahedron, 2011, 67, 390–400.
[74] Bazgir, A, Seyyedhamzeh, M, Yasaei, Z, Mirzaei, P. A novel three-component method for the synthesis of triazolo[1,2-a]indazole-triones. Tetrahedron Lett, 2007, 48, 8790–8794.
[75] Chandam, DR, Mulik, AG, Patil, PP, Jagdale, SD, Patil, DR, Deshmukh, MB. (±)-Camphor-10-sulfonic acid catalyzed atom efficient and green synthesis of triazolo[1,2-a]indazole-triones and spiro triazolo[1,2-a]indazole-tetraones. Res Chem Intermed, 2015, 41, 761–771.
[76] Shekouhy, M, Sarvestani, AM, Khajeh, S, Nezhad, AK. Glycerol: A more benign and biodegradable promoting medium for catalyst-free one-pot multi-component synthesis of triazolo[1,2-a]indazole-triones. RSC Adv, 2015, 5, 63705–63710.
[77] Tavakoli, HR, Moosavi, SM, Bazgir, A. $ZrOCl_2.8H_2O$ as an efficient catalyst for the three-component synthesis of triazoloindazoles and indazolophthalazines. J Kor Chem Soc, 2013, 57, 472–475.
[78] Hamidian, H, Fozooni, S, Hassankhani, A, Mohammadi, SZ. One-pot and efficient synthesis of triazolo[1,2-a]indazole-triones via reaction of arylaldehydes with urazole and dimedone catalyzed by silica nanoparticles prepared from rice husk. Molecules, 2011, 16, 9041–9048.
[79] Khazaei, A, Zolfigol, MA, Faal-Rastegar, T, Chehardoli, G, Mallakpour, S. Melamine trisulfonic acid (MTSA) as an efficient catalyst for the synthesis of triazolo[1,2-a]indazole-triones and some 2*H*-indazolo[2,1-b]phthalazine-triones. Iran J Catal, 2013, 3, 211–220.
[80] Sadeghzadeh, SM. Quinuclidine stabilized on $FeNi_3$ nanoparticles as catalysts for efficient, green, and one-pot synthesis of Triazolo[1,2-a]indazole-triones. ChemPlusChem, 2014, 79, 278–283.
[81] Hassankhani, A, Mosaddegh, E, Ebrahimipour, SY. Tungstosilicic acid as an efficient catalyst for the one-pot multicomponent synthesis of triazolo[1,2-a]indazole-1,3,8-trione derivatives under solvent-free conditions. Arab J Chem, 2016, 9, S936–S939.
[82] Verma, D, Sharma, V, Okram, GS, Jain, S. Ultrasound-assisted high-yield multicomponent synthesis of triazolo[1,2-a]indazole-triones using silica-coated ZnO nanoparticles as a heterogeneous catalyst. Green Chem, 2017, 19, 5885–5899.
[83] Naeimi, H, Didar, A. Efficient sonochemical green reaction of aldehyde, thiobarbituric acid and ammonium acetate using magnetically recyclable nanocatalyst in water. Ultrason Sonochem, 2017, 34, 889–895.
[84] Brahmachari, G, Banerjee, B. Facile and one-pot access to diverse and densely functionalized 2-amino-3-cyano-4H-pyrans and pyran-annulated heterocyclic scaffolds *via* an eco-friendly multicomponent reaction at room temperature using urea as a novel organo-catalyst. ACS Sustainable Chem Eng, 2014, 2, 411–422.
[85] Brahmachari, G, Banerjee, B. Facile and chemically sustainable one-pot synthesis of a wide array of fused O- and N-heterocycles catalyzed by trisodium citrate dihydrate under ambient conditions. Asian J Org Chem, 2016, 5, 271–286.

[86] Brahmachari, G, Laskar, S, Banerjee, B. Eco-friendly, one-pot multicomponent synthesis of pyran annulated heterocyclic scaffolds at room temperature using ammonium or sodium formate as non-toxic catalyst. J Heterocyclic Chem, 2014, 51, E303–E308.
[87] Amr, AGE, Mohamed, AM, Mohamed, SF, Abdel-Hafez, NA, Hammam, AEFG. Anticancer activities of some newly synthesized pyridine, pyrane, and pyrimidine derivatives. Bioorg Med Chem, 2006, 14, 5481–5488.
[88] Paliwal, PK, Jetti, SR, Jain, S. Green approach towards the facile synthesis of dihydropyrano (c)chromene and pyrano[2,3-d]-pyrimidine derivatives and their biological evaluation. Med Chem Res, 2013, 22, 2984–2990.
[89] Abdelrazeka, FM, Metza, P, Farrag, EK. Synthesis and molluscicidal activity of 5-oxo-5,6,7,8-tetrahydro-4*H*-chromene derivatives. Arch Pharm Pharm Med Chem, 2004, 337, 482–485.
[90] Kemnitzer, W, Drewe, J, Jiang, S, Zhang, H, Zhao, J, Crogan-Grundy, C, Xu, L, Lamothe, S, Gourdeau, H, Denis, R, Tseng, B, Kasibhatla, S, Cai, SX. Discovery of 4-aryl-4H-chromenes as a new series of apoptosis inducers using a cell- and caspase- based high through put screening assay. 3. Structure-activity relationships of fused rings at the 7,8 positions. J Med Chem, 2007, 50, 2858–2864.
[91] Erichsen, MN, Huynh, THV, Abrahamsen, B, Bastlund, JF, Bundgaard, C, Monrad, O, Jensen, AB, Nielsen, CW, Frydenvang, K, Jensen, AA, Bunch, L. Structure-activity relationship study of first selective inhibitor of excitatory amino acid transporter subtype 1:2-amino-4-(4-methoxyphenyl)-7-(naphthalen-1-yl)-5-oxo-5,6,7,8-tetrahydro-4*H*-chromene-3-carbonitrile (UCPH-101). J Med Chem, 2010, 53, 7180–7191.
[92] Bhavanarushi, S, Kanakaiah, V, Yakaiah, E, Saddanapu, V, Addlagatta, A, Rani, VJ. Synthesis, cytotoxic, and DNA binding studies of novel fluorinated condensed pyrano pyrazoles. Med Chem Res, 2013, 22, 2446–2454.
[93] Kumar, D, Reddy, VB, Sharad, S, Dube, U, Kapur, S. A facile one-pot green synthesis and antibacterial activity of 2-amino-4*H*-pyrans and 2-amino-5-oxo-5,6,7,8-tetrahydro-4*H*-chromenes. Eur J Med Chem, 2009, 44, 3805–3809.
[94] Smith, CW, Bailey, JM, Billingham, MEJ, Chandrasekhar, S, Dell, CP, Harvey, AK, Hicks, CA, Kingston, AE, Wishart, GN. The anti- rheumatic potential of a series of 2,4-di-substituted-4*H*-naphtho[1,2-*b*]pyran-3-carbonitriles. Bioorg Med Chem, 1995, 5, 2783–2788.
[95] Esmaeilpour, M, Javidi, J, Dehghaniaand, F, Dodeji, FN. A green one-pot three-component synthesis of tetrahydrobenzo[b]pyran and 3,4-dihydropyrano[c]chromene derivatives using a Fe_3O_4@SiO_2–imid–PMA^n magnetic nanocatalyst under ultrasonic irradiation or reflux conditions. RSC Adv, 2015, 5, 26625–26633.
[96] Saha, M, Das, B, Pal, A. Synthesis of Pyran Derivatives under Ultrasound Irradiation Using Ni Nanoparticles as Reusable Catalysts in Aqueous Medium. C R Chimie, 2013, 16, 1079–1085.
[97] Chen, D-H, Wu, S-H. Synthesis of nickel nanoparticles in water-in-oil microemulsions. Chem Mater, 2000, 12, 1354–1360.
[98] Safari, J, Javadian, L. Ultrasound assisted the green synthesis of 2-amino-4H-chromene derivatives catalyzed by Fe_3O_4-functionalized nanoparticles with chitosan as a novel and reusable magnetic catalyst. Ultrason Sonochem, 2015, 22, 341–348.
[99] Mulakayala, N, Murthy, PVNS, Rambabu, D, Aeluri, M, Adepu, R, Krishna, GR, Reddy, CM, Prasad, KRS, Chaitanya, M, Kumar, CS, Rao, MVB, Pal, M. Catalysis by molecular iodine: A rapid synthesis of 1,8-dioxo-octahydroxanthenes and their evaluation as potential anticancer agents. Bioorg Med Chem Lett, 2012, 22, 2186.
[100] Fan, X-S, Li, Y-Z, Zhang, X-Y, Hu, X-Y, Wang, -J-J. $FeCl_3.6H_2O$ catalyzed condensation of aromatic aldehydes with 5,5-dimethyl-1,3-cyclohexanedione in ionic liquids. Chin J Org Chem, 2005, 25, 1482–1486.

[101] Banerjee, B, Brahmachari, G. Ammonium chloride catalysed one-pot multicomponent synthesis of 1,8-dioxo-octahydroxanthenes and N-aryl-1,8-dioxodecahydroacridines under solvent free conditions. J Chem Res, 2014, 38, 745–750.
[102] Fan, X, Hu, X, Zhang, X, Wang, J. $InCl_3{\cdot}4H_2O$-promoted green preparation of xanthenedione derivatives in ionic liquids. Can J Chem, 2005, 83, 16–20.
[103] Li, -J-J, Tao, X-Y, Zhang, Z-H. An effective bismuth trichloride-catalyzed synthesis of 1,8-dioxo-octahydroxanthenes. Phosphorus Sulfur Silicon Relat Elem, 2008, 183, 1672–1678.
[104] Das, B, Thirupathi, P, Mahender, I, Reddy, VS, Rao, YK. Amberlyst-15: An efficient reusable heterogeneous catalyst for the synthesis of 1,8-dioxo-octahydroxanthenes and 1,8-dioxo-decahydroacridines. J Mol Catal A Chem, 2006, 247, 233–239.
[105] Rostamizadeh, S, Amani, AM, Mahdavinia, GH, Amiri, G, Sepehrian, H. Ultrasound promoted rapid and green synthesis of 1,8-dioxo-octahydroxanthenes derivatives using nanosized MCM-41-SO_3H as a nanoreactor, nanocatalyst in aqueous media. Ultrason Sonochem, 2010, 17, 306.
[106] Mahdavinia, GH, Rostamizadeh, S, Amani, AM, Emdadi, Z. Ultrasound-promoted greener synthesis of aryl-14*H*-dibenzo[*a, j*]xanthenes catalyzed by $NH_4H_2PO_4/SiO_2$ in water. Ultrason Sonochem, 2013, 16, 7–10.
[107] Chate, AV, Rathod, UB, Kshirsagar, JS, Gaikwad, PA, Mane, KD, Mahajan, PS, Nikam, MD, Gill, CH. Ultrasound assisted multicomponent reactions: A green method for the synthesis of N-substituted 1,8-dioxo-decahydroacridines using β-cyclodextrin as a supramolecular reusable catalyst in water. Chin J Catal, 2016, 37, 146–152.
[108] Dandia, A, Parewa, V, Jain, AK, Rathore, KS. Step-economic, efficient, ZnS nanoparticle-catalyzed synthesis of spirooxindole derivatives in aqueous medium via knoevenagel condensation followed by Michael addition. Green Chem, 2011, 13, 2135–2145.
[109] Arya, K, Rawat, DS, Sasai, H. Zeolite supported Brønsted-acid ionic liquids: An eco approach for synthesis of spiro[indole-pyrido[3,2-*e*]thiazine] in water under ultrasonication. Green Chem, 2012, 14, 1956–1963.
[110] Ying, A, Wang, L, Qiu, F, Hua, H, Yang, J. Magnetic nanoparticle supported amine: An efficient and environmental benign catalyst for versatile Knoevenagel condensation under ultrasound irradiation. C R Chimie, 2015, 18, 223–232.
[111] Zhang, Z, Zha, Z, Gan, C, Pan, C, Zhou, Y, Wang, Z, Zhou, -M-M. Catalysis and regioselectivity of the aqueous heck reaction by Pd(0) nanoparticles under ultrasonic irradiation. J Org Chem, 2006, 71, 4339.
[112] Zhang, J, Yang, F, Ren, G, Mak, TCW, Song, M, Wu, Y. Ultrasonic irradiation accelerated cyclopalladated ferrocenylimines catalyzed Suzuki reaction in neat water. Ultrason Sonochem, 2008, 15, 115–118.
[113] Ziarati, A, Safaei-Ghomi, J, Rohani, S. Sonochemically synthesis of pyrazolones using reusable catalyst CuI nanoparticles that was prepared by sonication. Ultrason Sonochem, 2013, 20, 1069–1075.

Arruje Hameed

4 Applications of nanomaterials in aqueous-mediated heterogeneous catalysis

4.1 Introduction

4.1.1 Role of water in heterogeneous catalysis

Over the last few decades, there has been a great focus on exploring the role of water as reactant, intermediate, impurity, and solvent in several organic reactions. Water/moisture has established its worth in the designing of new reaction procedures and methodologies due to its inhibitory or promotional effects in chemical reactions [1]. Recent studies have especially explored the important advantages of water in heterogeneous catalysis. On the surface of a catalyst, the water may exist in a molecular state or dissociate to form OH^- and H^+. Water could mediate a promotional role in chemical reactions under heterogeneous catalysis through three main aspects.

a) The molecular water could play a promotional role through H_2O-mediated H-transfer or through solvation-like effects.
b) The promotional role of H^+ and OH^- species
c) By blocking of active sites or surface reconstruction

These three aspects of water interaction could influence the selectivity and reaction rate. Depending on the thermodynamic conditions and surface types, water can exist in its three physical states [2]. The dissociated products of water, molecular water, and water clusters have been observed on metal surfaces during different chemical reactions. In the case of metal oxide surfaces, the oxygen anions and metal cations could absorb water or dissociate to generate two OH^- groups. The presence of OH^- groups influences thermal stability, wetting behavior, and catalytic activities. In liquid–solid phase or gas–solid phase heterogeneous reactions in aqueous media, the water exhibits a strong execrating effect while acting as a solvent-like polar spectator. Water electrochemistry is vital for controlling chemical reactions because the dissociated OH^- and H^+ can exchange electrons with the substrate. It has been well established that molecular water could mediate H^+–transfer or act as a solvent and usually does not participate directly in chemical reactions [3].

Arruje Hameed, Department of Biochemistry, Government College University Faisalabad, 38000 Fisalabad, Pakistan, e-mail: arrujeh@yahoo.com

https://doi.org/10.1515/9783110733846-004

4.1.2 Designing and preparation of nanocatalysts

Chemical industries and chemical biology do heavily rely on heterogeneous catalysis; which has emerged at the forefront chemical science over the last few decades. Under the current scenario of environmental change and green chemistry concepts, it has been desirous to design and develop active and robust catalytic processes with zero emissions and minimal wastage. The anthropogenic CO_2 emissions and ever-increasing demands of chemical products and energy implicate the idea of urgent rational designing of efficient catalysts for water splitting, CO_2 reduction, and upgrading of biomass. Ideally, materials designed with self-regenerating active sites at the atomic level could serve the purpose [4, 5]. Over the last few decades, catalysis has been merged as a promising chemical domain involved in a number of synthetic conversions and basic at the industrial level. The catalysis makes chemical reactions eco-friendly and economical because they control waste production, lessen reaction temperatures, and enhance reaction selectivity, thus result in product formation in lesser time. In fact, catalysis controls the reaction mechanisms for a green and sustainable process for the formation of pure products. The creation of perfect catalysis has been a focused area of research in synthetic chemistry over the last many years. To this end, heterogeneous, homogeneous, and enzyme-based catalysis have been well explored for a number of chemical conversions with varying degrees of success. The catalysis process utilizing heterogeneous and homogeneous catalysis have shown a number of merits and demerits related to their structural chemistry. Therefore, there has always been a requirement of a synergist framework with high recoverability like heterogeneous catalysis and dynamic like homogeneous catalysis. Both of these concepts of interest have been well joined in the structuring of nanocatalysis [6].

The development of efficient catalysts reduces energy consumptions and elevates hazardous effects on the environment. The designing of new catalytic processes relies on a strong understanding of surface reactions, experimental and theoretical methodology. The theoretical modeling helps to design efficient catalysts from new materials with controlled size, shape, and morphological properties. Both heterogeneous and homogeneous catalyses have a few limitations and drawbacks which persuade the development of new model catalyst having only the combined advantages of the two. Such model catalysts are expected to be highly selective, energy-efficient, easily recoverable, and reusable. Fortunately, these qualities have been displayed by many tailored nanostructures reported over the last two decades (Figure 4.1).

The nanosized catalyst offers a significantly high number of active sites providing efficient contact with reactants thus increase the catalytic rate much higher compared to the bulk catalyst. Good adsorption properties and variable oxidation states of transition metals (Cu, Ag, Au, Pd, and Pt) have made them attractive for heterogeneous and homogeneous catalysis in a number of chemical transformations. Generally,

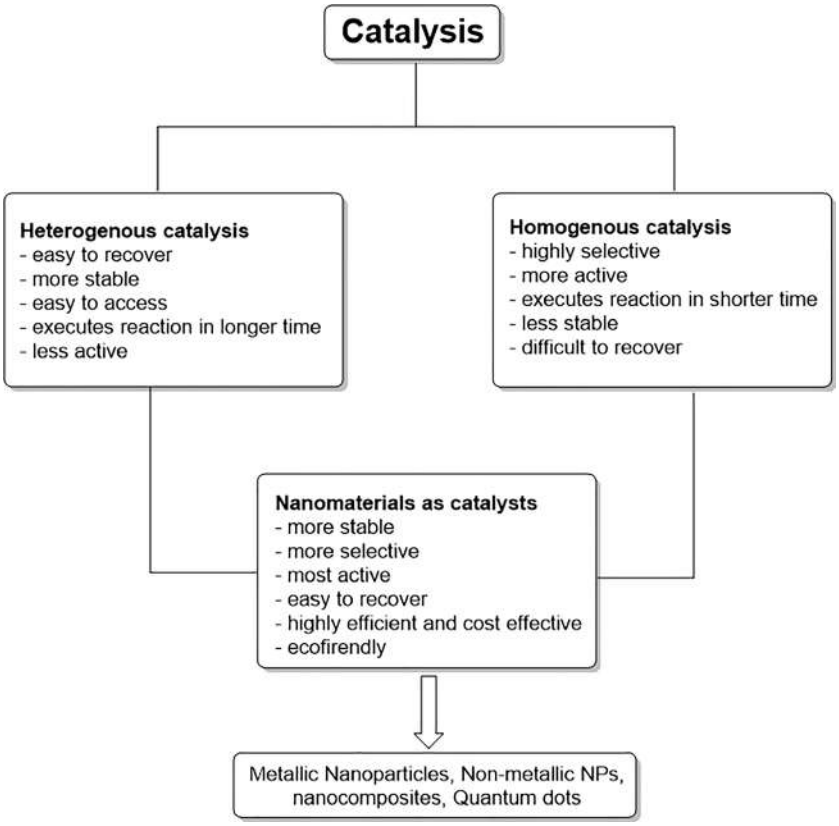

Figure 4.1: From catalysis to nanocatalysis.

transition metals or their compounds are coated on the surface of the catalyst to find highly active sites in heterogeneous catalysts. Thus, heterogeneous catalysis involves catalysts that are in different phase with respect to reactants. The conventional heterogeneous catalysts are increasingly substituted with metallic nanoparticles (NPs) which have a higher number of available active sites due to high surface area. They show higher catalytic efficiency due to the high number of contacts with reactants. This increased selective efficiency marks them as homogeneous catalysts. At the same time, they resemble heterogeneous catalysts because they are easy to separate from the reaction mixture. Thus, nanocatalysts are applied in heterogeneous catalysis with properties of homogeneous catalysts. A change in the size of NPs affects the adsorption capacity, electronic state, and coordination environment of the surface atom. The size-dependent electronic environment confers unique properties in NPs that are entirely different from their bulk counterparts. The structural composition of nanocatalysts affect their catalytic efficiency; in this regard, the concept of bimetallic NPs was introduced to achieve synergistic catalytic properties from different parent component

metals. The variation of amounts of component metals changes the composition and modifies the electronic structures resulting in the change of catalytic efficiency. Thus, the optimum ratios display composition-dependent catalytic efficiency. NPs tend to agglomerate due to high surface energies. The functionalizing agents such as stabilizers, polymers, and surfactants are used to retain the catalytic efficiency of NPs by avoiding their aggregation. Such surface tailoring affects the electronic structure and influences the catalytic efficiency [7].

Nanocatalysis involves the use of nanomaterials as catalyst for a broad spectrum of chemical transformations. Nanocatalysts execute chemical conversions with high selectivity, simplicity, and ease of catalysis separations at the end of a process. At the nanoscale, the contacts between reacting molecules and catalysis increase remarkably as just in the case of homogeneous catalysis. However, insolubility in reaction media confers the benefits of heterogeneous catalysis. Nanocatalysis influences the reactions due to structure, size, and shape-dependent properties. The designing and preparation of nanocatalysts are controlled by the use of stabilizing agents like polymers, surfactants, and ligands. Thus, control of composition, surface structure, and morphology impacts the reactivity and selectivity of nanocatalysts (Figures 4.2 and 4.3).

The key superiorities of nanocatalysis are expected to be

1. Low consumption of energy, enhanced selectivity, high reactivity, and reusability
2. Avoidance of use of heavy metals in bulk

The abovementioned characteristics could be achieved by controlling the electronic, structural and thermal properties of the nanocomponents. Over the last few years, a large variety of nanomaterials like NPs, nanocomposites, nanocrystals, and carbon dots (CDs) have been well exploited for their unprecedented capacity to act as nanocatalysts. For the preparation of nanocatalysts, the methodologies are applied to control structures of NPs, non-support, and their assembly. In fact, the development of complex and stable nanostructures has always been a challenging task for nanotechnology [8].

4.2 Nanoparticles as nanocatalysts

4.2.1 Nanoparticles as nanocatalysts in catalytic degradation

The synthesis of stable NPs is one of the growing areas of nanotechnology due to their enormous scope of applications. Accordingly, a number of synthetic methodologies like hydrothermal, chemical co-precipitation, micro-emulsion, and sol–gel methods have been developed for the preparation of NPs with controlled size, shape, and surface properties. In nanocatalysis, the size and shape of NPs is well controlled by

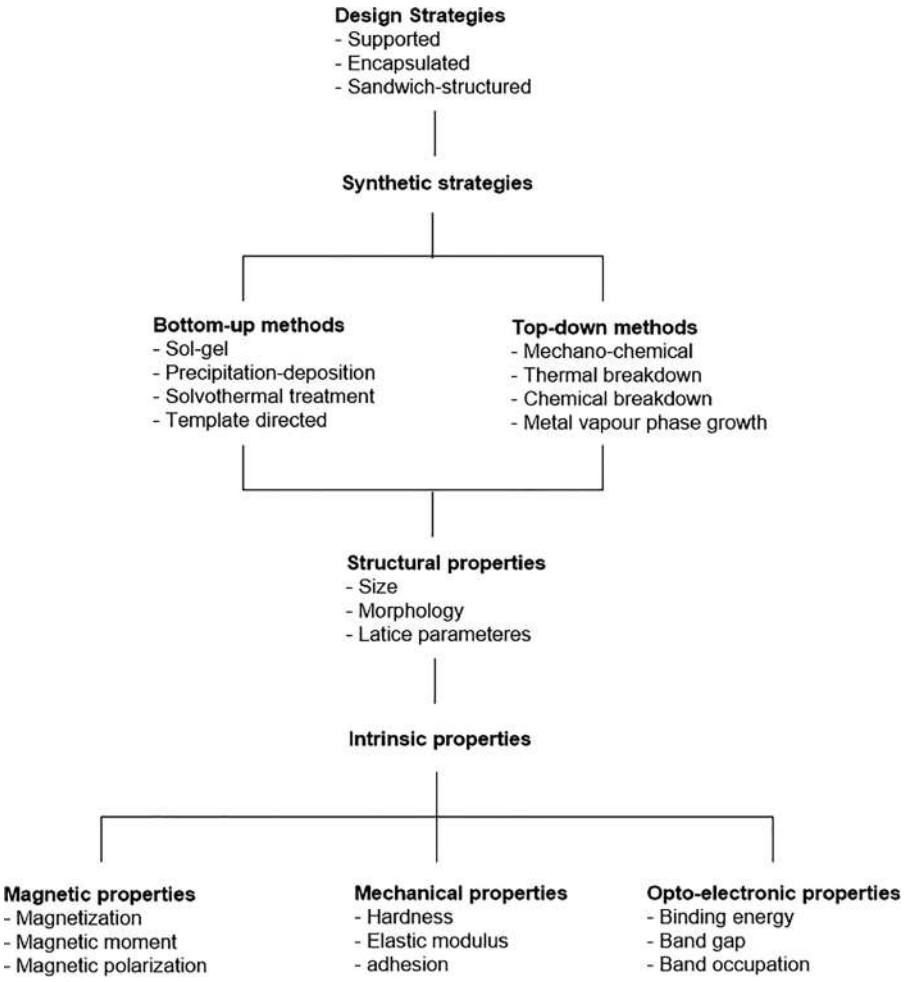

Figure 4.2: Designing and preparation of nanocatalysts.

employing a bottom-up strategy. This technique relies on stabilizing agents to control the size of NPs. The molecular approach helps to develop nanocatalysts with high selectivity. The catalytic performance of NPs could be tailored by using capping agents. The nature of the capping agents influences the growth and surface morphologies of NPs in terms of crystal structure and size. Metallic NPs have shown the promising role of heterogeneous nanocatalysts due to their higher thermal and mechanical stability. Such exciting salient features have prompted the use of NPs as heterogeneous catalysts across a number of scientific domains. Metal NPs have shown a number of promising applications in different fields like bioimaging, drug delivery, biomedical, agrochemicals, and catalysis. Different types of NPs could be prepared for their use as catalysts [9, 10].

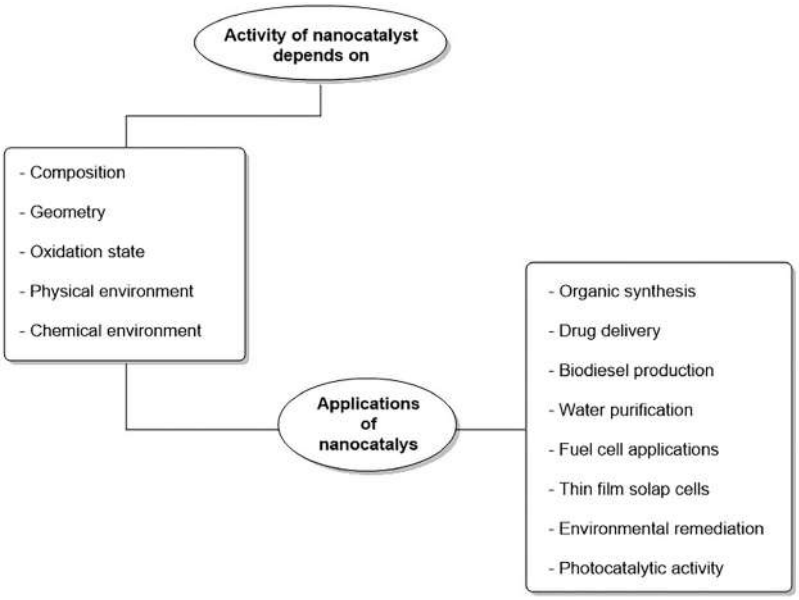

Figure 4.3: Main applications of nanocatalysts.

Over the years, silver NPs have been prepared using phytochemicals, chemical reduction, and hydrothermal techniques for their application as catalysts. The specific surface area and special electronic properties of nanosized silver NPs made them an attractive choice as heterogeneous catalysis [11, 12]. 4-Nitrophenol is a toxic chemical with wide applications in pharmaceuticals and dyes industries. 4-Nitophenol is converted into 4-aminophenol through chemical reduction for further applications in the pharmaceutical industry. In 2016, Kalantari et al. [13] prepared silver NPs through an ecofriendly green and facile approach. They used tapioca starch under alkaline conditions for the preparation of silver NPs. The prepared nanocatalyst efficiently reduced 4-nitrophenol in aqueous media within 15 min. Further, the heterogeneous nanocatalyst exhibited significant antioxidant activity. Thus, the prepared silver NPs were economical, biocompatible, and heterogeneous catalyst for expected biomedical and commercial applications.

Living beings are posed to severe ecotoxicological threats due to the discharge of wastewater effluents from industries like paper, leather, cement, and textiles. Among all, textile industries are the real threat due to the discharge of carcinogenic dyes, toxic auxiliary compounds, and heavy amounts of salts. Over the last two decades, textile industries have been compelled for wastewater treatments to control organic pollutants. The azodyes or one of the frequently used synthetic compounds and their removal from effluents is generally challenging due to their water solubility and

stable chemical structure. Accordingly, a number of physical, chemical, and biological procedures have been developed for their removal from wastewater [14, 15].

However, none of the methods completely degrade and remove azodyes. Thus, the severity of the environmental issues remains the same. Over the last few years, as an alternative strategy, nanosized zero-valent Fe has successfully been used for the degradation of organic pollutants and dye molecules in wastewater. Catalytic efficiency of this efficient and low-cost nanocatalyst reduces due to its surface corrosion issues. Many efforts were made to increase the reusability of nanosized zero-valent Fe by using partial coverage of other metals such as Ag, Cu, Ni, and Pd. Such bimetallic nanosystems were found efficient for the degradation of organic pollutants but they are also showed issues with their stability.

Considering such instability issues in mind, Kgatle and his research group [16] came up with an idea of highly efficient trimetallic nanocatalysts. Very recently they developed a trimetallic nanocatalyst using Fe/Cu/Ag for laboratory-scale study. For the development of trimetallic nanocatalyst with desired shape and structure, iron was coupled with silver and copper using $NaBH_4$ reduction method. The prepared trimetallic nanocatalyst very efficiently degraded 100% of methyl orange dye within 1 min in acidic conditions (Figure 4.4). Further, the solution pH, dye concentration, and concentration of nanocatalyst were varied to establish the optimum conditions for the best efficiency of prepared NPs. High dosage of NPs, low concentration of dye, and lower pH are favored by the catalyst for maximum catalytic activity. The prepared nanocatalyst proved as an efficient alternative for wastewater remediation.

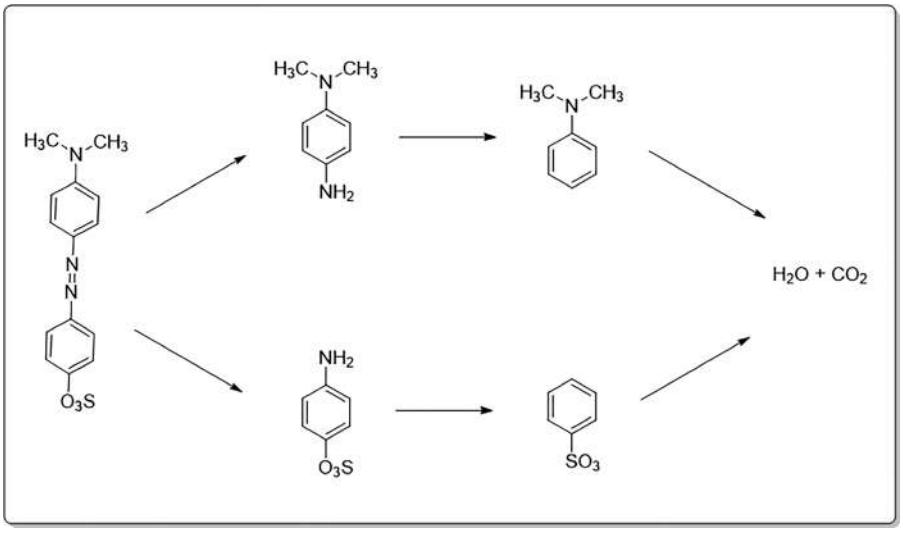

Figure 4.4: Degradation of methyl orange using trimetallic nanocatalyst.

Vanadium(V) has unique physiochemical properties and is widely used in the chemical industry and metallurgy. It is also frequently distributed in the natural environments and biological systems. Benzotriazole has been extensively been used as a corrosion and rust inhibitor. Its high water solubility, bioaccumulative capacity, and persistent nature make it toxic for the environment. Its removal from wastewater becomes hard using conditional, biological, and physicochemical methods. Last year, Liu and his team [17] employed hydrothermal method for the preparation of Cu (II)-doped V_2O_5 NPs. The prepared nanocatalyst was characterized using surface-sensitive techniques and subsequently used as heterogeneous catalyst for persulfate activation. The prepared samples degraded benzotriazoles with persulfate with much higher efficiency than pure V_2O_5 (Figure 4.5). For optimization studies, pH, persulfate concentration, doping content, and amount of nanocatalyst were varied systematically. The benzotriazole degradation was more than 80% even after three cycles of Cu–V_2O_5 catalytic activity through persulfate activation. The study revealed that persulfate radical was mainly responsible for benzotriazole degradation while the other free radicals such as O_2^- and OH^- were also involved in catalytic oxidation.

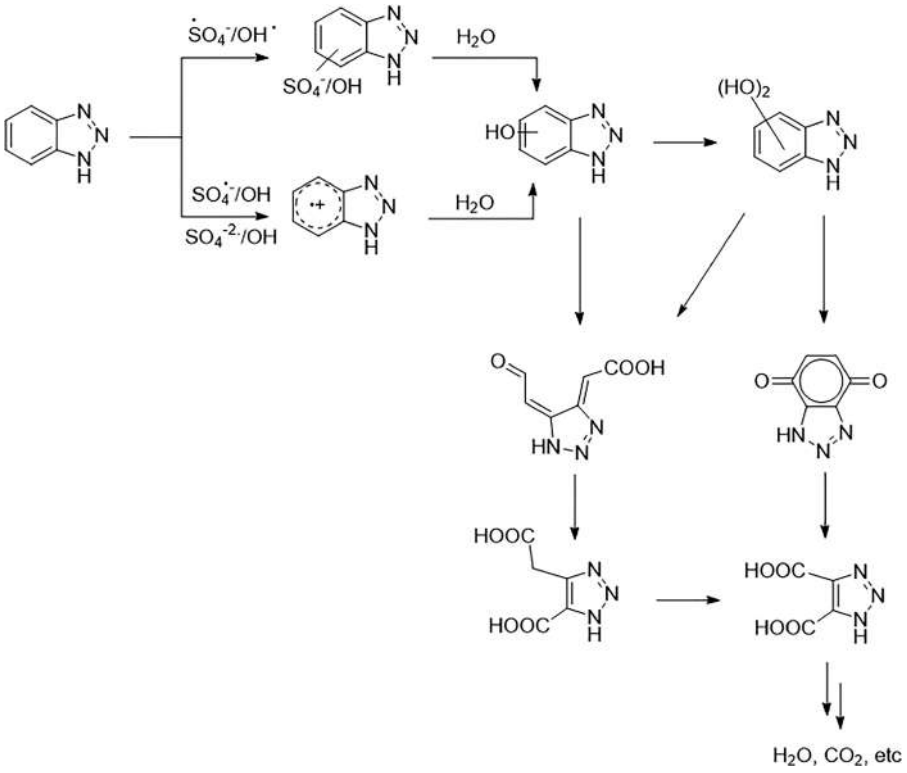

Figure 4.5: Cu(II)-doped V_2O_5-NPs for catalytic degradation of benzotriazoles.

The hazardous contaminants in water and air are continuously posing serious threats to living beings. The undegradable, toxic, and water-soluble nature of organic contaminants exposes them as endocrine-disrupting chemicals. Different physiochemical, photodegradation, filtration, and electrooxidation techniques are applied for wastewater treatments, especially for the removal of organic dyes. However, all these wastewater treatment techniques failed to produce desired results. In this regard, nanomaterial-mediated catalytic reduction of organic contaminants has emerged as a facile and economical method. In a recent study, Veisi et al. [18] prepared Au-NPs-decorated biguanidine-modified mesoporous silica KIT-5 as a nanocatalyst (Figure 4.6). The biguanidine ligand acted as a stabilizer for Au-NPs. The prepared nanocatalyst efficiently degraded organic water contaminants like rhodamine B, methyl orange, and methylene blue at room temperature (Figure 4.7). The dye reduction efficiency of the nanocatalyst increased with higher catalyst load.

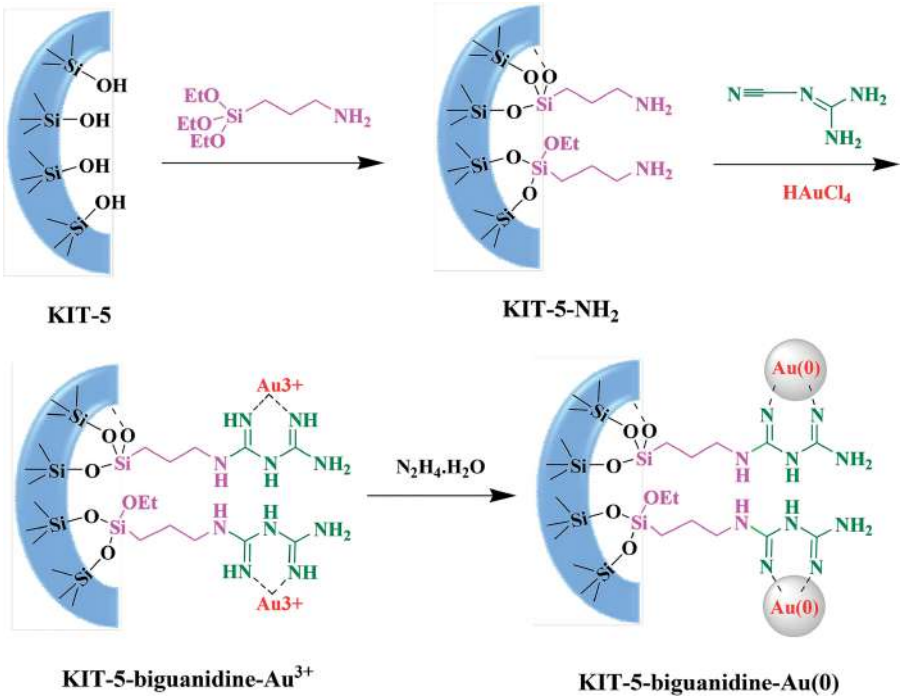

Figure 4.6: Preparation of KIT-5-biguanidine-Au(0) as nanocatalyst [18].

In the recent past, mesoporous silica materials have shown a variety of applications as heterogeneous catalysts in the field of environmental remediation, energy storage, chemical synthesis, and biomedicines. Accordingly, a number of methodologies have been developed for the preparation of Si-based porous materials of different structures and morphologies. In recent years, great efforts have been made for the preparation of

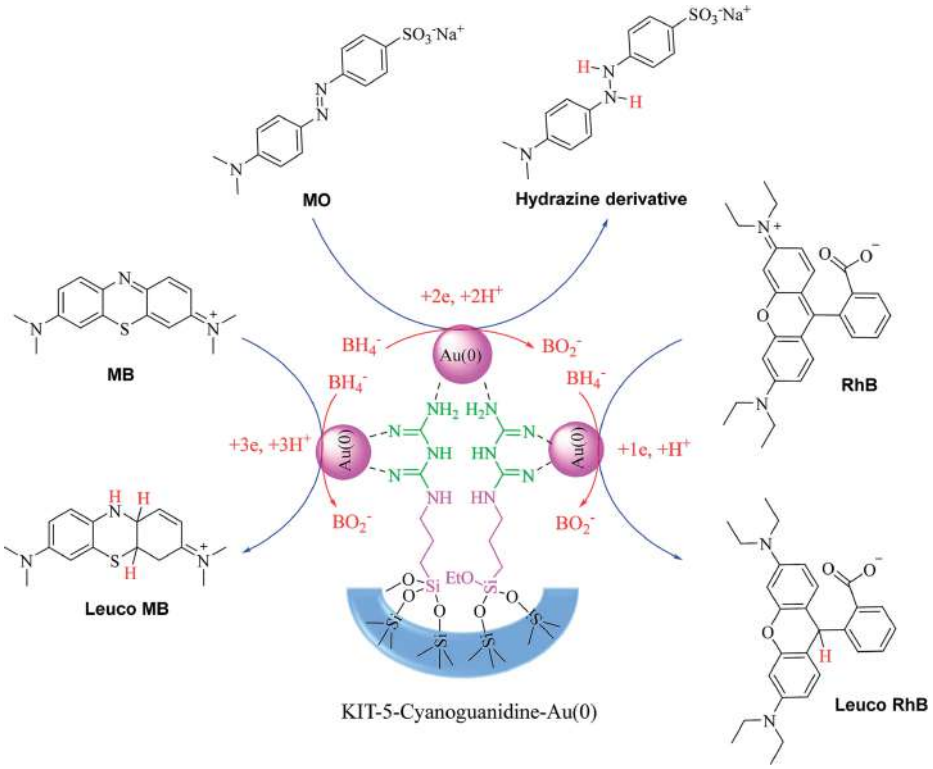

Figure 4.7: Application of KIT-5-biguanidine-Au(0) for degradation of organic dyes [18].

mesoporous silica nanospheres with polymer/surfactant-mediated controlled pore size and morphology. In one of the studies, the hydrothermal method has been employed for the preparation of novel dendritic fibrous silica nanospheres (DFNS) was prepared with large pore size and high surface area. Owing to the functional ability of fibers, the DFNS have widely been utilized as solid support materials for homogeneous and heterogeneous catalysts. Various organic transformations including Suzuki cross-coupling reactions have been managed using a catalyst prepared from metal NPs immobilized on amine-supported DFNS. However, it has been observed that the guest molecules do not get desirous excess to the functional moieties due to the non-uniform pore size of Si nanospheres. Such morphological shortcomings limit their much-anticipated applications in heterogeneous catalysis. In a very recent study, Shabir et al. [19] reported a successful synthesis of dendritic fibrous core–shell silicon NPs. The prepared DFNS have a uniform and vertical nanochannels with cubic morphology. The prepared DNFS have a high core diameter and surface area and were subsequently loaded with silver NPs and the fibers were functionalized with amines. The resultant nanostructure was used as a reusable catalyst for the reductive degradation of the organic dyes, nitro, and toxic aromatics compounds. The fibrous morphology facilitated the Ag-NPs to interact

properly with the organic pollutants and resulted in the higher catalytic activity of prepared materials.

4.2.2 NPs as nanocatalysts in organic synthesis

1,2,3-Triazoles generated from 1,3-dipolar cycloaddition of azides and alkynes are important heterocycles with a broad range of applications. The classical Huisgen methodology provides a mixture of 1,4- and 1,5-regioisomers of 1,2,3-triazoles under harsh conditions. In 2002, a Cu-catalyzed approach was introduced for regioselective synthesis of 1,4-disubsitiuted 1,2,3-triazoles under mild conditions. This highly efficient, versatile, and facile reaction met some issues due to the involvement of stabilizing agents, reducing agents, and recyclability of catalysts. Thus, it is highly desirable to develop a sustainable and environmentally benign Cu catalyst for such a versatile reaction. Considering the concept of nanocatalysis as a sustainable alternative for various organic synthetic reactions, Chetia et al. [20] introduced the use of copper NPs as a green catalyst for the preparation of 1,2,3-triazoles (Figure 4.8). They reported Cu-NPs supported on nanocellulose as a green and efficient catalyst for ecofriendly preparation of 1,2,3-triazoles. The as-prepared nanocatalyst provided excellent product yield without losing catalytic efficiency even after five cycles.

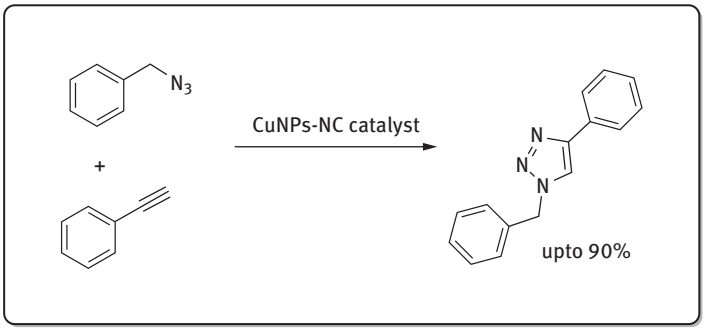

Figure 4.8: Cu-NPs supported on nanocellulose for synthesis of 1,2,3-triazoles.

Over the last few years, great attention has been focused on the development of magnetic heterogeneous metal catalysts for a variety of synthetic reactions due to ease of separation, high reusability, and stability. Very recently, Rajabi-Moghaddam et al. [21] prepared Cu-coated magnetic core–shell NPs (Fe_3O_4@SiO_2) as a novel and efficient heterogeneous nanocatalyst for the preparation of 1,2,3-triazoles (Figures 4.9 and 4.10). During the reaction, the prepared Cu(II) MNPs provided Cu(I) for the execution of the cycloaddition reaction. This highly efficient heterogeneous nanocatalyst showed superior catalytic activity up to six consecutive runs in an aqueous environment.

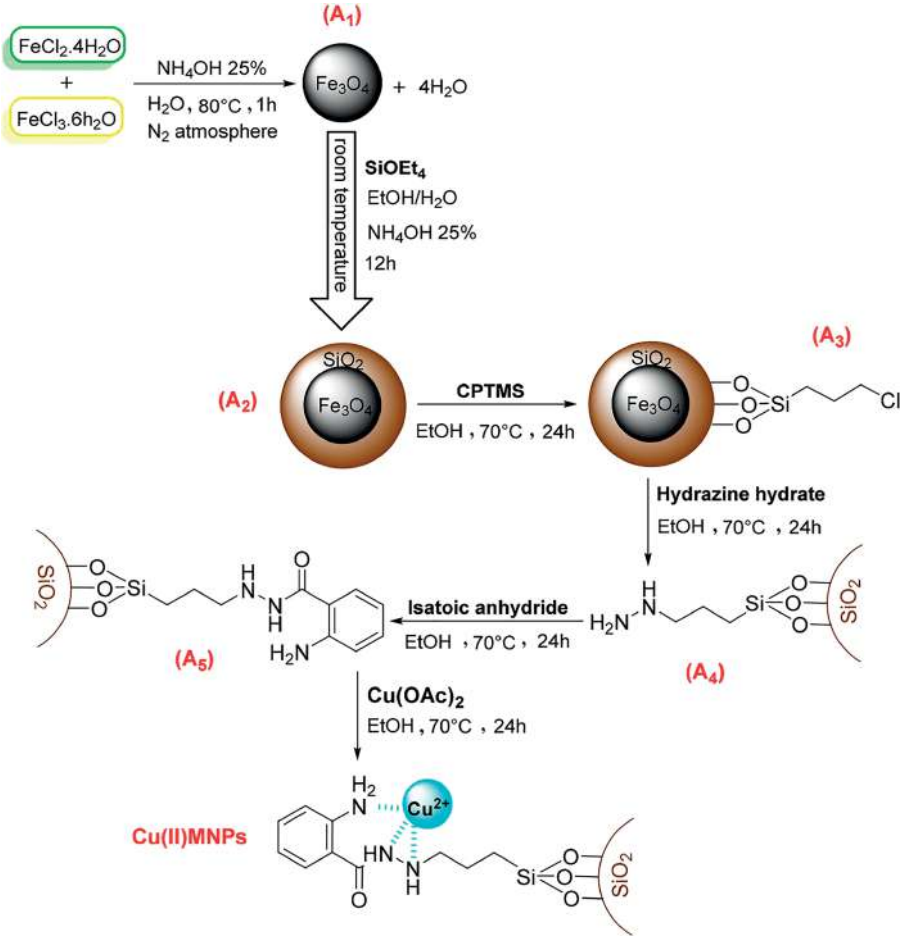

Figure 4.9: Preparation of Cu-MNPs nanocatalyst [21].

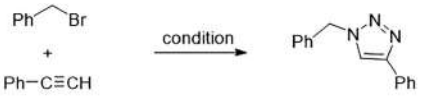

Conditions and product yield:

NO Catalyst Sodium ascorbate NaN_3, 18h, 50oC No reaction	0.025 g Catalyst Sodium ascorbate NaN_3, 3h, 50oC 98% Yield	0.1 g Catalyst Sodium ascorbate NaN_3, 3h, 50oC 98% Yield	0.05 g Catalyst Sodium ascorbate NaN_3, 3h, 50oC 98% Yield	0.05 g Catalyst Sodium ascorbate NaN_3, 3 hr, rt 90% Yield

Figure 4.10: Cu-coated magnetic core-shell nanoparticles for the preparation of 1,2,3- triazoles.

Considering the application of heterogeneous nanocatalysis, the importance of triazoles, and the use of environmentally benign reaction media, Paplal et al. [22] prepared Bi_2WO_6 NPs as a novel catalyst for the preparation of 1,2,3-triazoles from chalcones and β-nitrostyrenes in water (Figure 4.11). Further, the combined applications of Bi_2WO_6 NPs and click conditions furnished functionalized 1,4-disubsitiuted triazoles in very short reaction times.

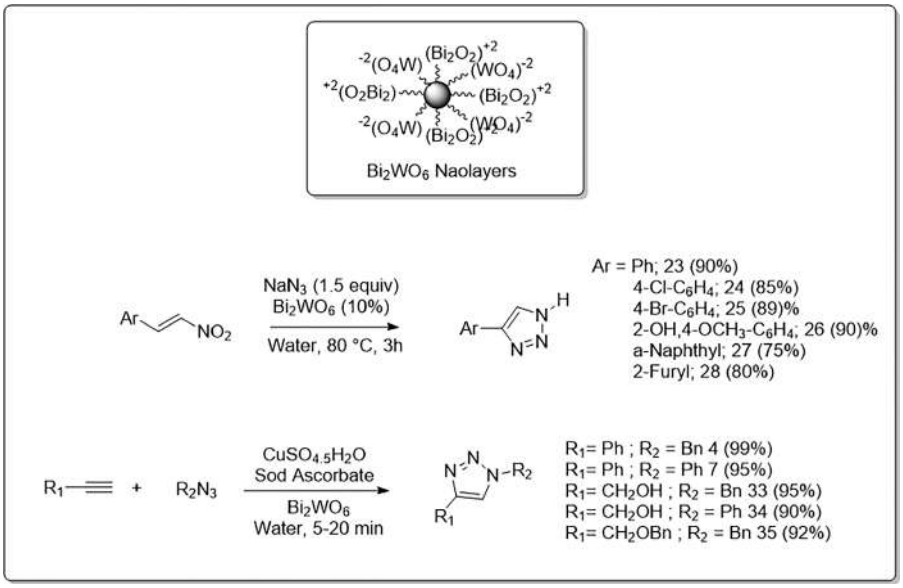

Figure 4.11: Bi_2WO_6 NPs-assisted preparation of 1,2,3-triazoles.

Generally, metallic NPs are prepared under the concept of wet chemistry which involved the applications of different chemical reductants under harsh conditions. The chemical-mediated synthesis of NPs involved stabilizers, reducing agents, and potentially hazardous solvents. There has been a growing interest in the development of facile and ecofriendly approaches for the synthesis of NPs by avoiding the use of toxic chemicals. Accordingly, various environment-friendly approaches have been developed for the preparation of metallic NPs. One such alternative green approach involves bioreductants for the preparation of NPs in aqueous media. In one such effort, Khan et al. [23] employed aqueous extract of *Salvadora persica L.* as bioreductants for ecofriendly synthesis of Pd-NPs (Figure 4.12). The aqueous extract not only facilitated the synthesis of Pd-NPs but also functionalized their surface. The prepared NPs displayed higher catalytic activity in Suzuki cross-coupling reactions in aqueous media. This Pd-based nanocatalyst was found highly efficient with superior reusability under aerobic conditions. Previously, few reports have described the application of Pd NPs in cross-

coupling reactions. However, in most cases, Pd nanocatalysts were synthesized using various toxic chemicals.

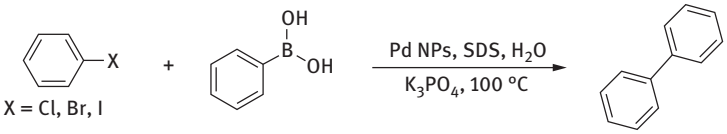

Figure 4.12: Pd NPs-mediated cross-coupling reactions.

Over the last few years, attention has been diverted on the development of highly efficient Pd-based heterogeneous nanocatalysts with superior reusability. To this end, highly efficient Pd-based bimetallic NPs were prepared using Ni, Au, Pt, and Co. The CuO supports are preferred for the development of Pd-based nanocatalysts to prevent agglomeration of NPs. In 2018, Elazeb et al. reported a green and highly reliable procedure for the preparation of Pd-NPs supported on CuO (Figure 4.13). The preparation involved microwave-assisted reduction of Pd and Cu salts in aqueous media. The as-prepared NPs exhibited high catalytic activity in cross-coupling reaction under ligand-free conditions. The bimetallic nanocatalyst executed chemical reactions in a shorter time without losing catalytic activity even after five cycles. The bimetallic catalyst was stable, efficient, and reusable compared to unsupported NPs.

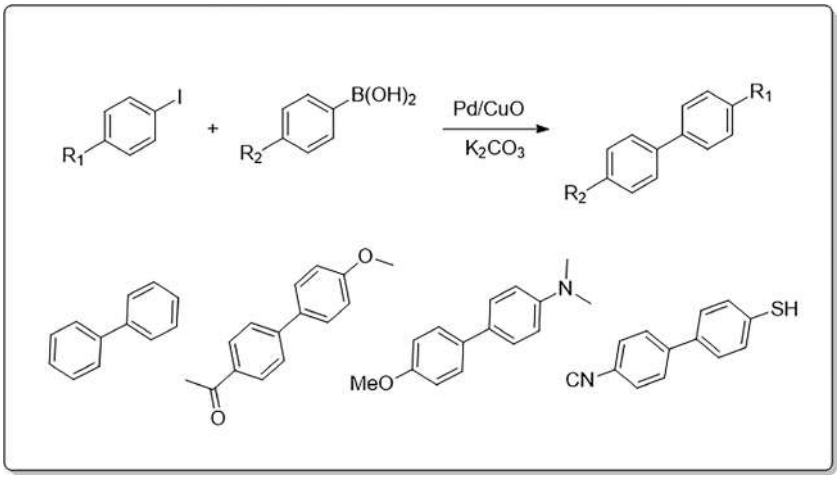

Figure 4.13: Pd–CuO nanocatalyst for Suzuki cross-coupling reactions.

Over the last few years, bio-based nanomaterials have received considerable attention in heterogeneous catalysis due to their unique morphological, structural, and sustainable properties. Cellulose nanocrystals can stabilize highly dispersive metal

NPs because of their diversely functional and highly soluble nature. Such heterogeneous structures could act as catalysts for a variety of synthetic reactions. Very recent studies have reported the preparation of highly active catalysts by stabilizing highly disperse Au on the surface of bio-based nanocrystals for coupling reactions. Very recently, Jin et al. [24] prepared heterogeneous catalysts using chitosan and chitin nanocrystals as supports for Pd-NPs (Figure 4.14). The Pd salt was reduced and directly deposited on nanocrystals in one-pot reaction. This bio-based nanocatalyst showed superior catalytic activity in HECK coupling reactions (Figure 4.15). The efficient heterogeneous catalyst was prepared by immobilizing Pd-NPs on sustainable biomaterial supports.

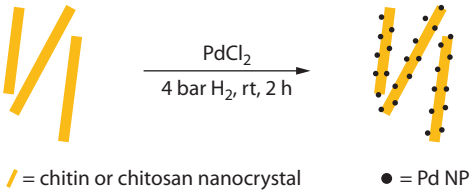

Figure 4.14: Preparation of nanocatalyst by depositing Pd-NPs on biomaterials [24].

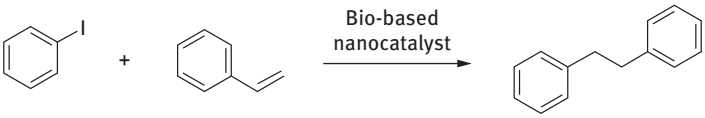

Figure 4.15: Bio-based nanocatalyst for HECK coupling reactions.

4.3 Nanocomposites as nanocatalysts

4.3.1 Nanocomposites as nanocatalysts in catalytic degradation

The sustainability of aquatic ecosystems faces severe threats due to oxygen desolation and sunlight penetration issues caused by wastewater organic pollution. Such organic pollutants are heavily discharged by the plastic, textile, paper, and pharmaceutical industries. As described earlier, the discharge waste must be treated properly to reserve water resources and to avoid negative impacts of the environment [25]. Accordingly, a number of physiochemical methods and techniques have been developed with limited to high success over the last few decades.

With the recent advancements in nanotechnology, nanocomposites have gained much attention as a heterogeneous catalysts for catalytic degradation of hazardous pollutants in industrial effluents [26]. A variety of nanocomposites for degradation of

organic pollutants have been prepared using conventional methods such as rapid solidification process, grafting melt intercalation, electrospinning, and high energy ball milling. All these methods are non-ecofriendly due to the involvement of hazardous chemicals thus, have limited applications in environmental remediation. In recent years, nanocomposite preparation through green and sustainable methods have gained considerable attention especially for the degradation of organic pollutants. Researchers have been exploiting a variety of phytochemicals as reducing and stabilizing agents for environmental friendly preparation of nanocomposites [27, 28]. Last year, Maham et al. used *Ageratum conyzoides L.*, extract for the biosynthesis of $Ag–ZrO_2$ nanocomposite through an in-situ green method [29]. This facile method involved a reduction of Ag^+ and the prepared Ag-NPs were subsequently dispersed on the surface of ZrO_2. The prepared nanocomposite was highly stable because the phytochemical avoided the aggregation of silver NPs. the prepared nanocatalyst exhibited high catalytic efficiency for the reduction of pollutants like congored, negrosin, 4-nitrophenol, and 2,4-dinitrophenyl hydrazine in aqueous media (Figure 4.16). This heterogeneous catalyst did not lose its catalytic efficiency seriously even after multiple runs due to synergistic interaction between Ag-NPs and the support.

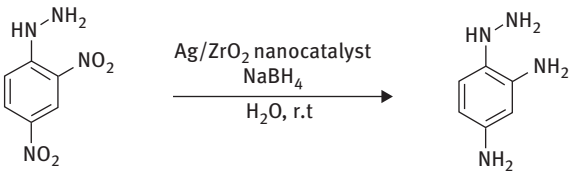

Figure 4.16: Catalytic reduction of pollutants.

Rhodamine B is a widely used cationic fluorescent dye. It is a neurotoxin and carcinogenic and can cause gene mutations and damage to respiratory tract, eyes, and skin. It is frequently found in effluents of pharmaceutical, foodstuff and textile industries. Over the years, the adsorption process has been regarded as the economical and simple approach for the removal of organic dyes from wastewater. Owing to the abundantly present negatively charged oxygenated groups, the graphene oxide (GO) could develop strong interactions with cationic rhodamine B. The GO also show high solution dispersibility, water stability, and hydrophilic character. Furthermore, the physiochemical properties of GO could be tailored using a number of available chemical modifications. The metal-organic frameworks (MOFs) are highly ordered class of adsorbents with high catalytic activity, excellent adsorbability, high porosity, and surface area. Hence, the MOFs could be combined with GO to prepare composite materials with improved adsorptive properties. Very recently, Kumar and his group employed one-pot process for the preparation of MOF-5@GO nanocomposites (Figure 4.17) [30]. Initially, the GO was prepared from hummer's method and the salvo-thermal process produced MOF-5. This

prepared nanocomposite was found to be reusable, economical, and highly efficient for the removal of rhodamine B in an aqueous solution (Figure 4.18). Further, the catalytic efficiency was optimized by varying dye concentration, time and pH of the solution.

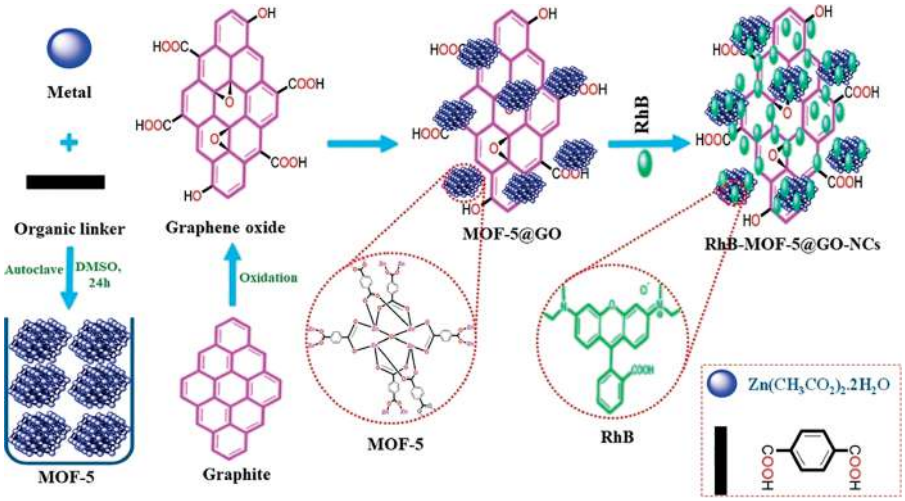

Figure 4.17: Preparation of MOF-5@GO nanocomposites (reproduced with permission [30], https://pubs.acs.org/doi/abs/10.1021/acsomega.1c00143).

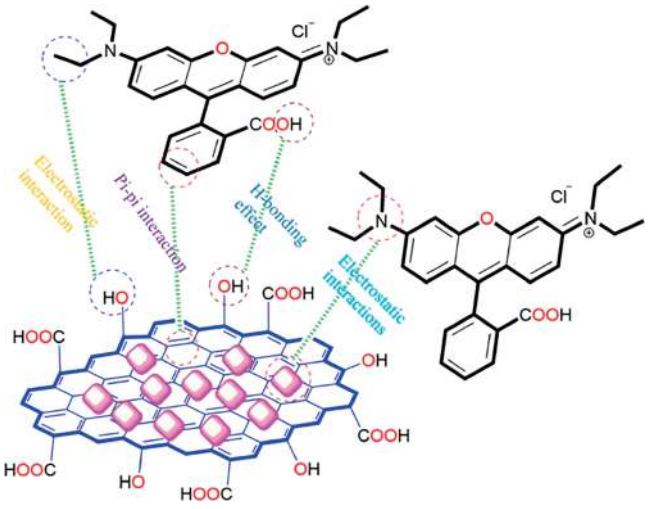

Figure 4.18: Adsorption of organic dye on MOF-5@GO nanocomposites (reproduced with permission [30], https://pubs.acs.org/doi/abs/10.1021/acsomega.1c00143).

In 2021, Jinendra et al. [31] described the application of reduced graphene oxide–nickel (RGO-Ni) nanocomposites for the efficient removal of rhodamine B from aqueous solution (Figure 4.19). The prepared nanocomposite was used for the removal of organic dye at different pH, adsorbent dosage, dye concentration, and contact time. The nanocomposite was found highly efficient with repeated useable capacity.

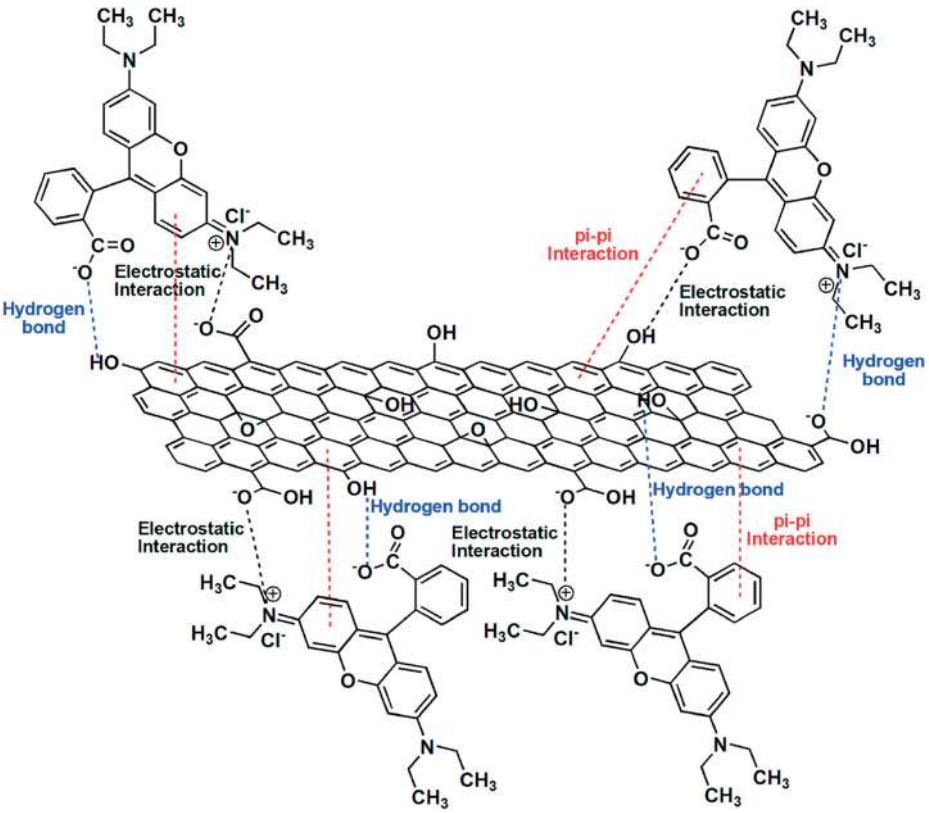

Figure 4.19: Interaction between RGO-Ni Nanocomposite and organic dye [31].

The remains of pharmaceutical products in wastewater effluents threaten the environment due to their water solubility and persistent nature. Metronidazole is a highly recommended antibiotic and it poses serious threats to the environment due to its high mutagenic, carcinogenic, and toxic nature. It shows low biological degradation and high water solubility; producing an urgent need to develop methods for its effective degradation. Therefore, multifunctional and efficient processes are required for cost-effective removal and degradation of such organic compounds. The currently used physiochemical processes like chlorination, membrane filtration,

and adsorption techniques have many disadvantages [32, 33]. Nanotechnology is at the forefront for environmental remediation and producing solutions to various challenges related to the conventional wastewater treatment techniques. Nanomaterials have gained exceptional attraction as catalysts for the degradation of organic pollutants including medical waste. Nasseh et al., in 2018, developed a heterogeneous $FeNi_3/SiO_2$ magnetic nanocomposite for the catalytic degradation of metronidazole in the presence of H_2O_2 [34]. The Fenton-like catalytic process was studied by varying concentrations of H_2O_2, pH, the concentration of metronidazole, and nanocomposite. The highly efficient nanocomposite lost its catalytic activity only 8% even after six periodic cycles.

As described earlier, the frequently used antibiotics have become major environmental issues due to their water solubility and stable chemical structures. The large-scale production and economic availability of tetracycline (TC) have increased its application in veterinary, agriculture, and human health management. Such huge administration of TC increases the risks of its discharge into the environment. Its release damages the ecosystem and creates toxic effects on human and aquatic life. Thus, it is highly desirable to develop an efficient, productive, and economical method for the removal of TC from polluted bodies. In general, the removal of TC is managed through adsorption methods due to their efficient nature and lack of by-product formation. Although, other techniques like advanced oxidation, photolysis, and biological processes are frequently used with significant success [35, 36].

As discussed earlier, the GO has unique physiochemical properties due to oxygen-containing functional groups, making it an attractive adsorbent for organic pollutants including antibiotics. Further, magnetic separation technology has gained attention in the field of environmental remediation, analytical chemistry, and medicine. GO has been coupled with quite a few magnetic materials for the induction of magnetic properties in the adsorbent [37, 38]. Likewise, in 2017, Hu et al. [39] prepared magnetically separable Fe_3O_4 @GO by directly coupling Fe_3O_4-MNPs with GO. The prepared nanocomposite was used for the removal of TC from wastewater by varying temperature, TC concentration, humic acid, and pH. The prepared nanocomposites exhibited high adsorption capacity at low pH. The affinity of TC to nanocomposite was influenced by the presence of humic acid. The as-prepared nanocomposite exhibited high reusability and good regeneration in the treatment of antibiotic wastewater.

Various NP systems have also been used for the degradation of contaminants like antibiotics through an advanced oxidation processes. The NPs show high suitability for the oxidation process because of their economic availability, high stability, and photocatalytic activity in aqueous solutions. Over the last few years, the concepts of biosorption have gain interest in the field of wastewater treatment due to some main attributes like high efficiency, increased selectivity, and rapid adsorption rate. The biosorbents like yeast, algae, fungi, and bacteria have become attractive alternatives for the replacement of in-use carbon-based adsorption techniques [40–42].

A couple of years ago, Gupal et al. [43] used bionanocomposites for the adsorption and degradation of TC in wastewater (Figure 4.20). Initially, chemical precipitation for the preparation of iron oxide, then TiO_2 was prepared. Finally, the bionanocomposite was prepared by mixing dead biomass of *Acinetobacter sp*. The prepared nanobiocomposite efficiently adsorbs and degrades the TC in wastewater. The degradation reaction conditions for TC degradation were optimized by varying pH, TC, and bionanocomposite concentration. The as-prepared nanobiocomposite exhibited excellent catalytic activity due to photocatalytic potential of nanomaterial and sorption capacity of antibiotic-resistant bacterial biomass.

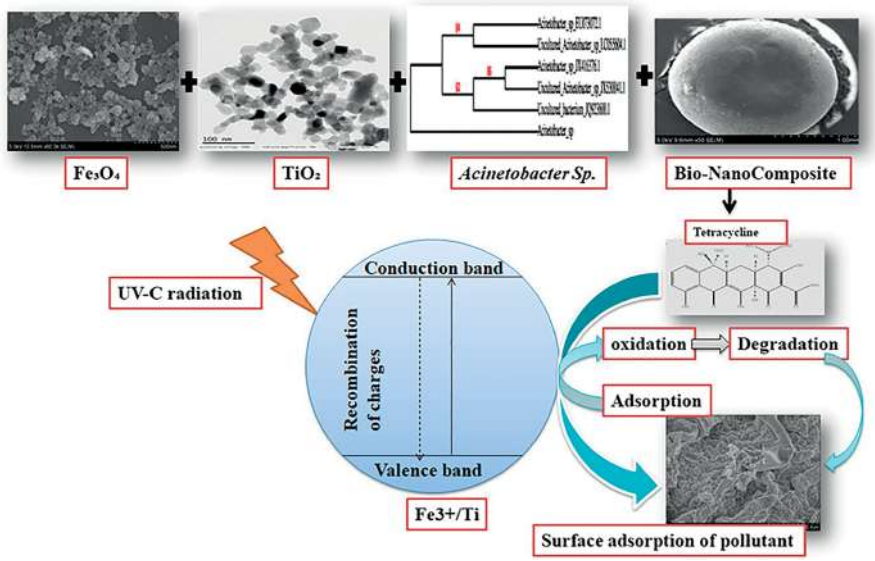

Figure 4.20: Adsorption and degradation of tetracycline using bionanocomposite (reproduced with permission from [43], https://pubs.acs.org/doi/10.1021/acsomega.9b02339).

4.3.2 Nanocomposites as nanocatalysts in organic synthesis

The preparation of industrially important amino aromatics from nitro compounds do rely on catalytic hydrogenation. For the highly efficient reduction process, the efforts have always been diverted for the development of next-generation green and economical catalysts. Over the last decade, the efficiency of catalytic systems has greatly improved by the introduction of metallic NPs and nanocomposites as heterogeneous catalysts [44, 45]. Generally, the heterogeneous catalysts are prepared from expensive metals like Ru, Pt, and Pd. Hence, they are not used on large scale in chemical industries due to cost-related issues. Therefore, there is a great emphasis for the preparation of greener and economical nanocatalysts with a broader scope of

application. To this end, hybrid nanocomposites offer improved catalytic properties due to the synergistic effects of NPs and support [46].

As discussed earlier, graphene can act as green support for NPs in a heterogeneous catalyst. Highly active hybrid nanocomposites show a synergistic effect due to the exceptional conductivity of graphene and highly stable NPs. In reaction media, graphene promotes the donation of reductant's electrons and enhances reduction capacity of nanocatalyst. Keeping this in view, Zhang et al. [47] used a facile hydrothermal self-assembly process for the preparation of CuO/GO hybrid nanocomposite. The prepared nanocomposite was employed as a catalyst for the reduction of a variety of nitro-aromatics (Figure 4.21). The nanocatalyst exhibited excellent catalytic activity due to the synergetic effect of GO and NPs in the presence of $NaBH_4$ in aqueous media. The heterogeneous catalyst could be recycled six times without losing selectivity and reduction performance. The as-prepared nanocatalyst was suggested as a suitable candidate for industrial reduction processes due to simple and low-cost preparation.

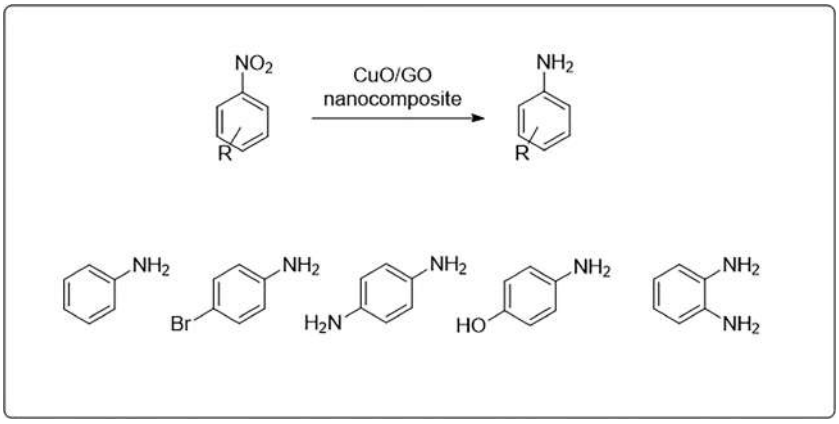

Figure 4.21: Reduction of nitro-aromatics using CuO/GO hybrid nanocomposite.

To tackle the cost-related issues with the production of heterogeneous catalysts, efforts have been made to prepared nanostructures using known novel metals like iron for large-scale applications. The high abundance, non-toxic, and ecofriendly nature represent it as an attractive element for the preparation of heterogeneous nanocatalysts. The magnetic properties of iron NPs enable them to be easily separated from the reaction media by the use of an external magnet [48, 49]. Further, water tolerant property is exhibited by Fe_2O_3 NPs enable them to be used as a catalyst in aqueous media. A number of hydrocarbons are prepared using Fe-based nanocatalysts. Supported Fe_2O_3 NPs have efficiently acted as nanocatalysts in a number of chemical processes like hydrogenation, oxidation, cross-coupling, and acid-catalyzed reactions [50, 51]. Considering the importance and industrial applications of amino-aromatics,

Sohail et al. [52] reported the economical preparation of Fe-based nanostructures with high catalytic efficiency for selective conversion of nitro-aromatics to corresponding amines (Figure 4.22). The preparation of $Fe_9TiO_{15}@TiO_2$ was managed using a simple sol–gel method employing THF, titanium isopropoxide, and ferrocene as precursors. The nano-TiO_2 acted as a support for Fe–Ti bimetallic NPs in this as prepared nanocomposite. The reported methodology efficiently controlled the morphology of NPs and the composition of nanocomposites. A number of structurally different nitro-aromatics were reduced to corresponding anilines using this nanomaterial as a selective, efficient, and sustainable heterogeneous catalyst. The economical production and high catalytic efficiency suggested the industrial application of this novel nanocatalyst because the resulting anilines are highly important for the chemical industry, dye industry and life sciences.

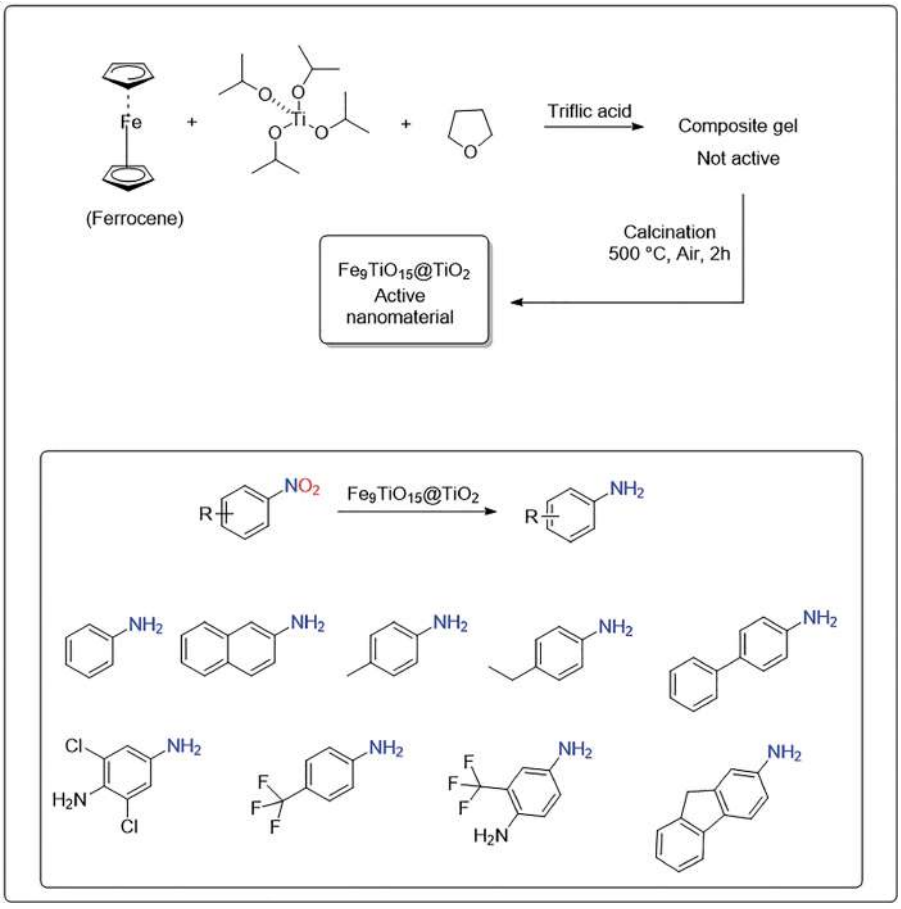

Figure 4.22: Fe-based highly efficient nanostructures for the reduction reaction.

As described earlier, 1,2,3-triazollic moiety has a wide range of applications in a number of scientific domains including drug delivery in biological and medicinal chemistry. Accordingly, a number of heterogeneous and homogeneous copper catalysts have successfully been prepared for the regioselective synthesis of 1,4-disubstituted 1,2,3-triazoles [53]. In addition to the conventionally used copper catalyst, a number of NPs-based nanocatalytic structures have been developed. Recently, the Ni-catalyzed preparation of 1,2,3-triazoles has emerged as an alternative methodology to avoid the issues of Cu contamination, especially in biological systems [54].

However, the Ni-based variant of cycloaddition reaction is less efficient because it produces a mixture of both regeoisomers. A Ni-catalyst supported on rGO-furnished poor yield of triazole however, its catalytic performance was better in cross-coupling reactions. At the same time, microporous zeolites have emerged as versatile host materials for the preparation of a novel catalyst. They show high hydrothermal stability, surface area, and intrinsic nanosized pore cavities for mass transport. A novel Ni-zeolite nanocatalyst provided only 52% maximum yield when employed as a catalyst for cycloaddition reactions. Considering these facts, Choudhury et al. [55] envisioned that rGO-zeolite hybrid could act as better support for Ni-NPs for high catalytic performance. They prepared a recyclable, robust and efficient heterogeneous catalyst Ni–rGO–zeolite nanocomposite. Initially, they performed protonation of Na–Y–zeolite for the preparation of GO–zeolite hybrid. Afterward, Ni-acetate was added under reducing conditions. Subsequently, the GO was converted to rGO along with the formation of Ni (0). The as-prepared nanocomposite was employed as heterogeneous catalyst for regioselective preparation of 1,2,3-triazoles (Figure 4.23). The nanocomposite was found to be highly efficient in aqueous media.

As described earlier, the preparation of novel nanocatalysts by incorporating metal NPs on a support has become a focused research area in nanotechnology. The development of new methods for the preparation and recyclization of catalysts has become hot research area for environmental remediation and chemical synthesis [56, 57]. In a recent report, Daraie et al. [58] disclosed a novel heterogeneous nanocomposite efficiently catalyzing KA^2 and A^3 coupling reactions and cycloaddition reactions. They used Fe_3O_4/g-C_3N_4/alginate as substrate immobilized Ag-NPs for the preparation of novel nanocomposite (Figure 4.24). The as-prepared nanostructure efficiently catalyzed the cycloaddition reactions. Further, it also efficiently catalyzed $KA^2$and A^3 coupling reactions in reagent-free aqueous conditions. No loss of catalytic activity was observed even after several runs, suggesting the nanocomposite as an efficient, highly selective, and ecofriendly nanocatalyst.

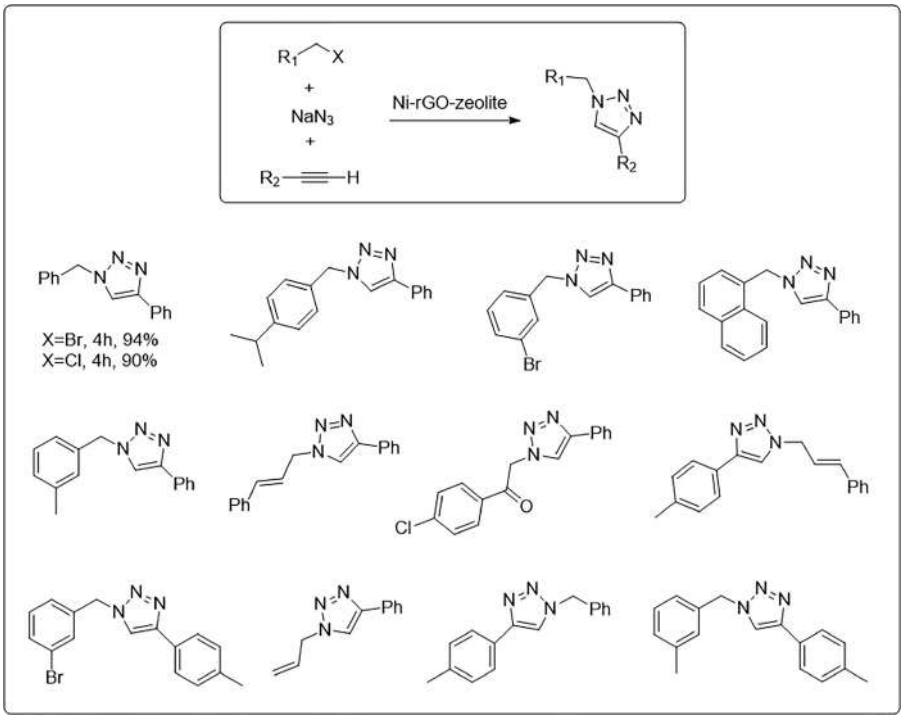

Figure 4.23: Ni–rGO–zeolite-mediated synthesis of triazoles.

4.4 Quantum dots as heterogeneous nanocatalysts

4.4.1 Quantum dots as nanocatalysts in catalytic degradation

As described earlier, a number of organic pollutants including synthetic dye in wastewaterare photocatalytically degraded using various types of metallic NPs. The photocatalytic degradation process is controlled by the band-gap of semiconducting metal oxides. However, generally the metal oxide NPs have low water solubility and are carcinogenic in nature. They lose their photocatalytic efficiency after several cycles and their remains become toxic for aquatic organisms. Other demerits include expensive precursors and high energy-consuming methods for their production. The research area of environmental pollution remediation has been revolutionized with the introduction of heterogeneous semiconductor photocatalysis. This approach efficiently degrade organic pollutants without causing the production of secondary pollutants [59, 60].

The semiconductor quantum dots (QDs) exhibit exceptionally catalytic potential due to high surface area, small size and quantum confinement effects. In recent years,

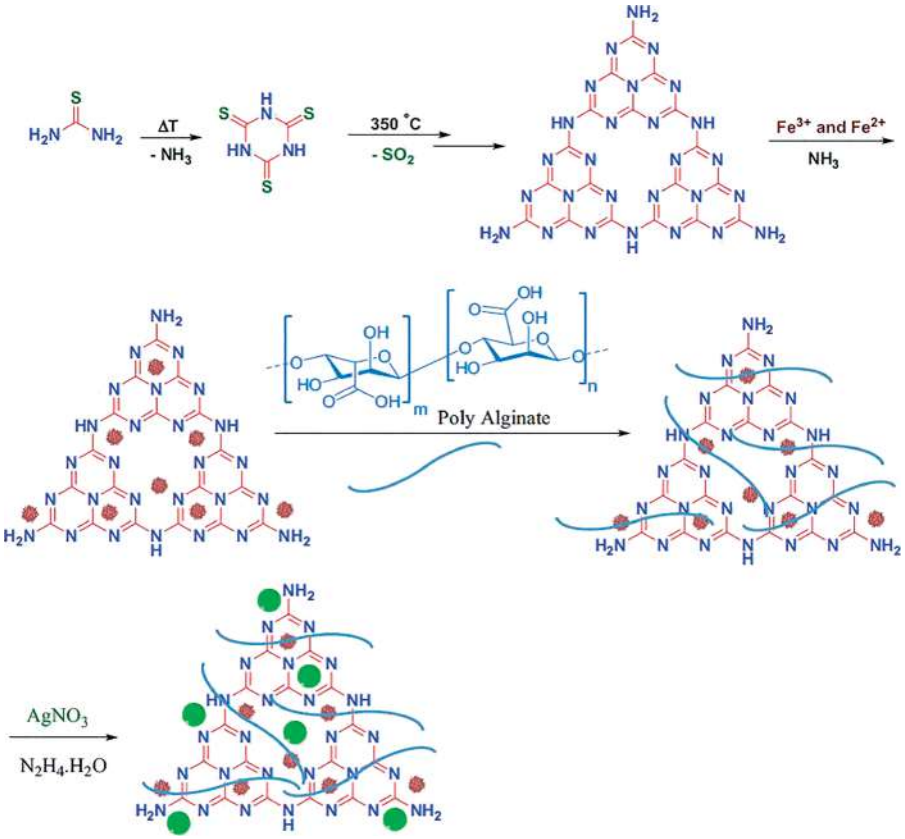

Figure 4.24: Preparation of Ag incorporated nanocomposite [58].

the graphene quantum dots (GQDs) have shown promising application in drug delivery, bioimaging and electrochemical sensing, and so on due to its zero-dimensional surface and biocompatible nature. The GQDs have emerged as a new type of nanomaterials with photo-luminescence properties [61]. Mandal et al. [62] used pyrocatechol for the preparation of GQDs at different pH. The prepared GQDs were used for the photocatalytic degradation of methyl orange and methyl blue under visible light radiation (Figure 4.25). The dye degradation process was optimized by varying GQDs dosage, reaction time, and pH of the GQDs. At pH 10, the successfully prepared GQDs were 8 nm in size and spherical in shape. Thus, the GQDs exhibited photocatalytic degradation of dyes and future applications for wastewater treatment.

The photoexcitation generates electron–hole pairs which provide the unique catalytic potential to transition metal sulfides such as zinc sulfide (ZnS). ZnS shows a high negative reduction potential compared to TiO_2 and ZnO. The easy excess of electron–hole pair in sulfide nanomaterials highlights their superior photocatalytic activity. The higher conduction band position in photocatalyst causes high negative

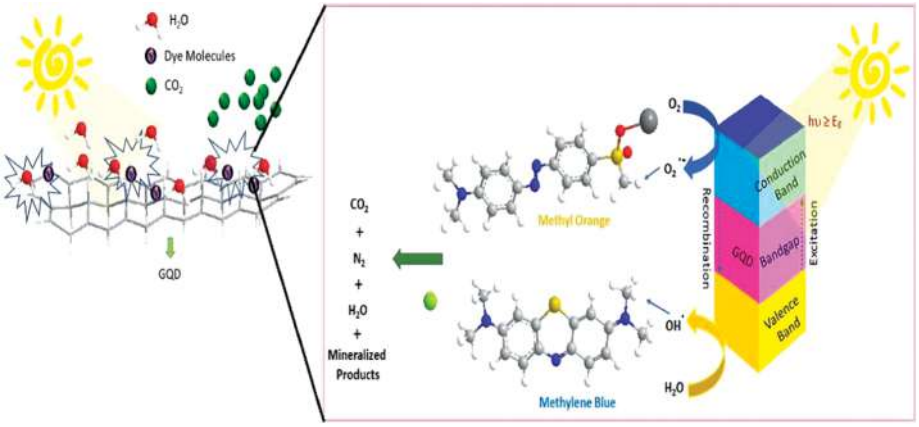

Figure 4.25: Photocatalytic action of GQDs [62].

reduction potential in aqueous solution [63]. The photocatalytic activities, mechanical stability, and morphology of nanostructures could easily be tuned through functionalization with different chemical agents. Efforts have been made to control the optoelectronic properties without the involvement of hazardous chemical capping agents.

Sood et al. [64] used a simple sol–gel method for chemical-free preparation of TiO_2 QDs. The as-prepared QDs were around 8 nm in size and highly crystalline in nature. Under UV irradiation, the QDs displayed excellent photocatalytic degradation of indigo carmine dye in aqueous media. The maximum catalytic activity was observed under acidic conditions with pseudo first-order kinetic. Very recently, Rafiq et al. [65] used simple and fast co-precipitation methods for the preparation of ZnS-QDs using 2-mercaptoethanol as a capping agent. The prepared ZnS-QDs were 4.2 nm with rhombohedral cubic structure. However, the capped ZnS were nanorod shaped. The Fourier-transform infrared spectroscopy (FTIR) analysis confirmed strong chemical bonding and functional group on the surface of prepared QDs. The prepared ZnS-QDs were suggested to show effective degradation of organic pollutants of leather, textile and chemical industries. The reported procedure provided guidelines for the preparation of ZnS-QDs with controlled band gap and structural morphology.

Due to some unique properties like high water solubility, photoluminescence activity, easy surface functionalization, and non-toxic nature the CDs have become attractive entities over the last decade. Therefore, CDs have found wide applications in bioimaging, drug delivery, and photocatalysis. They are prepared using the bottom-up approach which relies on CD synthesis from smaller units while the top-down approach means breaking of big structures into NPs (Figure 4.26). They have been employed as photocatalysts after doping with certain metal ions (Cu, Pi, and Zn) and

heteroatoms (N, P, and S). The doping promotes redox reactions on CDs surface which infect improve the electron acceptance and donation capacity (Figure 4.27) [66, 67]. Owing to such properties, the CDs are frequently used in hydrogen generation and industrial effluent treatments. The CDs-mediated photodegradation could be classified as (a) CDs as up-conversion materials, (b) CDs as electron accepter/mediators, (c) CDs as photo sensitizers, and (d) CDs as photocatalysts (Figure 4.28).

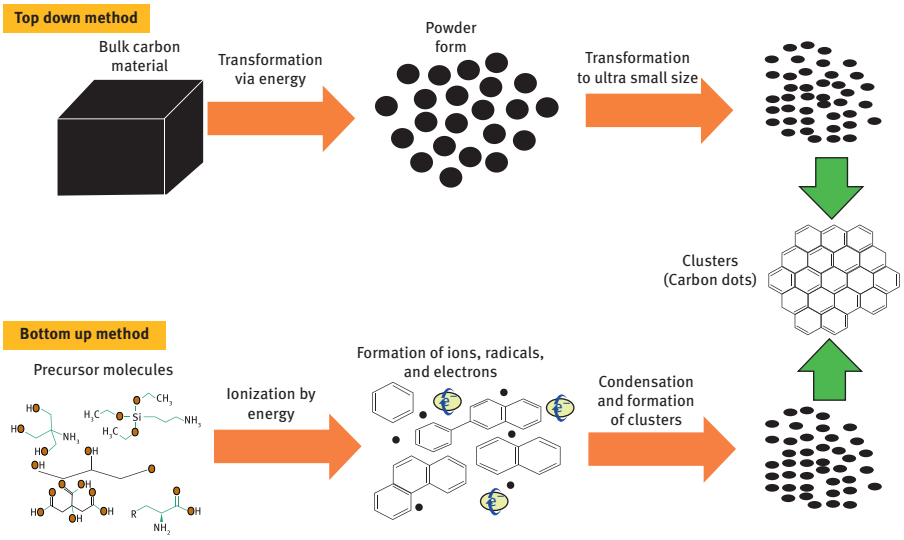

Figure 4.26: Synthetic methods for the preparation of carbon dots [66].

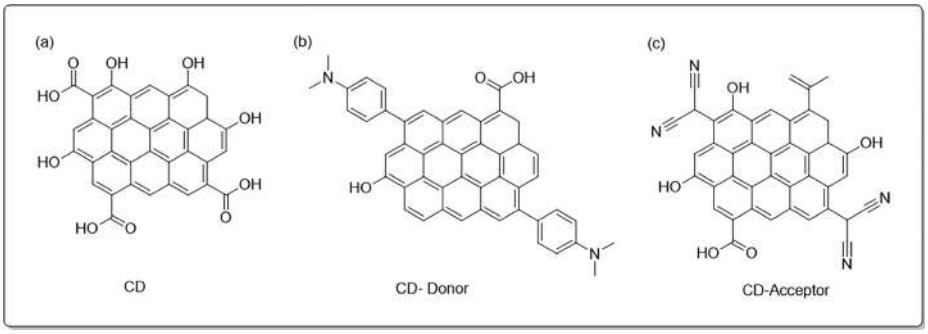

Figure 4.27: CDs with electron acceptance and donation capacity.

The bare CDs are not generally used for the photodegradation of organic pollutants and only the hybrids of CDs are utilized for this purpose. Sharma et al. [68] performed photodegradation of antibiotic and synthetic dye pollutants using

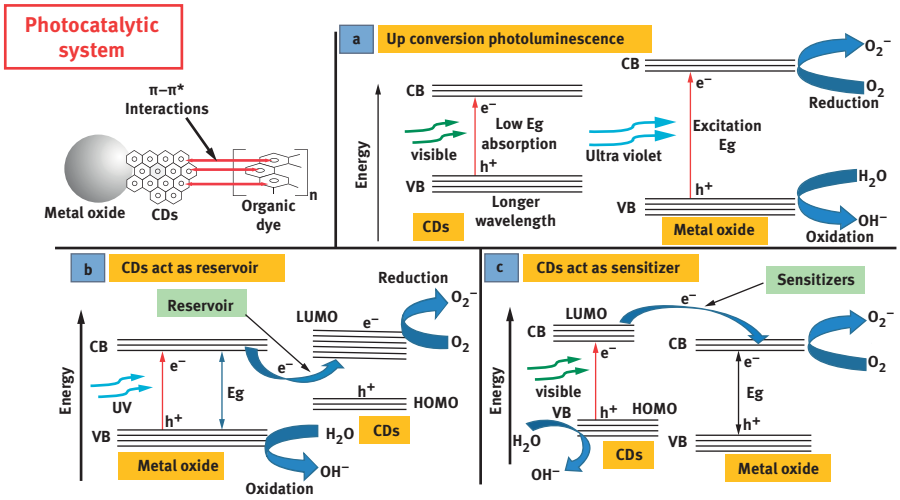

Figure 4.28: Mechanistic approaches for CD-based photocatalysis [66].

trimetallic hybrids of CDs using visible light. The CDs mediated photocatalytic degradationremoved malachite green dye (75%) and ampicillin antibiotic (45%) in just 4 h. During light absorbing event, semiconductors produce and donate photogenerated electrons to CDs causing an effective charge separation. The charge separation directly boast the photodegradation capacity of photocatalyst. Di et al., in 2015 [69], used Bi_2WO_4 and its hybrid with CDs for photocatalytic degradation of antibiotics such as TC and ciprofloxacin, and organic pollutants like bis-phenol a and b and rhodamine dye under visible light. The CDs/Bi_2WO_4 hybrid was found highly efficient photocatalyst for the photo degradation of organic dye and antibiotics in aqueous solution.

In another study, CDs/Zn hybrids were used for photocatalytic degradation of organic pollutants including ciprofloxacin, rhodamine B and methylene blue under visible light irradiation [70]. Here again, the enhanced charge separation and role of CDs in light absorption was reported as a major factor for photodegradation of organic molecules. The CDs absorb visible light and emit it in the form of shorter wavelength which is subsequently absorbed by semi-conductor where electron–hole pairs are generated. This phenomenon enhances the photocatalytic degradation of organic pollutants. Nanostructures of ZnS have become attractive semi-conductors for photocatalytic applications owing to their high stability, non-toxic nature, and wide band gaps. They show high redox potential because they rapidly produce maximum photo-generated electron–hole pairs under visible light [71, 72]. Thus, they can act as heterogeneous catalysts for photodegradation of organic effluents. Keeping these facts in mind, Wei et al. [73] used the hydrothermal method for the preparation of ZnS-QDs. The prepared QDs were used as

photocatalysts for the degradation ciprofloxacin under UV radiation, the prepared QDs efficiently degraded organic pollutants however its catalytic activity was only 45% under visible light. Thus the prepared QDs were suggested as efficient photocatalysts for the degradation of antibiotics in wastewater effluents. Rajabi et al. [74] disclosed a water-based preparation of ZnS-QDs using a sono-assisted chemical precipitation method. The successfully prepared pure and doped ZnS-QDs using 1-cysteine as a capping agent. The sono-assisted preparation methods proceeded efficiently in a short reaction time at room temperature. The as-prepared QDs were further employed as catalysts for the photodegradation of synthetic dye contaminants (Vitoria blue R). Under UV radiation, the maximum photocatalytic degradation of dye was observed at 10.5 pH with the minimum QDs amount. The photodegradation properties of the QDs were retained with a low percentage of dopants.

4.4.2 QDs as nanocatalysts in organic synthesis

Over the last few decades, the phenomenal advancements in photo redox catalysis have revolutionized the synthetic chemistry. This important tool has given excess to different complex molecules through simpler and greener new routes. To this end, semiconductor QDs have become interesting candidates due to broader absorption spectra, long-lived excited states, and high photostability [75, 76]. The controlled morphology could help to the tune redox potential of QDs even for single specific photochemical reactions. As described earlier, the readily available elements like S, Se, Zn, and Cd could easily be used for the preparation of QDs which could subsequently be functionalized differently [77]. However, the QDs remain unexplored for application in C–C bond forming redox reactions. Caputo et al., in 2017 (78), explored the C–C bond forming reactions using low loading of CdSe QDs as redox photocatalyst. The prepared QDs serve as metal free, robust, and efficient photoredox catalysts for at least five photo-assisted redox reactions namely decarboxylative radical formation, amine arylation, dehalogenation, β-amino alkylation, and β-alkylation. The single-sized tested QDs advantageously replaced frequently used Ru- and Ir-based photoredox catalysts for the aforementioned organic reactions. The quinazolinones have become promising motifs in a variety of biopotent molecules displaying a range of bioactivities like antimicrobial, antiviral, and anticancer [79, 80]. Classically, they are prepared using hazardous oxidants and chemically unstable aldehydes as precursors. As an alternative strategy, a two-step oxidation pathway has been developed which requires a highly selective and efficient catalyst. The high yielding approach lost its efficacy due to the involvement of precious metal-based catalyst, complex workup, hazardous waste, and organic solvents [81, 82].

Therefore, great attention has been diverted for developing greener and sustainable methods. So, it is highly desirous to prepare economical, stable, and recyclable

heterogeneous catalysts for organic synthesis in an aqueous media. Majumdar et al., in 2018 [83], reported Fe_2O_3-CD nanocomposites as a magnetically recoverable and biocompatible catalyst for the preparation of quinazolinones in an aqueous medium. The CDs were used as stabilizing agents for Fe_2O_3-NPs and the nanosystems acted as heterogeneous catalysts in cyclooxidative tandem reactions. The high yields of the quinazolinones under control experiments confirmed the synergistic role of CDs in the catalytic activity of the nanocomposites. Further, the catalyst was used over several cycles and recovered efficiently due to its inherent magnetic nature.

The nanosized and tunable phase behavior have been made as CDs for promising materials as support or catalyst. They have emerged as an alternative to conventional heterogeneous supports due to their thermostable nature, high surface area, and tunable functionalities. So, they could act as economical and ecofriendly supports for metal-based catalysts. The CDs as sub-nanometric carbonaceous supports could add advantages of both homogeneous and heterogeneous catalysis [84]. Very recently, Rezaei et al., in 2021 [85], performed selective oxidative cleavage of alkenes for the preparation of aldehydes using tungstate-decorated amphiphilic CDs as pseudo-homogeneous catalyst (Figures 4.29 and 4.30). This amphiphilic nanocatalyst was prepared through one-step hydrothermal method. The oxidative organic transformation was executed using H_2O_2 and water as green oxidant, and the novel catalyst exhibited high recycle ability.

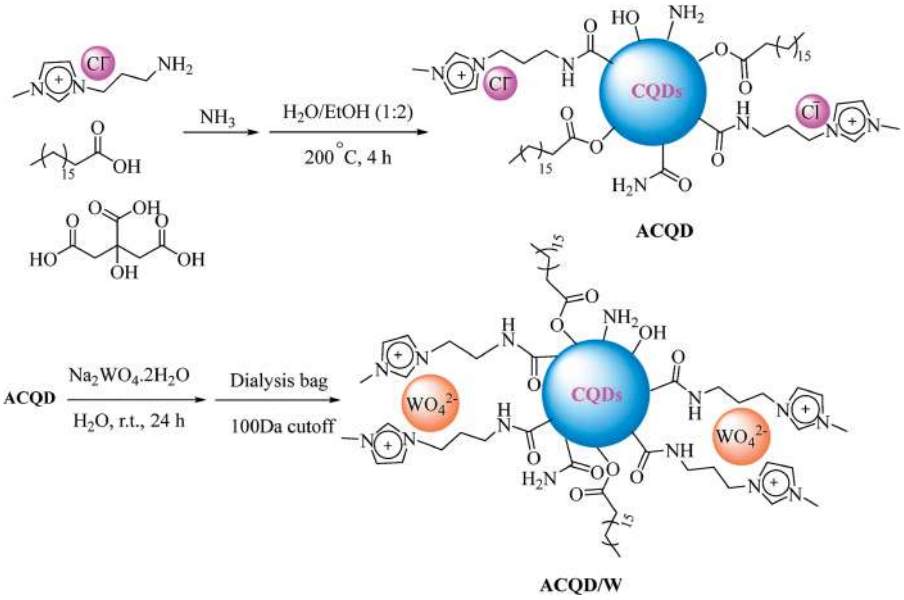

Figure 4.29: Preparation of amphiphilic CDs as pseudo-homogeneous nanocatalyst [85].

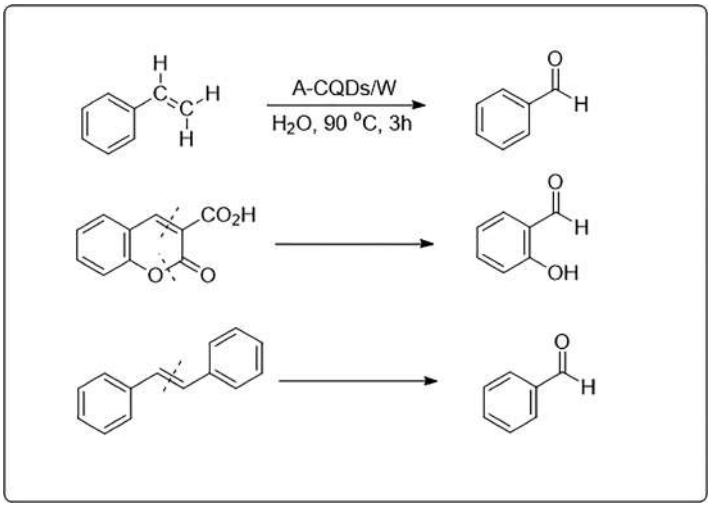

Figure 4.30: Oxidative cleavage of alkenes.

Over the last few decades, arylboronates have become promising building blocks in medicinal chemistry, material science, and synthetic organic chemistry. Their preparation through classical approaches requires highly anhydrous conditions and produces higher amounts of metal-containing wastes. The other highly robust and efficient alternative methods require heavy metal-based catalysts. Thus, it has been desirous to develop economical, scalable, and greener methods for the preparation of arylboronates [86]. As described earlier, the outlook of synthetic chemistry has greatly been influenced by the photoredox catalysis. The QDs have become superior next-generation photocatalysts for a variety of organic reactions. Chandrashekar et al. [87] successfully performed borylation of diazonium salts using water-soluble 3-mercaptopropionic acid capped CdSe-QDs in aqueous media (Figure 4.31). The catalyst exhibited high catalytic activity, reusability, and high photostability.

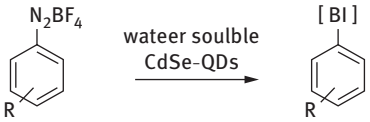

Figure 4.31: CdSe-QDs-mediated borylation reactions.

4.5 Conclusions

The ever-increasing potential of nanoscience has facilitated the economical and ecofriendly development of highly efficient nanocatalysts for synthetic chemistry and pollutant remediation applications. Various synthetic approaches have been developed to calibrate the size, shape, and intrinsic properties of nanostructures for selective applications. Herein, NPs, nanocomposites, and QD have been presented as efficient heterogeneous catalysts in aqueous-mediated cross-coupling, cycloaddition reactions, and photocatalytic degradation of organic pollutants. The latest examples regarding the facile preparation of nanocatalysts and case studies about their applications as heterogeneous catalysts validate the revolutionary concept of nanocatalysis in synthesis and water purification studies.

References

[1] Butler, RN, Coyne, AG. Water: Nature's Reaction Enforcer-Comparative Effects for Organic Synthesis "In-Water" and "On-Water". Chem Rev, 2010, 110, 6302–6337.
[2] Akiya, N, Savage, PE. Roles of water for chemical reactions in high-temperature water. Chem Rev, 2002, 102, 2725–2750.
[3] Chang, CR, Huang, ZQ, Li, J. The promotional role of water in heterogeneous catalysis: Mechanism insights from computational modeling. Wiley Interdiscip Rev Comput Mol Sci, 2016, 6, 679–693.
[4] Liu, M, Liu, M, Wang, X, Kozlov, SM, Cao, Z, De, LP. et al., Quantum-dot-derived catalysts for CO_2 reduction reaction. Joule, 2019, 3, 1703–1718.
[5] Chen, C, Yan, X, Wu, R, Wu, Y, Zhu, Q, Hou, M. et al., Quasi-square-shaped Cadmium Hydroxide Nanocatalysts for Electrochemical CO2 Reduction with High Efficiency. Chem Sci, 2021, 12 (35), 11914–11920.
[6] Prinsen, P, Luque, R. Introduction to Nanocatalysts. Nanoparticle Design and Characterization for Catalytic Applications in Sustainable Chemistry, 38, 2019, 1.
[7] Philippot, K, Serp, P. Concepts in nanocatalysis. In: Philippe Serp, Karine Philippot (eds.). Nanomaterials in catalysis. First Edition. Wiley-VCH Verlag & Co., Weinheim, Germany, 2013, 1–54.
[8] Zeng, HC. Hierarchy Concepts in Design and Synthesis of Nanocatalysts. ChemCatChem, 2020, 12, 5303–5311.
[9] Rodrigues, TS, da Silva, AG, Camargo, PH. Nanocatalysis by noble metal nanoparticles: Controlled synthesis for the optimization and understanding of activities. J Mater Chem A, 2019, 7, 5857–5874.
[10] Astruc, D. Introduction: Nanoparticles in catalysis. Chem Rev, 2020, 120, 461–463.
[11] Shenashen, MA, El-Safty, SA, Elshehy, EA. Synthesis, morphological control, and properties of silver nanoparticles in potential applications. Part Part Syst Charact, 2014, 31, 293–316.
[12] Beyene, HD, Werkneh, AA, Bezabh, HK, Ambaye, TG. Synthesis paradigm and applications of silver nanoparticles (AgNPs), a review. Sustainable Mater Technol, 2017, 13, 18–23.
[13] Kalantari, K, Afifi, ABM, Bayat, S, Shameli, K, Yousefi, S, Mokhtar, N. et al., Heterogeneous catalysis in 4-nitrophenol degradation and antioxidant activities of silver nanoparticles embedded in Tapioca starch. Arabian J Chem, 2019, 12, 5246–5252.

[14] Chen, M, Ding, W, Wang, J, Diao, G. Removal of azo dyes from water by combined techniques of adsorption, desorption, and electrolysis based on a supramolecular sorbent. Ind Eng Chem Res, 2013, 52, 2403–2411.
[15] Singh, PK, Singh, RL. Bio-removal of azo dyes: A review. Internat J Appl Sci Biotech, 2017, 5, 108–126.
[16] Kgatle, M, Sikhwivhilu, K, Ndlovu, G, Moloto, N. Degradation Kinetics of Methyl Orange Dye in Water Using Trimetallic Fe/Cu/Ag Nanoparticles. Catalysts, 2021, 11, 428.
[17] Liu, Y, Guo, W, Guo, H, Ren, X, Cu, XQ. (II)-doped V_2O_5 mediated persulfate activation for heterogeneous catalytic degradation of benzotriazole in aqueous solution. Sep Purif Technol, 2020, 230, 115848.
[18] Veisi, H, Abassi, P, Mohammadi, P, Tamoradi, T, Karmakar, B. Gold nanoparticles decorated biguanidine modified mesoporous silica KIT-5 as recoverable heterogeneous catalyst for the reductive degradation of environmental contaminants. Sci Rep, 2021, 11, 1–17.
[19] Shabir, J, Rani, S, Sharma, M, Garkoti, C, Mozumdar, S. Synthesis of dendritic fibrous nanosilica over a cubic core (cSiO 2@ DFNS) with catalytically efficient silver nanoparticles for reduction of nitroarenes and degradation of organic dyes. RSC Adv, 2020, 10, 8140–8151.
[20] Chetia, M, Ali, AA, Bordoloi, A, Sarma, D. Facile route for the regioselective synthesis of 1, 4-disubstituted 1, 2, 3-triazole using copper nanoparticles supported on nanocellulose as recyclable heterogeneous catalyst. J Chem Sci, 2017, 129, 1211–1217.
[21] Rajabi-Moghaddam, H, Naimi-Jamal, M, Tajbakhsh, M. Fabrication of copper (II)-coated magnetic core-shell nanoparticles Fe 3 O 4@ SiO 2-2-aminobenzohydrazide and investigation of its catalytic application in the synthesis of 1, 2, 3-triazole compounds. Sci Rep, 2021, 11, 1–14.
[22] Paplal, B, Nagaraju, S, Palakollu, V, Kanvah, S, Kumar, BV, Kashinath, D. Synthesis of functionalized 1, 2, 3-triazoles using Bi_2 WO_6 nanoparticles as efficient and reusable heterogeneous catalyst in aqueous medium. RSC Adv, 2015, 5, 57842–57846.
[23] Khan, M, Albalawi, GH, Shaik, MR, Khan, M, Adil, SF, Kuniyil, M. et al., Miswak mediated green synthesized palladium nanoparticles as effective catalysts for the Suzuki coupling reactions in aqueous media. J Saudi Chem Soc, 2017, 21, 450–457.
[24] Jin, T, Hicks, M, Kurdyla, D, Hrapovic, S, Lam, E, Moores, A. Palladium nanoparticles supported on chitin-based nanomaterials as heterogeneous catalysts for the Heck coupling reaction. Beilstein J Org Chem, 2020, 16, 2477–2483.
[25] Ng, WJ Industrial wastewater treatment: World Scientific 2006.
[26] Lu, F, Astruc, D. Nanocatalysts and other nanomaterials for water remediation from organic pollutants. Coord Chem Rev, 2020, 408, 213180.
[27] Zhao, B, Li, H, Li, Z, Ge, S, Qin, X, Zhang, S. et al, Green strategy of scaleably synthesizing copper nanocomposites with remarkable catalytic activity for wastewater treatment. J Mater Sci Technol, 2021, Volume 95, 158–166.
[28] Aldalbahi, A, El-Naggar, M, Khattab, T, Abdelrahman, M, Rahaman, M, Alrehaili, A. et al., Development of green and sustainable cellulose acetate/graphene oxide nanocomposite films as efficient adsorbents for wastewater treatment. Polymers, 2020, 12, 2501.
[29] Maham, M, Nasrollahzadeh, M, Sajadi, SM. Facile synthesis of Ag/ZrO2 nanocomposite as a recyclable catalyst for the treatment of environmental pollutants. Composites Part B: Eng, 2020, 185, 107783.
[30] Kumar, G, Masram, DT. Sustainable Synthesis of MOF-5@ GO Nanocomposites for Efficient Removal of Rhodamine B from Water. ACS Omega, 2021, 6, 9587–9599.
[31] Jinendra, U, Bilehal, D, Nagabhushana, B, Kumar, AP. Adsorptive removal of Rhodamine B dye from aqueous solution by using graphene–based nickel nanocomposite. Heliyon, 2021, 7, e06851.

[32] Akpotu, SO, Oseghe, EO, Ayanda, OS, Skelton, AA, Msagati, TA, Ofomajam, AE. Photocatalysis and biodegradation of pharmaceuticals in wastewater: Effect of abiotic and biotic factors. Clean Technol Environ Policy, 2019, 21, 1701–1721.
[33] Renita, AA, Kumar, PS, Srinivas, S, Priyadharshini, S, Karthika, M. A review on analytical methods and treatment techniques of pharmaceutical wastewater. Desalination and Water Treatment, 2017, 87, 160–178.
[34] Nasseh, N, Taghavi, L, Barikbin, B, Nasseri, MA, Allahresani, A. FeNi3/SiO2 magnetic nanocomposite as an efficient and recyclable heterogeneous fenton-like catalyst for the oxidation of metronidazole in neutral environments: Adsorption and degradation studies. Composites Part B: Eng, 2019, 166, 328–340.
[35] Wang, J, Zhuan, R. Degradation of antibiotics by advanced oxidation processes: An overview. Sci Total Environ, 2020, 701, 135023.
[36] Shao, S, Wu, X. Microbial degradation of tetracycline in the aquatic environment: A review. Crit Rev Biotechnol, 2020, 40, 1010–1018.
[37] Kyzas, GZ, Deliyanni, EA, Matis, KA. Graphene oxide and its application as an adsorbent for wastewater treatment. J Chem Technol Biotechnol, 2014, 89, 196–205.
[38] Thakur, K, Kandasubramanian, B. Graphene and graphene oxide-based composites for removal of organic pollutants: A review. J Chem Eng Data, 2019, 64, 833–867.
[39] Hu, X, Zhao, Y, Wang, H, Tan, X, Yang, Y, Liu, Y. Efficient removal of tetracycline from aqueous media with a Fe3O4 nanoparticles@ graphene oxide nanosheets assembly. Int J Environ Res Public Health, 2017, 14, 1495.
[40] Aksu, Z. Application of biosorption for the removal of organic pollutants: A review. Process Biochem, 2005, 40, 997–1026.
[41] Fomina, M, Gadd, GM. Biosorption: Current perspectives on concept, definition and application. Bioresour Technol, 2014, 160, 3–14.
[42] Biosorption:, TE. A review of the latest advances. Processes, 2020, 8, 1584.
[43] Gopal, G, Roy, N, Chandrasekaran, N, Mukherjee, A. Photo-assisted removal of tetracycline using bio-nanocomposite-immobilized alginate beads. ACS Omega, 2019, 4, 17504–17510.
[44] Shi, J. On the synergetic catalytic effect in heterogeneous nanocomposite catalysts. Chem Rev, 2013, 113, 2139–2181.
[45] Narayanan, R. Synthesis of green nanocatalysts and industrially important green reactions. Green Chem Lett Rev, 2012, 5, 707–725.
[46] Zhao, Z, Dai, Y, Ge, G, Mao, Q, Rong, Z, Wang, G, Facile, A. Approach to Fabricate an N-Doped Mesoporous Graphene/Nanodiamond Hybrid Nanocomposite with Synergistically Enhanced Catalysis. ChemCatChem, 2015, 7, 1070–1077.
[47] Zhang, K, Suh, JM, Lee, TH, Cha, JH, Choi, JW, Jang, HW. et al., Copper oxide–graphene oxide nanocomposite: Efficient catalyst for hydrogenation of nitroaromatics in water. Nano Convergence, 2019, 6, 1–7.
[48] Soares, PI, Lochte, F, Echeverria, C, Pereira, LC, Coutinho, JT, Ferreira, IM. et al., Thermal and magnetic properties of iron oxide colloids: Influence of surfactants. Nanotechnol, 2015, 26, 425704.
[49] Kuang, Y, Wang, Q, Chen, Z, Megharaj, M, Heterogeneous, NR. Fenton-like oxidation of monochlorobenzene using green synthesis of iron nanoparticles. J Colloid Interface Sci, 2013, 410, 67–73.
[50] Rajabi, F, Karimi, N, Saidi, MR, Primo, A, Varma, RS, Luque, R. Unprecedented selective oxidation of styrene derivatives using a supported iron oxide nanocatalyst in aqueous medium. Adv Synth Catal, 2012, 354, 1707–1711.

[51] Wei, J, Sun, J, Wen, Z, Fang, C, Ge, Q, Xu, H. New insights into the effect of sodium on Fe_3O_4-based nanocatalysts for CO 2 hydrogenation to light olefins. Catal Sci Technol, 2016, 6, 4786–4793.
[52] Sohail, M, Tahir, N, Rubab, A, Beller, M, Sharif, M. Facile Synthesis of Iron-Titanate Nanocomposite as a Sustainable Material for Selective Amination of Substitued Nitro-Arenes. Catalysts, 2020, 10, 871.
[53] Farooq, T Advances in Triazole Chemistry: Elsevier Science 2020.
[54] Miura, T, Yamauchi, M, Murakami, M. Nickel-catalysed denitrogenative alkyne insertion reactions of N-sulfonyl-1, 2, 3-triazoles. Chem Commun, 2009, 12, 1470–1471.
[55] Choudhury, P, Chattopadhyay, S, De, G, Basu, B. Ni–rGO–zeolite nanocomposite: An efficient heterogeneous catalyst for one-pot synthesis of triazoles in water. Mater Adv, 2021, 2, 3042–3050.
[56] White, RJ, Luque, R, Budarin, VL, Clark, JH, Macquarrie, DJ. Supported metal nanoparticles on porous materials. Methods and applications. Chem Soc Rev, 2009, 38, 481–494.
[57] Ndolomingo, MJ, Bingwa, N, Meijboom, R. Review of supported metal nanoparticles: Synthesis methodologies, advantages and application as catalysts. J Mater Sci, 2020, 55, 6195–6241.
[58] Daraie, M, Heravi, MM, Mohammadi, P, Daraie, A. Silver incorporated into g-C3N4/Alginate as an efficient and heterogeneous catalyst for promoting click and A3 and KA2 coupling reaction. Sci Rep, 2021, 11, 14086.
[59] Chatterjee, D, Dasgupta, S. Visible light induced photocatalytic degradation of organic pollutants. J Photochem Photobiol C: Photochem Rev, 2005, 6, 186–205.
[60] Pirilä, M, Saouabe, M, Ojala, S, Rathnayake, B, Drault, F, Valtanen, A. et al., Photocatalytic degradation of organic pollutants in wastewater. Topics in Catal, 2015, 58, 1085–1099.
[61] Yan, Y, Gong, J, Chen, J, Zeng, Z, Huang, W, Pu, K. et al., Recent advances on graphene quantum dots: From chemistry and physics to applications. Adv Mater, 2019, 31, 1808283.
[62] Mandal, P, Nath, KK, Saha, M. Efficient Blue Luminescent Graphene Quantum Dots and their Photocatalytic Ability Under Visible Light. Biointerface Res Appl Chem, 2021, 11, 8171–8178.
[63] Fang, X, Zhai, T, Gautam, UK, Li, L, Wu, L, Bando, Y. et al., ZnS nanostructures: From synthesis to applications. Prog Mater Sci, 2011, 56, 175–287.
[64] Sood, S, Kumar, S, Umar, A, Kaur, A, Mehta, SK, Kansal, SK. TiO_2 quantum dots for the photocatalytic degradation of indigo carmine dye. J Alloys Compd, 2015, 650, 193–198.
[65] Rafiq, A, Imran, M, Ikram, M, Naz, M, Aqeel, M, Majeed, H. et al., Photocatalytic and catalytic degradation of organic dye by uncapped and capped ZnS quantum dots. Mater Res Express, 2019, 6, 055801.
[66] Sharma, A, Das, J. Small molecules derived carbon dots: Synthesis and applications in sensing, catalysis, imaging, and biomedicine. J Nanobiotechnol, 2019, 17, 1–24.
[67] Akbar, K, Moretti, E, Vomiero, A. Carbon Dots for Photocatalytic Degradation of Aqueous Pollutants: Recent Advancements. Adv Opt Mater, 2021, 95, 2100532.
[68] Sharma, G, Bhogal, S, Naushad, M, Kumar, A, Stadler, FJ. Microwave assisted fabrication of La/Cu/Zr/carbon dots trimetallic nanocomposites with their adsorptional vs photocatalytic efficiency for remediation of persistent organic pollutants. J Photochem Photobiol A Chem, 2017, 347, 235–243.
[69] Di, J, Xia, J, Ge, Y, Li, H, Ji, H, Xu, H. et al., Novel visible-light-driven CQDs/Bi2WO6 hybrid materials with enhanced photocatalytic activity toward organic pollutants degradation and mechanism insight. Appl Catal B, 2015, 168, 51–61.
[70] Ming, F, Hong, J, Xu, X, Wang, Z. Dandelion-like ZnS/carbon quantum dots hybrid materials with enhanced photocatalytic activity toward organic pollutants. RSC Adv, 2016, 6, 31551–31558.

[71] Boxi, SS, Paria, S. Effect of silver doping on TiO 2, CdS, and ZnS nanoparticles for the photocatalytic degradation of metronidazole under visible light. RSC Adv, 2014, 4, 37752–37760.
[72] Khaparde, R, Acharya, S. Effect of isovalent dopants on photodegradation ability of ZnS nanoparticles. Spectrochim Acta A Mol Biomol Spectrosc, 2016, 163, 49–57.
[73] Wei, M, Yang, L, Yan, Y, Ni, L. Preparation of ZnS quantum dot photocatalyst and study on photocatalytic degradation of antibiotics. Mater Express, 2019, 9, 413–418.
[74] Rajabi, HR, Karimi, F, Kazemdehdashti, H, Kavoshi, L. Fast sonochemically-assisted synthesis of pure and doped zinc sulfide quantum dots and their applicability in organic dye removal from aqueous media. J Photochem Photobiol B, 2018, 181, 98–105.
[75] Pal, A, Ghosh, I, Sapra, S, König, B. Quantum dots in visible-light photoredox catalysis: Reductive dehalogenations and C–H arylation reactions using aryl bromides. Chem of Mater, 2017, 29, 5225–5231.
[76] Smyder, JA, Krauss, TD. Coming attractions for semiconductor quantum dots. Mater Today, 2011, 14, 382–387.
[77] Ranishenka, B, Ulashchik, E, Kruhlik, A, Tatulchenkov, MY, Radchanka, A, Shmanai, V. et al., Controlled Functionalization of Water-Soluble Semiconductor Quantum Dots for Bioconjugation. J Appl Spectrosc, 2020, 86, 1064–1070.
[78] Caputo, JA, Frenette, LC, Zhao, N, Sowers, KL, Krauss, TD, Weix, DJ. General and efficient C–C bond forming photoredox catalysis with semiconductor quantum dots. J Am Chem Soc, 2017, 139, 4250–4253.
[79] Reddy, MM, Sivaramakrishna, A. Remarkably flexible quinazolinones – Synthesis and biological applications. J Heterocycl Chem, 2020, 57, 942–954.
[80] Xing, Z, Wu, W, Miao, Y, Tang, Y, Zhou, Y, Zheng, L. et al., Recent advances in quinazolinones as an emerging molecular platform for luminescent materials and bioimaging. Org Chem Front, 2021, 8, 1867–1889.
[81] Ge, W, Zhu, X, Wei, Y. Iodine-catalyzed oxidative system for cyclization of primary alcohols with o-aminobenzamides to quinazolinones using DMSO as the oxidant in dimethyl carbonate. RSC Adv, 2013, 3, 10817–10822.
[82] Maiden, T, Harrity, J. Recent developments in transition metal catalysis for quinazolinone synthesis. Org Biomol Chem, 2016, 14, 8014–8025.
[83] Majumdar, B, Sarma, D, Jain, S, Sarma, TK. One-Pot Magnetic Iron Oxide–Carbon Nanodot Composite-Catalyzed Cyclooxidative Aqueous Tandem Synthesis of Quinazolinones in the Presence of tert-Butyl Hydroperoxide. ACS Omega, 2018, 3, 13711–13719.
[84] Liu, Z, Zhang, B, Yu, H, Wu, KH, Huang, X. Carbon Catalysis: Focus on Sustainable Chemical Technology. Front Chem, 2020, 8, 308.
[85] Rezaei, A, Hadian-Dehkordi, L, Samadian, H, Jaymand, M, Targhan, H, Ramazani, A. et al., Pseudohomogeneous metallic catalyst based on tungstate-decorated amphiphilic carbon quantum dots for selective oxidative scission of alkenes to aldehyde. Sci Rep, 2021, 11, 1–13.
[86] Merino, P, Tejero, T. Expanding the limits of organoboron chemistry: Synthesis of functionalized arylboronates. Angewandte Chemie International Edition, 2010, 49, 7164–7165.
[87] Chandrashekar, HB, Maji, A, Halder, G, Banerjee, S, Bhattacharyya, S, Maiti, D. Photocatalyzed borylation using water-soluble quantum dots. Chem Commun, 2019, 55, 6201–6204.

Puja Basak, Pranab Ghosh*

5 Metal-composite-catalyzed C–C coupling reactions in water

5.1 Introduction

Carbon–carbon (C–C) bond formation reactions are the essence of the synthesis in organic chemistry. Kolbe's fundamental laboratory-based C–C bond formation in 1845 for his well-known acetic acid synthesis played an important role in shaping chemical synthesis [1]. The enzymatic processes must take place in an aqueous environment in nature, but water has been avoided as a reaction medium in common organic synthesis. Since the historic study of Breslow for Diels–Alder reactions [2], the recognition of water as a solvent in C–C coupling reactions has been increased and proved to be advantageous over organic solvents [3]. Generally, protection and deprotection processes under aqueous solvent in organic synthesis can be simplified and there has already been great advance to understand the organic reaction in water at high temperatures, and its broad scopes vary from the source of life to energy and fuels to chemical synthesis [4]. In the twentieth century, carbon–carbon bond formation reactions have shown a new paradigm that has amplified the effectiveness of organic chemists appreciably in synthesizing complex molecular frameworks, which has substituted our thinking completely about organic synthesis. Based on transition metal catalysis, the C–C bond formation reactions joining functionalized and sensitive substrates are fundamental for organic molecule synthesis and provide new opportunities in medicinal chemistry as well as nanotechnology. In organic chemistry, the C–C coupling reaction is a general term for a wide variety of organic reactions, where in the presence of metal catalysts, two fragments are combined together. Generally, two types of coupling reactions have been identified: homocoupling and heterocoupling reactions. Homocoupling reaction occurs when two identical chemical species are joined together to afford a single product. Heterocoupling reaction (also known as cross-coupling) occurs when two dissimilar chemical species are combined to form a single product. Among the homocoupling reactions, the Wurtz reaction [5], Pinacol coupling reaction [6], Glaser coupling [7], and Ullmann reaction [8] are important. On the other hand, some important hetero C–C cross-coupling reactions include Cadiot–Chodkiewicz coupling [9], Castro–Stephens coupling [10], Corey–House synthesis [11], Kumada coupling [12], Heck reaction [13], Sonogashira coupling [14],

*Corresponding author: **Pranab Ghosh,** Department of Chemistry, University of North Bengal, Dist-Darjeeling, West Bengal, India, e-mail: pizy12@yahoo.com
Puja Basak, Department of Chemistry, University of North Bengal, Dist-Darjeeling, West Bengal, India.

https://doi.org/10.1515/9783110733846-005

Negishi coupling [15], Stille cross-coupling [16], Suzuki reaction [17], Murahashi coupling [18], Hiyama coupling [19], Fukuyama coupling [20], and Liebeskind–Srogl coupling [21]. Over the past 30 years, the development of C–C cross-coupling reactions catalyzed by transition metals has profoundly revolutionized the protocols for the synthesis of natural products, organic materials, and polymers (building blocks for supramolecular chemistry), and medicinal chemistry from simpler moieties. In 2010, E. Negishi, R. Heck, and A. Suzuki were awarded the Nobel Prize in chemistry for developing direct bond formation between carbon atoms (palladium-catalyzed C–C cross-coupling reaction). However, the growth of highly active catalysts has drawn much consideration for the development of efficient, green, and cost-effective synthesis in organic chemistry. Metal–nanoparticle (NP)-based catalysts can be assumed as an intermediate between homogeneous and heterogeneous catalysts, and they are considered half-heterogeneous catalysts [22]. Due to the small size of metal–NPs, they are not easily removed from the reaction mixture and this problem is usually solved by binding NPs with structural support. Therefore, there is a need for heterogeneous catalysts via immobilization of metal NPs on solid supports to achieve high catalytic activity, high mechanical and thermal stability, easy regeneration, and separation procedures [23–26]. Metal–NPs on structural support or metal-composite catalysts (composite materials are combinations of two or more materials having different phases) are being investigated as a new dimension of catalysis [27–29]. Normally, composites are composed of two types of different materials, one is called a binder or matrix, which binds the fragments together or fibers of the other materials and is termed reinforcement. If one of the combining elements of the composite is in the nanometer dimension, then it is called a nanocomposite [30]. As the subject is very vast, in this chapter, we have shown the application of different nanostructured materials as host elements for the heterogeneous PdNP-catalyzed Suzuki, Heck, and Sonogashira coupling reactions. This chapter generally covers the Pd chemistry of cross-coupling performed in water as the sole reaction medium or solvent.

5.2 General outline of C–C cross-coupling reaction mechanism

The mechanism of the C–C cross-coupling reaction generally comprises three important steps:

1. Oxidative addition
2. Transmetalation
3. Reductive elimination

The oxidative addition and reductive elimination are generally multistep processes as they involve ligand association and dissociation processes, respectively.

On the other hand, the transmetalation process involves ligand exchange between two metal centers.

5.2.1 Suzuki coupling

The Suzuki coupling is categorized as a C–C cross-coupling reaction, where two dissimilar fragments such as boronic acid and organohalide or triflate are combined to yield substituted biphenyls in the presence of palladium(0) complex catalyst [31]. The relative reactivity order of halides and triflate is R-I > R-OTf > R-Br ≫ R-Cl. Since its discovery in 1979, this reaction becomes utmost acceptable process for the carbon framework expansion in organic molecules. Suzuki–Miyaura coupling reaction is extremely helpful for the assembly of a conjugated diene, polyene systems, and biaryl systems with high stereoisomeric purity. Suzuki–Miyaura coupling using inactivated alkyl halides to form C (sp^2)–C (sp^3) and even C (sp^3)–C (sp^3) bonds has made incredible progress in the field of coupling reaction [32, 33]. The first step of the Suzuki coupling mechanism (Figure 5.1) is the oxidative addition of Pd(0) to the aryl halide (**1**) to form the organopalladium species (**2**). After that, intermediate (**3**) is formed by the reaction with a base, which again forms the organopalladium species via transmetalation (**4**) with the complex (boronate complex) formed by the reaction of boronic acid (**5**) with base. The last step is reductive elimination, which yields the biaryl

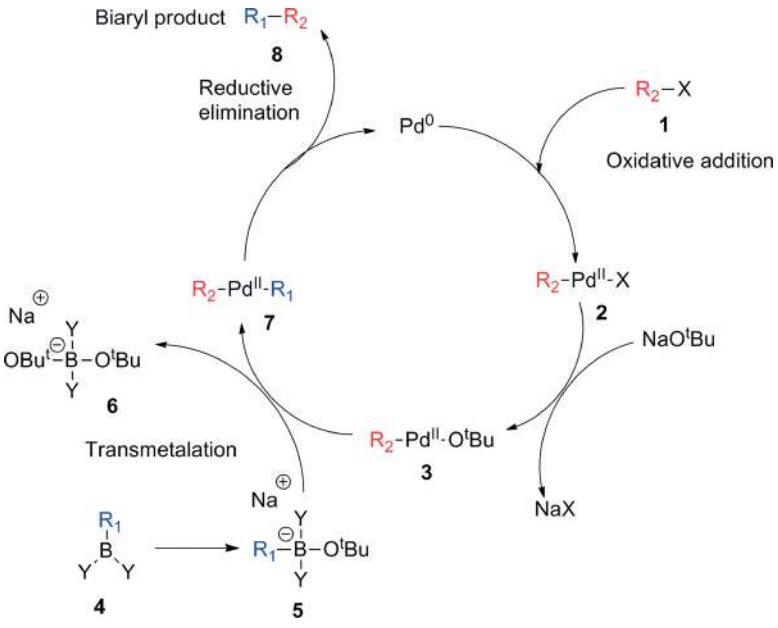

Figure 5.1: Suzuki coupling reaction mechanism.

product (**8**) and brings back the original Pd(0) catalyst. The Suzuki coupling reaction occurs in the presence of the base and the base has three roles in this coupling reaction: formation of the palladium complex, formation of trialkyl borate, and acceleration of the reductive elimination by the reaction with Pd complex.

5.2.2 Heck reaction

The Heck reaction is the cross-coupling reaction (also known as Mizoroki–Heck reaction), where halides or triflates with unsaturation are joined with an alkene to form substituted alkene in the presence of a base and a palladium (Pd^0) catalyst (or palladium nanomaterial-based catalyst) [34]. Tsutomu Mizoroki (1971) described the synthesis of stilbene (**11**) from iodobenzene (**9**) and styrene (**10**) in the presence of potassium acetate as base and $PdCl_2$ as catalyst at 120 °C (Figure 5.2).

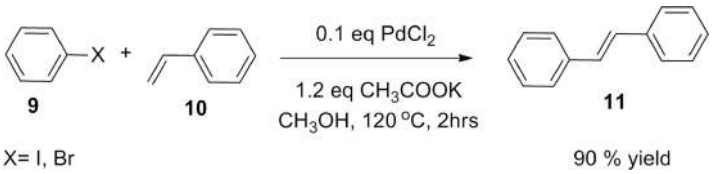

Figure 5.2: Mizoroki–Heck C–C cross-coupling reaction.

In 1972, Heck appreciated the Mizoroki publication and discovered the same reaction independently with different conditions (palladium acetate as catalyst, catalyst loading 0.01 equivalent, a hindered amine as base, and in the absence of solvent) [34]. The mechanism of the Heck reaction involves several steps. At first, palladium (II) acetate [$Pd(OAc)_2$] is reduced by triphenylphosphine (PPh_3) to bis(triphenylphosphine)palladium (0). Step 1 of the coupling reaction involves the insertion of Pd(0) into the aryl halide bond (**9**) (Figure 5.3). In step 2, alkene (**12**) and Pd form a C–Pd bond (**13**) in a *syn*-addition fashion. In step 3, a Pd–alkene π complex (**14**) is generated through β-hydride elimination. The Pd(0) compound is then reformed by the reductive elimination of Pd(II) complex with the help of a base in the final step of the coupling reaction.

5.2.3 Sonogashira coupling

The Sonogashira cross-coupling reaction utilizes a Pd catalyst along with copper (Cu) cocatalyst to form a C–C bond between (Figure 5.4) a terminal alkyne (**16**) and an aryl halide (**15**) or vinyl halide [35]. The reaction is carried out normally under

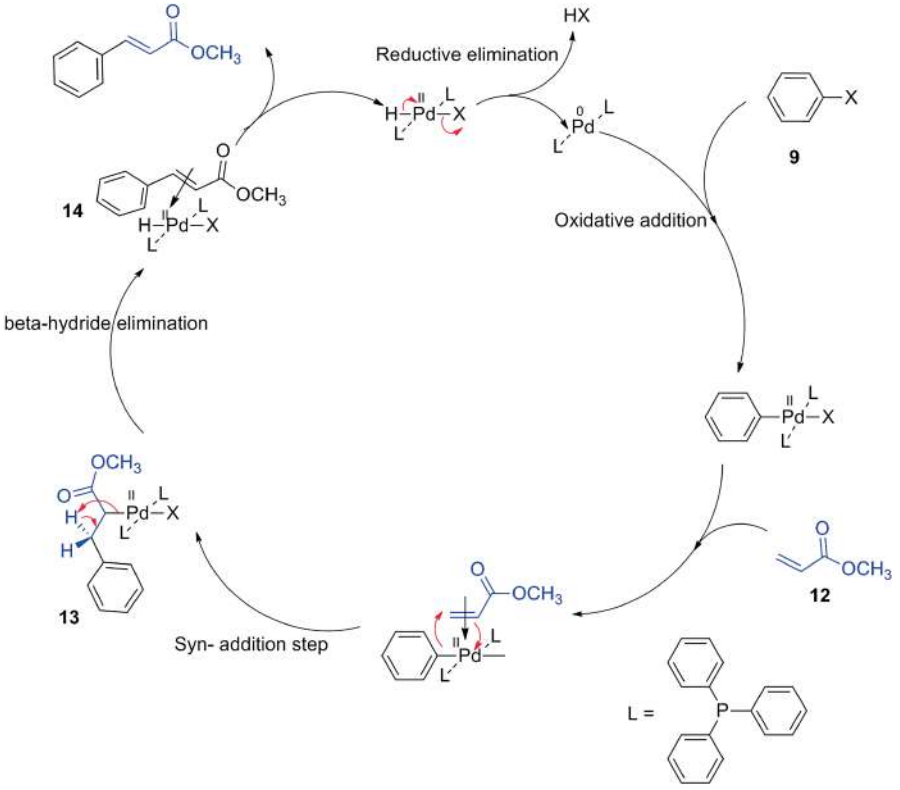

Figure 5.3: Pd-catalyzed Heck coupling reaction mechanism.

mild reaction conditions as in aqueous media, at room temperature, and using a mild base to form the disubstituted alkyne (**17**). This coupling reaction has been engaged in pharmaceuticals, natural products, and organic material synthesis. The synthesis of tazarotene [35] is used for the treatment of psoriasis and acne, and the synthesis of SIB-1508Y (known as Altinicline) [36], a nicotinic receptor agonist, involves the Sonogashira coupling reaction.

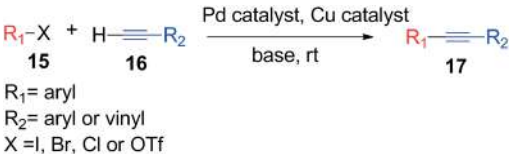

Figure 5.4: Sonogashira cross-coupling reaction.

The Pd precatalyst is activated to form a reactive Pd^0 under the coupling reaction condition (Figure 5.5). The Pd^0 catalyst then undergoes an oxidative coupling reaction with aryl or vinyl halide to form a Pd^{II} complex. This complex reacts with Cu acetylide and is converted into a new complex through the transmetalation step. In this final complex, reductive elimination occurs and the desired substituted alkyne is generated along with the regeneration of the Pd species. Although the Cu cycle is not discussed appropriately, it is proposed that π-alkyne complex (**19**) is formed using a base from terminal alkyne and Cu salt (**18**) and results in the formation of Cu acetylide (**20**) due to the increased acidity of terminal alkyne. This Cu acetylide then participates in transmetalation with the Pd intermediate.

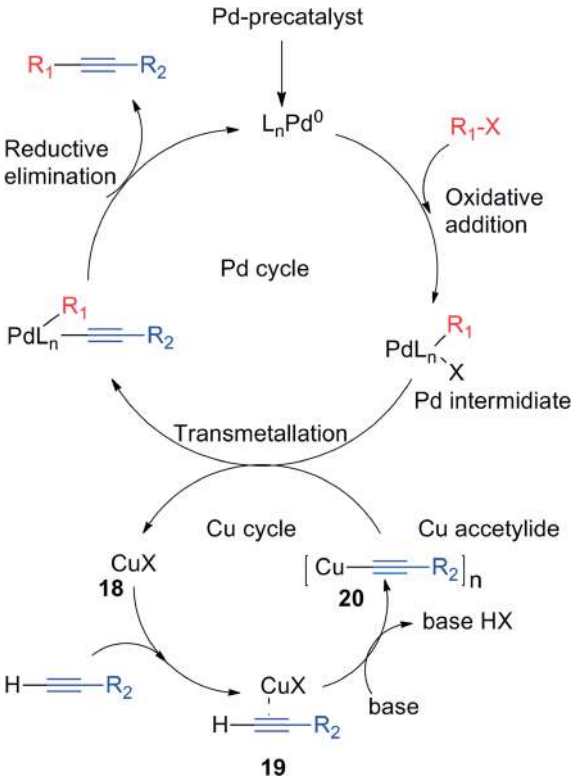

Figure 5.5: Sonogashira coupling reaction mechanism.

5.3 Background of heterogeneous metal-composite catalyst for cross-coupling

Heck, Suzuki, and Sonogashira cross-coupling reactions are typically catalyzed by Pd-based homogeneous systems (in Sonogashira coupling Cu cocatalyst is needed) that involve ligands (phosphine or *N*-heterocyclic) to design active catalytic systems. As a consequence, the separation of the homogeneous catalyst after the reaction is the biggest problem in the field of catalyst. Accordingly, the catalyst may be incorporated in the final product, thus resulting in the loss of the catalyst in the reaction, and a devalued product is formed from a pharmaceutical point of view. The main challenge is to develop heterogeneous catalytic systems for C–C cross-coupling reactions and establish the nature of the active catalyst species. The literature of the coupling reaction with homogeneous catalytic systems is well developed, but the same remained inadequate for heterogeneous systems [37]. Some researchers claim to develop solid precatalyst of soluble catalytically active Pd species [38–40], while others recognize absolutely heterogeneous systems, where catalysis takes place on the surface of Pd-based solid heterogeneous catalyst [41, 42]. The effectiveness of a good catalytic system is generally decided by the activity, selectivity, and lifetime of the prepared catalyst [43]. The activity of the catalyst is measured by the percentage of reactants converted into a product; however, the selectivity is measured by the percentage of reactants that are transformed into the desired final products, and the lifetime of the catalyst is the time when the catalyst attains its activity and selectivity to the expected level.

PdNPs have become attractive forms of heterogeneous catalyst due to their size and shape dependence and efficient catalytic activity in C–C cross-coupling reaction [37, 44]. Nevertheless, their use as a catalyst has been restricted because of scantiness of efficient separation procedures, and techniques like centrifugation and filtration are not much effective to recover the NPs completely. Moreover, due to the agglomeration and sintering properties of NPs upon heating, they are leached to form the insoluble noncatalytic Pd black [37]. Supported Pd catalyst has drawn profound interest due to their easy reusability in the C–C cross-coupling reaction. Most often, PdNPs immobilized on solid support become less catalytically active, and better understanding of the activity of PdNPs leads to design more effective heterogeneous catalysts in the cross-coupling reaction. Supported metal catalyst or metal-composite catalyst can be categorized as inorganic, organic, and inorganic–organic materials.

5.3.1 Inorganic support

5.3.1.1 PdNPs on carbonaceous supports

In C–C cross-coupling reaction, the use of carbonaceous nanomaterial-supported PdNPs opened up a new paradigm in the field of heterogeneous catalysis [45–47]. Among them, due to the commercial availability of activated charcoal, often Pd/C, is used as a heterogeneous catalyst. In addition, different solid supports like alumina and silica possess lower surface area than the charcoal support [47]. From literature, it is observed that Pd/C is stable in air, water, acid, and bases and does not require any inert atmospheric condition to be performed [47, 48]. Xu and his coworkers developed a pathway for the reaction between water-soluble bromoarenes (**21**) with sodium tetraphenylborate (**22**) to synthesize substituted biphenyl (**23**) (Figure 5.6) in the presence of 0.0025 mol% of Pd/C under reflux in water (reaction time varied from 1 to 7 h) [49]. The comparison between inorganic bases showed that sodium bases are more effective than potassium bases in this reaction. The catalyst was recycled up to five cycles with a gradual loss of reactivity.

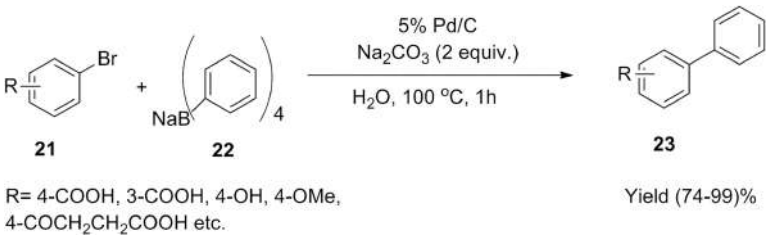

Figure 5.6: Suzuki–Miyaura reaction by Xu and coworkers.

Previous reports showed that surfactants are used as an additive to increase the solubility of the reactant aryl halides (**24**). Kohler and his coworkers performed the coupling reaction of aryl chlorides with aryl boronic acids (**25**) (Figure 5.7) in the presence of ligand-less Pd/C catalyst in water [50]. All reactions were carried out under an ambient condition to minimize the chance of homocoupling, although a lower Pd concentration (0.2–0.5 mol%) is required for activated aryl chlorides and higher Pd concentration (2 mol%) is needed for deactivated chloroarenes. The addition of surfactant tetrabutylammonium bromide (TBAB) as an additive and application of NaOH among the inorganic bases have a profound role in this reaction. Not only the aryl boronic acids but the boronate esters (**26**) and potassium trifluoroborates (**27**) are equally effective under this optimized reaction condition. The reactivation of the catalyst [Pd(0) to Pd(II)] using iodine as an oxidizing agent was carried out to recycle the catalyst in successive runs.

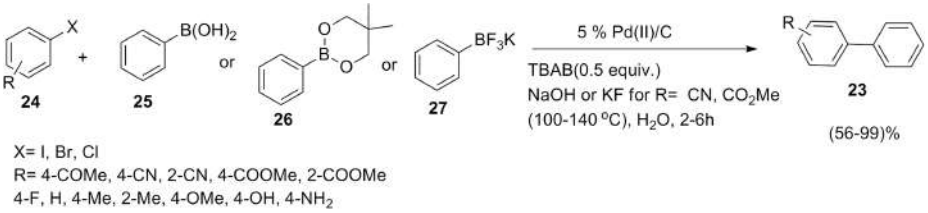

Figure 5.7: Suzuki coupling reaction by Kohler and coworkers.

Among the nanomaterials, graphene is solely able to stand out far ahead of all other nanomaterials because of its unique structure and exclusive characteristics [51]. Graphene and its derivatives have been widely used as a catalyst support due to their high flexibility and strength like solid substrates. They exhibit a high surface area and are homogeneously embedded into metal matrices which make graphene and its derivatives a viable candidate to be used as a catalyst support. Due to the immobilization of metal NPs on the surface of graphene and its derivatives, the surface area of the composite material increases, thereby increasing the distance between the sheets. The catalytic activity of these metal composite materials successfully enhances the productivity of the most studied C–C cross-coupling reactions [52–57]. Zhang et al. reported graphene-modified PdNPs by reducing $Pd(OAc)_2$ (Figure 5.8) using a surfactant sodium dodecyl sulfate (SDS) [58]. The use of SDS can be shown as a surfactant as well as a reducing agent. The prepared catalyst was highly efficient under aqueous as well as in aerobic conditions and exerted the product within 5 min. The recovery of the catalyst was done by filtration process

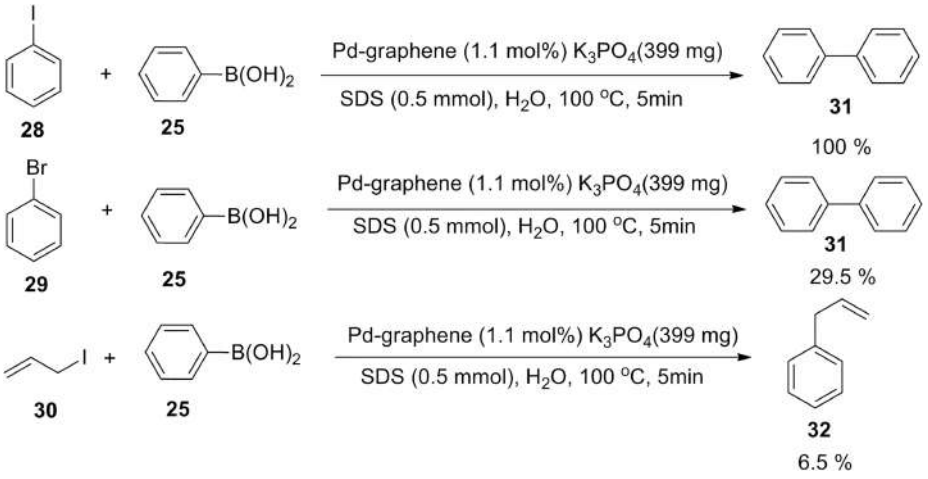

Figure 5.8: Pd–graphene composite-catalyzed synthetic approach by Zhang and coworkers.

and reused up to ten consecutive cycles. Allyl iodides (**30**) and bromobenzene (**29**) were also employed in this coupling reaction but resulted in a lower yield of allylbenzene (**32**) and biphenyl (**31**).

Shendage and his coworkers electrochemically deposited PdNPs on nafion–graphene support (Pd/Nf-G) which showed the eminent catalytic activity for the Suzuki coupling reaction to produce substituted biphenyls (**34**) from substituted aryl boronic acids (**33**) (Figure 5.9) under ethanol/water mixture at 80 °C [59]. Under the reaction temperature, Nafion is chemically and thermally stable. It is used to disperse and stabilize graphene on the electrode surface. The electrochemical process is generally heterogeneous in nature and allows easy recovery of the desired product. Besides this, no side product formation, short time of reaction, simple operation, and high purity of the desired product make this process advantageous than conventional processes.

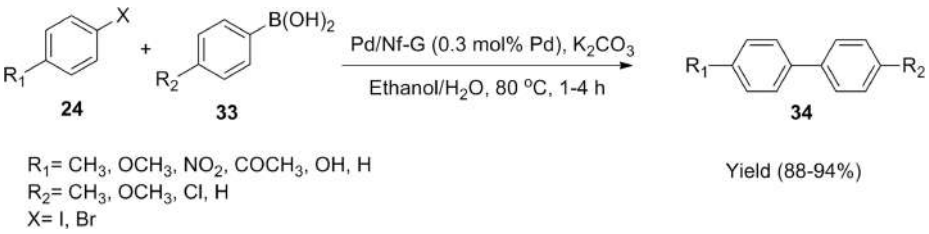

Figure 5.9: The Suzuki coupling reaction using Pd/Nf-G catalyst.

The formation of PdNPs on Nf-G support was confirmed by scanning electron microscopy with energy-dispersive X-ray analysis, X-ray diffraction analysis, transmission electron microscopy, and thermogravimetric analysis. The reaction between different aryl iodides and arylboronic acid was studied using a Pd/Nf–G catalyst. The electron-donating and electron-withdrawing aryl iodides afforded the product with excellent yield; however, aryl bromides require longer reaction time. Gómez-Martínez et al. used boron-derived nucleophiles like potassium aryltrifluoroborates or boronic acid esters as reactants and aryl halide (**35**) to afford biaryls (**36**) for Suzuki coupling reaction using PdNPs (6% Pd w/w) supported on graphene (PdNPs-G) and reduced graphene oxide (PdNPs–rGO). They prepared three types of catalysts (Figure 5.10). Catalyst 1 is PdNPs immobilized on rGO sheets functionalized with octadecylamine

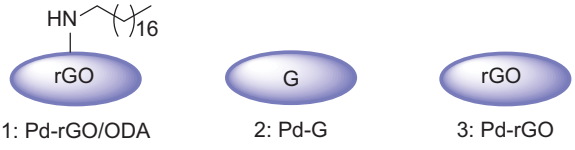

Figure 5.10: Pd(0) NP-supported catalyst employed in Suzuki coupling.

(PdNPs–rGO/ODA), where 13 nm average size Pd(0) NPs have been immobilized. Catalyst 1 disperses better in organic solvents due to the presence of amino-functional groups. Catalyst 2 is (PdNPs–G) where 5 nm average size Pd(0) NPs are distributed on the sheets of graphene oxide, while catalyst 3 (PdNPs–rGO) contains Pd(0) NPs with an average size of 6.9 nm. Catalysts 2 and 3 are well dispersed in an aqueous medium. Due to the better dispersibility in water, both catalysts 2 (PdNPs–G) and 3 (PdNPs–rGO) are highly active in this process with a solvent ratio ($MeOH/H_2O$:3/1) (Figure 5.11). Under the microwave irradiation, catalyst 2 was reused up to eight consecutive cycles without the loss of its catalytic activity. However, the catalytic activity dropped significantly under the conventional heating reaction conditions after five consecutive cycles.

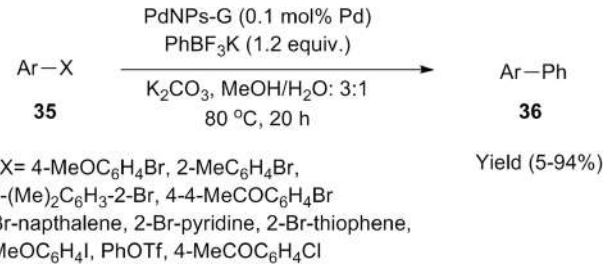

Figure 5.11: Suzuki coupling catalyzed by Pd(0) NPs supported GO and rGO.

5.3.1.2 Zeolite support (inorganic support)

Among the catalyst support, zeolites having an anionic framework provide high surface area and it is conducive to the high dispersion and adsorption of metal species [60, 61]. As crystalline nanoporous materials, zeolite can trap or recover heavy metals including Pd from industrial wastewater due to its well-distributed microporous space [62]. Wang et al. prepared the zeolite-supported Pd(II) catalysts by placing Pd(II) species on the solid surface of zeolite with an anion framework based on the charge balance principle (Figure 5.12). They developed a highly efficient zeolite-supported Pd catalyst (0.84% Pd@zeolite USY) for "in water" C–C cross-coupling reaction using tetrapropylammonium hydroxide as base (Figure 5.13) [63]. This catalyst was successfully employed to produce substituted alkynes (**38**) and biaryl (**39**) from terminal alkynes (**37**) and aryl boronic acids (**33**).

The interaction between metal and support may be varied due to the interaction between metal reactant and the form of the metal [64]. In an aqueous system, the Pd species migrate in the catalytic process and the Pd(II) intermediate undergoes ion exchange with cations (Na^+, K^+, etc.) present in an aqueous medium and easily escapes from the zeolite support. Therefore, it is quite necessary for the metal species to get

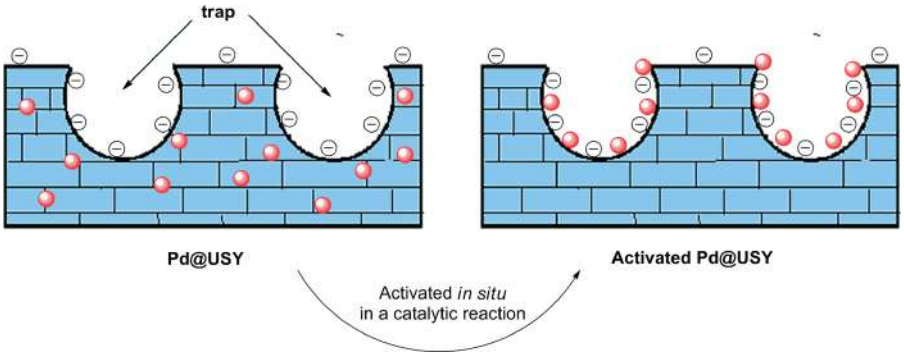

Figure 5.12: The migration of Pd during the activation in catalysis.

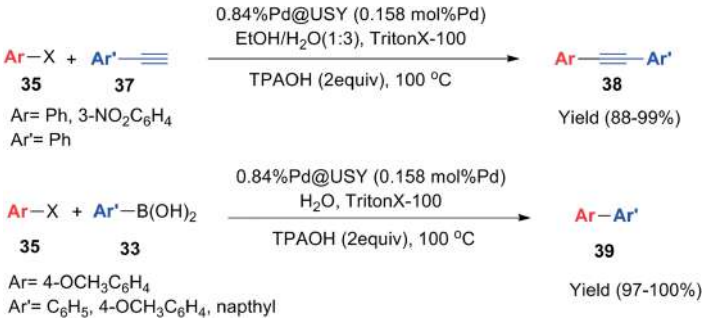

Figure 5.13: Pd@zeolite USY-catalyzed Sonogashira and Suzuki coupling reaction.

stabilized on the catalytic support during the reaction. They observed that in some alkaline aqueous systems, Pd(II) intermediate species uses zeolites (with an anionic framework) as a sink for coupling reaction; therefore, the position of Pd on the surface of zeolites can be controlled by release/capture capability of metal ions [65].

5.3.2 PdNPs on organic–inorganic support

Basak et al. developed a ligand-free low Pd(0)-loaded GO-polymer composite to catalyze Suzuki and Heck C–C cross-coupling reaction efficiently in water medium (Figure 5.14) [66]. Poly(methyl methacrylate) (PMMA) is a nonconductive polymer and it makes a thermally stable composite with GO. Their work involves the formation of GO-PMMA through in situ polymerization of methyl methacrylate (MMA) and deposition of Pd (0) NPs on the composite surface successively (Figure 5.15) [67].

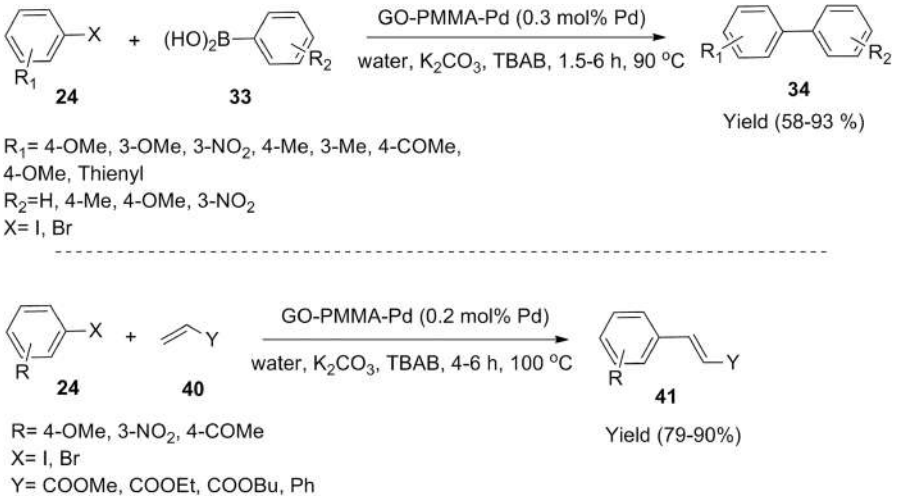

Figure 5.14: GO-PMMA-Pd(0) composite-catalyzed Suzuki and Heck reaction.

Several substituted aryl halides and aryl bromides (**24**) were coupled successfully with aryl boronic acids (**33**) in the presence of GO-PMMA-Pd catalyst (0.3 mol% Pd), K_2CO_3 as base, and TBAB as surfactant in aqueous medium at 90 °C. In the case of Heck reaction, aryl halides efficiently reacted with methyl/ethyl acrylates (**40**) in the presence of GO-PMMA-Pd catalyst (0.2 mol% Pd), TBAB as the surfactant, and K_2CO_3 as base at 100 °C to yield substituted alkene (**41**).

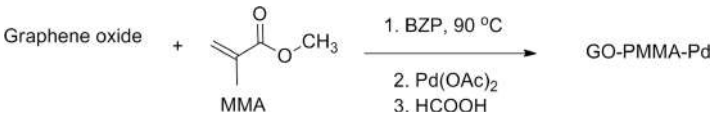

Figure 5.15: The schematic representation of the synthesis of GO-PMMA-Pd(0) catalyst.

5.3.3 Organic support

Among various polymeric supports, the natural polysaccharide of chitosan (CS) is cheap, nontoxic, and has excellent complexation capability with transition metal due to the presence of polar functional groups. Moreover, CS is very easy to process into different forms, such as microspheres, films, and fibers. Cotugno et al. developed an efficient protocol for Suzuki cross-coupling reaction using Pd(0) CS composite catalyst [68]. Excellent yield and selectivity were achieved using this catalyst at a relatively short reaction time (5 h). They carried out the reaction between different aryl halides and aryl boronic acids using K_2CO_3 as a base, PdNPs@CS (0.1 mol%)

catalyst, molten TBAB at 70–90 °C under aqueous medium (Figure 5.16). To obtain the catalyst, in the presence of TBAB, $Pd(OAc)_2$ was reduced electrochemically on the surface of CS. Subsequently, the PdNPs metallic core is stabilized by tetrabutylammonium cations mixed with Br^- and $[PdBr_4]^-$, and the core–shell nanostructured catalyst is further chemically absorbed on CS surface (Figure 5.17).

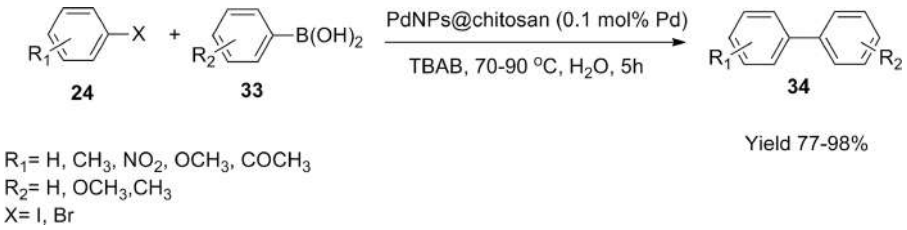

Figure 5.16: Suzuki cross-coupling reaction catalyzed by PdNPs@chitosan.

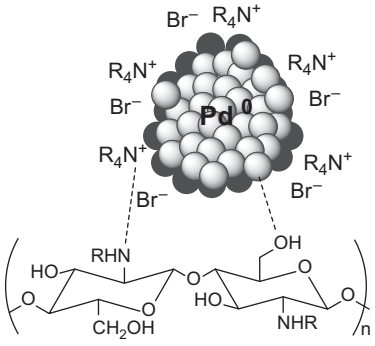

Figure 5.17: The core–shell structure of Pd nanoparticles is chemisorbed on chitosan in tetraalkylammonium-based ionic liquids (ILs).

Mondal and his coworkers synthesized PdNPs grafted mesoporous organic polymer catalyst by reacting (Figure 5.18) $Pd(OAc)_2$ and poly-triallylamine (MPTA-1) in methanol [69]. The mesoporous materials generally exhibit high surface area, and the active metal centers are distributed on this large surface to run organic transformation effectively [70]. These materials act as an ideal tethering agent to bind the active metals strongly at their surface. Cross-linking polymers minimize the chance of metal leaching from its surface and extensively stabilizes the metal in long term and hence are extensively used as long-term stabilization of the metals, which minimizes the possibility of leaching of metals under reaction conditions [71]. They observed the Heck coupling reaction between different aryl and heteroaryl halides (**35**) with substituted alkenes (**40**) to form disubstituted alkene (**42**) using this heterogeneous Pd–MPTA-1 catalyst in a water. Substituted chlorobenzenes underwent this C–C coupling reaction but took a longer reaction time along

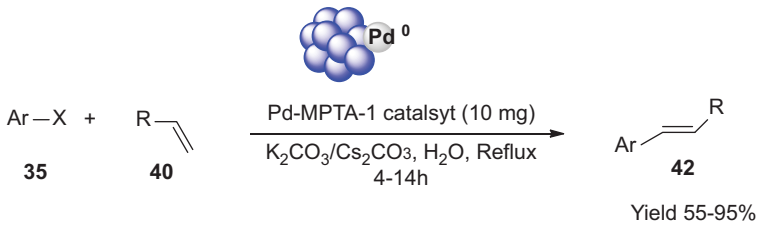

Figure 5.18: Heck reaction catalyzed by Pd-MPTA-1 catalyst in water media.

with a lower yield of the product compared to the corresponding bromobenzene and iodobenzene.

Lee et al. synthesized PdNPs immobilized on poly(*N*-isopropylacrylamide-*co*-4-vinylpyridine) [poly(NIPAM-*co*-4-VP)] copolymer hydrogel for Suzuki, Heck, and Sonogashira cross-coupling reactions in water (Figure 5.19) [72]. Poly(*N*-isopropylacrylamide) (PNIPAM) is an example of temperature-responsive polymer which shows a phase transition from coil to globule in an aqueous solution at 32 °C which is the lower critical solution temperature (LCST) [73]. The swelling of PNIPAM polymer hydrogels is due to changes in the H-bonding of the PNIPAM polymer with water molecules [74]. At temperature above the LCST of PNIPAM, some H-bonds are dissociated and hydrophobic interactions are dominant among the PNIPAM network. Therefore, it is possible to carry out Suzuki coupling reaction with hydrophobic substrates in the absence of surfactants and organic solvents. Moreover, PNIPAM can be easily recovered from an aqueous medium by simple filtration above its LCST. Due to the versatile properties of PNIPAM, PdNPs immobilized on it have been utilized as recyclable heterogeneous catalysts [75, 76]. They observed that the PNIPAM matrix could not be restored after recycle, and leaching of Pd occurred. To resolve this difficulty they used temperature-responsive poly(*N*-isopropylacrylamide-*co*-4-vinylpyridine) [poly(NIPAM-*co*-4-VP)] copolymers [77] as the PdNPs support (Figure 5.20). The poly(NIPAM-*co*-4-VP) copolymer-stabilized PdNPs were prepared by reducing the Pd(II) precursor on the copolymer surface using $NaBH_4$ as reducing agent in MeOH. This Pd-grafted poly(NIPAM-*co*-4-VP) catalyst was equally capable to synthesize biaryls (**34**) from aryl bromide (**43**), butyl cinnamates (**46**), and 1,2-disubstituted alkynes (**48**) from aryl iodides (**44**).

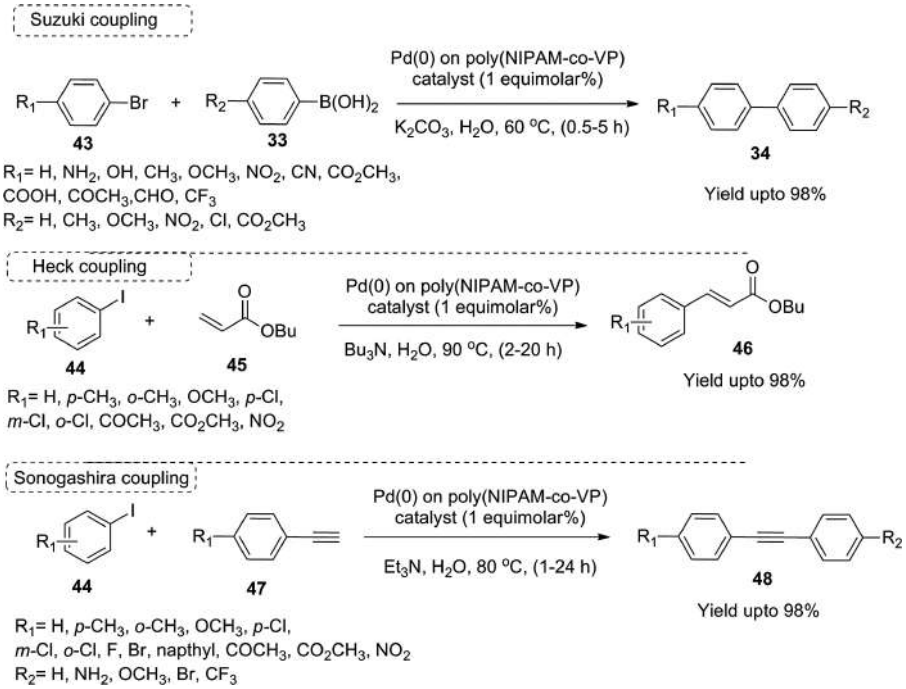

Figure 5.19: Suzuki, Heck, and Sonogashira coupling reactions catalyzed by Pd(0) [poly(NIPAM-*co*-4-VP)] catalyst.

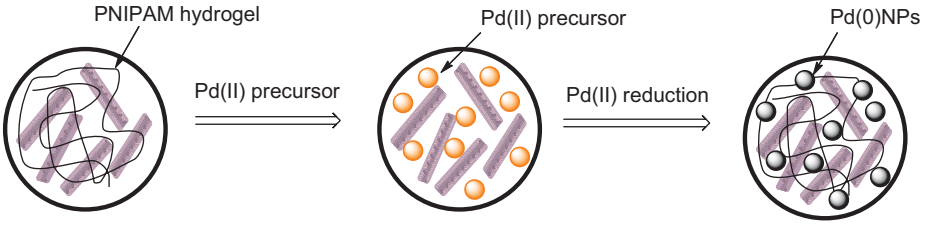

Figure 5.20: Pd(0) grafted on poly(*N*-isopropylacrylamide-*co*-4-vinylpyridine) [poly(NIPAM-*co*-4-VP)] copolymer hydrogel.

5.4 Conclusions

The Suzuki, Heck, and Sonogashira cross-coupling reactions have been widely exploited for decades for the expeditious C–C, C = C, C ≡ C bond formation which is used for the development of organic compounds, polymers, and natural products in drug discovery. From the industrial point of view, Pd-catalyzed coupling reactions in greener way using alternative reaction media are the current area of interest.

Among the green solvents, the utmost choice is water due to its environmental benefits, safeties, and cost. The use of homogeneous Pd catalyst is not appropriate in industrial purposes due to their lower stability, higher cost of synthesis, problem in their separation procedure, and difficulty in reusability. To overcome the drawbacks of a homogeneous catalyst, the concept of PdNPs immobilized on a solid support has attracted much interest to merge all the advantages of homogeneous and heterogeneous catalysts. The PdNP-immobilized nanostructured catalysts having high surface to volume ratio, low cost of processibility, good mechanical and thermal stability, and high reusability, and hence have been used in long-lasting, cost-effective cross-coupling reaction.

Abbreviation

NP	Nanoparticle
$[Pd(OAc)_2]$	Palladium (II) acetate
TBAB	Tetrabutylammonium bromide
SDS	Sodium dodecyl sulfate
Pd/Nf-G	Nafion-graphene support
PdNPs–G	PdNPs supported on graphene
PdNPs–rGO	Reduced graphene oxide
Pd@zeolite USY	Zeolite-supported Pd catalyst
PMMA	Poly(methyl methacrylate)
CS	Chitosan
MPTA	Poly-triallylamine
poly(NIPAM-*co*-4-VP)	Poly(*N*-isopropylacrylamide-*co*-4-vinylpyridine)

References

[1] Kolbe, H. Untersuchungenüber die elektrolyseorganischerverbindungen. Ann Chem Pharm, 1849, 69, 257–294.
[2] Breslow, R. Hydrophobic effects on simple organic reactions in water. Acc Chem Res, 1991, 24, 159–164.
[3] Li, CJ, Chan, TH. Organic Reactions in Aqueous Media. John Wiley & Sons: New York, 1997.
[4] Siskin, M, Katritzky, AR. Reactivity of Organic Compounds in Hot Water: Geochemical and Technological Implications. Science, 1991, 254, 231–237.
[5] Wurtz, A. UebereineneueKlasseorganischerRadicale. Justus Liebigs Ann Chem, 1855, 96, 364–375.
[6] Fittig, R. Uebereinigeproducte der trockenendestillationessigsaurersalze. Justus Liebigs Ann Chem, 1859, 110, 23–45.
[7] Glaser, C. Untersuchungenübereinige Derivate der Zimmtsäure [Studies on some derivatives of cinnamic acid]. Justus Liebigs Ann Chem, 1870, 154, 137–171.
[8] Ullmann, F, Bielecki, J. UeberSynthesen in der Biphenylreihe. ChemischeBerichte, 1901, 34, 2174–2185.

[9] Cadiot, P, Chodkiewicz, W. In chemistry of acetylenes, Viehe, HG, Dekker, M ed., New York, 1969, 597–647.
[10] Stephens, RD, Castro, CE. The substitution of aryl iodides with cuprous acetylides. A synthesis of tolanes and heterocyclics. J Org Chem, 1963, 28, 3313–3315.
[11] Corey, EJ, Posner, GH. Selective formation of carbon-carbon bonds between unlike groups using organocopper reagents. J Am Chem Soc, 1967, 89, 3911–3912.
[12] Tamao, K, Sumitani, K, Kumada, M. Selective carbon-carbon bond formation by cross-coupling of Grignard reagents with organic halides. Catalysis by nickel-phosphine complexes. J Am Chem Soc, 1972, 94, 4374–4376.
[13] Heck, RF. Palladium-catalyzed vinylation of organic halides. Org React, 1982, 27, 345–390.
[14] Sonogashira, K. Development of Pd-Cu catalyzed cross-coupling of terminal acetylenes with sp^2-carbon halides. J Organomet Chem, 2002, 653, 46–49.
[15] King, AO, Okukado, N, Negishi, E. Highly general stereo-, regio-, and chemo-selective synthesis of terminal and internal conjugated enynes by the Pd-catalysed reaction of alkynylzinc reagents with alkenyl halides. J C S Chem Comm, 1977, 19, 683–684.
[16] Stille, JK. The palladium-catalyzed cross-coupling reactions of organotin reagents with organic electrophiles. Angew Chem Int Ed, 1986, 25, 508–524.
[17] Miyaura, N, Yamada, K, Suzuki, A. A new stereospecific cross-coupling by the palladium-catalyzed reaction of 1-alkenylboranes with 1-alkenyl or 1-alkynyl halides. Tetrahedron Lett, 1979, 20, 3437–3440.
[18] Murahashi, S, Yamamura, M, Yanagisawa, K, Mita, N, Kondo, K. Stereoselective synthesis of alkenes and alkenyl sulfides from alkenyl halides using palladium and ruthenium catalysts. J Org Chem, 1979, 44, 2408–2417.
[19] Hatanaka, Y, Hiyama, T. Cross-coupling of organosilanes with organic halides mediated by a palladium catalyst and tris(diethylamino)sulfonium difluorotrimethylsilicate.J. Org Chem, 1988, 53, 918–920.
[20] Tokuyama, H, Yokoshima, S, Yamashita, T, Fukuyama, T. A novel ketone synthesis by a palladium-catalyzed reaction of thiol esters and organozinc reagents. Tetrahedron Lett, 1998, 39, 3189–3192.
[21] Liebeskind, L, Srogl, J. Thiol Ester-Boronic Acid Coupling. A Mechanistically Unprecedented and General Ketone Synthesis. J Am Chem Soc, 2000, 122, 11260–11261.
[22] Astruc, D, Lu, F, Aranzaes, JR. Nanoparticles as recyclable catalysts: The frontier between homogeneous and heterogeneous catalysis. Angew Chem Int Ed, 2005, 44, 7852–7872.
[23] Saravanan, R, Thirumal, E, Gupta, VK, Narayanan, V, Stephen, A. The photocatalytic activity of zno prepared by simple thermal decomposition method at various temperatures. J Mol Liq, 2013, 177, 394–401.
[24] Saravanan, R, Gupta, VK, Mosquera, E, Gracia, F. Preparation and characterization of V_2O_5/ZnO nanocomposite system for photocatalytic application. J Mol Liq, 2014, 198, 409–412.
[25] Saleh, TA, Gupta, VK. Functionalization of tungsten oxide into MWCNT and its application for sunlight-induced degradation of rhodamine B. J Colloid Interface Sci, 2011, 362, 337–344.
[26] Saleh, TA, Gupta, VK. Photo-catalyzed degradation of hazardous dye methyl orange by use of a composite catalyst consisting of multi-walled carbon nanotubes and titanium dioxide. J Colloid Interface Sci, 2012, 371, 101–106.
[27] Astruc, D. Palladium nanoparticles as efficient green homogeneous and heterogeneous carbon-carbon coupling precatalysts: A unifying view. Inorg Chem, 2007, 46, 1884–1894.
[28] Liu, J. Catalysis by supported single metal atoms. ACS Catal, 2017, 7, 34–59.
[29] Wang, D, Astruc, D. The recent development of efficient Earth-abundant transition-metal nanocatalysts. Chem Soc Rev, 2017, 46, 816–854.
[30] Singh, NB, Agarwal, S. Nanocomposites: An overview. Emerg Mater Res, 2016, 5, 5–43.

[31] Miyaura, N, Suzuki, A. Palladium-catalyzed cross-coupling reactions of organoboron compounds. Chem Rev, 1995, 95, 2457–2483.
[32] Budagumpi, S, Haque, RA, Salman, AW. Stereochemical and structural characteristics of single-and double-site Pd(ii)-n-heterocyclic carbene complexes: Promising catalysts in organic syntheses ranging from cc coupling to olefin polymerizations. Coord Chem Rev, 2012, 256, 1787–1830.
[33] Kantchev, EAB, O'Brien, CJ, Organ, MG. Palladium complexes of n-heterocyclic carbenes as catalysts for cross-coupling reactions-a synthetic chemist's perspective. Angew Chem Int Ed, 2007, 46, 2768–2813.
[34] de Meijere, A, Meyer, FE. Fine Feathers Make Fine Birds: The heck reaction in modern garb. Angew Chem Int Ed Engl, 1994, 33, 2379–2411.
[35] King, AO, Yasuda, N. A practical and efficient process for the preparation of tazarotene. Org Process Res Dev, 2005, 9, 646–650.
[36] King, AO, Yasuda, N. Palladium-catalyzed cross coupling reactions in the synthesis of pharmaceuticals organometallics in process chemistry. Top Organomet Chem, 2004, 6, 205–245.
[37] Veerakumar, P, Thanasekaran, P, Lu, KL, Lin, KC, Rajagopal, S. Computational studies of versatile heterogeneous palladium-catalyzed Suzuki, Heck and Sonogashira coupling reactions. ACS Sustain Chem Eng, 2017, 5, 8475–8490.
[38] Phan, NTS, Van Der Sluys, M, Jones, CW. On the nature of the active species in palladium catalyzed Mizoroki-Heck and Suzuki-Miyaura couplings-homogeneous or heterogeneous catalysis, a critical review. Adv Synth Catal, 2006, 348, 609–679.
[39] Ananikov, VP, Beletskaya, IP. Toward the ideal catalyst: From atomic centers to a "cocktail" of catalysts. Organometallics, 2012, 31, 1595–1604.
[40] Amoroso, F, Colussi, S, Del Zotto, A, Llorca, J, Trovarelli, A. Room-temperature Suzuki–Miyaura reaction catalyzed by Pd supported on rare earth oxides: Influence of the point of zero charge on the catalytic activity. Catal Lett, 2013, 143, 547–554.
[41] Sanjaykumar, SR, Mukri, BD, Patil, S, Madras, G, Hegde, MS. Ce0.98Pd0.02O2-δ: Recyclable, ligand free palladium (II) catalyst for Heck reaction. J Chem Sci, 2011, 123, 47–54.
[42] Khalili, D, Banazadeh, AR, Etemadi-Davan, E. Palladium stabilized by amino-vinyl silica functionalized magnetic carbon nanotube: Application in Suzuki-Miyaura and Heck-Mizoroki coupling reactions. Catal Lett, 2017, 147, 2674–2687.
[43] Chorkendorff, IB, Niemantsverdriet, JW. Introduction to catalysis in concepts of modern catalysis and kinetics, WILEY-VCH Verlag GmbH & Co. KGaA: Weinheim, Germany, 2003, 1–22.
[44] Astakhov, AV, Khazipov, OV, Chernenko, AY, Pasyukov, DV, Kashin, AS, Gordeev, EG, Khrustalev, VN, Chernyshev, VM, Ananikov, VP. A new mode of operation of Pd-NHC systems studied in a catalytic Mizoroki–Heck reaction. Organometallics, 2017, 36, 1981–1992.
[45] Felpin, FX, Ayad, T, Mitra, S. Pd/C: An old catalyst for new applications-Its use for the Suzuki-Miyaura reaction. Eur J Org Chem, 2006, 2006, 2679–2690.
[46] Felpin, FX. Ten years of adventures with Pd/C catalysts: From reductive processes to coupling reactions. Synlett, 2014, 25, 1055–1067.
[47] Cini, E, Petricci, E, Taddei, M. Pd/C catalysis under microwave dielectric heating. Catalysts, 2017, 7, 89.
[48] Wang, Y, Mao, Y, Lin, Q, Yang, J. Preparation of nano Pd/C catalyst and catalysis for Heck reaction. HuagongXinxingCailiao, 2014, 42, 132–135.
[49] Lu, G, Franzen, R, Zhang, Q, Xu, Y. Palladium charcoal-catalyzed, ligandless Suzuki reaction by using tetraarylborates in water. Tetrahedron Lett, 2005, 46, 4255–4259.

[50] Lysen, M, Kohler, K. Palladium on activated carbon – a recyclable catalyst for Suzuki-Miyaura cross-coupling of aryl chlorides in water. Synthesis, 2006, 692.
[51] Novoselov, KS, Fal'ko, VI, Colombo, L, Gellert, PR, Schwab, MG, Kim, K. A roadmap for graphene. Nature, 2012, 490, 192–200.
[52] Scheuermann, GM, Rumi, L, Steurer, P, Bannwarth, W, Mülhaupt, R. Palladium nanoparticles on graphite oxide and its functionalized graphene derivatives as highly active catalysts for the Suzuki-Miyaura coupling reaction. J Am Chem Soc, 2009, 131, 8262–8270. Rumi L, Scheuermann GM, Mülhaupt R, Bannwarth W. Palladium nanoparticles on graphite oxide as catalyst for Suzuki-Miyaura, Mizoroki-Heck, and Sonogashira reactions. Helv Chim Acta 2011, 94, 966–976.
[53] Xiang, G, He, J, Li, T, Zhuang, J, Wang, X. Rapid preparation of noble metal nanocrystals via facile coreduction with graphene oxide and their enhanced catalytic properties. Nanoscale, 2011, 3, 3737–3742. Hoseini SJ, Dehghani M, Nasrabadi H. Thin film formation of Pd/reduced-graphene oxide and Pd nanoparticles at oil-water interface, suitable as effective catalyst for Suzuki-Miyaura reaction in water. Catal Sci Technol 2014, 4, 1078–083.
[54] Moussa, S, Siamaki, AR, Gupton, BF, El-Shall, MS. Pd-partially reduced graphene oxide catalysts (Pd/PRGO): Laser synthesis of Pd nanoparticles supported on PRGO nanosheets for carbon-carbon cross coupling reactions. ACS Catal, 2012, 2, 145–154.
[55] Hu, J, Wang, Y, Han, M, Zhou, Y, Jiang, X, Sun, P. A facile preparation of palladium nanoparticles supported on magnetite/s-graphene and their catalytic application in Suzuki-Miyaura reaction. Catal Sci Technol, 2012, 2, 2332–2340.
[56] Shang, N, Gao, S, Feng, C, Zhang, H, Wang, C, Wang, Z. Graphene oxide supported N-heterocyclic carbene-palladium as a novel catalyst for the Suzuki-Miyaura reaction. RSC Adv, 2013, 3, 21863–21868.
[57] Shang, N, Feng, C, Zhang, H, Gao, S, Tang, R, Wang, C, Wang, Z. Suzuki-Miyaura reaction catalyzed by graphene oxide supported palladium nanoparticles. Catal Commun, 2013, 40, 111–115.
[58] Li, Y, Fan, X, Qi, J, Ji, J, Wang, S, Zhang, G, Zhang, F. Palladium nanoparticle-graphene hybrids as active catalysts for the Suzuki reaction. Nano Res, 2010, 3, 429–437.
[59] Shendage, SS, Patil, UB, Nagarkar, JM. Electrochemical synthesis and characterization of palladium nanoparticles on nafion-graphene support and its application for Suzuki coupling reaction. Tetrahedron Lett, 2013, 54, 3457–3461.
[60] Li, J, Corma, A, Yu, J. Synthesis of new zeolite structures. Chem Soc Rev, 2015, 44, 7112–7127.
[61] Bhattacharyya, S, Samanta, D, Roy, S, Haveri Radhakantha, VP, Maji, TK. In situ stabilization of Au and Co nanoparticles in a redox-active conjugated microporous polymer matrix: Facile heterogeneous catalysis and electrocatalytic oxygen reduction reaction activity. ACS Appl Mater Interfaces, 2019, 11, 5455–5461.
[62] Kumbhar, A. Palladium catalyst supported on zeolite for cross-coupling reactions: An overview of recent advances. Top Curr Chem, 2017, 375, 2.
[63] Wang, Y, Liao, J, Xie, Z, Zhang, K, Wu, Y, Zuo, P, Zhang, W, Li, J, Gao, Z. Zeolite-enhanced sustainable Pd-catalyzed C-C cross-coupling reaction: Controlled release and capture of palladium. ACS Appl Mater Interfaces, 2020, 12, 11419–11427.
[64] Shamzhy, M, Opanasenko, M, Concepcion, P, Martínez, A. New trends in tailoring active sites in zeolite-based catalysts. Chem Soc Rev, 2019, 48, 1095–1149.
[65] Wang, N, Sun, Q, Bai, R, Li, X, Guo, G, Yu, J. In situ confinement of ultrasmall Pd clusters within nanosized silicalite-1 zeolite for highly efficient catalysis of hydrogen generation. J Am Chem Soc, 2016, 138, 7484–7487.

[66] Basak, P, Ghosh, P. Poly (methyl methacrylate)-graphene oxide supported palladium catalyst: A ligand free protocol for Suzuki and Heck coupling reaction in water medium. Synth Commun, 2018, 48, 2584–2599.
[67] Pham, VH, Dang, TT, Hur, SH, Kim, EJ, Chung, JS. Highly conductive poly(methyl methacrylate) (PMMA)-reduced graphene oxide composite prepared by self-assembly of PMMA latex and graphene oxide through electrostatic interaction. ACS Appl Mater Interfaces, 2012, 4, 2630–2636.
[68] Cotugno, P, Casiello, M, Nacci, A, Mastrorilli, P, Dell'Anna, MM, Monopoli, A. Suzuki coupling of iodo and bromoarenes catalyzed by chitosan-supported Pd-nanoparticles in ionic liquids. J Organomet Chem, 2014, 752, 1–5.
[69] Mondal, J, Modak, A, Bhaumik, A. One-pot efficient Heck coupling in water catalyzed by palladium nanoparticles tethered into mesoporous organic polymer. J Mol Catal A Chem, 2011, 350, 40–48.
[70] Zhang, YL, Wei, S, Liu, FJ, Du, YC, Liu, S, Ji, YY, Yokoi, T, Tatsumi, T, Xiao, FS. Superhydrophobic nanoporous polymers as efficient adsorbents for organic compounds. Nano Today, 2009, 4, 135–142.
[71] Cho, JK, Najman, R, Dean, TW, Ichihara, O, Muller, C, Bradley, M. Captured and cross-linked palladium nanoparticles. J Am Chem Soc, 2006, 128, 6276–6277.
[72] Lee, Y, Hong, MC, Ahn, H, Yu, J, Rhee, H. Pd nanoparticles immobilized on poly (NIPAM-co-4-VP) hydrogel: Highly active and reusable catalyst for carbon-carbon coupling reactions in water. J Organomet Chem, 2014, 769, 80–93.
[73] Hirokawa, Y, Tanaka, T, Matsuo, ES. Volume phase transition in a non-ionic gel. J Chem Phys, 1984, 81, 6379–6380. Kubota K, Fujishige S, Ando I. Single-chain transition of poly(N-isopropylacrylamide) in water. J Phys Chem, 1990, 94, 5154–5158.
[74] Shibayama, M, Suetoh, Y, Nomura, S. Structure relaxation of hydrophobically aggregated poly(n-isopropylacrylamide) in water. Macromolecules, 1996, 29, 6966–6968.
[75] Bergbreiter, DE, Case, BL, Liu, YS, Caraway, JW. Poly(n-isopropylacrylamide) soluble polymer supports in catalysis and synthesis. Macromolecules, 1998, 31, 6053–6062.
[76] Mei, Y, Lu, Y, Polzer, F, Ballauff, M, Drechsler, M. Catalytic activity of palladium nanoparticles encapsulated in spherical polyelectrolyte brushes and core-shell microgels. Chem Mater, 2007, 19, 1062–1069. Bergbreiter DE, Osburn PL, Wilson A, Sink EM. Palladium-catalyzed C-C coupling under thermomorphic conditions. J Am Chem Soc, 2000, 122, 9058–9064.
[77] Melendez-Ortiz, HI, Bucio, E, Burillo, G. Radiation-grafting of 4-vinylpyridine and N-isopropylacrylamide onto polypropylene to give novel pH and thermo-sensitive films. Radiat Phys Chem, 2009, 78, 1–7. Nur H, Pinkrah VT, Mitchell JC, Benee LS, Snowden MJ. Synthesis and properties of polyelectrolyte microgel particles. Adv Colloid Interface Sci, 2010, 158, 15–20.

Debashis Ghosh, Sumit Ghosh, Alakananda Hajra*

6 Gold nanoparticles as promising catalyst for electrochemical CO_2 reduction in aqueous medium

6.1 Introduction

Conversion of carbon dioxide into energy-enriched materials is one of the keys and essential projects to mitigate global warming and to fulfill global energy demand [1–3]. Among the numerous methods to mitigate CO_2 concentration, the electrochemical reduction is one of the suitable methods due to its simple feasibility under normal reaction condition and controllability of the technique (i.e., by altering overpotential) [4, 5]. The initial problem realizes direct single-electron reduction of linear CO_2 to bent $CO_2^{\bullet-}$ as it is a thermodynamically uphill process having the corresponding reduction potential of –1.90 V [6] or –1.99 V [7] versus standard hydrogen electrode at pH 7 in aqueous medium. However, various proton-coupled multiple electron reductions of CO_2 to CO, formate, methanol, and methane can favorably be achieved at less negative potentials than –1.90 V [6]. Because of the resemblance of their proton-coupled reduction potentials, the product selectivity remains a potential issue. Additionally, the availability of proton source under CO_2 reduction condition can encourage a side reaction, like hydrogen evolution reaction (HER) in aqueous medium. To resolve these practical problems and yield a desired product selectively, one effective solution is to develop an efficient catalyst. Catalytic activity of bulk metals has been studied in detail in recent years for electrochemical CO_2 reduction; however, they have several disadvantages with regard to low activity and readily get deactivation [8]. Out of different metals, gold (Au) and silver (Ag) display distinct behavior with high selectivity toward the evolution of CO [9]. According to literature reports, efficient conversion of CO_2 to CO under electrochemical condition in aqueous medium depends on relative energies of the intermediates generated on active metal surfaces [10–12].

The overall process involves the following reactions (reactions 1–5, Figure 6.1) where the star (*) implies either a surface-attached species or an unfilled catalytically active site [13, 14]. Production of CO depends on both the formation (reaction 1) and reduction (reaction 2) of COOH*, and on potential of the catalyst to release

*Corresponding author: Alakananda Hajra, Department of Chemistry, Visva-Bharati (A Central University), Santiniketan 731235, India, e-mail: alakananda.hajra@visva-bharati.ac.in
Debashis Ghosh, Department of Chemistry, St. Joseph's College (Autonomous), Bangalore 560027, Karnataka, India
Sumit Ghosh, Department of Chemistry, Visva-Bharati (A Central University), Santiniketan 731235, India

https://doi.org/10.1515/9783110733846-006

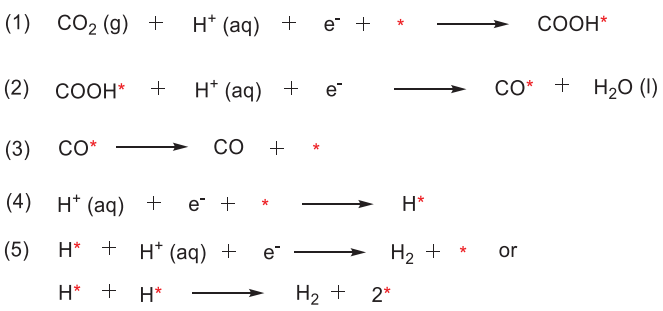

Figure 6.1: General schematic representation for CO_2 reduction and HER on catalyst surface.

CO (reaction 3). To achieve significant CO_2 to CO conversion selectivity, it is the catalyst that should balance reactions 1–3 as well as suppress the HER (reactions 4–5), the main side reaction that is frequently detected in examining reduction of CO_2 under electrochemical condition [14]. Nanostructured Au catalysts have recently been explored as efficient electrocatalysts for CO_2 reduction to CO in aqueous electrolyte [4]. It is expected that nanoparticle (NP) catalysts should show high catalytic activity toward electrochemical CO_2 reduction owing to high surface area. Furthermore, the surface of NP catalyst generally accommodates a significant part of edge (i.e., low-coordinated sites), whose catalytic performance is markedly different from their bulk counterparts (having fully coordinated sites) [15, 16].

In this chapter, we discuss the recent progress of nanostructured Au catalysts toward electrochemical CO_2 reduction, which includes the synthetic strategy for various Au-based nanostructured materials, their distinct catalytic properties, and investigation of reaction mechanism.

6.2 Various nanostructured Au catalysts

6.2.1 Dispersed Au nanoparticle catalysts on carbon electrode

In 2012, a new type of Au NP catalyst (oxide-derived AuNP film, Figure 6.2a) has been prepared by anodic oxidation and subsequent electrochemical reduction of Au foils. This synthesized AuNP film selectively reduced CO_2 to CO with current densities within 2–4 mA/cm^2 and Faradaic efficiencies (FEs) around 96% (which is much better than polycrystalline Au, Figure 6.2b) at mild negative potential (−0.35 V vs reversible hydrogen electrode (RHE)) [13].

According to the authors, the improved stability of the reduced CO_2 radical or the COOH* and the enfeebled CO attachment on the Au surface (especially in case of oxide-derived Au electrodes, Figure 6.3) caused selective CO_2 reduction to CO [13].

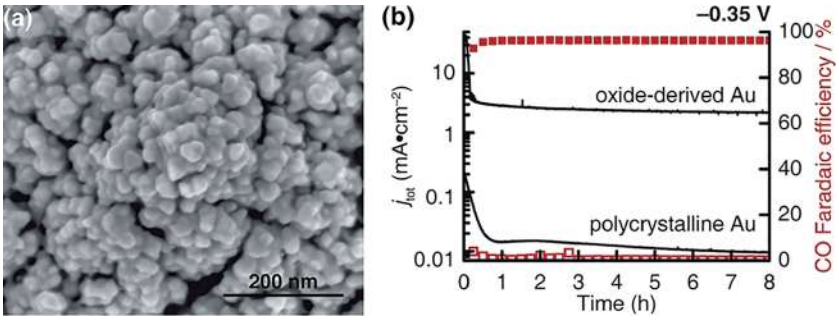

Figure 6.2: (a) SEM image of oxide-derived AuNP film surface. (b) Comparative study of CO_2 reduction activity between polycrystalline Au and oxide-derived AuNP film. Reprinted with permission from ref. [13]. Copyright © 2012 American Chemical Society.

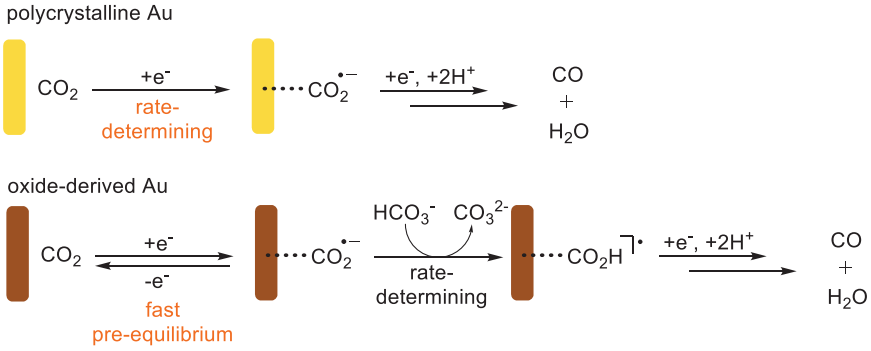

Figure 6.3: Proposed pathway for CO_2 reduction to CO as reported by Y. Chen et al. [13].

In view of the size and surface effects usually noticed in NPs with encouraging results obtained from AuNPs, Zhu et al. in 2013 [14] studied monodispersed AuNPs as catalysts for electrocatalytic CO_2 reduction under ambient condition. The authors synthesized various AuNPs (4, 6, 8, and 10 nm, respectively) deposited on carbon support (C-Au paste). Each type of C-Au paste was coated on a carbon paper under suitable conditions and used as a working electrode. Authors have screened all coated AuNPs and reported that 8 nm AuNPs showed best CO_2 reduction ability; FE reaching 90% at −0.67 V (vs RHE) into CO (Figure 6.4a). Applying density functional theory (DFT) calculations on different crystal faces and a 13-atom Au cluster (Au_{13}), they summarized that the edge sites on gold NP surfaces were suitable for CO_2 reduction, whereas the corner sites accommodated the HER pathway. The correlation between the density of active surface sites and the Au cluster size was depicted in Figure 6.4b. The DFT studies indicated that the 8 nm gold NPs having 4 nm crystallite diameter were appropriate to supply an optimal number of edge sites active for CO_2 reduction to CO and diminish the number of corner sites suitable for the HER.

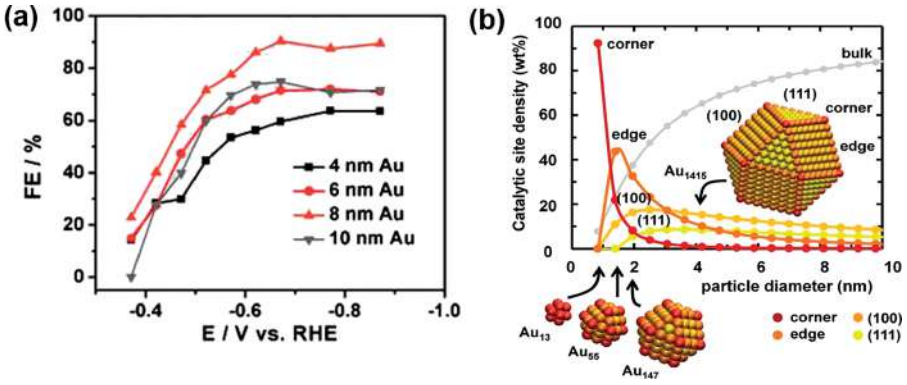

Figure 6.4: (a) FEs for CO production by AuNPs during CO_2 electroreduction at different redox potentials. (b) Density of adsorption sites (yellow, light orange, dark orange, and red symbols for (111), (0 0 1), edge, or corner on-top sites, respectively). Reprinted with permission from ref. [14]. Copyright © 2013 American Chemical Society.

Subsequently in 2014, W. Zhu et al. [17] further developed ultrathin Au nanowires (NWs) (500–15 nm) deposited onto a Ketjen carbon support (designated as C-Au-500, C-Au-100, and C-Au-15, respectively) and tested their CO_2 electroreduction abilities under ambient conditions at different reduction potentials (Figure 6.5). The authors reported that at −0.35 V, the FE_{CO} reached to 94% for C-Au-500 and maintained at least for 6 h without any activity changes. Based on theoretical calculations, they suggested that the Au NWs performed well for this reaction due to high mass density of active edge sites (≥16%) and poor CO binding on these sites.

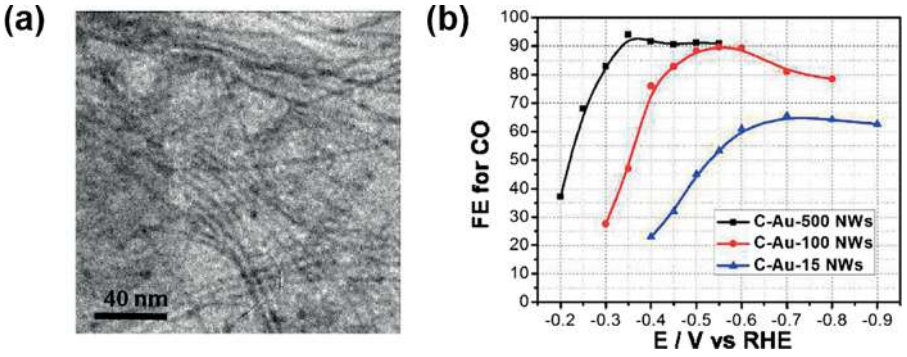

Figure 6.5: (a) TEM image of the C-Au-500 NWs. (b) FEs of C-Au-500, C-Au-100, and C-Au-15 NWs for electrocatalytic reduction of CO_2 to CO. Reprinted with permission from ref. [17]. Copyright © 2014 American Chemical Society.

Later in 2016, E. B. Nursanto et al. [18] reported thin Au nanofilm deposited on carbon paper as catalysts for electrochemical reduction of CO_2 (at −0.59 V vs RHE) at room temperature. The authors synthesized various Au nanofilms (with thicknesses 0.5–30 nm) coated on carbon paper (referred to as Au-T samples). Authors reported that the FE value for CO production increased proportionally with the gold amount and reached a saturation point of ~78% (at −0.59 V vs RHE) for samples thicker than Au-4 and the FE value was similar to that of commercial gold foil (Figure 6.6a). They further determined the CO production rate (by multiplying the current density with FE value for CO) for these synthesized Au-T samples. Moreover, CO formation rate (measured at the same experimental potential) increased from Au-0.5 to Au-30 (Figure 6.6b). In particular, gold loadings higher than 7 nm thickness exhibited better CO formation rate than that of gold foil. Based on the experimental evidences and by comparing with literature [13], they suggested that the slowest step was an electron transfer for the formation of CO_2 radical anion on the catalyst surface.

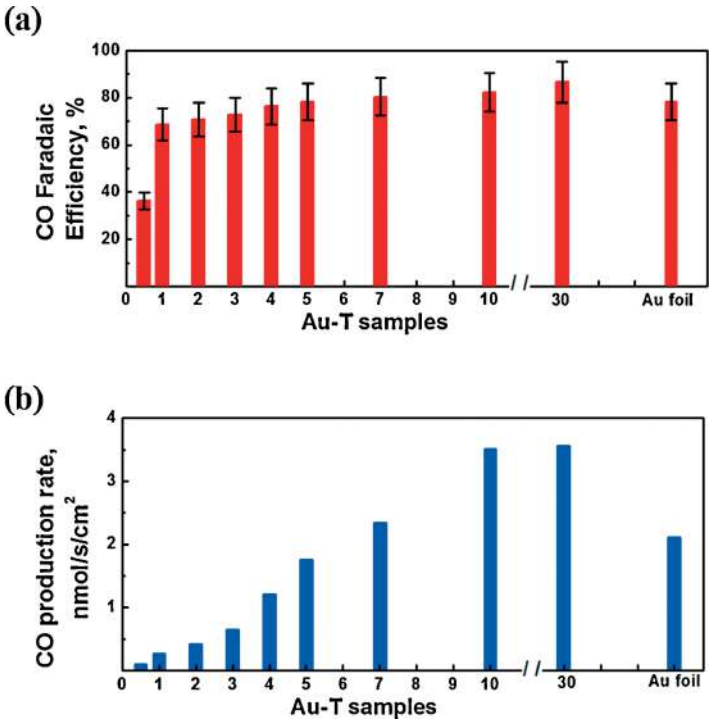

Figure 6.6: (a) FEs for CO production by Au-T samples during electrochemical CO_2 reduction. (b) CO formation rates determined at applied potential = −0.59 V. Reproduced with permission from ref. [18].

Two years later in 2018, Y. Kim and his group [19] synthesized highly dispersive AuNPs (with average diameters ranging from 5.8 (±2.4) to 2.0 (±0.4) nm) on carbon black (in general represented as AuNPs/CB) in situ in the presence of two different reducing agents of $NaBH_4$ at several concentrations (12, 4, 1.3, 0.4, 0.2, and 0.04 mM, respectively) and citrate at a fixed concentration (3 mM). The electrocatalytic activity for CO_2 reduction by AuNPs/CB-0.2 (i.e., 2 nm AuNPs on carbon support with 0.2 mM $NaBH_4$) was reported with scanning electrochemical microscopy (SECM) as well as bulk electrolysis in an H-type cell. From the SECM voltammograms (Figure 6.7), it is clear that CO_2 reduction was feasible at a potential near –0.62 V (vs saturated calomel electrode; SCE) (Figure 6.7). Although authors reported that selective CO_2 reduction to CO was achieved by applying AuNPs/CB-0.2 substrate electrode at potential ≥–0.725 V (vs SCE), reliable quantification was done by supplying a relatively larger overpotential (at –1.07 V), where FE_{CO} was 74.9% and FE_{H2} was 24.1%.

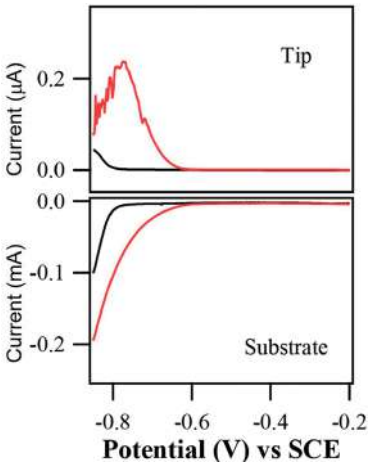

Figure 6.7: SECM voltammograms utilizing AuNPs/CB-0.2 electrode (substrate) and Sn/Pt (tip). Taken from ref. [19]. Copyright © 2018 Wiley-VCH Verlag GmbH & Co. KGaA, Weinheim.

6.2.2 Modified graphene-supported gold nanoparticles

Presently, graphene nanosheets are used as good support materials for catalyst because of their high conductivities, large surface areas, and less manufacturing costs [20–22]. The 2D sheet structure of graphene with large surface area yielded homogeneous dispersion of catalyst NPs. Many active sites containing edges and defects, which were present in the graphitic layer, showed the capability to change the electronic behavior of catalysts attached on it. This changed electronic behavior of the catalyst could alter the reaction mechanism and eventually the final product of the chemical transformation [23].

Narrow graphene nanoribbons (GNRs) are an exciting high-performance material that has currently become available via large-scale, solution-based bottom-up

synthesis [24–28]. C. Rogers et al. (in 2017) [29] explored structurally defined GNRs as a suitable support for AuNPs in electrocatalytic CO_2 reduction (Figure 6.8).

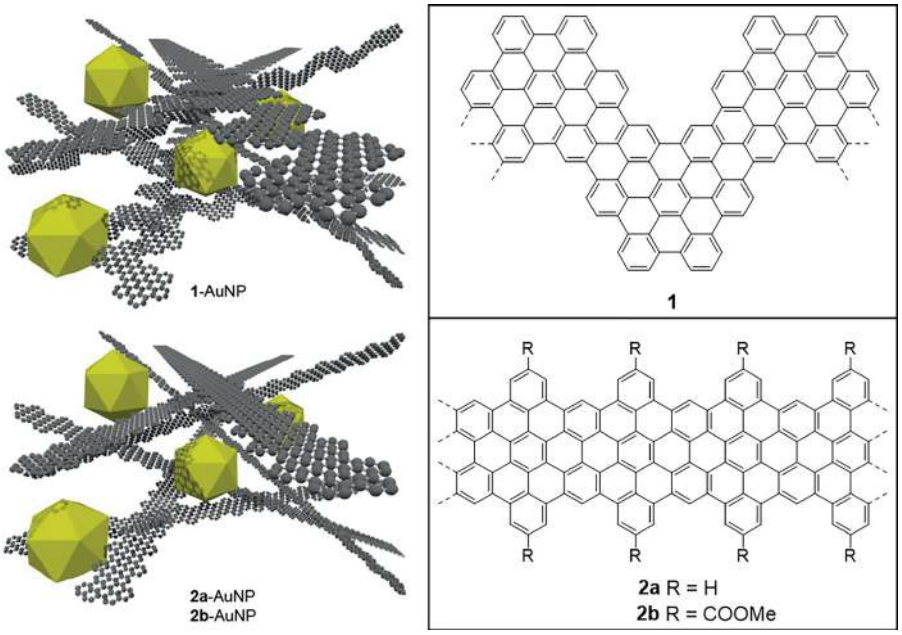

Figure 6.8: Design of GNR-AuNP composite materials. Slight modification from ref. [29]. Reprinted with permission from ref. [29]. Copyright © 2017 American Chemical Society.

The authors synthesized GNR-AuNP combined electrodes (**2a**-AuNP and **2b**-AuNP) and measured their cyclic voltammograms (CVs) in CO_2-saturated aqueous electrolyte (Figure 6.9a). There was marked increase in current for GNR-AuNPs combined electrodes than the electrodes obtained from AuNPs alone, or AuNPs supported by a C_{black} matrix. The authors further measured CVs of GNR electrodes without any added AuNPs and observed negligible current over the similar potential range, thereby confirming that the GNRs themselves were not active under present electrochemical condition. Controlled potential electrolysis (for 1 h) across a potential window between −0.87 to −0.37 V was performed by the authors. The CO Faraday efficiency (FE_{CO}) (Figure 6.9b) for reduction of CO_2 by GNR-AuNP composite electrodes significantly outstripped those of C_{black}-AuNP over a wide potential range. Furthermore, C_{black}-AuNP degraded rapidly, yielding only 22% FE_{CO} after 3 h. Notably, GNR-AuNP composites maintained high catalytic ability for more than 10 h of controlled potential electrolysis as reported by the authors. To clarify the source of the increased performance showed by **2b**-AuNP composites, the authors studied the kinetics of CO_2 reduction for each of the composites via Tafel plot. The observed Tafel slope for **2b**-AuNP composites is much less (only 66 mV/decade) than other composites

(141–129 mV/decade), thereby suggesting a pre-equilibrating single-electron transfer followed by a rate-determining chemical step (similar to Figure 6.3).

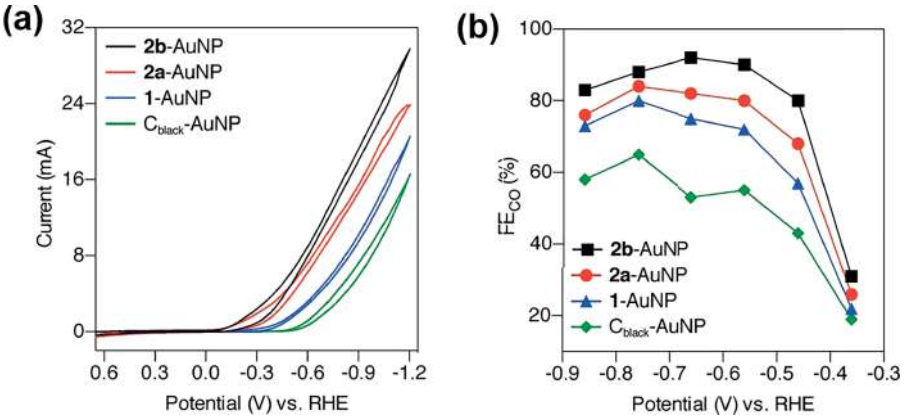

Figure 6.9: (a) CVs of various composite electrodes. (b) FE_{CO} by various composite electrodes. Reprinted with permission from ref. [29]. Copyright © 2017 American Chemical Society.

In 2018, Saquib et al. [30] have developed gold NPs on the reduced graphene oxide (RGO) support and examined CO_2 electroreduction by these new composite materials. Based on TEM data, they confirmed well dispersion of AuNPs on RGO support. Using energy-dispersive X-ray spectroscopy data, they confirmed the weight percentage of Au which was 13.72% in the RGOAu catalyst (with uniform distribution of AuNPs over the RGO support). To find out the effect of Au content on the conversion of CO_2 to CO, the authors prepared another composite material of Au, denoted by RGOAu (35.51 wt%). The CV measurements indicated a large positive shift of onset potential for RGOAu (35.51 wt%) as shown in Figure 6.10. This result suggested that RGOAu (35.51 wt%) was a more active catalyst than RGOAu (13.72 wt%) for reduction of CO_2. Further, by investigating Tafel plots for both supported catalysts, the authors clarified that RGOAu (13.72 wt%) electrode showed comparatively slow kinetics than the RGOAu (35.51 wt%), thereby, they have concluded that the $CO_2^{\bullet-}$ intermediate was significantly stabilized by RGOAu (35.51 wt%) over RGOAu (13.72 wt%), and consequently, enhanced CO_2 reduction rate.

Based on the experimental evidence, the authors proposed a mechanism for CO_2 reduction (Figure 6.11). They suggested enhanced stability of the intermediate $*COO^{\bullet-}$ by excess negative charge on the oxygen atoms owing to back donation from Au. This facilitated more abstraction of proton in the aqueous medium and eventual formation of CO by elimination of HO^-. The authors further suggested that the defects present on RGO enabled easy desorption of CO from gold surfaces by transfer of electron from RGO to Au.

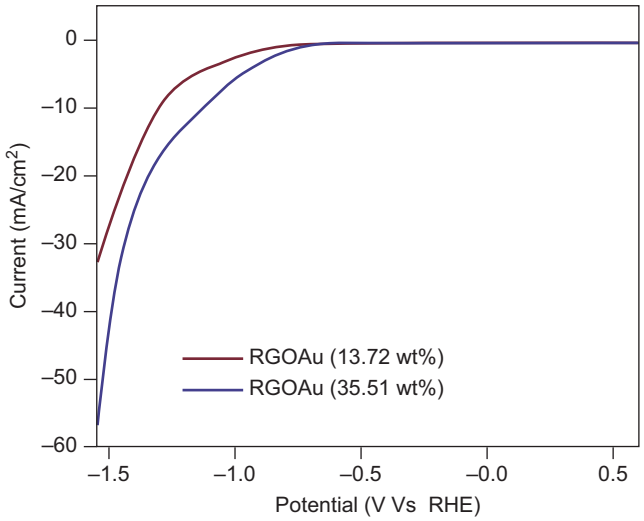

Figure 6.10: CVs of RGOAu catalysts (35.51 wt%, blue and 13.72 wt%, red in the CV). Reproduced with permission from ref. [30]. Copyright © Springer Science + Business Media B.V., part of Springer Nature 2018.

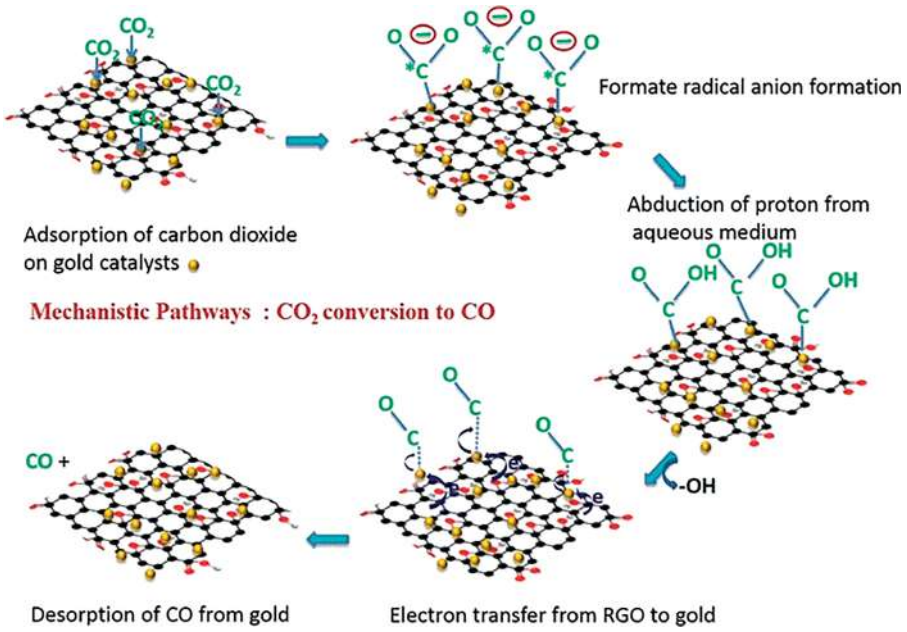

Figure 6.11: Proposed mechanism for CO_2 reduction by RGO-Au catalyst. Reproduced with permission from ref. [30]. Copyright © Springer Science + Business Media B.V., part of Springer Nature 2018.

6.2.3 Surface-functionalized gold nanoparticles

From the aforementioned discussion, it is clear that metal NPs (e.g., Au) could be one of the promising candidates among many electrocatalysts because of their high conductivities, large surface areas, and greater stabilities under the required CO_2 reduction potentials [8, 13, 14, 29, 31–34]. However, metal NPs mostly require surfactants having extended alkyl chains for stabilizing the NP surfaces. Moreover, these surfactants can reduce the catalytic activity of NPs by blocking the catalytically active sites [14, 17, 29, 34]. Additionally, these surfactants, being monodentate in nature, may leach out from NP surface under the electrocatalytic reaction condition, thereby inducing particle aggregation and resulting in loss of activity [29, 32, 34]. Therefore, concurrent stabilization of the catalyst surface and keeping catalytically active sites via appropriate designing of surface capping ligands of the NPs is required. In 2016, Z. Cao et al. [34] developed suitable *N*-heterocyclic carbene-functionalized Au NPs (represented as Au-Cb NP) as catalyst (Figure 6.12) and attached this catalyst with carbon paper electrode via appropriate synthetic modification. The AuNP/C combination was also prepared for relative comparison of activity. The authors have evaluated activities of these AuNP catalysts toward CO_2 reduction and compared with free carbene and a molecular Au-Cb complex using linear sweep voltammetry (Figure 6.13a). Under optimized reaction conditions, the control substances exhibited a negligible current response, further indicating superior catalytic activity for the Au-Cb NP.

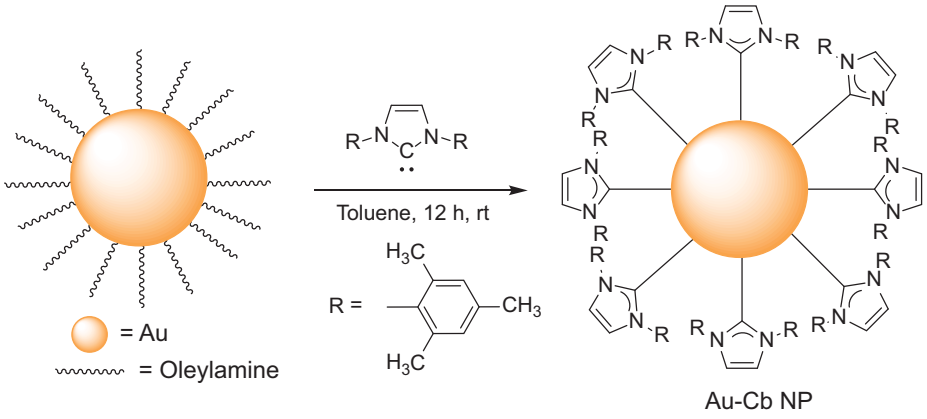

Figure 6.12: Cb ligand exchange reaction on AuNPs as reported by Z. Cao et al. [34].

The authors performed controlled potential electrolysis across a potential window between –0.27 and –0.87 V (vs RHE) to quantify CO_2 reduction products. Under all applied potentials studied, the Au-Cb NP catalyst exhibited greater FEs for CO and lesser FEs for H_2 than that of AuNP/C (Figure 6.13b). Based on various experimental evidences, the authors suggested that the significant σ-donation from the carbenes

made the Au NP surface very electron-rich in case of Au-Cb NP and thereby a quick electron transfer to CO_2 happened before the rate-limiting step (as shown in Figure 6.3). This destabilization might force to re-organize the gold NP surface, thus enhancing the number of defect sites with improved kinetics for the CO_2 reduction.

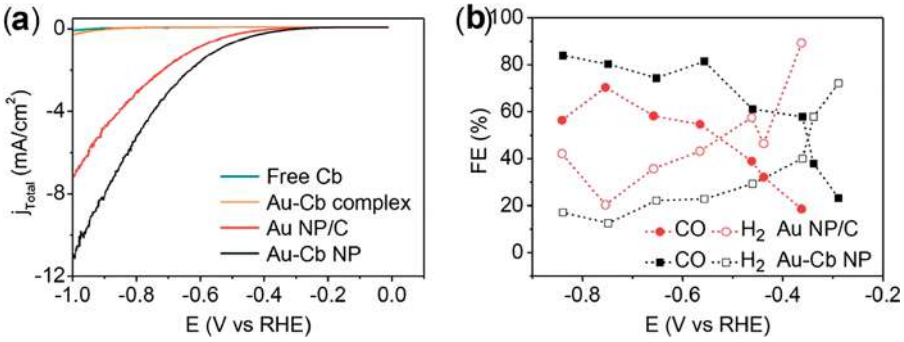

Figure 6.13: (a) Linear sweep voltammetry scans of Au-Cb NP, AuNP/C, free carbene, and molecular Au-Cb complex. (b) FEs of products obtained during CO_2 reduction by Au-Cb NP and AuNP/C. Reprinted with permission from ref. [34]. Copyright © 2016 American Chemical Society.

In 2018, Z. Cao et al. [35] explored a tetradentate porphyrin molecule to chelate on the surface of oleyl amine capped AuNP, therefore, successfully regulating the electrocatalytic CO_2 reduction efficiency and enhancing the catalyst stability. Firstly, the authors synthesized oleyl amine-capped AuNPs (represented as **OAm-AuNP**), and thereafter, by using ligand exchange process prepared the porphyrin-functionalized AuNPs (denoted as **P1-AuNP**) (Figure 6.14).

The catalytic activity of **P1-AuNP** and **OAm-AuNP** for electrochemical CO_2 reduction was then studied (using CV, Figure 6.15a) in a custom-made cell by using aqueous electrolyte solution. The CV measurements (Figure 6.15a) indicated that **P1-AuNP** showed much higher total current density and less negative onset potential (at −0.16 V vs RHE) compared to **OAm-AuNP** electrode. The authors carried out bulk electrolysis in CO_2-saturated $KHCO_3$ buffers across a range of applied potentials between −0.30 and −0.70 V (Figure 6.15b). The catalyst **P1-AuNP** showed higher FE_{CO} value (optimal FE_{CO} value = 93%) than that of **OAm-AuNP** under all applied potentials. Based on kinetic measurement data, the authors proposed that **P1-AuNP** might undergo single-electron transfer followed by a rate-determining chemical step [29, 34]. Further, based on DFT calculation, authors concluded that the reduction of CO_2 to CO on **P1-Au**(111) surface was energetically more favored than that of bare Au(111) surface.

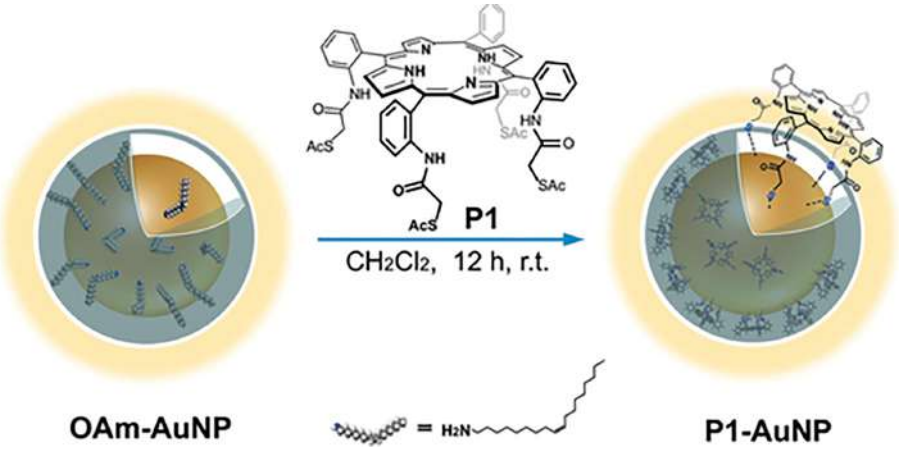

Figure 6.14: Preparation of **P1-AuNP**. Reproduced with permission from ref. [35]. Copyright © 2018 Wiley-VCH Verlag GmbH & Co. KGaA, Weinheim.

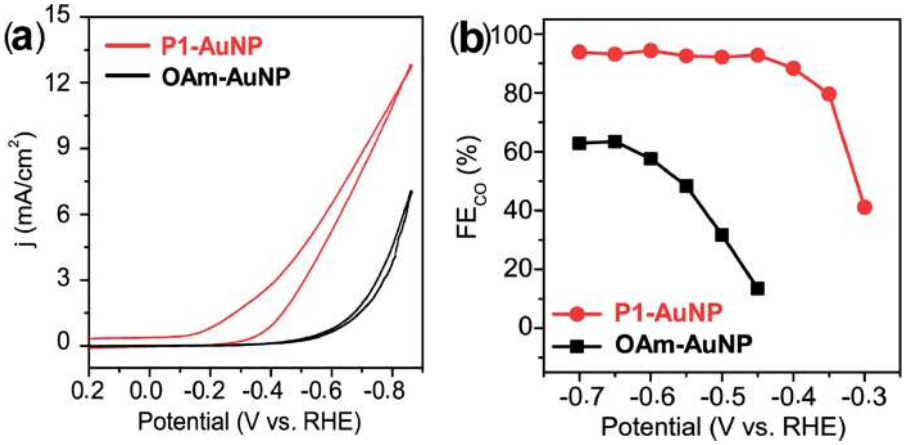

Figure 6.15: (a) CVs of **OAm-AuNP** and **P1-AuNP** electrodes. (b) FE_{CO} values for CO_2 reduction by **OAm-AuNP** and **P1-AuNP** electrodes. Reproduced with permission from ref. [35]. Copyright © 2018 Wiley-VCH Verlag GmbH & Co. KGaA, Weinheim.

6.3 Summary and outlook

Considering global energy demand and keeping environmental issues in mind, CO_2 conversion to energy-enrich compounds is of current research interest worldwide. Toward this goal, CO_2 electroreduction is one among the various sustainable approaches. However, single electron reduction of CO_2 to $CO_2^{\bullet-}$ requires large negative

overpotential. Moreover, H_2 evolution reaction competes with CO_2 reduction in aqueous medium. Thus, designing of appropriate catalyst is crucial for achieving selective CO_2 reduction over H_2 evolution, particularly, in aqueous medium. Recent studies showed that AuNPs with suitable structural modification (on the surface of the NPs) can significantly reduce the overpotential for initial reduction of CO_2 to $CO_2^{\bullet-}$ and follow-up reaction leads to CO as the main reduction product. Although a wide range of Au nanostructured materials have been reported as efficient catalysts for the electroreduction of CO_2 to CO, they follow a general reaction pathway as shown in Figure 6.16 [13, 14, 36]. Other than CO detachment, each single step in the mechanisms proceeds via concerted proton-coupled electron transfer pathway. In general, production of CO depends on both the formation (reaction Ia) and reduction (reaction Ib) of a COOH*, and further on the efficiency of the catalyst to release CO that is produced (reaction Ic). Additionally, to achieve high CO selectivity, the catalyst requires to promote reactions Ia–Ic while suppressing the HER reduction (reactions IIa–IIb).

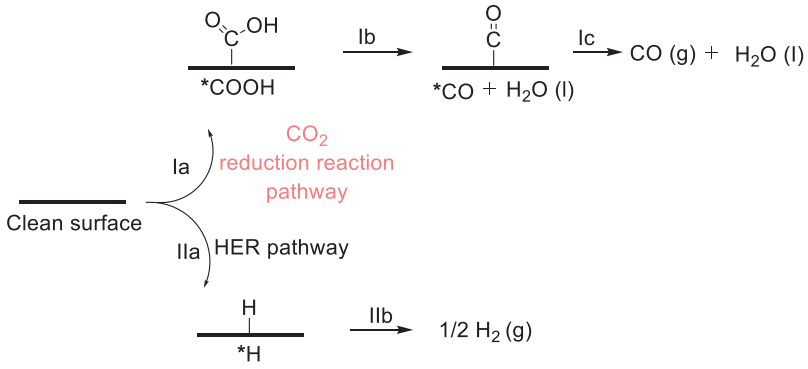

Figure 6.16: Proposed mechanisms for the electrocatalytic CO_2 reduction and hydrogen evolution reaction on nanostructured Au surfaces [36].

It is worth mentioning here that CO_2 electroreduction to CO using space confinement (which signifies those chemical reactions that occur inside nanoscale or even sub-nanoscale pockets) between gold NPs could also be considered as a viable approach according to a very recent report [36]. In this report, K. Chang et al. [36], using quantum chemical calculation, demonstrated that decreasing the limited space helped to stabilize *COOH adsorption (Figure 6.16), which altered the free energy of electrocatalytic reduction of CO_2 to CO and shifted the onset potential to less negative value. Alternatively, space restraint has a very small effect on the adsorption energy of *H. Therefore, decreasing the limited space did not disturb the free energy of the HER. Consequently, by the impact of space restraint, more amount of electricity was operated in the direction of required electrocatalytic CO_2 reduction from the competitive HER. We hope that this chapter will attract a broad readership

in the field of sustainable chemistry, help to dig deep inside the topic, and lead to the generation of new gold catalyst with superior efficiency that may assist to solve one of the most important global problems.

References

[1] Jacobson, MZ. Review of solutions to global warming, air pollution, and energy security. Energy Environ Sci, 2009, 2, 148–173.
[2] Lewis, NS, Nocera, DG. Powering the planet: Chemical challenges in solar energy utilization. Pnas, 2006, 103, 15729–15735.
[3] Climate Change, UN Conference COP 25. Chile, Dec 2–13, 2019.
[4] Lu, Q, Rosen, J, Jiao, F. Nanostructured Metallic Electrocatalysts for Carbon Dioxide Reduction. ChemCatChem, 2015, 7, 38–47.
[5] Francke, R, Schille, B, Roemelt, M. Homogeneously Catalyzed Electroreduction of Carbon Dioxide-Methods, Mechanisms, and Catalysts. Chem Rev, 2018, 118, 4631–4701.
[6] Matsubara, Y, Grills, DC, Kuwahara, Y. Thermodynamic Aspects of Electrocatalytic CO_2 Reduction in Acetonitrile and with an Ionic Liquid as Solvent or Electrolyte. ACS Catal, 2015, 5, 6440–6452.
[7] Schwarz, HA, Dodson, RW. Reduction potentials of CO_2- and the alcohol radicals. J Phys Chem, 1989, 93, 409–414.
[8] Hori, Y. Electrochemical CO_2 Reduction on Metal Electrodes, Springer: New York, 2008, 89–189.
[9] Zhao, S, Jin, R, Jin, R. Opportunities and challenges in CO_2 reduction by gold- and silver-based electrocatalysts: from bulk metals to nanoparticles and atomically precise nanoclusters. ACS Energy Lett, 2018, 3, 452–462.
[10] Peterson, AA, Norskov, JK. Activity descriptors for CO_2 electroreduction to methane on transition-metal catalysts. J Phys Chem Lett, 2012, 3, 251–258.
[11] Peterson, AA, Abild-Pedersen, F, Studt, F, Rossmeisl, J, Norskov, JK. How copper catalyzes the electroreduction of carbon dioxide into hydrocarbon fuels. Energy Environ Sci, 2010, 3, 1311–1315.
[12] Hansen, HA, Varley, JB, Peterson, AA, Norskov, JK. Understanding Trends in the Electrocatalytic Activity of Metals and Enzymes for CO_2 Reduction to CO. J Phys Chem Lett, 2013, 4, 388–392.
[13] Chen, Y, Li, CW, Kanan, MW. Aqueous CO_2 reduction at very low overpotential on oxide-derived Au Nanoparticles. J Am Chem Soc, 2012, 134, 19969–19972.
[14] Zhu, W, Michalsky, R, Metin, O, Lv, H, Guo, S, Wright, CJ, Sun, X, Peterson, AA, Sun, S. Monodisperse Au nanoparticles for selective electrocatalytic reduction of CO_2 to CO. J Am Chem Soc, 2013, 135, 16833–16836.
[15] Kibsgaard, J, Chen, Z, Reinecke, BN, Jaramillo, TF. Engineering the surface structure of MoS2 to preferentially expose active edge sites for electrocatalysis. Nat Mater, 2012, 11, 963–969.
[16] Chen, C, Kang, Y, Huo, Z, Zhu, Z, Huang, W, Xin, HL, Snyder, JD, Li, D, Herron, JA, Mavrikakis, M, Chi, M, More, KL, Li, Y, Markovic, NM, Somorjai, GA, Yang, P, Stamenkovic, VR. Highly crystalline multimetallic nanoframes with three-dimensional electrocatalytic surfaces. Science, 2014, 343, 1339–1343.

[17] Zhu, W, Zhang, YJ, Zhang, H, Lv, H, Li, Q, Michalsky, R, Peterson, AA, Sun, S. Active and selective conversion of CO_2 to CO on ultrathin Au nanowires. J Am Chem Soc, 2014, 136, 16132–16135.
[18] Nursanto, EB, Jeon, HS, Kima, C, Jee, MS, Koh, JH, Hwang, YJ, Min, BK. Gold catalyst reactivity for CO_2 electro-reduction: From nano particle to layer. Catalysis Today, 2016, 260, 107–111.
[19] Kim, Y, Jo, A, Ha, Y, Lee, Y, Lee, D, Lee, Y, Lee, C. Highly Dispersive Gold Nanoparticles on Carbon Black for Oxygen and Carbon Dioxide Reduction. Electroanalysis, 2018, 30, 2861–2868.
[20] Stankovich, S, Dikin, DA, Dommett, GH, Kohlhaas, KM, Zimney, EJ, Stach, EA, Piner, RD, Nguyen, ST, Ruoff, RS. Graphene-based composite materials. Nature, 2006, 442, 282–286.
[21] Geim, AK, Novoselov, KS. The rise of graphene. Nat Mater, 2007, 6, 183–191.
[22] Park, S, Ruoff, RS. Chemical methods for the production of graphenes. Nat Nanotechnol, 2009, 4, 217–224.
[23] Antolini, E. Carbon supports for low-temperature fuel cell catalysts. Appl Catal B Environ, 2009, 88, 1–24.
[24] Vo, TH, Shekhirev, M, Kunkel, DA, Morton, MD, Berglund, E, Kong, L, Wilson, PM, Dowben, PA, Enders, A, Sinitskii, A. Large-scale solution synthesis of narrow graphene nanoribbons. Nat Commun, 2014, 5, 3189.
[25] Narita, A, Feng, X, Hernandez, Y, Jensen, SA, Bonn, M, Yang, H, Verzhbitskiy, IA, Casiraghi, C, Hansen, MR, Koch, AH, Fytas, G, Ivasenko, O, Li, B, Mali, KS, Balandina, T, Mahesh, S, Feyter, SD, Müllen, K. Synthesis of structurally well-defined and liquid-phase-processable graphene nanoribbons. Nat Chem, 2014, 6, 126–132.
[26] Müllen, K. Evolution of Graphene Molecules: Structural and Functional Complexity as Driving Forces behind Nanoscience. ACS Nano, 2014, 8, 6531–6541.
[27] Narita, A, Verzhbitskiy, I, Frederickx, W, Mali, K, Jensen, S, Hansen, M, Bonn, M, Feyter, SD, Casiraghi, C, Feng, X, Müllen, K. Bottom-up synthesis of liquid-phase-processable graphene nanoribbons with near-infrared absorption. ACS Nano, 2014, 8, 11622–11630.
[28] Narita, A, Feng, X, Müllen, K. Bottom-up synthesis of chemically precise graphene nanoribbons. Chem Rec, 2015, 15, 295–309.
[29] Rogers, C, Perkins, WS, Veber, G, Williams, TE, Cloke, RR, Fischer, FR. Synergistic enhancement of electrocatalytic CO_2 reduction with gold nanoparticles embedded in functional graphene nanoribbon composite electrodes. J Am Chem Soc, 2017, 139, 4052–4061.
[30] Saquib, M, Halder, A. Reduced graphene oxide supported gold nanoparticles for electrocatalytic reduction of carbon dioxide. J Nanopart Res, 2018, 20, 46.
[31] Liu, M, Pang, Y, Zhang, B, Luna, PD, Voznyy, O, Xu, J, Zheng, X, Dinh, CT, Fan, F, Cao, C, Arquer, F, Safaei, TS, Mepham, A, Klinkova, A, Kumacheva, E, Filleter, T, Sinton, D, Kelley, SO, Sargent, EH. Enhanced electrocatalytic CO_2 reduction via field-induced reagent concentration. Nature, 2016, 537, 382–386.
[32] Kim, D, Resasco, J, Yu, Y, Asiri, AM, Yang, P. Synergistic geometric and electronic effects for electrochemical reduction of carbon dioxide using gold–copper bimetallic nanoparticles. Nat Commun, 2014, 5, 4948.
[33] Shang, H, Wallentine, SK, Hofmann, DM, Zhu, Q, Murphy, CJ, Baker, LR. Effect of surface ligands on gold nanocatalysts for CO_2 reduction. Chem Sci, 2020, 11, 12298.

[34] Cao, Z, Kim, D, Hong, D, Yu, Y, Xu, J, Lin, S, Wen, X, Nichols, EM, Jeong, K, Reimer, JA, Yang, P, Chang, CJ. A Molecular Surface Functionalization Approach to Tuning Nanoparticle Electrocatalysts for Carbon Dioxide Reduction. J Am Chem Soc, 2016, 138, 8120–8125.

[35] Cao, Z, Zacate, SB, Sun, X, Liu, J, Hale, EM, Carson, WP, Tyndall, SB, Xu, J, Liu, X, Liu, X, Song, C, Luo, J, Cheng, MJ, Wen, X, Liu, W. Tuning Gold Nanoparticles with Chelating Ligands for Highly Efficient Electrocatalytic CO_2 Reduction. Angew Chem Int Ed, 2018, 57, 12675–12679.

[36] Chang, K, Jian, X, Jeong, HM, Kwon, Y, Lu, Q, Cheng, MJ. Improving CO_2 Electrochemical Reduction to CO Using Space Confinement between Gold or Silver Nanoparticles. J Phys Chem Lett, 2020, 11, 1896–1902.

Rajib Sarkar, Chhanda Mukhopadhyay*

7 Copper-based heterogeneous catalysis for the synthesis of small organic molecules in aqueous medium

7.1 Introduction

Water is ubiquitous in nature and plays a key role as solvent in biological transformations in living organisms. Therefore, by utilizing the omnipresent water as the solvent for heterogeneous catalysis has been a focus of study for many years [1–6]. This idea to take benefits of water as solvent has resulted in altering the activity as well as selectivity of heterogeneous catalystsbased on metal complexes, nanomaterials, microporous supports, and others [7, 8].

In this perspective, Cu-based heterogeneous catalysts are mostly attractive due to high natural abundance and low cost. Being a 3d transition metal, copper has interesting physical and chemical properties [9]. Moreover, copper is very much compatible with the chemical transformations at high-temperature and high-pressure including vapor-phase chemical reactions and microwave-assisted reactions [10–12]. Such distinctive properties of copper and its alloys are favorable for the construction of new, efficient, and selective catalytic protocols [13, 14].

The applications of these economical copper catalysts, including Cu-based nanoparticles (NPs), have potential interest in current years, particularly in the field of heterogeneous catalysis in water. Additionally, having variable oxidation states (Cu^{III}, Cu^{II}, Cu^{I}, and Cu^{0}), Cu-based catalysts can promote a range of reactions via one- as well as two-electron change pathways. The convenient and straightforward numerous ways of developing Cu-based heterogeneous catalystsalso makes its applications more general [15–20]. Remarkably, the potential modification of the copper-based NPs and their catalytic activity in aqueous conditions have been intensely studied. Till date, researchers in heterogeneous catalysis have projected many catalytic processes in aqueous medium [21]. Despite the considerable development of aqueous

Acknowledgments: The first author thanks the Prabhu Jagatbandhu College for their kind support. The authors are also thankful to CAS-V (UGC), Department of Chemistry, University of Calcutta.

***Corresponding author: Chhanda Mukhopadhyay,** Department of Chemistry, University of Calcutta, 92 APC Road, Kolkata 700009, India, e-mail: cmukhop@yahoo.co.in
Rajib Sarkar, Department of Chemistry, University of Calcutta, 92 APC Road, Kolkata 700009, India, rajib007park@gmail.com; Department of Chemistry, Prabhu Jagatbandhu College, Jhorehat, Andul-Mouri, Howrah 711302, India

https://doi.org/10.1515/9783110733846-007

heterogeneous catalytic protocols, at present the literature does not have any systematic review of this field.

This chapter addresses several aspects of copper-based heterogeneous catalytic reactions in water reported so far. The key aim of this chapter is to appraise the copper-based heterogeneous catalysis in water for synthesizing small organic molecules. We suppose this critical evaluation will provide required formations to develop the future applications of Cu-based heterogeneous catalysis in water. The discussion in the first part covers the heterogeneous catalysis by Cu-based NPs in aqueous medium. The second part emphasizes the synthetic protocols catalyzed by other supported heterogeneous copper catalysts in water.

7.2 Cu-based nanoparticles: applications in organic synthesis

The catalytic applications of NPs correspond to a wealthy source for chemical methods, employed in convenient transformations [22, 23]. NPs have been used in various procedures, including biological protocols, chemical industry, energy storage, and environmental equipment [24, 25]. The great potential of nanocatalysis has encouraged the synthesis of various diversely substituted organic molecules in aqueous medium.

Nanomaterials have developed from earth-abundant inexpensive copper (Cu) metal, and have received significant attention due to their prospective as possible alternatives to the expensive and rare noble metal catalysts used in several commercial chemical methods [26]. The copper NPs often show catalytic activity dissimilar from that of the related bulk resources due to their different shapes and sizes.

In this part, we focus on the heterogeneous catalytic applications of Cu-based NPsin water for the synthesis of diverse organic molecules. To simplify our idea on the reactions catalyzed by copper-based NPs, we have outlined them into two different categories: (i) click chemistry of azide–alkyne cycloaddition and (ii) coupling reactions.

7.2.1 Click chemistry of azide–alkyne cycloaddition

In 2011, Borah et al. [27] have studied the 1,3-dipolar cycloaddition reaction between terminal alkynes (**1**) and alkyl azides (**2**) for the synthesis of 1,2,3-triazoles (**3**) catalyzed by in situ-generated Cu(0)-NPs embedded in nanopores of a modified montmorillonite (Figure 7.1). The modification has been carried out through activating montmorillonite by H_2SO_4 under controlled environment, where the generated nanopores act as “host” for Cu(0)-NPs. The generated Cu(0)-NPs were spherical in shape

and the size is around 10 nm. The catalyst acts as an effective green catalyst for the click reaction of azide–alkyne cycloaddition to give regioselective 1,4-disubstituted-1,2,3-triazoles (**3**) with good to excellent yields under aqueous environment. The method is compatible with linear as well as branched alkylazides, including hindered azides. The nanocatalysts were also reused in next reactions without considerable loss of catalytic activity. Easy to employ and recyclability of the catalyst under environmentally benign reaction conditions make the protocol attractive and suitable for large-scale preparation of triazole-based drug molecules.

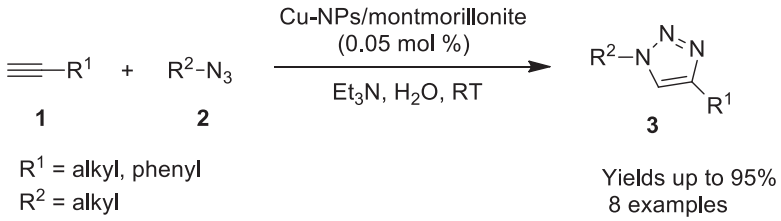

Figure 7.1: Cu-NP/montmorillonite-catalyzed synthesis of 1,2,3-trizoles.

Copper NPs immobilized on charcoal (Cu NPs/C) were developed by Alonso et al. in 2011 (Figure 7.2) [28]. This versatile and reusable catalyst consisting of oxidized Cu NPs on activated charcoal effectively catalyzed the three-component synthesis of disubstituted 1,2,3-triazoles (**3**) in water. A wide range of 1,4-disubstituted triazoles (**3**) have been synthesized from organic halides (**4**) or diazonium salts (**5**) or aryl primary amines (**6**) with sodium azide (**7**) and different terminal alkynes (**1**). The catalyst gave high yields of 1,2,3-triazoles (**3**) and also showed excellent recyclability. The catalyst was fully characterized and the copper NPs were found mostly to be in the oxidized forms (Cu_2O and CuO). Two protocols involving anilines or its diazonium salts as aryl–azide precursor were described in this click reaction. The developed catalytic protocol and described methodologies follow most of the principles of green chemistry.

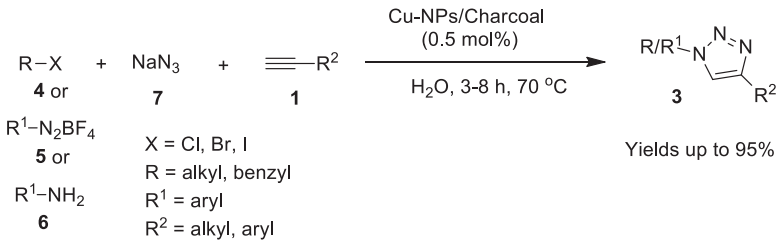

Figure 7.2: Cu-NPs/charcoal-catalyzed synthesis of 1,2,3-triazoles.

In 2011, Alonso et al. [29] reported copper NPs on activated carbon-catalyzed synthesis of a wide range of β-hydroxy 1,4-disubstituted 1,2,3-triazoles (**3a**) in aqueous medium (Figure 7.3). This is a multicomponent 1,3-dipolar cycloaddition protocol involving variety of epoxides (**8**) with alkynes (**1**) and sodium azide (**7**) in water at 70 °C. Herein the regioselective 1,4-adducts, the epoxide azidolysis extremely depends on the steric as well as electronic properties of the epoxides. The catalyst is reusable and easy to prepare, and also exhibits remarkable catalytic activity up to fourth cycles. The regio- and stereoselectivities of the synthesis have been recognized by NMR experiment as well as X-ray crystallographic analyses. Mechanistic investigation of the reaction revealed the generation of copper(I) acetylides and triazolides as intermediates of the reaction.

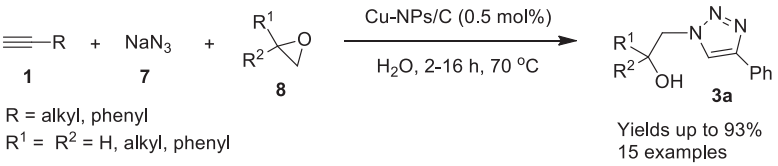

Figure 7.3: Cu-NP/C-catalyzed synthesis of triazoles by epoxide azidolysis.

In 2013, Radivoy et al. [30] reported a magnetically recoverable CuNPs onto silica-coated maghemite to catalyze a multicomponent course involving in situ formation of organic azide followed by 1,3-dipolar cycloaddition with terminal alkynes (**1**) in water at 70 °C (Figure 7.4). The catalyst was easily prepared by the addition of magnetic silica to a suspension of copper NPsprepared through reducing cupric chloride ($CuCl_2$) by Li along with 4,4′-di-*tert*-butylbiphenyl in THF as solvent at room temperature. The catalyst was recycled by a magnet and used again without substantial loss of catalytic activity. The TEM experiments revealed that the catalyst composed of 3.0 nm copper NPs on silica-coated maghemite NPs of 5–30 nm. This new reusable copper-based heterogeneous catalyst also has shown efficient catalytic activity for several reactions such as Glaser alkyne dimerization, Huisgen 1,3-dipolar cycloaddition,and multicomponent synthesis of propargyl amines under sustainable conditions.

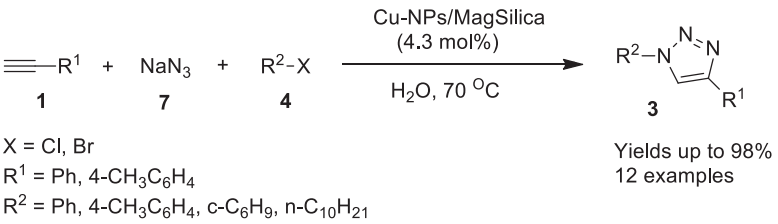

Figure 7.4: Cu NPs on MagSilica-catalyzed synthesis of triazoles.

Pourjavadi and coworkers [31] reported a heterogeneous Cu(II) species of poly (ionic liquid)-coated magnetic NP-catalyzed one-pot three-component synthesis of disubstituted 1,2,3-triazole (**3b**) derivatives by click reactions in 2015 (Figure 7.5). The catalyst has remarkable catalytic activity and is used in small weight percent to catalyze the reaction of halides or tosylates (**9**) with azide salt (**7**) and terminal alkynes (**1**) in the presence of aqueous sodium ascorbate at room temperature to produce triazole derivatives (**3b**). The distinctive nanocatalyst composition and the multilayered structure of coated polymer of vinyl imidazolium ionic liquid based on the magnetite Fe_3O_4 surface will result in the excellent catalytic activity toward click reactionsshowing exceptional substrate scope with broad versatility. The catalyst was reused up to fifth cycle and used to produce more than 30 diverse ranges of products from different combinations of reactants in excellent yields. This present green protocol is also useful for industrial applications.

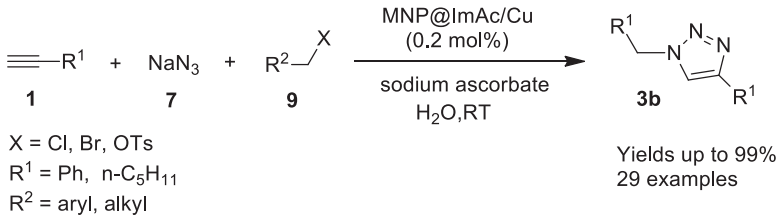

Figure 7.5: Huisgen 1,3-dipolar cycloaddition, catalyzed by MNP@ImAc/Cu.

7.2.2 Coupling reactions

In 2013, Honraedt and coworkers [32] described copper oxide NPs supported by graphite (CuO NPs/Gr) catalyzed C–H arylation of benzoquinone derivatives (**10**) in water (Figure 7.6). This protocol is the first instance of a heterogeneously catalyzed Meerwein arylation. The CuONP/Gr catalyst was prepared in MeOH from the $Cu(OAc)_2$ and graphite under H_2. The generality of the reaction was examined with various diversely substituted aniline derivatives (**6**) having alkynes, nitriles, halogens, ketones, and ester substituents. Various naphthoquinone derivatives (**10**) can also be used as the reacting partner without affecting the reaction's efficiency. The addition of DMSO as cosolvent was used to increase the solubility of reactants, while the use of $CaCO_3$ maintains the solution buffer. The sturdiness of the CuONPs/Gr heterogeneous catalyst was performed up to five recycling experiments for the coupling between benzoquinones (**10**) and substituted anilines(**6**) under mild and simple conditions.

In 2008, Ranu and coworkers [33] reported a green synthesis of *S*-aryl- and *S*-styrenyl-dithiocarbamates (**15** and **16**) through a one-pot three-component reaction of a secondary amine (**14**), carbon disulfide (**13**) with styrenyl bromides (**12**) or aryl iodides (**4a**) by using spherical Cu NPs as catalyst in water (Figure 7.7). The experimental

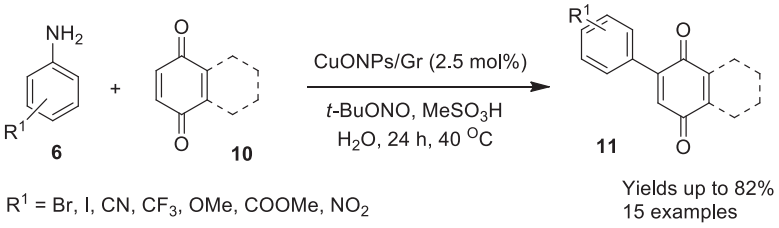

Figure 7.6: Graphite-supported CuO NP-catalyzed synthesis of C–H arylation of benzoquinones.

protocol is very efficient and convenient requiring only refluxing water, and no additional ligand or base or additives are required. The reaction was investigated with various secondary acyclic amines like diethylamine, dimethylamine, and also with cyclic amines including piperidine, pyrrolidine, and morpholine with good yields of the products. This protocol using spherical copper NPs showed excellent stereoselectivity for (*E*)- and (*Z*)-styrenyl dithiocarbamates and also catalyst recyclability up to four times with almost same catalytic activity.

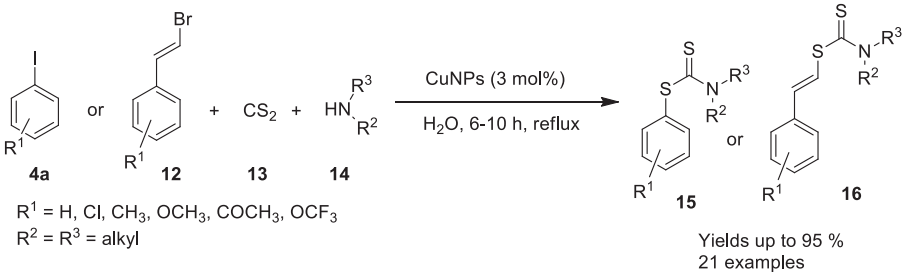

Figure 7.7: Cu NP-catalyzed synthesis of S-aryl and S-vinyldithiocarbamates.

In 2012, Duan et al. [34] reported a novel copper NP for the reduction of aryl nitro compounds (**17**) with sodium borohydride (**18**) in aqueous medium at 50 °C (Figure 7.8). Many aromatic nitro derivatives (**17**) were reduced to the corresponding amino products (**6**) in high yields in 1:2 mixture of THF–water and catalyzed by Cu NPs. The copper nanocatalyst was prepared from cupric sulfate ($CuSO_4$) by using hydrazine as the reducing reagent and recycled for several reaction cycles with high catalytic efficiency. This reaction protocol provides the advantages of easier separation of products with higher yields at lower cost compared with the other usual methods of the reduction of nitro compounds.

In 2014, Sen and coworkers [35] outlined a one-pot three-component protocol for the synthesis of 2,3-dihydro-isoindolinones (**21**) using cuprous oxide NPs as the catalyst in aqueous medium (Figure 7.9). This is an efficient cost-effective environmentally benign protocol involving substituted indoles/pyrroles (**20**), 2-iodo-*N*-

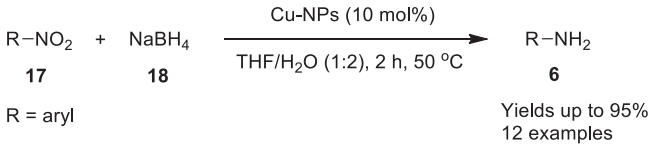

Figure 7.8: Cu-NP-catalyzed reduction of aromatic nitro compounds.

phenylbenzamides (**19**), and terminal alkynes (**1**) in water at 50 °C. The scope of the reaction is broad, and versatility of the reaction also covers the aliphatic alkynes without any alkyne dimerization. The catalyst Cu_2O NPs were prepared by hydrolysis of $CuCl_2$, followed by addition of fructose as the reducing as well as capping agent via the formation of $Cu(OH)_2$. The nanocatalysts were efficiently employed and recycled under environmentally benign aerobic and inert conditions without using additional ligands or any surfactants. The formation of 2,3-dihydro-isoindolinones (**21**) through domino Sonogashira cyclization reaction followed by regioselective nucleophilic addition was also established during mechanistic investigation.

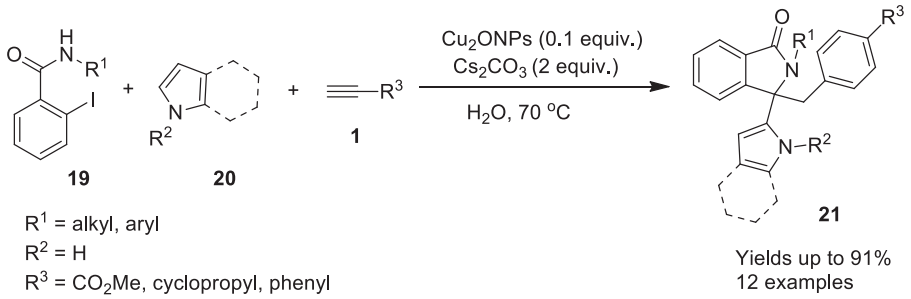

Figure 7.9: Synthesis of isoindolinones catalyzed by Cu_2O NPs.

In 2013, Ghahremanzadeh and coworkers [36] demonstrated a three-component green protocol involving cylohexane-1,3-diones (**22**), active cyanomethanes (**24**) along with isatins (**23**), catalyzed by copper ferrite NPs in refluxing water (Figure 7.10). This is the preparation of spirooxindole fused heterocycles (**25**) by using magnetically recoverable as well as reusable copper ferrite NP catalyst under mild reaction conditions having broad substrate scope, promoting the synthesis of 19 oxindoles (**25**) with high yields of products with purity. The catalyst copper ferrite NPs having a size of 35 nm were prepared from aqueous sodium hydroxide solution through coprecipitation of Fe $(NO_3)_2$ and $Cu(NO_3)_2$. The operational simplicity, easy workup procedures, and excellent catalyst recyclability up to many cycles by magnetic separation of the nanocatalyst make the process more attractive.

In 2015, Sarkar et al. [37] reported a reusable nanocopper(I) oxide-catalyzed C–C coupling for the synthesis of amides (**27**) in water (Figure 7.11). This is a cost-effective

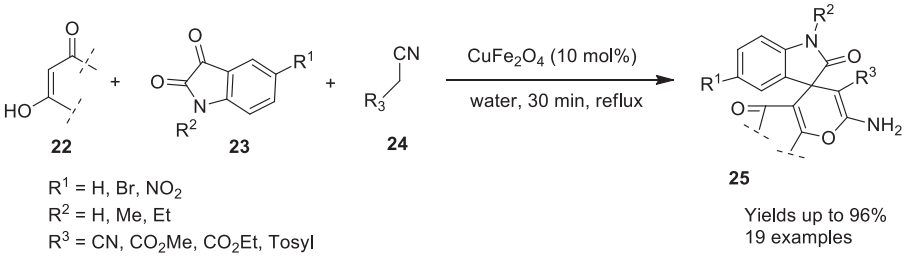

Figure 7.10: Synthesis of spirooxindoles catalyzed by copper ferrite NPs.

green amidation involving aryl halides (**4**) and isocyanides (**26**) showing broad substrate scope with no additives or additional ligands. The product amides were synthesized in good to excellent yields by using a variety of aliphatic or aryl isocyanides with aryl halides. The catalyst was effectively recycled and reused up to four cycles with same robustness in water under aerobic conditions.

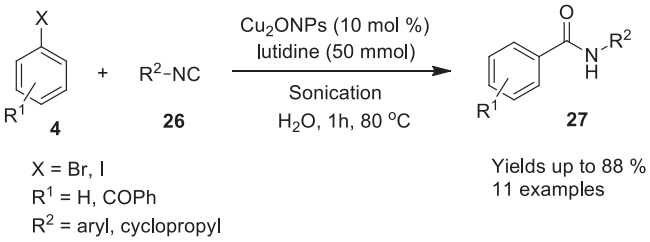

Figure 7.11: Copper(I) oxide NPs catalyzed synthesis of amides in aqueous medium.

In 2014, Patel and coworkers [38] established the synthesis of *o*-hydroxyanilides (**29**) and benzoxazoles (**30**) from *o*-haloanilides (**28**) catalyzed by CuONPs in refluxing water (Figure 7.12). The use of Cs_2CO_3 (inorganic base) promoted the formation of *o*-hydroxyanilides (**29**) as the major product, while the organic base *N*,*N*,*N*′,*N*′-tetramethylethane-1,2-diamine enabled the selective formation of benzoxazoles (**30**). A range of *o*-halophenyl alkylamides selectively provided either *o*-hydroxylated products (**29**) or benzoxazoles (**30**) depending on the base used with the CuO nanocatalyst under both the reaction conditions showing the reaction versatility with broad substrate scope. The catalyst was also reusable up to five reaction cycles with comparable catalytic activity, and thereafter the catalytic activity decreases due to aggregation.

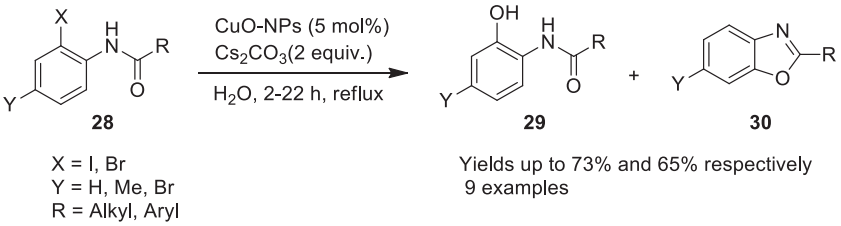

Figure 7.12: CuO-NP-catalyzed formation of benzoxazoles and *o*-hydroxyanilides.

7.3 Synthetic protocols catalyzed by other supported heterogeneous copper catalysts

In 2015, Pourjavadi et al. [39] reported a heterogeneous graphene oxide/poly(vinyl imidazole)-supported copper(II) polymeric catalyst and used in click synthesis of substituted 1,2,3-triazole (**3**) in water at 50 °C (Figure 7.13). This is a one-pot multicomponent cycloaddition of sodium azide (**7**) and halides (**4**) along with terminal alkynes (**1**) producing 1,4-disubstittued 1,2,3-triazoles (**3**) in excellent yields under mild reaction conditions. The heterogeneous catalyst was prepared by immobilization of copper(II) ions in a nanocomposite of graphene oxide/poly(vinyl imidazole). The catalyst has high catalytic activity for the click synthesis of 1,2,3-triazoles (**3**) carried out in water and is suitable to a wide substrate scope (alkyl/benzyl halides and aromatic/aliphatic alkynes). The catalyst was readily recovered and recycled up to eight times without significant loss of activity and can be utilized for large-scale preparation of 1,2,3-triazole derivatives (**3**).

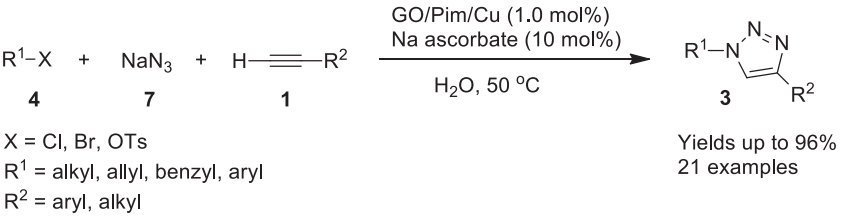

Figure 7.13: Graphene oxide/poly(vinyl imidazole)-supported heterogeneous copper(II) polymeric-catalyzed synthesis of 1,2,3-triazole.

In 2015, Kobayashi and coworkers [40] reported a nonimmobilized chiral heterogeneous catalysts of copper(II) for the enantioselective addition of silylboronates (**32**) with various α, β-unsaturated ketones (**31**) in water at room temperature (Figure 7.14). The catalyst was prepared from copper acetylacetonate ($Cu(acac)_2$) with a chiral bipyridine ligand (**34**). Most significantly, the reactions proceed efficiently only in water, leading to high yields with enantioselectivities and did not undergo well in

organic or in mixed organic/water solvents. In this copper-based heterogeneously catalytic protocol, water has an important role in promoting sterically confined transition states as well as accelerating the successive protonation to attain high yields of the enantioselective products (**33**) with wide substrate scope.

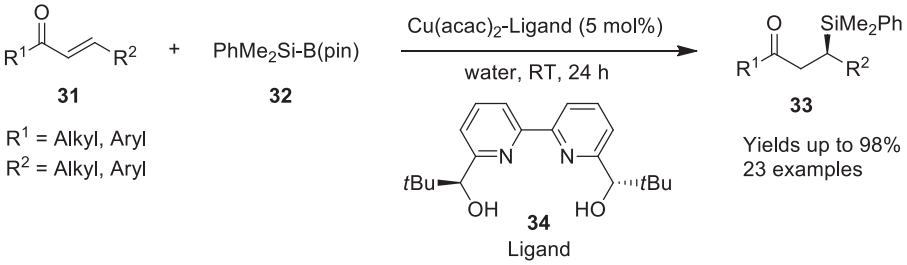

Figure 7.14: Copper(II) acetylacetonate-chiral bipyridine catalyzed asymmetric silyl addition in water.

In 2016, Tubío et al. [41] synthesized Cu/Al_2O_3 catalyst of woodpile porous composition by 3D printing followed by sintering at elevated temperature. The copper species are immobilized into Al_2O_3 matrix to obtain a copper-supported rigid arrangement having high mechanical strength and high surface-to-volume ratio with controlled macroporosity. The prepared catalyst exhibits high catalytic efficiency and excellent recyclability in various Ullmann reactions with large substrate scope (Figure 7.15). Ease of catalyst preparation, remarkable reactivity, recyclability, and little metal leaching make this 3D printing method a good alternative strategy for fabricating different kinds of metal/oxide heterogeneously catalyzed protocols.

In 2018, Rhee and coworkers [42] synthesized two different types of solid supports for the development of two heterogeneous catalysts. One is reverse phase silica gel of aminopropyl functionality and another is a thermoresponsive poly(*N*-isopropylacrylamide-co-4-vinylpyridine) (*p*-NIPAM-VP). The reverse-phase silica gel solid supports have an end-capped hydrophobic alkyl group and another solid support shows hydrophobicity and hydrophilicity depending on the temperature. The catalyst was obtained by the immobilization of Cu(I) and Cu(II) species onto these two types of solid supports and catalytically used in the azide–alkyne cycloaddition reaction in water at 60 °C. Several 1,4-disubstituted-1,2,3-triazoles (**3b**) were prepared with broad substrate diversity using the synthesized copper catalysts (Figure 7.16). These catalysts are stable in air and can be reused in multiple cycles furnishing good to outstanding yields of the triazoles (**3b**).

In 2017, Pogula et al. [43] established a convenient green synthesis of quinoxalines (**42**) and substituted benzimidazoles (**37b**) catalyzed by copper NPsstabilized on alumina (Figure 7.17). The reaction is carried out in aqueous medium at room temperature with no additional oxidant or surfactant. Various substituted *o*-

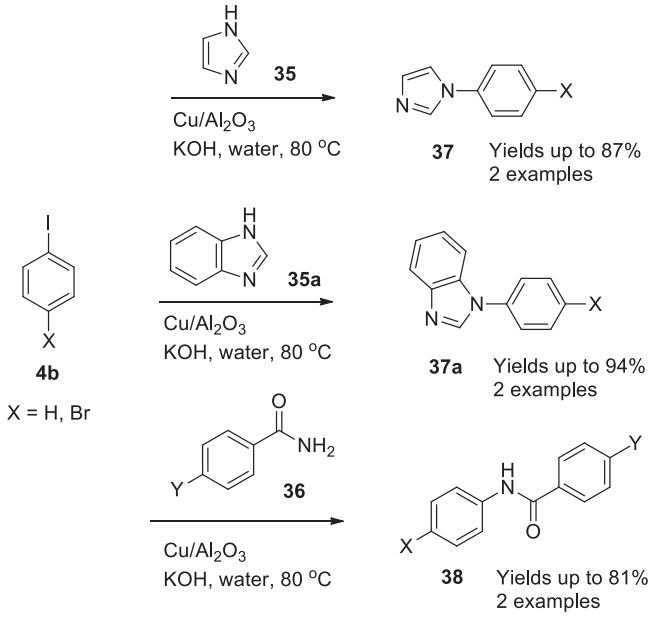

Figure 7.15: Cu/Al_2O_3 catalytic system-catalyzed Ullmann reactions.

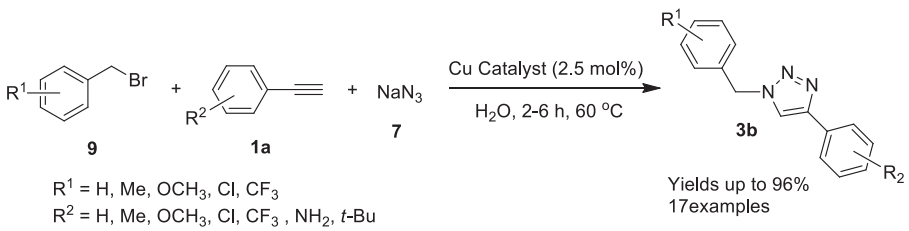

Figure 7.16: Solid-supported Cu-catalyzed synthesis of 1,2,3-triazoles.

phenylenediamines (**39**) with α-bromo ketones (**40**) or aldehydes (**41**) were used to generate broad ranges of functionalized heterocyclic compounds (**42** and **37b**) in high yields. The catalyst can be recovered and reused up to five cycles with almost same activity under this environmentally benign protocol.

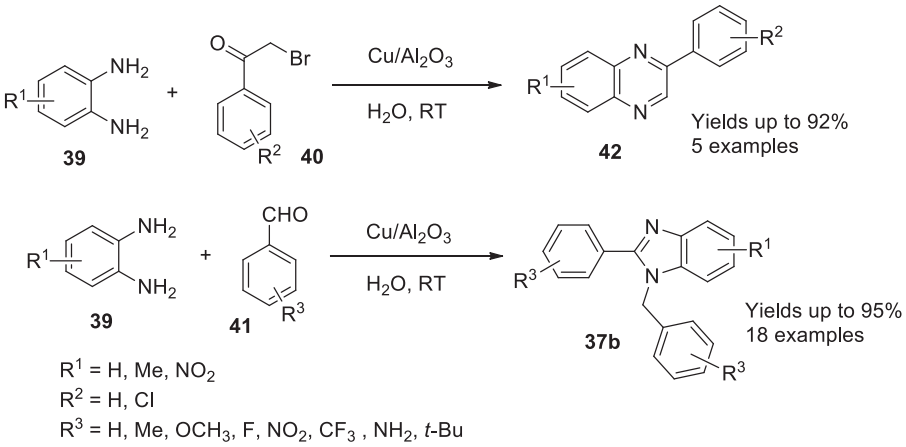

Figure 7.17: Cu(0)/Al_2O_3-catalyzed synthesis of quinoxalines and 1,2-disubstituted benzimidazoles.

7.4 Conclusions

Copper-based heterogeneous catalystsare found to be very effective for the synthesis of a variety of substituted organic molecules. As a result, the last decade has seen tremendous outburst to design new heterogeneously catalyzed protocols for the synthesis of various small organic molecules under aqueous reaction conditions. Under this direction, among heterogeneous catalysis, recently solid supported catalysts have gained considerable attention. This chapter summarized the applications of copper-based heterogeneous catalysts for the synthesis of various organic molecules such as aromatic amines, substituted amides, *o*-hydroxyanilides, 1,2-disubstituted imidazoles or benzimidazoles, benzoxazoles, 1,2,3-triazoles or β-hydroxy-1,2,3-triazoles, quinoxalines, C-H arylated benzoquinones, 2,3-dihydro-isoindolinones, spirooxindole fused heterocycles, as well as *S*-aryl- and *S*-styrenyl-dithiocarbamates.

References

[1] Ball, P. Water an Active Constituent in Cell Biology. Chem Rev, 2008, 108, 74–108.
[2] Herrerías, CI, Yao, X, Li, Z, Li, C-J. Reactions of C-H Bonds in Water. Chem Rev, 2007, 107, 2546–2562.
[3] Walter, MG, Warren, EL, McKone, JR, Boettcher, SW, Mi, Q, Santori, EA, Lewis, NS. Solar Water Splitting Cells. Chem Rev, 2010, 110, 6446–6473.
[4] Forneris, F, Mattevi, A. Enzymes Without Borders: Mobilizing Substrates, Delivering Products. Science, 2008, 321, 13–216.
[5] Feng, L, Yan, H, Wu, Z, Yan, N, Wang, Z, Jeffrey, PD, Shi, Y. Structure of a Site-2 Protease Family Intramembrane Metalloprotease. Science, 2007, 318, 1608–1612.

[6] Snyder, PW, Mecinović, J, Moustakas, DT, Thomas, SW, Harder, M, Mack, ET, Lockett, MR, Héroux, A, Sherman, W, Whitesides, GM. Mechanism of the Hydrophobic Effect in the Biomolecular Recognition of Arylsulfonamides by Carbonic Anhydrase. Proc Natl Acad Sci U S A, 2011, 108, 17889–17894.
[7] Zhao, M, Ou, S, Wu, C-D. Porous Metal-Organic Frameworks for Heterogeneous Biomimetic Catalysis. Acc Chem Res, 2014, 47, 1199–1207.
[8] Xuereb, DJ, Raja, R. Design Strategies for Engineering Selectivity in Bio-Inspired Heterogeneous Catalysts. Catal Sci Technol, 2011, 1, 517–534.
[9] Zhang, J, Liu, J, Peng, Q, Wang, X, Li, Y. Nearly Monodisperse Cu_2O and CuO Nanospheres: Preparation and Applications for Sensitive Gas Sensors. Chem Mater, 2006, 18, 867–871.
[10] Yoshida, K, Gonzalez-Arellano, C, Luque, R, Gai, PL. Efficient Hydrogenation of Carbonyl Compounds using Low-Loaded Supported Copper Nanoparticles under Microwave Irradiation. Appl Catal A, 2010, 379, 38–44.
[11] Ranu, BC, Saha, A, Jana, R. Microwave-Assisted Simple and Efficient Ligand Free Copper Nanoparticle Catalyzed Aryl-Sulfur Bond Formation. Adv Synth Catal, 2007, 349, 2690–2696.
[12] Reymond, S, Cossy, J. Copper-Catalyzed Diels-Alder Reactions. Chem Rev, 2008, 108, 5359–5406.
[13] Decan, MR, Impellizzeri, S, Marin, ML, Scaiano, JC. Copper Nanoparticle Heterogeneous Catalytic 'Click' Cycloaddition Confirmed by Single-Molecule Spectroscopy. Nat Commun, 2014, 5, 4612.
[14] Shaygan Nia, A, Rana, S, Döhler, D, Jirsa, F, Meister, A, Guadagno, L, Koslowski, E, Bron, M, Binder, WH. Carbon-Supported Copper Nanomaterials: Recyclable Catalysts for Huisgen [3+2] Cycloaddition Reactions. Chem Eur J, 2015, 21, 10763–10770.
[15] Evano, G, Blanchard, N, Toumi, M. Copper-Mediated Coupling Reactions and Their Applications in Natural Products and Designed Biomolecules Synthesis. Chem Rev, 2008, 108, 3054–3131.
[16] Li, G, Li, XH, Zhang, ZJ. Preparation Methods of Copper Nanomaterials. Prog Chem, 2011, 23, 1644–1656.
[17] Huang, H, Huang, W, Xu, Y, Ye, X, Wu, M, Shao, Q, Ou, G, Peng, Z, Shi, J, Chen, J, Feng, Q, Zan, Y, Huang, H, Hu, P. Catalytic Oxidation of Gaseous Benzene with Ozone over Zeolite-Supported Metal Oxide Nanoparticles at Room Temperature. Catal Today, 2015, 258, 627–633.
[18] Ahmed, A, Elvati, P, Violi, A. Size-and Phase-Dependent Structure of Copper(II) Oxide Nanoparticles. RSC Adv, 2015, 5, 35033–35041.
[19] Mondal, J, Biswas, A, Chiba, S, Zhao, Y. Cu0 Nanoparticles Deposited on Nanoporous Polymers: A Recyclable Heterogeneous Nanocatalyst for Ullmann Coupling of Aryl Halides with Amines in Water. Sci Rep, 2015, 5, 8294.
[20] Baig, NBR, Varma, RS. Copper Modified Magnetic Bimetallic Nano-Catalysts Ligand Regulated Catalytic Activity. Curr Org Chem, 2013, 17, 2227–2237.
[21] Li, X, Zhang, L, Wang, S, Wu, Y. Recent Advances in Aqueous-Phase Catalytic Conversions of Biomass Platform Chemicals Over Heterogeneous Catalysts. Front Chem, 2020, https://doi.org/10.3389/fchem.2019.00948.
[22] Senanayake, SD, Stacchiola, D, Rodriguez, JA. Unique Properties of Ceria Nanoparticles Supported on Metals: Novel Inverse Ceria/Copper Catalysts for CO Oxidation and the Water-Gas Shift Reaction. Acc Chem Res, 2013, 46, 1702–1711.
[23] Bordiga, S, Groppo, E, Agostini, G, van Bokhoven, JA, Lamberti, C. Reactivity of Surface Species in Heterogeneous Catalysts Probed by In Situ X-Ray Absorption Techniques. Chem Rev, 2013, 113, 1736–1850.
[24] Laurent, S, Forge, D, Port, M, Roch, A, Robic, C, Vander Elst, L, Muller, RN. Magnetic Iron Oxide Nanoparticles: Synthesis, Stabilization, Vectorization, Physicochemical Characterizations, and Biological Applications. Chem Rev, 2008, 108, 2064–2110.

[25] Gawande, MB, Branco, PS, Parghi, K, Shrikhande, JJ, Pandey, RK, Ghumman, CAA, Bundaleski, N, Teodoro, O, Jayaram, RV. Synthesis and Characterization of Versatile MgO-ZrO_2 Mixed Metal Oxide Nanoparticles and Their Applications. Catal Sci Technol, 2011, 1, 1653–1664.
[26] Zaera, F. Nanostructured Materials for Applications in Heterogeneous Catalysis. Chem Soc Rev, 2013, 42, 2746–2762.
[27] Borah, BJ, Dutta, D, Saikia, PP, Barua, NC, Dutta, DK. Stabilization of Cu(0)-Nanoparticles into the Nanopores of Modified Montmorillonite: An Implication on the Catalytic Approach for "Click" Reaction Between Azides and Terminal Alkynes. Green Chem, 2011, 13, 3453–3460.
[28] Alonso, F, Moglie, Y, Radivoy, G, Yus, M. Click Chemistry from Organic Halides, Diazonium Salts and Anilines in Water Catalysed by Copper Nanoparticles on Activated Carbon. Org Biomol Chem, 2011, 9, 6385–6395.
[29] Alonso, F, Moglie, Y, Radivoy, G, Yus, M. Multicomponent Click Synthesis of 1,2,3-Triazoles from Epoxides in Water Catalyzed by Copper Nanoparticles on Activated Carbons. J Org Chem, 2011, 76, 8394–8405.
[30] Nador, F, Volpe, MA, Alonso, F, Feldhoff, A, Kirschning, A, Radivoy, G. Copper Nanoparticles Supported on Silica Coated Maghemite as Versatile, Magnetically Recoverable and Reusable Catalyst for Alkyne Coupling and Cycloaddition Reactions. Appl Catal A, 2013, 455, 39–45.
[31] Pourjavadi, A, Tajbakhsh, M, Farhang, M, Hosseini, SH. Copper-loaded Polymeric Magnetic Nanocatalysts as Retrievable and Robust Heterogeneous Catalysts for Click Reactions. New J Chem, 2015, 39, 4591–4600.
[32] Honraedt, A, Le Callonnec, F, Le Grognec, E, Fernandez, V, Felpin, F-XC-H. Arylation of Benzoquinone in Water through Aniline Activation: Synergistic Effect of Graphite-Supported Copper Oxide Nanoparticles. J Org Chem, 2013, 78, 4604–4609.
[33] Bhadra, S, Saha, A, Ranu, BC. One-Pot Copper Nanoparticle-Catalyzed Synthesis of S-Aryl- and S-Vinyl Dithiocarbamates in Water: High Diastereoselectivity Achieved for Vinyl Dithiocarbamates. Green Chem, 2008, 10, 1224–1230.
[34] Duan, ZY, Ma, GL, Zhang, WJ. Preparation of Copper Nanoparticles and Catalytic Properties for the Reduction of Aromatic Nitro Compounds. Bull Korean Chem Soc, 2012, 33, 4003–4006.
[35] Sarkar, S, Chatterjee, N, Roy, M, Pal, R, Sarkar, S, Sen, AK. Nanodomain Cubic Cuprous Oxide as Reusable Catalyst in One-Pot Synthesis of 3-Alkyl/Aryl-3-(Pyrrole-2-yl/Indole-3-yl)-2-Phenyl-2,3- Dihydro-Isoindolinones in Aqueous Medium. RSC Adv, 2014, 4, 7024–7029.
[36] Bazgir, A, Hosseini, G, Ghahremanzadeh, R. Copper Ferrite Nanoparticles: An Efficient and Reusable Nanocatalyst for a Green One-Pot, Three-component Synthesis of Spirooxindoles in Water. ACS Comb Sci, 2013, 15, 530–534.
[37] Sarkar, S, Pal, R, Roy, M, Chatterjee, N, Sarkar, S, Sen, AK. Nanodomain Cubic Copper (I) Oxide as Reusable Catalyst for the Synthesis of Amides by Amidation of Aryl Halides with Isocyanides. Tetrahedron Lett, 2015, 56, 623–626.
[38] Khatun, N, Guin, S, Rout, SK, Patel, BK. Divergent Reactivities of O-Haloanilides with CuO Nanoparticles in Water: A Green Synthesis of Benzoxazoles and O-Hydroxyanilides. RSC Adv, 2014, 4, 10770–10778.
[39] Pourjavadi, A, Safaie, N, Hosseini, SH, Bennett, C. Graphene oxide/poly(vinyl imidazole) nanocomposite: An effective support for preparation of highly loaded heterogeneous copper catalyst. Appl Organometal Chem, 2015, 29, 601–607.
[40] Kitanosono, T, Zhu, L, Liu, C, Xu, P, Kobayashi, S. An Insoluble Copper(II) Acetylacetonate-Chiral Bipyridine Complex that Catalyzes Asymmetric Silyl Conjugate Addition in Water. J Am Chem Soc, 2015, 137, 15422–15425.
[41] Tubío, CR, Azuaje, J, Escalante, L, Coelho, A, Francisco Guitián, F, Eddy Sotelo, E, Gil, A. 3D printing of a heterogeneous copper-based catalyst. J Catal, 2016, 334, 110–115.

[42] Lim, M, Lee, H, Kang, M, Yoo, W, Rhee, H. Azide-alkyne cycloaddition reactions in water via recyclable heterogeneous Cu catalysts: Reverse phase silica gel and thermoresponsive hydrogels. RSC Adv, 2018, 8, 6152–6159.
[43] Pogula, J, Laha, S, Likhar, PR. Nano Copper(0)-Stabilized on Alumina: Efficient and Recyclable Heterogeneous Catalyst for Chemoselective Synthesis of 1,2-Disubstituted Benzimidazoles and Quinoxalines in Aqueous Medium. Catal Lett, 2017, 147, 2724–2735.

Yogesh A. Tayade, Dipak S. Dalal*

8 β-Cyclodextrin-based heterogeneous catalysts in aqueous medium

8.1 Introduction

Supramolecular chemistry involves noncovalent bonding interactions, where covalent bonds are formed between the interacting species, that is, molecules, ions, or radicals [1]. Supramolecular catalyst β-cyclodextrin (β-CD) is a cyclic oligosaccharide, hollow truncated cone-shaped macro-ring made up of seven glucopyranose units [2] with the wider face formed by the secondary –OH at C-2 and C-3, and the narrower side by the primary –OH at C-6 (Figure 8.1). The inner cavity size and its hydrophobicity made it suitable for encapsulating a variety of guests such as organic compounds [3]. Due to the presence of this hydrophobic cavity, CDs provide a suitable environment to catalyzed organic reactions [6], through noncovalent interactions. Cyclodextrins (CDs) have been recognized as versatile enzyme mimics [4–5] and also show a supramolecular host for organometallic complexes [6]. Bhosale and coworkers reported β-CD-catalyzed organic synthesis till the end of 2006 [7]. In continuation of our work on β-CD [8–13], most of the organic reactions catalyzed by β-CD were carried out in aqueous medium.

Most extensively used organic solvents are flammable, volatile, environmentally hazardous, and highly toxic. Thus, the demand for greener solvent is increasing due to stringent environmental policy [14–20]. So, it is a necessity to replace the volatile organic solvents by using greener solvent "water" [21]. In view of sustainable development in organic synthesis, development of aqueous phase transformation is most important. Being a unique and universal solvent, water is used in nature for various biological as well as chemical processes [22]. Water is the solvent of supreme solution of scientists as it is environment friendly, economically cheap, incombustible, ample in source, low cost, and easily available [23–25]. In addition, the aspects like hydrogen bonding, latent heat capacity, interfacial tension, high polarity, and high cohesive energy have shown significant characteristic properties of water that can make

Acknowledgments: The first author Y. A. Tayade thanks the principal of Dhanaji Nana Mahavidyalaya, Faizpur, India, for the kind support. D. S. Dalal thanks UGC and DST for financial grants under UGC-SAP-DSA-I program, and FIST-DST, School of Chemical Sciences, KBC NMU, Jalgaon.

***Corresponding author: Dipak S. Dalal,** School of Chemical Sciences, Kavayitri Bahinabai Chaudhari North Maharashtra University, Jalgaon 425 001, Maharashtra, India,
E-mail: dsdalal2007@gmail.com
Yogesh A. Tayade, Department of Chemistry, Dhanaji Nana Mahavidyalaya, Faizpur 425503, Maharashtra, India

https://doi.org/10.1515/9783110733846-008

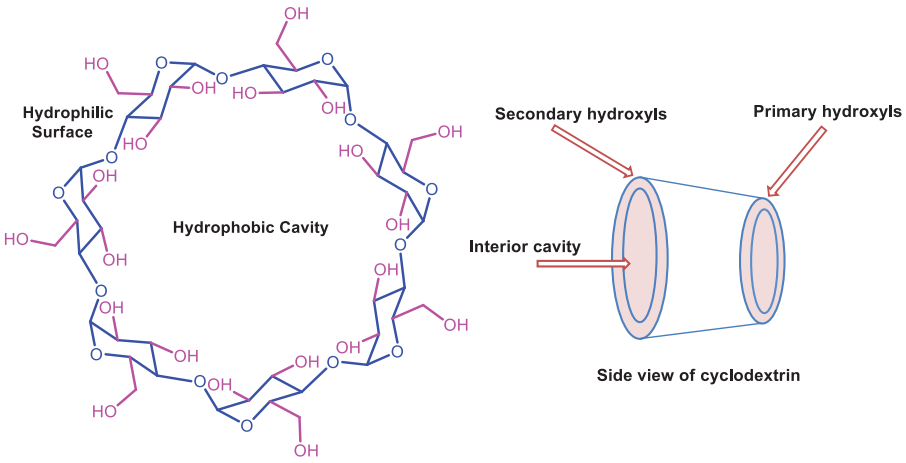

Figure 8.1: β-Cyclodextrin and its side view.

the water more suitable and valuable for organic reactions [26]. About 90% of chemicals have been produced worldwide by using heterogeneous catalysis [27]. Due to its great importance, researchers in chemical and energy area are attracted toward the development of this field [28]. Heterogeneous catalysis has traditionally focused on developing and improving catalysts for optimizing chemical processes [29]. Both mixed catalysis, that is, homogeneous and heterogeneous, made huge contributions to the progress of society. Both types of catalysis have their own numerous advantages; however, heterogeneous catalysis appears to be more appropriate for industrial large-scale setup that prefers endless flow systems [30–33]. The safe handling, toughness, inertness to common conditions (moisture, air, etc.), longer ledge life are the major advantages [34]. In addition to this, the heterogeneous aqueous phase catalysis has attracted special attention of scientists due to easy reuse and recovery of the catalyst.

This chapter focuses on to design and synthesize some novel heterogeneous catalysts based on β-CD and its synthetic utility in aqueous medium. In this chapter, we have summarized various aqueous-phase organic transformation catalyzed by β-CD-based heterogeneous catalyst (Figure 8.2).

8.2 Applications of β-cyclodextrin-based heterogeneous catalysts in water

8.2.1 Suzuki–Miyaura reaction

The supramolecular catalyst β-CD has been examined for coupling reactions. This cross-coupling reaction is useful for C-C bond formation and form compounds with

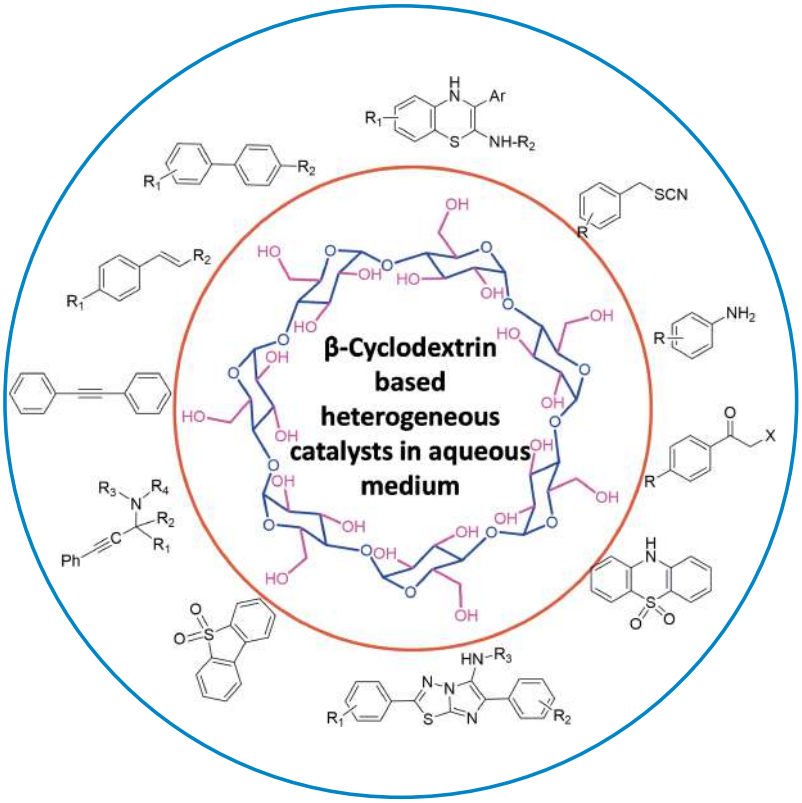

Figure 8.2: Organic transformation catalyzed by β-cyclodextrin-based heterogeneous catalyst.

easily accessible methods [35–37]. A water-soluble palladium complex supported by triazolyl β-CD (PdLn@β-CD) was designed, prepared, and studied for applications in coupling reactions between substituted aryl halide (**1a**) and aryl boronic acid (**2b**) in water (Figure 8.3) to form biaryl compounds (**3a**). The catalyst shows high TONs and TOFs [38].

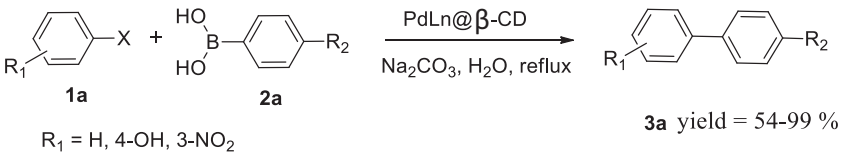

Figure 8.3: Suzuki–Miyaura reactions catalyzed by using catalyst PdLn@β-CD.

First, β-CD reacted with tosyl chloride and sodium azide to form 6-monodeoxy-6-monoazido-β-CD, after that it undergoes click reaction with 2-ethynylpyridine [39–41]

in DMSO–H_2O to form Ln@β-CD. Ln@β-CD reacted with palladium acetate in dry toluene for 12 h to form the desire catalyst PdLn@β-CD as light yellow powder. This prepared catalyst has showed greater solubility in water. The detailed synthesis of PdLn@β-CD is shown in Figure 8.4.

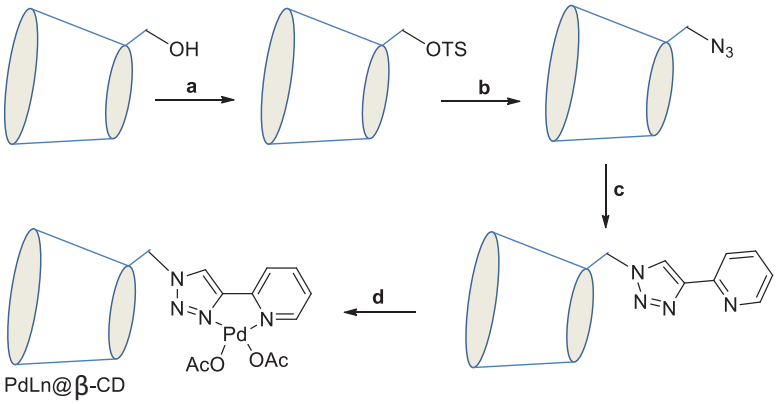

Figure 8.4: Methods of preparation of PdLn@β-CD catalyst. (a) Tosyl chloride, NaOH/H_2O, 0–5 °C, 4 h; (b) NaN_3, DMF, 75 °C, 4 h; (c) 2-ethynylpyridine, $CuSO_4$/sodium ascorbate, DMSO-H_2O, r.t., 1 day; (d) palladium acetate in toluene, at r.t., 12 h.

Heravi et al. [42] reported Suzuki–Miyaura reactions (Figure 8.5) between aryl halides **(1b)** and phenyl boronic acids **(2b)** to form bisaryl derivatives (**3b**). They designed, prepared, and characterized the M-GO/(AM-MBA-β-CD@Pd) [M-GO (magnetic graphene oxide), AM (acrylamide) and MBA (methylenebisacrylamide)] nanocomposite and explored its utility as an efficient and magnetically separable catalyst for the Suzuki–Miyaura reaction. The reported nanocatalyst was easily magnetically separable and reusable for several cycles without loss of its catalytic potential.

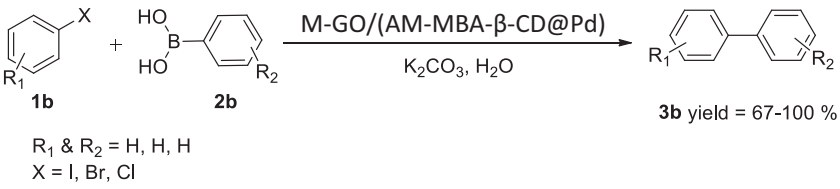

Figure 8.5: M-GO/(AM-MBA-β-CD@Pd) nanocomposite-catalyzed Suzuki–Miyaura reaction.

8.2.2 C–C coupling reactions

Aqueous-phase C–C coupling reactions have emerged as an important tool in catalysis research [43]. Ghosh et al. [44] have prepared the novel heterogeneous catalyst Pd-NPs-β-CD graphene nanosheets (Pd@CD–GNS) and investigated its applications for Suzuki–Miyaura reaction of aryl halide (**3a**) and phenyl boronic acid (**3b**) to form product **(3c)** (Figure 8.6) and Heck–Mizoroki reactions between aryl halide (**4a**) and alkene (**5a**) (Figure 8.7) in aqueous medium without ligand and aerobic conditions to form product (**6a**).

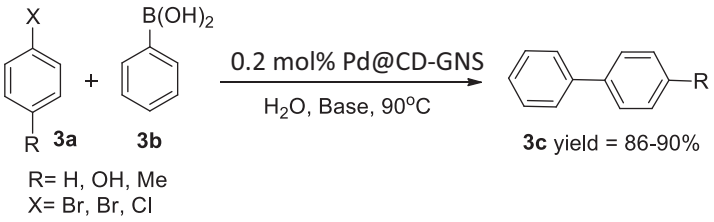

Figure 8.6: Pd@CD-GNS-catalyzed Suzuki–Miyaura C–C bond formation reaction in H_2O.

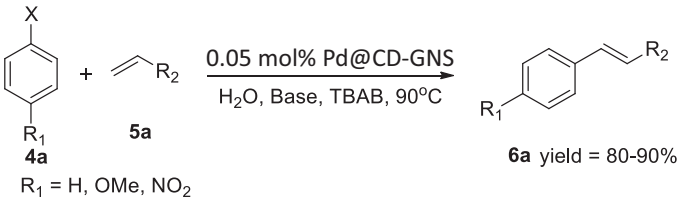

Figure 8.7: Pd@CD–GNS-catalyzed Heck–Mizoroki cross-coupling reaction in H_2O.

8.2.3 Heck reaction in water

A practically simple method was developed for Heck reaction (Figure 8.8) for substituted stilbene derivative synthesis (**6b**) via C–C coupling reaction between aryl halide (**4b**) and styrene (**5b**) in aqueous medium in the presence of the catalyst PdNP-SβCD [45].

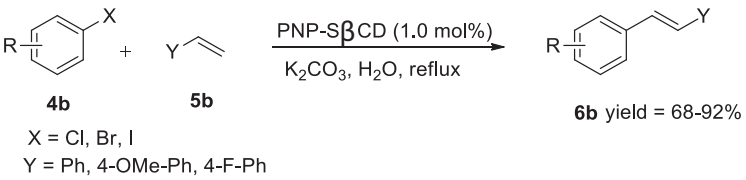

Figure 8.8: Synthesis of stilbene derivatives catalyzed by PdNP-SβCD in water.

This report includes the preparation of silica- CD (SCD) substrate (Figure 8.9) by the reaction of silica with thionyl chloride ($SOCl_2$) at reflux condition to form silica chloride. Silica chloride is treated with CD to form SCD substrate. The substrate is treated with palladium acetate nanoparticles (NP) in ethanol at room temperature for 24 h to form the PdNP-S-β-CD catalyst (Figure 8.10). To test the catalytic activity, this prepared catalyst was applied to the Heck reaction and shows good results with high yields of products in aqueous media.

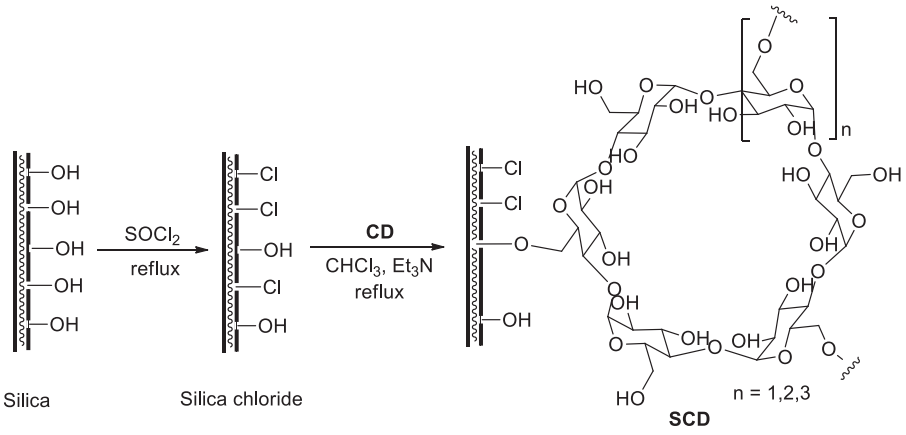

Figure 8.9: Preparation of silica-cyclodextrin substrates (SDC).

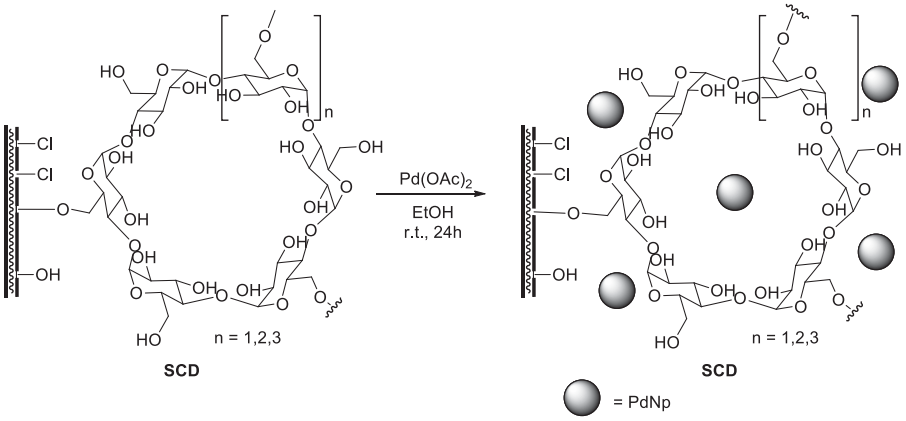

Figure 8.10: Preparation of PdNP-S-β-CD catalyst.

8.2.4 Sonogashira reactions

Sonogashira coupling is Pd–Cu-catalyzed reaction between substituted aryl halides and terminal acetylenes. This coupling reaction is the most significant and widely used sp^2–sp carbon–carbon coupling reaction to form diaryl-substituted acetylenes [46]. The reaction is generally carried out in organic phase with amines as base, cocatalyst CuI and $Pd(PPh_3)_2Cl_2$ or $Pd(PPh_3)_4$ homogeneous catalyst, which makes the parting procedure dull with product palladium contamination. To overcome these difficulties, Liu et al. reported Sonogashira coupling reaction (Figure 8.11) between aryl halide **(7)** and terminal alkynes **(8)** catalyzed by heterogeneous catalyst β-CD-supported Pd-NPs in water at room temperature to form product (**9**). This coupling reaction progressed well at room temperature without co-catalyst (CuI) and ligand phosphine (PPh_3) to form products with good yields [47].

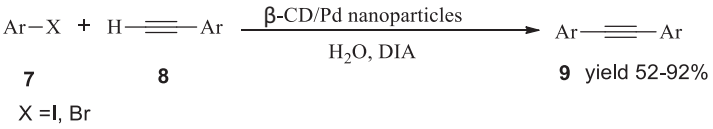

Figure 8.11: Aqueous-phase Sonogashira reactions catalyzed by β-CD-Pd NPs.

8.2.5 Combined aqueous-phase Sonogashira and Heck reaction

Halloysite nanoclay ($Al_2(OH)_4Si_2O_5 \cdot 2H_2O$) is composed of tetrahedral siloxane on external surface and aluminol groups on the internal surface. In Halloysite nanotubes (HNTs), the water molecules are located between the inner spaces [48–49]. HNTs show very similar properties like Kaolin [50–51]. It is inert in nature and its structure, biodegradability, high mechanical as well as chemical stability, and surface area make this clay a valuable for number of applications [52].

Sadjadi et al. [53], first time, prepared a heterogeneous Pd@HNTs-CDNS-g-C_3N_4 catalyst from halloysite nanotubes, CD nanosponges, and g-C_3N_4 and used for copper-free aqueous-phase Sonogashira and Heck coupling reactions. The cyclodextrin nanosponges (CDNS) having the capability to form host–guest complex with substrates catalyzed the reactions. The g-C_3N_4 is used to suppress the Pd leaching. The involvement of all components and its synergistic effect between them result in great catalytic activity.

8.2.6 A^3 and KA^2 coupling reactions

Propargylamines are key intermediates for the synthesis of various natural products and bioactive nitrogen containing heterocycles [54–57]. It can be prepared by the

three-component reaction between amines, aldehydes, and alkynes and is designated as A^3 coupling reaction [58]. Sadjadi and his group [59] designed and prepared the catalyst h-Fe_2O_3@SiO_2-CD/Ag and studied its application for A^3 and KA^2 coupling reactions under simple and ecofriendly reaction condition. The catalyst is synthesized from γ-Fe_2O_3 and SiO_2 shell to form h-Fe_2O_3@SiO_2 with 3-*N*-(2-(trimethoxysilyl)ethyl) methanediamine and treated with tosylated CD to form the catalyst. The precatalyst h-Fe_2O_3@SiO_2-CD is doped with silver nanoparticles by using hollyhock flower extract as the reducing agent to form the actual catalyst h-Fe_2O_3@SiO_2-CD/Ag (Figure 8.12). To test the catalytic performance of γ-Fe_2O_3@SiO_2-CD/Ag for propargylamine **(13)** synthesis, the reaction of carbonyl compounds (**10**) and secondary amines **(11)** with terminal alkynes (**12**) was carried out in the presence of the catalyst (20 mg) under ultrasound irradiation using power input of 70 W (Figure 8.13). The terminal C–H bond of phenylacetylene is activated by silver NPs forming Ag–acetylide (**14**). Then, progress of the reaction involves alkyne C–H bond activation with interaction by metal NPs (**M**). Metalacetylide intermediate (**14**) is generated from terminal alkyne. Aldehydes, activated by Ag, undergo condensation with the amines to form the imminium ion **(15)**. Subsequently, the intermediate (**14**) attacks on the imminium ion **(15)** to form the product propargylamine **(16)**. The plausible mechanism of this conversion is shown in Figure 8.14.

8.2.7 Synthesis of imidazothiadiazolamine derivatives

Ionic liquids (ILs) are molten salts with melting point below the boiling point of water. This distinctive feature of ILs has made them an alternative solvent as well as the catalyst for organic transformations [60, 61]. Mahdavi et al. [62] reported a novel magnetically separable, β-CD-based IL anchored to magnetic starch catalyst, denoted as β-CD-IL@M-starch for the synthesis of diphenylimidazo[2,1-*b*][1,3,4]thiadiazol-5-amine derivatives (**21**) (Figure 8.15) by the reaction between substituted aromatic aldehydes **(17)**, semicarbazide **(18)**, benzaldehydes **(19)**, and isocyanides **(20)**.

8.2.8 Hydrogenation reaction

In heterogeneous catalysis, the active coordination site containing supported materials and metal nanomaterials has great importance [63–65]. Klaus-Viktor Peinemann et al. [66] designed and prepared a polymer network cross-linked β-CD (CPN) catalyst from various nanomaterials to obtain the catalyst PdNPs@CPN and used for the hydrogenation reaction (Figure 8.16) of nitroarene (**22**) to form the product arylamine (**23**).

To prepare a stable CPN, the fixed ratio of cross-linker with per-(6-azido-6-deoxy)-β-cyclodextrins (**24**) was used for formation of CPN. 1,4-Diethynylbenzene (**25**) has

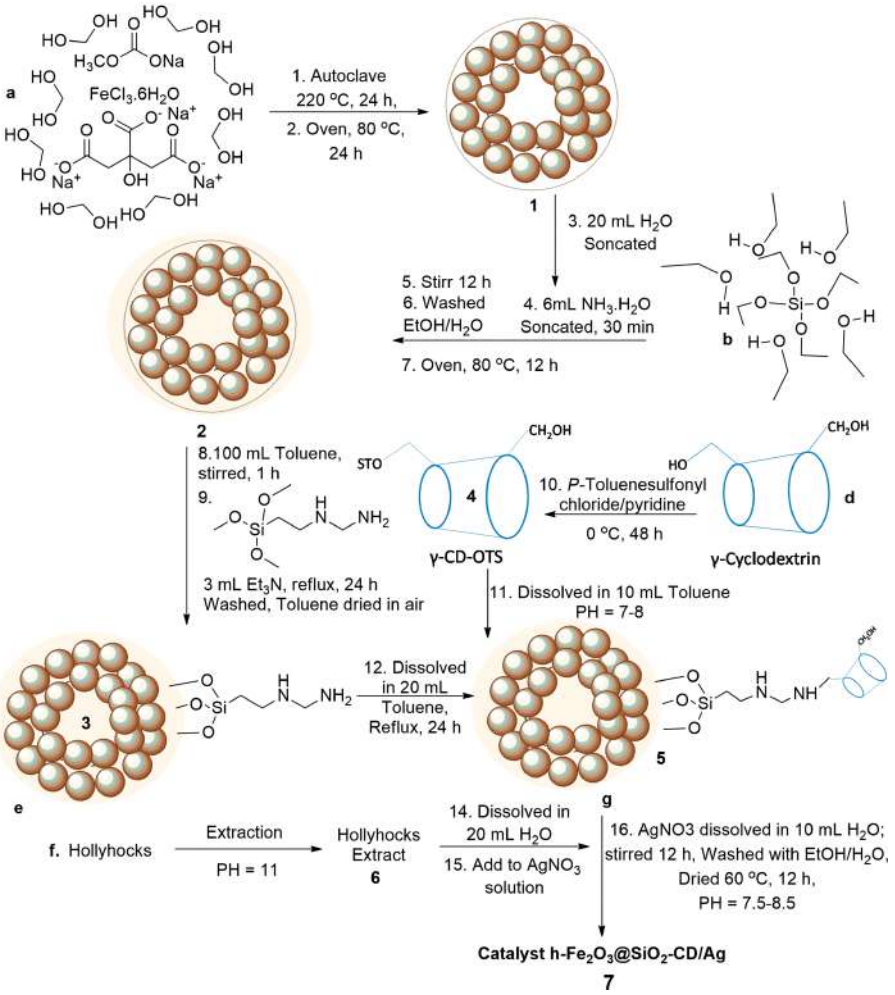

Figure 8.12: The process of formation of hollow sphere catalyst h-Fe_2O_3@SiO_2-CD/Ag.

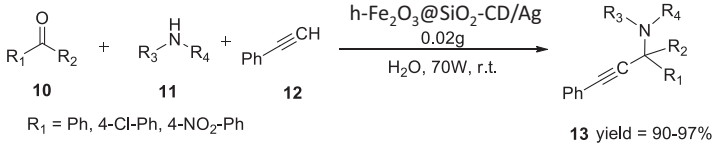

Figure 8.13: Synthesis of propargylamine derivatives.

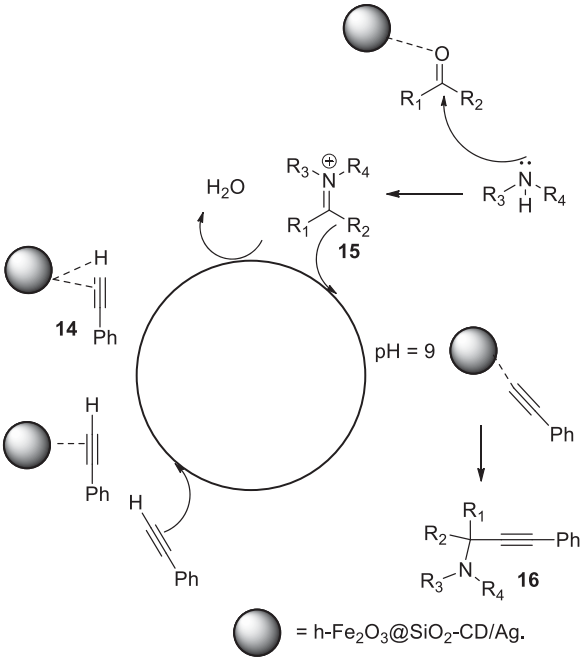

Figure 8.14: Plausible mechanism for propargylamine synthesis.

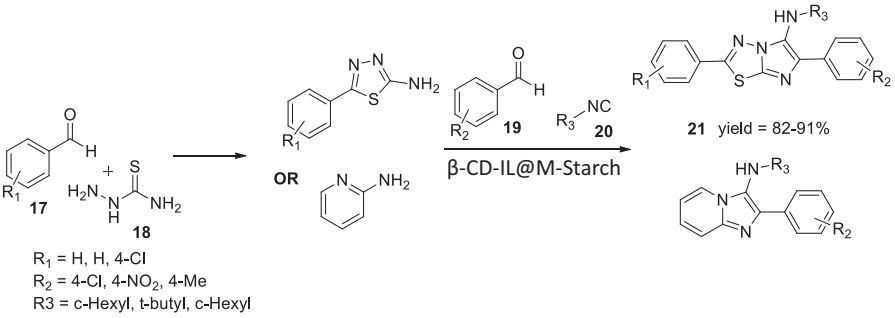

Figure 8.15: Imidazo[2,1-*b*][1,3,4]thiadiazol-5-amine derivative synthesis.

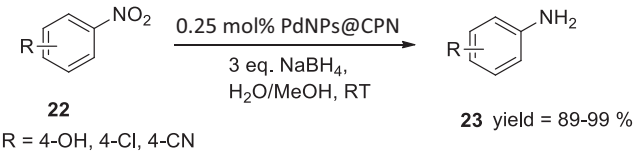

Figure 8.16: Hydrogenation reactions catalyzed by PdNPs@CPN.

been used as the cross-linker to synthesize CPN. The mixture of per-(6-azido-6-deoxy) -β-cyclodextrins, 1,4-diethynylbenzene, and $CuSO_4 \cdot 5H_2O$ in DMF was treated with sodium ascorbate under inert atmosphere for 7 days at 60 °C. The brown color product that was obtained by centrifugation was freeze-dried for 3 days to form pale yellow powder CPN (**26**) with good yield of product (Figure 8.17).

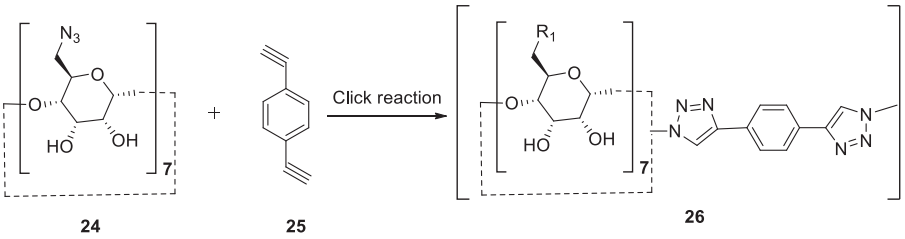

24 25 26

Figure 8.17: Preparation of CPN.

8.2.8.1 Preparation of metal NPs@CPN

The pale yellow color CPN is treated with Pd(OAc) in dichloromethane under overnight stirring at room temperature to obtain the crude product PdNPs@CPN. The crude product was redispersed in dichoromethane for 1 h to remove excess Pd $(OAc)_2$ and dried overnight in vacuum at 30 °C to form orange solid catalyst Pd(II) @CPN. This was reduced in alcoholic solution of $NaBH_4$ to get the final gray solid PdNPs@CPN catalyst. A total of 6 wt% of Pd content was found in PdNPs@CPN.

8.2.9 Thiocyanation of alkyl halides in water

Alkyl thiocyanates have great importance in the field of organosulfur chemistry [67]. It found various applications for the synthesis of biologically active heterocycles. Thiocyanation is generally done by nucleophilic substitution reaction using thiocyanate anions [68–71]. Ali Reza et al. [72] reported the synthesis of thiocyanation product (**28**) from alkyl halide (**27**) (Figure 8.18) and phenacyl derivatives (**30**) from α-bromo ketone (**29**) (Figure 8.19) by the reaction of potassium thiocyanate, azide, or acetate by employing the heterogeneous catalyst-immobilized β-CD onto Dowex Resin (Dowex-β-CD) in water.

Figure 8.20 shows the enzyme biomimetic role of Dowex-β-CD in water. The reaction is catalyzed via formation of host–guest complex of β-CD with phenacyl bromides via hydrogen bonding formed between outer -OH of β-CD and α-bromo ketones, after that it undergoes the attack of nucleophiles to form the product.

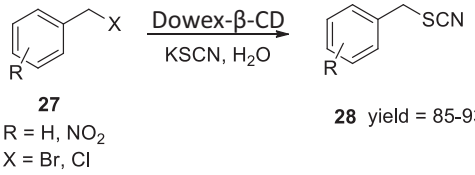

Figure 8.18: Dowex-β-CD-assisted thiocyanation reaction of alkyl halides.

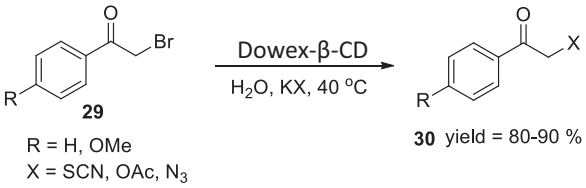

Figure 8.19: Synthesis of phenacyl derivatives catalyzed by Dowex-β-CD.

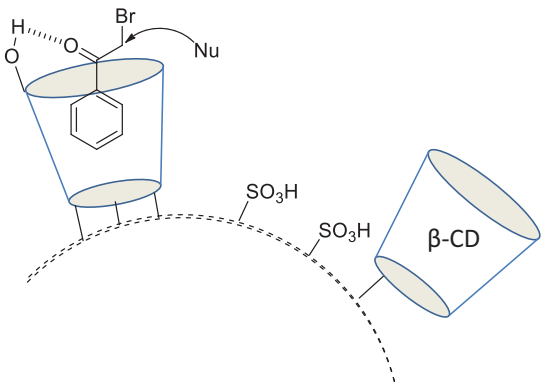

Figure 8.20: Host–guest interaction of β-CD with phenacyl bromides.

8.2.10 3-Aryl-4*H*-benzo[1,4]thiazin-2-amine synthesis in water

NPs offer huge surface area for greater contact among the reactants and catalyst to enhance the rate of reaction and reduce the required quantity of catalyst [73, 74]. Heterogeneous catalysts are insoluble in most of the reaction media and hence they have been easily separated from the reaction mixture [75, 76]. The ZnO-NPs are non-toxic, less corrosive, with good recyclability, and prepared easily from cheap starting materials. ZnO-NPs have very widespread applications for organic synthesis [77, 78]. In addition to these merits, ZnO-NPs are environmentally friendly in terms of discarding [79, 80] and elimination of chemicals as well as biopollutants for contaminated water treatment [81]. These features make the ZnO-NPs greener and efficient

catalyst as compared to other catalysts. Siddiqui et al. [82] reported the efficient, green, and recyclable heterogeneous catalytic system of ZnO-NP-β-CD for the preparation of 3-aryl-4*H*-benzo[1,4]thiazin-2-amine (**34**) through single pot, MCRs between *o*-aminothiophenol **(31),** substituted aldehydes **(32)** and isocyanides (**33)** (Figure 8.21) in aqueous media at 60 °C.

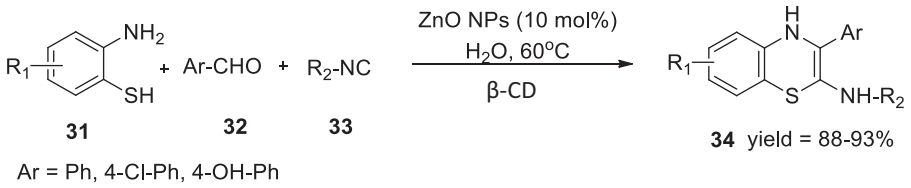

Figure 8.21: Aqueous-phase synthesis of 3-aryl-4*H*-benzo[1,4]thiazin-2-amines catalyzed by ZnO-β-CD NPs.

The reaction goes forward with the formation of intermediate **(35)** by the reaction between *o*-aminothiophenol with aldehyde in the presence of ZnO-NPs. The activation of intermediate (**35**) through ZnO-NPs favoring the attack of nucleophile isocyanide to form **(36)** in which the sulfur undergoes intramolecular nucleophile trapping to form **(37)**, which leads to product **(34)**. The proposed mechanism for the formation of (**34)** is shown in Figure 8.22.

8.2.11 Deep oxidative desulfurization of gas oil

To get deep clean gas oil, Rezvani et al. [83] synthesized a novel TBA-SiWCd@β-CD blended catalyst by using tetrabutyl ammonium salts with sandwich-type polysilicotungstate on β-CD as a versatile catalyst for aerobic or oxidative desulfurization of dibenzothiophene (DBT) **(38)** to dibenzothiophenoxide (DBTO) **(39)** and dibenzothiophenodioxide ($DBTO_2$) (**40**) (Figure 8.23). This study explored the utilization of TBA-SiWCd@β-CD catalyst to remove harmful sulfur containing substrates from gas oil fuel.

8.2.12 Degradation of 4-chlorophenol (4-CP) by using catalyst Fe_3O_4@β-CD

The Fenton reaction is one of the most successful advanced oxidation processes which produce · OH, and after that fluorine is another powerful oxidizing agent for effective degradation of pollutants [84–86]. The Fenton process has great benefits, such as operation simplicity, easy handling, high decadence efficiency, and affordable materials [87, 88]. Zhan et al. [89] reported a magnetically separable Fe_3O_4@β-CD catalyst

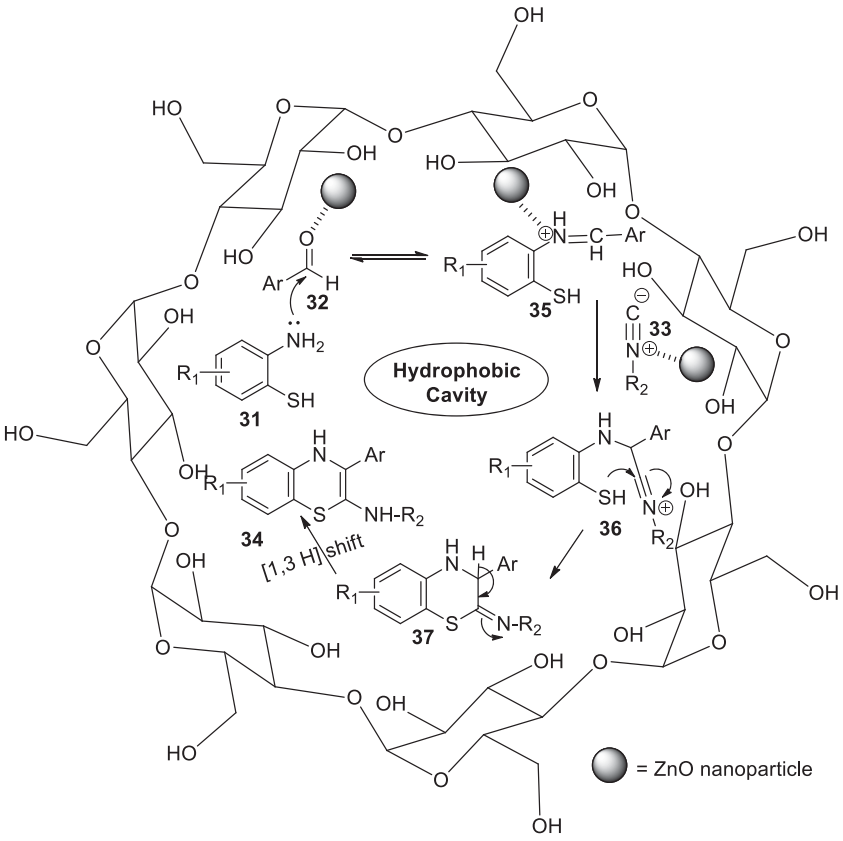

Figure 8.22: Proposed mechanism for the synthesis of 3-aryl-4*H*-benzo[1,4]thiazin-2 amine.

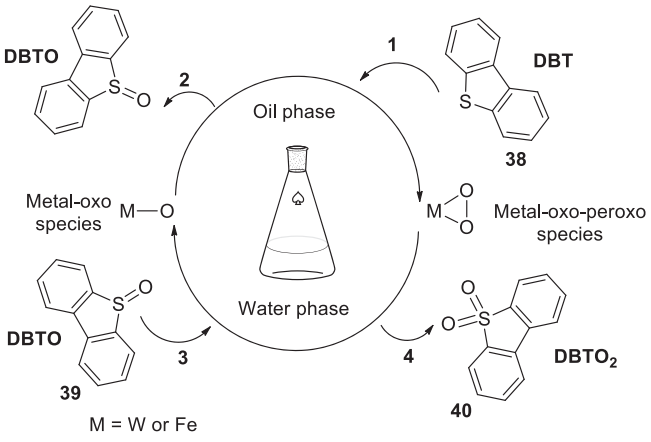

Figure 8.23: TBA-SiWCd@β-CD-catalyzed ODS process of DBT.

prepared from Fe ions and β-CD (Figure 8.24) and studied its applications for degradation of 4-chlorophenol (4-CP) (**41**) to form water and carbon dioxide (**42**) as final products (Figure 8.25). The Fe_3O_4@β-CD nanocomposite shows a greater catalytic activity than normal Fe_3O_4 for 4-CP degradation with rate constants (k_{obs}) of 0.0373 min^{-1} for Fe_3O_4@β-CD, and 0.0162 min^{-1} for normal Fe_3O_4. Formation of a tertiary complex (Fe^{2+}-β-CD-pollutant) favors to generate hydroxyl radicals (·OH) that directly attack on pollutants to increase the solubility of organic pollutant. A viable reaction method of 4-CP degradation influenced by · OH was studied through the analysis of degradation intermediates and chloride ions. β-CD and 4-CP form inclusion complexes to offer the uniqueness of decomposed intermediate due to the systematic structural arrangement of β-CD, and this study was investigated with density functional theory.

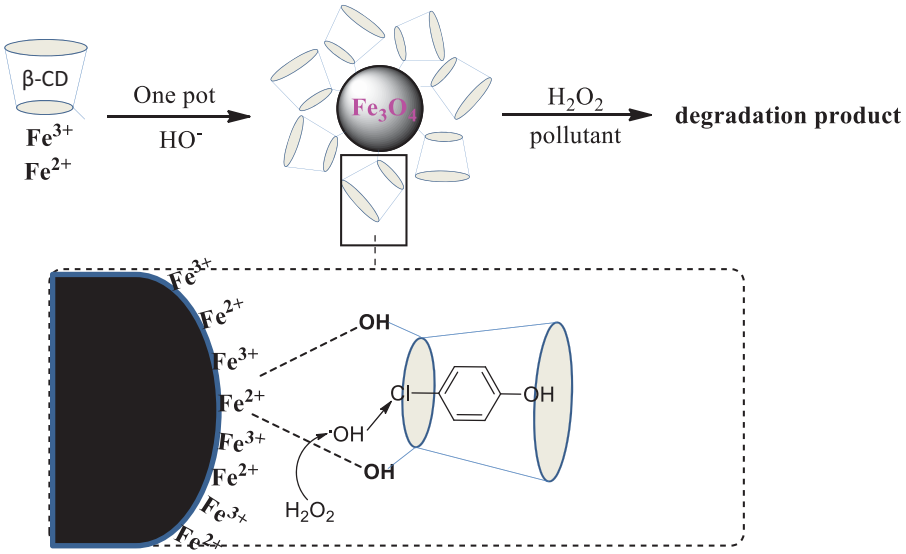

Figure 8.24: Preparation method of Fe_3O_4@-β-CD.

8.2.13 Degradation of methylene blue in aqueous suspension

Cerium oxide (CeO_2) NPs were formed from the reaction of cerium with oxygen [90]. It exists in fluorite structure with two distinct Ce^{3+} and Ce^{4+} oxidation states with high oxygen depository and release ability [91]. Gogoi and Sarma in 2016 [92] reported a new catalyst β-CD-CeO_2 from β-CD-based CeO_2 nanocomposite for degradation of organic dye methylene blue (MB) (Figure 8.26) in the presence of H_2O_2 and absence of light in water at room temperature. The catalyst β-CD-CeO_2 has diameter of 14 ± 2 nm with 4.93 eV of band gap. The degradation of MB **(43)** produces LMB sulfone

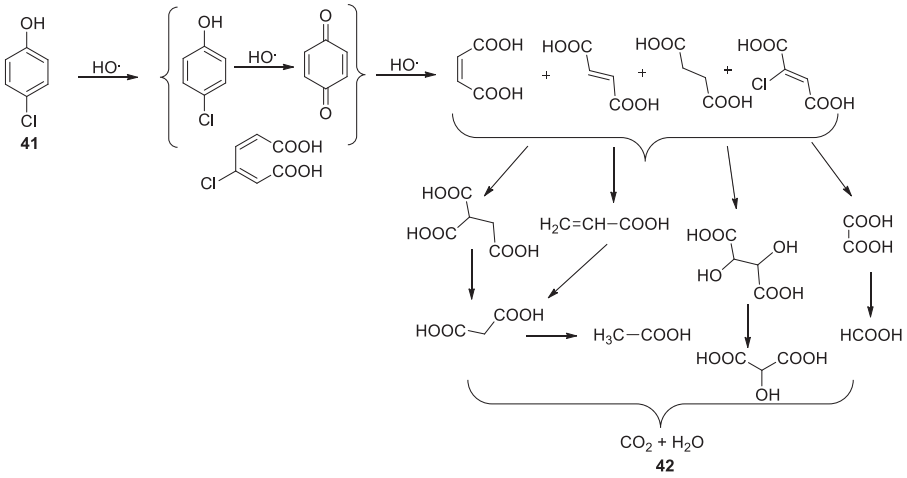

Figure 8.25: Plausible mechanism for 4-CP degradation.

(44) with $m/z = 317$ amu; LMB sulfone undergoes the loss of single or both of its dimethylamine groups to form **(45)** with $m/z = 273$ amu and (**46**) with $m/z = 229$ amu. In the presence of the catalyst β-CD-CeO_2, the complete degradation of MB occurred within 1 h, whereas CeO_2 took higher time to degrade MB.

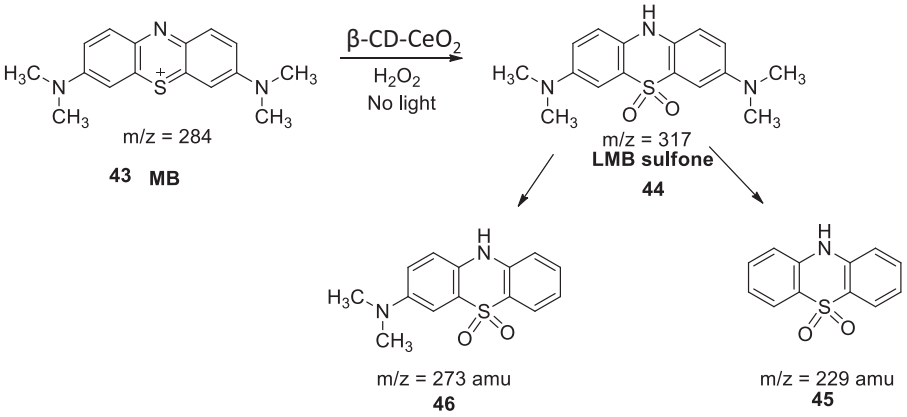

Figure 8.26: Degradation process of methylene blue.

8.2.14 Degradation of persistent organic pollutant

The persistent organic pollutants (POPs) cause a vast hazard to living organism and water safety [93, 94]. The organic compound bisphenol A (BPA) is a endocrine disruptor and a hazard to living organism [95]. Due to its harmful effect, it is very essential

to eliminate it from wastewater. A newer magnetic nanocomposite Fe_3O_4@β-CD-*N*,*N*″-carbonyldiimidazole (CDI) was prepared and studied for its applications for the adsorption and decomposition of POPs in aqueous medium [96]. The catalyst Fe_3O_4@β-CD-CDI catalytically degrades BPA **(47)** via Fenton-like process in the presence of hydrogen peroxide (Figure 8.27). Fe_3O_4@β-CD-CDI was prepared by the treatment of Zn ions to Fe_3O_4 NP surface and treated with β-CD-CDI **(49)** obtained by the reaction of β-CD with CDI **(48)**. Fast degradation of BPA can be possible only due to the production of · OH close to β-CD and can attack directly on the encapsulated BPA pollutants. This study shows that Fe_3O_4@β-CD-CDI **(50)** has significant importance in purification of wastewater persistent with organic pollutants.

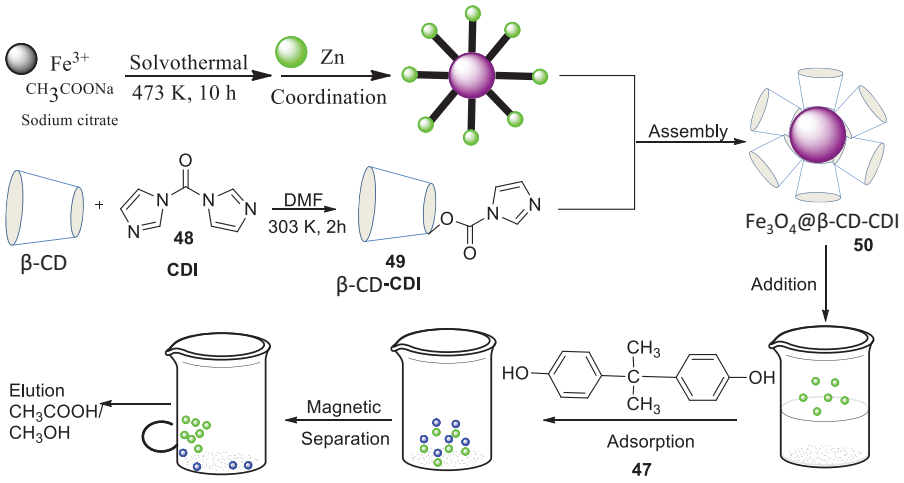

Figure 8.27: Mechanistic pathway of Fe_3O_4@β-CD-CDI composites.

8.3 Conclusions

β-CD-based heterogeneous catalyst is a highly efficient, magnetically separable, and environmentally friendly catalyst for organic synthesis. Because of the great potential of β-CD, it draws researchers' attention toward its ability to promote aqueous-phase organic transformations. β-CD-based heterogeneous catalyst is useful for variety of carbon–carbon bond formation reactions such as Suzuki–Miyaura, Sonogashira, Heck, A^3, and KA^2 coupling reactions. β-CD-based heterogeneous catalyst has been applicable for imidazothiadiazolamine synthesis, hydrogenation reaction, thionation of alkyl halide, synthesis of phenacyl derivatives, and 3-aryl-4*H*-benzo[1,4]thiazin-2-amine synthesis. It has been also useful in deep aerobic desulfurization of gas oil, degradation of 4-CP, and degradation of MB in aqueous suspension.

References

[1] Szejtli, J. Introduction and general overview of cyclodextrin chemistry, Chem Rev, 1998, 98, 1743–1754.

[2] Szeitli, J. Cyclodextrin Technology, Klwner Academic publications: Dordracht, 1988.

[3] Bender, ML, Komiyama, M. Cyclodextrin Chemistry, Springer Verlag. berlin-Heidelberg-New York, 1978.

[4] Komiyama, M, Bender, ML. In the Chemistry of Enzyme Action, Page, M, I, Elsevier, 1984, 505.

[5] Iglesias, E. Cyclodextrins as Enzyme Models in Nitrosation and in Acid- Base-Catalyzed Reactions of Alkyl Nitrites. J Am Chem Soc, 1998, 120, 13057–13069, (b) Yuan, DQ., Lu, J., Atsumi, M., Izuka, A., Kai, M., Fujita, K. The first successful investigation into a cyclodextrin-based enzyme model as an efficient catalyst for luminol chemiluminescent reaction. Chem Commun 2002, 730–731.

[6] Hapiot, F, Tilloy, S, Monflier, E. Cyclodextrins as supramolecular hosts for organometallic complexes, Chem Rev, 2006, 106, 767–781.

[7] Bhosale, SV, Bhosale, SV. β-Cyclodextrin as a catalyst in organic synthesis, Mini-Rev in Org Chem, 2007, 4, 231–242.

[8] Tayade, YA, Dalal, DS. β-Cyclodextrin as a Supramolecular Catalyst for the Synthesis of 1H-Pyrazolo [1, 2-b] phthalazine-5, 10-dione Derivatives in Water, Catal Lett, 2017, 147, 1411–1421.

[9] Tayade, YA, Patil, DR, Wagh, YB, Jangle, AD, Dalal, DS. An efficient synthesis of 3-indolyl-3-hydroxy oxindoles and 3, 3-di (indolyl) indolin-2-ones catalyzed by sulfonated β-CD as a supramolecular catalyst in water, Tetrahedron Lett, 2015, 56, 666–673.

[10] Patil, DR, Wagh, YB, Ingole, PG, Singh, K, Dalal, DS. β-Cyclodextrin-mediated highly efficient [2+ 3] cycloaddition reactions for the synthesis of 5-substituted 1 *H*-tetrazoles, New J Chem, 2013, 37, 3261–3266.

[11] Tayade, YA, Jangale, AD, Dalal, DS. Simple and Highly Efficient Synthesis of Thioamide Derivatives Using β-Cyclodextrin as Supramolecular Catalyst in Water, Chem Select, 2018, 3, 8895–8900.

[12] Dalal, DS, Patil, DR, Tayade, YA. β-Cyclodextrin: A Green and Efficient Supramolecular Catalyst for Organic Transformations, The Chem Rec, 2018, 18, 1560–1582.

[13] Patil, DR, Ingole, PG, Singh, K, Dalal, DS. Inclusion complex of Isatoic anhydride with β-cyclodextrin and supramolecular one-pot synthesis of 2, 3-dihydroquinazolin-4 (1*H*)-ones in aqueous media, J Incl Phenom Macrocycle Chem, 2013, 76, 327–332.

[14] Hofstetter, TB, Capello, C, Hungerbühler, K. Environmentally preferable treatment options for industrial waste solvent management: A case study of a toluene containing waste solvent, Process Saf Environ Prot, 2003, 81, 189–202.

[15] Amelio, A, Genduso, G, Vreysen, S, Luis, P, Van der Bruggen, B. Guidelines based on life cycle assessment for solvent selection during the process design and evaluation of treatment alternatives, Green Chem, 2014, 16, 3045–3063.

[16] Figoli, A, Marino, T, Simone, S, Di Nicolo, E, Li, XM, He, T, Tornaghi, S, Drioli, E. Towards non-toxic solvents for membrane preparation: A review, Green Chem, 2014, 16, 4034–4059.

[17] Drioli, E, Brunetti, A, Di Profio, G, Barbieri, G. Process intensification strategies and membrane engineering, Green Chem, 2012, 14, 1561–1572.

[18] Szekely, G, Jimenez-Solomon, MF, Marchetti, P, Kim, JF, Livingston, AG. Sustainability assessment of organic solvent nanofiltration: From fabrication to application, Green Chem, 2014, 16, 4440–4473.

[19] Kim, JF, Székely, G, Valtcheva, IB, Livingston, AG. Increasing the sustainability of membrane processes through cascade approach and solvent recovery-pharmaceutical purification case study. Green Chem, 2014, 16, 1, 133–145.

[20] da Silva Burgal, J, Peeva, L, Livingston, A. Towards improved membrane production: Using low-toxicity solvents for the preparation of PEEK nanofiltration membranes, Green Chem, 2016, 18, 2374–2384.
[21] (a) Gawande, MB, Bonifacio, VDB, Luque, R, Branco, PS, Varma, RS. Benign by Design: Catalyst-Free in-Water, on-Water Green Chemical Methodologies in Organic Synthesis. Chem Soc Rev, 2013, 42, 5522–5551. (b) Ghashang, M., Mansoor, SS., Mohammad, MR. Green Chemistry Preparation of MgO Nanopowders: Efficient Catalyst for the Synthesis of Thiochromeno[4,3-b] pyran and Thiopyra-no[4,3-b]pyran Derivatives. J Sulfur Chem 2016, 37, 377–390.
[22] Butler, RN, Coyne, AG. Water: Nature's Reaction Enforcer-Comparative Effects for Organic Synthesis "In-Water" and "On-Water", Chem Rev, 2010, 110, 6302–6337.
[23] Tsukinoki, T, Nagashima, S, Mitoma, Y, Tashiro, M. Organic reaction in water Part 4. New synthesis of vicinal diamines using zinc powder promoted carbon-carbon bond formation, Green Chem, 2000, 2, 117–119.
[24] Bigi, F, Conforti, ML, Maggi, R, Piccinno, A, Sartori, G. Clean synthesis in water: Uncatalysed preparation of ylidenemalononitriles, Green Chem, 2000, 2, 101–103.
[25] Head-Gordon, T, Hura, G. Water structure from scattering experiments and simulation, Chem Rev, 2002, 102, 2651–2670.
[26] Sagar Vijay Kumar, P, Suresh, L, Vinodkumar, T, Reddy, BM, Chandramouli, GV. Zirconium doped ceria nanoparticles: An efficient and reusable catalyst for a green multicomponent synthesis of novel Phenyldiazenyl–chromene derivatives using aqueous medium, ACS Sustain Chem Eng, 2016, 4, 2376–2386.
[27] Rothenberg, G. Catalysis: Concepts and green applications, John Wiley & Sons, 2017.
[28] Ross, JR Heterogeneous catalysis: Fundamentals and applications. Elsevier; 2011.
[29] Muley, PD, Wang, Y, Hu, J, Shekhawat, D. Microwave-assisted Heterogeneous Catal. 2021, 33, 1–37.
[30] Somorjai, GA, Li, Y Introduction to surface chemistry and catalysis. John Wiley & Sons; 2010.
[31] Muhler, M, Thomas, JM, Thomas, WJ. Principles and Practice of Heterogeneous Catalysis, VCH: Weinheim, 1997, 1560.
[32] Horvath, IT. Encyclopedia of catalysis, Wiley-Interscience, 2003.
[33] Handbook of Heterogeneous Catalysis, Edi, Ertl, G, Wiley-VCH: Weinheim-New York, 2nd, 2008.
[34] Kokel, A, Schäfer, C, Török, B. Application of microwave-assisted heterogeneous catalysis in sustainable synthesis design, Green Chem, 2017, 19, 3729–3751.
[35] Miyaura, N, Suzuki, A. Palladium-catalyzed cross-coupling reactions of organoboron compounds, Chem Rev, 1995, 95, 2457–2483.
[36] Phan, NT, Van Der Sluys, M, Jones, CW. On the nature of the active species in palladium catalyzed Mizoroki–Heck and Suzuki–Miyaura couplings-homogeneous or heterogeneous catalysis, a critical review, Adv Synth Catal, 2006, 348, 609–667.
[37] Blangetti, M, Rosso, H, Prandi, C, Deagostino, A, Venturello, P. Suzuki-Miyaura cross-coupling in acylation reactions, scope and recent developments, Molecules, 2013, 18, 1188–1213.
[38] Zhang, G, Luan, Y, Han, X, Wang, Y, Wen, X, Ding, C, Gao, J. A palladium complex with functionalized β-cyclodextrin: A promising catalyst featuring recognition abilities for Suzuki–Miyaura coupling reactions in water, Green Chem, 2013, 15, 2081–2085.
[39] Kolb, HC, Finn, MG, Sharpless, KB. Angew Chem Int Ed, 2001, 40, 2004–2021.
[40] Poulain, A, Canseco-Gonzalez, D, Hynes-Roche, R, Müller-bunz, H, Schuster, O, Stoeckli-Evans, H, Neels, A, Albrecht, M. Synthesis and tunability of abnormal 1, 2, 3-triazolylidene palladium and rhodium complexes, Organometallics, 2011, 30, 1021–1029.
[41] Zhang, G, Wang, Y, Wen, X, Ding, C, Li, Y. Dual-functional click-triazole: A metal chelator and immobilization linker for the construction of a heterogeneous palladium catalyst and its application for the aerobic oxidation of alcohols, Chem Commun, 2012, 48, 2979–2981.

[42] Heidari, B, Heravi, MM, Nabid, MR, Sedghi, R, Hooshmand, SE. Novel palladium nanoparticles supported on β-cyclodextrin@graphene oxide as magnetically recyclable catalyst for Suzuki Miyaura cross-coupling reaction with two different approaches in bio-based solvents. Appl Organometal Chem, 2018, 1–13.
[43] Li, Y, Hong, XM, Collard, DM, El-Sayed, MA. Suzuki cross-coupling reactions catalyzed by palladium nanoparticles in aqueous solution, Org Lett, 2000, 2, 2385–2388.
[44] Putta, C, Sharavath, V, Sarkar, S, Ghosh, S. Palladium nanoparticles on β-cyclodextrin functionalised graphene nanosheets: A supramolecular based heterogeneous catalyst for C–C coupling reactions under green reaction conditions, RSC Adv, 2015, 5, 6652–6660.
[45] Khalafi-Nezhad, A, Panahi, F. Size-controlled synthesis of palladium nanoparticles on a silica–cyclodextrin substrate: A novel palladium catalyst system for the Heck reaction in water, ACS Sustain Chem Eng, 2014, 2, 1177–1186.
[46] Yin, L, Liebscher, J. Carbon-carbon coupling reactions catalyzed by heterogeneous palladium catalysts, Chem Rev, 2007, 107, 133–173.
[47] Xue, C, Palaniappan, K, Arumugam, G, Hackney, SA, Liu, J, Liu, H. Sonogashira reactions catalyzed by water-soluble, β-cyclodextrin-capped palladium nanoparticles, CatalLett, 2007, 116, 94–100.
[48] Pasbakhsh, P, Churchman, GJ, editors. Natural mineral nanotubes: Properties and applications, CRC Press, 2015.
[49] Szczepanik, B, Słomkiewicz, P. Photodegradation of aniline in water in the presence of chemically activated halloysite, Appl Clay Sci, 2016, 124, 31–38.
[50] Zhang, Y, Tang, A, Yang, H, Ouyang, J. Applications and interfaces of halloysite nanocomposites, Appl Clay Sci, 2016, 119, 8–17.
[51] Kumar-Krishnan, S, Hernandez-Rangel, A, Pal, U, Ceballos-Sanchez, O, Flores-Ruiz, FJ, Prokhorov, E, De Fuentes, OA, Esparza, R, Meyyappan, M. Surface functionalized halloysite nanotubes decorated with silver nanoparticles for enzyme immobilization and biosensing, J Mater Chem B, 2016, 4, 2553–2560.
[52] Zhang, Y, He, X, Ouyang, J, Yang, H. Palladium nanoparticles deposited on silanized halloysite nanotubes: Synthesis, characterization and enhanced catalytic property, Sci Rep, 2013, 3, 1–6.
[53] Sadjadi, S, Heravi, MM, Malmir, M. Pd@ HNTs-CDNS-g-C3N4: A novel heterogeneous catalyst for promoting ligand and copper-free Sonogashira and Heck coupling reactions, benefits from halloysite and cyclodextrin chemistry and g-C3N4 contribution to suppress Pd leaching, Carbohydr Polym, 2018, 186, 25–34.
[54] Albaladejo, MJ, Alonso, F, Moglie, Y, Yus, M. Three-component coupling of aldehydes, amines, and alkynes catalyzed by oxidized copper nanoparticles on titania, Eur J Org Chem, 2012, 16, 3093.
[55] Villaverde, G, Corma, A, Iglesias, M, Sánchez, F. Heterogenized gold complexes: Recoverable catalysts for multicomponent reactions of aldehydes, terminal alkynes, and amines, ACS Catal, 2012, 2, 399–406.
[56] Katkar, SV, Jayaram, RV. Cu–Ni bimetallic reusable catalyst for synthesis of propargylamines via multicomponent coupling reaction under solvent-free conditions, RSC Adv, 2014, 4, 47958–47964.
[57] Salam, N, Kundu, SK, Roy, AS, Mondal, P, Roy, S, Bhaumik, A, Islam, SM. Cu-grafted mesoporous organic polymer: A new recyclable nanocatalyst for multi-component, N-arylation and S-arylation reactions, Catal Sci Techn, 2013, 3, 3303–3316.

[58] Satyanarayana, KV, Ramaiah, PA, Murty, YL, Chandra, MR, Pammi, SV. Recyclable ZnO nano particles: Economical and green catalyst for the synthesis of A^3 coupling of propargylamines under solvent free conditions, Catal Commun, 2012, 25, 50–53.
[59] Sadjadi, S, Malmir, M, Heravi, MM. A green approach to the synthesis of Ag doped nano magnetic γ-Fe_2O_3@ SiO_2-CD core–shell hollow spheres as an efficient and heterogeneous catalyst for ultrasonic-assisted A^3 and KA^2 coupling reactions, RSC Adv, 2017, 7, 36807–36818.
[60] Dupont, J, de Souza, RF, Suarez, PA. Ionic liquid (molten salt) phase organometallic catalysis, Chem Rev, 2002, 102, 3667–3692.
[61] Rogers, RD, Seddon, KR. Ionic liquids–solvents of the future?, Science, 2003, 302, 792–793.
[62] Bahadorikhalili, S, Ansari, S, Hamedifar, H, Mahdavi, M. The use of magnetic starch as a support for an ionic liquid-β-cyclodextrin based catalyst for the synthesis of imidazothiadiazolamine derivatives, Int J Biol Macromol, 2019, 135, 453–461.
[63] Goulet, PJ, Lennox, RB. New insights into Brust-Schiffrin metal nanoparticle synthesis, J Am Chem Soc, 2010, 132, 9582–9584.
[64] Deraedt, C, Ye, R, Ralston, WT, Toste, FD, Somorjai, GA. Dendrimer-stabilized metal nanoparticles as efficient catalysts for reversible dehydrogenation/hydrogenation of N-heterocycles, J Am Chem Soc, 2017, 139, 18084–18092.
[65] Liu, L, Corma, A. Metal catalysts for heterogeneous catalysis: From single atoms to nanoclusters and nanoparticles, ChemRev, 2018, 118, 4981–5079.
[66] Huang, T, Sheng, G, Manchanda, P, Emwas, AH, Lai, Z, Nunes, SP, Peinemann, KV. Cyclodextrin polymer networks decorated with subnanometer metal nanoparticles for high-performance low-temperature catalysis, Sci Adv, 2019, 5, eaax6976.
[67] Guy, RG, Patai, S. The chemistry of cyanates and their thio derivatives, Part Wiley, 1977, 2, 819–886.
[68] Kamal, A, Chouhan, G. A task-specific ionic liquid[bmim] SCN for the conversion of alkyl halides to alkyl thiocyanates at room temperature, Tetrahedron Lett, 2005, 46, 1489–1491.
[69] Ju, Y, Kumar, D, Varma, RS. Revisiting nucleophilic substitution reactions: Microwave-assisted synthesis of azides, thiocyanates, and sulfones in an aqueous medium, J Org Chem, 2006, 71, 6697–6700.
[70] Kiasat, AR, Badri, R, Sayyahi, S. A facile and convenient method for synthesis of alkyl thiocyanates under homogeneous phase transfer catalyst conditions, Chin Chem Lett, 2008, 19, 1301–1304.
[71] Mokhtari, B, Azadi, R, Rahmani-Nezhad, S. In situ-generated N-thiocyanatosuccinimide (NTS) as a highly efficient reagent for the one-pot thiocyanation or isothiocyanation of alcohols, Tetrahedron Lett, 2009, 50, 6588–6589.
[72] Kiasat, AR, Zarinderakht, N, Sayyahi, S. β-Cyclodextrin Immobilized onto Dowex Resin: A Unique Microvessel and Heterogeneous Catalyst in Nucleophilic Substitution Reactions, Chin J Chem, 2012, 30, 699–702.
[73] Cheng, T, Zhang, D, Li, H, Liu, G. Magnetically recoverable nanoparticles as efficient catalysts for organic transformations in aqueous medium, Green Chem, 2014, 16, 3401–3427.
[74] Polshettiwar, V, Len, C, Fihri, A. Silica-supported palladium: Sustainable catalysts for cross-coupling reactions, Coord Chem Rev, 2009, 253, 2599–2626.
[75] Hu, A, Yee, GT, Lin, W. Magnetically recoverable chiral catalysts immobilized on magnetite nanoparticles for asymmetric hydrogenation of aromatic ketones, J Am Chem Soc, 2005, 127, 12486–12487.

[76] Luque, R, Baruwati, B, Varma, RS. Magnetically separable nanoferrite-anchored glutathione: Aqueous homocoupling of arylboronic acids under microwave irradiation. Green Chem, 2010, 12, 1540–1543.
[77] Rao, GD, Kaushik, MP, Halve, AK. An efficient synthesis of naphtha [1, 2-e] oxazinone and 14-substituted-14H-dibenzo [a, j] xanthene derivatives promoted by zinc oxide nanoparticle under thermal and solvent-free conditions, Tetrahedron Lett, 2012, 53, 2741–27444.
[78] Ghosh, PP, Das, AR. Nanocrystalline and Reusable ZnO Catalyst for the Assembly of Densely Functionalized 4 H-Chromenes in Aqueous Medium via One-Pot Three Component Reactions: A Greener "NOSE" Approach, J Org Chem, 2013, 78, 6170–6181.
[79] Moghaddam, FM, Saeidian, H, Mirjafary, Z, Sadeghi, A. Rapid and efficient one-pot synthesis of 1, 4-dihydropyridine and polyhydroquinoline derivatives through the Hantzsch four component condensation by zinc oxide. J Iran Chem Soc, 2009, 317–324.
[80] Mueller, NC. Nowack, B. Nanotechnology Developments for the Environment Sector-Report of the Observatory NANO EU FP7 project 2009.
[81] Diallo, MS, Savage, N. Nanoparticles and Water Quality. 2005, 7, 330–325.
[82] Sagir, H, Rai, P, Singh, PK, Siddiqui, IR. ZnO nanoparticle-β-cyclodextrin: A recyclable heterogeneous catalyst for the synthesis of 3-aryl-4 H-benzo [1, 4] thiazin-2-amine in water, New J Chem, 2016, 40, 6819–6824.
[83] Rezvani, MA, Khandan, S, Sabahi, N, Saeidian, H. Deep oxidative desulfurization of gas oil based on sandwich-type polysilicotungstate supported β-cyclodextrin composite as an efficient heterogeneous catalyst, Chin J Chem Eng, 2019, 27, 2418–2426.
[84] Hu, X, Liu, B, Deng, Y, Chen, H, Luo, S, Sun, C, Yang, P, Yang, S. Adsorption and heterogeneous Fenton degradation of 17α-methyltestosterone on nano Fe_3O_4/MWCNTs in aqueous solution, Appl Catal B: Environ, 2011, 107, 274–283.
[85] Mousset, E, Oturan, N, van Hullebusch, ED, Guibaud, G, Esposito, G, Oturan, MA. Influence of solubilizing agents (cyclodextrin or surfactant) on phenanthrene degradation by electro-Fenton process–study of soil washing recycling possibilities and environmental impact, Water Res, 2014, 48, 306–316.
[86] He, DQ, Wang, LF, Jiang, H, Yu, HQA. Fenton-like process for the enhanced activated sludge dewatering, Chem Eng J, 2015, 272, 128–134.
[87] Wang, Q, Lemley, AT. Kinetic model and optimization of 2, 4-D degradation by anodic Fenton treatment, Environ Sci Tech, 2001, 35, 4509–4514.
[88] Fukushima, M, Tatsumi, K, Morimoto, K. The fate of aniline after a photo-Fenton reaction in an aqueous system containing iron (III), humic acid, and hydrogen peroxide, Environ Sci Tech, 2000, 34, 2006–2013.
[89] Wang, M, Fang, G, Liu, P, Zhou, D, Ma, C, Zhang, D, Zhan, J. Fe_3O_4@ β-CD nanocomposite as heterogeneous Fenton-like catalyst for enhanced degradation of 4-chlorophenol (4-CP), Appl Catal B: Environ, 2016, 188, 113–122.
[90] Lin, Y, Ren, J, Qu, X. Catalytically active nanomaterials: A promising candidate for artificial enzymes, Acc Chem Res, 2014, 47, 1097–1105.
[91] Chen, SY, Lu, YH, Huang, TW, Yan, DC, Dong, CL. Oxygen vacancy dependent magnetism of CeO_2 nanoparticles prepared by thermal decomposition method, J Phys Chem C, 2010, 114, 19576–19581.
[92] Gogoi, A, Sarma, KC. Synthesis of the novel β-cyclodextrin supported CeO2 nanoparticles for the catalytic degradation of methylene blue in aqueous suspension, Mater Chem Phys, 2017, 194, 327–336.

[93] Careghini, A, Mastorgio, AF, Saponaro, S, Sezenna, E. Bisphenol A, nonylphenols, benzophenones, and benzotriazoles in soils, groundwater, surface water, sediments, and food: A review, Environ Sci Poll Res Int, 2014, 22, 5711–5741.
[94] Im, J, Loffler, FE. Fate of bisphenol a in terrestrial and aquatic environments, Environ Sci Technol, 2016, 50, 8403–8416.
[95] Zhou, Y, Chen, M, Zhao, F, Mu, D, Zhang, Z, Hu, J. Ubiquitous occurrence of chlorinated byproducts of bisphenol A and nonylphenol in bleached food contacting papers and their implications for human exposure, Environ Sci Technol, 2015, 49, 7218–7226.
[96] Liu, D, Huang, Z, Li, M, Li, X, Sun, P, Zhou, L. Construction of magnetic bifunctional β-cyclodextrin nanocomposites for adsorption and degradation of persistent organic pollutants, Carbohydr Polym, 2020, 230, 115564.

Payal Malik, Avtar Singh, Anupama Parmar, Harish Kumar Chopra*

9 Water-mediated heterogeneous catalysis for organic functional group transformations and synthesis

9.1 Introduction

Water is one of the most abundant substances on the Earth and plays a critical role in various biological, geological, and atmospheric processes [1]. Due to the unique physical and chemical properties of water, nature has chosen water as the medium. Water is an essential molecule for enzymatic catalysis: it helps in controlling the mass transfer rates of substrates as well as the products, proton transfer, and establishing molecular conformations which are responsible for the high efficiency and selectivity of enzymes in the living organisms [2]. Though most of the organic transformations are performed using organic solvents, in the recent past, synthetic chemists are forced to look for a replacement of organic solvents due to the associated limitations of these solvents such as toxicity, carcinogenicity, flammability, explosivity, cost, and their noticeable contribution to air, soil, and aquatic pollution. In this regard, water is an economical, greener, and more sustainable alternative to the organic solvents. There are several practical advantages of the use of water as solvent in organic synthesis, for instance, easy isolation of organic products by phase separation, recycling of the catalysts (water soluble), and elimination of hydrophobic derivatization. Although water is considered as the universal solvent, until recently, most of the synthetic organic chemists were trained in such a way that the presence of water in many fundamental organic reactions should be avoided [3]. This was probably due to detrimental effects of hydrolysis and water-insoluble nature of the organic compounds as for better chemical conversions solubility of reactants in the reaction medium is essential. On industrial scale, it is undesirable to replace the organic solvent by water at the expense of synthetic efficiency, since a small decrease in yield or selectivity of a reaction can lead to a significant increase in the cost. In the past few decades, the solubility issue of aqueous synthesis has been addressed, and the recent developments established that the unique solvating properties of water were shown to have advantageous effects on reactions in terms of both rate and selectivity.

*Corresponding author: **Harish Kumar Chopra,** Department of Chemistry, Sant Longowal Institute of Engineering and Technology, Longowal 148106, Sangrur, Punjab, India,
e-mail: hk67@rediffmail.com
Anupama Parmar, PG Department of Chemistry, M M Modi College, Patiala 147001
Payal Malik, Avtar Singh, Department of Chemistry, Sant Longowal Institute of Engineering and Technology, Longowal 148106, Sangrur, Punjab, India

https://doi.org/10.1515/9783110733846-009

In early reports, Fulhame [4] was the first to suggest that the water has promotional effect in the reduction of metals by hydrogen. The seminal work of Breslow group [5] set the stage for a paradigm shift in aqueous synthesis; they demonstrated that water as a reaction medium has positive effect on the rates and selectivity of the Diels–Alder reactions, and the hydrophobic effect played a key role in such reactions (Figure 9.1). These results have attracted attention of the scientific community [6]. In a major breakthrough, Sharpless et al. [7] performed the cycloaddition reaction of quadricyclanes with dimethylazodicarboxylates in water and aqueous suspension was obtained, and low miscibility of organic compounds with water was not detrimental; in fact, it accelerates the rate of reaction substantially and facilitates the isolation of products. They coined a new term "on-water" for the cases where reactants are not soluble in water. Since then, the field has witnessed tremendous growth, and the previous belief like highly reactive reagents and catalysts often decompose or are deactivated by water has changed now [8]. A variety of organic reactions have been carried out in aqueous media; in some cases, faster reaction rates and remarkable selectivity were observed. The results were comparable with the classic organic solvent-based systems [9]. Although reactions in aqueous media have extensively been explored in the recent past, their classification is still a topic of debate. Earlier the reactions are classified as "on water" and "in water" reactions; however, it is difficult to make a clear distinction between "on water" and "in water." This chapter provides an overview of the recent developments in the field of water-mediated organic transformations. We documented the promotional effect of water in a diverse range of synthetic organic reactions, such as cycloaddition, cross-coupling, C–H activation, and organometallic reactions. Comprehensive coverage of the field is beyond the scope of this chapter, mainly reactions in which hydrophobic interactions, cohesive energy density, hydrogen bonding, and proton transfer mechanisms that are operative have been discussed. The hydrophobic effects are associated with a negative volume of activation. High cohesive energy density and clathrate formation ability of water bring the organic molecules together and lead to the formation of tighter transition states, which influence the rate and stereoselectivity of the reactions. In the cases where hydrogen bonding is involved in the mechanism, strong H-bond acceptors within reactants interact with dangling –OH groups at the interface. These interactions accelerate the reaction rates by stabilizing the transition state. Reservoir and nano-to-nano effects are mainly associated with nanomicelles.

9.2 Cycloaddition reactions

Cycloaddition reactions are among one of the most important reactions in synthetic organic chemistry. They enable access to complex polycyclic compounds with a high degree of regio- and stereo-control. In pioneer studies, Breslow and Ride [10]

treated cyclopentadiene (**1**) with a range of dienophiles (**2**) and examined the effect of water as a solvent on the reaction, and the results revealed that water has a promotional effect on Diels–Alder [4 + 2] reaction. It enhances the rate of the reaction as well as *endo* selectivity (**3a**) significantly; and rate acceleration and an increase in *endo* selectivity were observed (Figure 9.1). The authors suggested that the hydrophobic effect was responsible for rate acceleration and better selectivity.

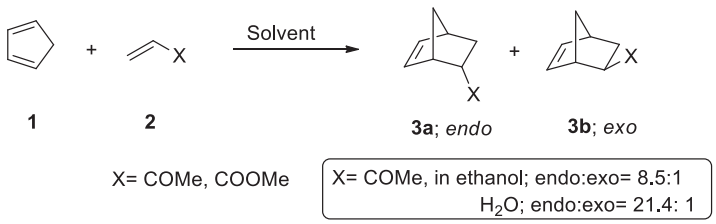

Figure 9.1: Diels–Alder reaction of cyclopentadiene with dienophiles using water as a solvent.

Since then, various organic transformations have been carried out using water as reaction media or cosolvent and the field of aqueous organic synthesis has observed remarkable growth in the past few decades [11]. Later, Griesback [12] reported Diels–Alder reaction of dimethylfulvene (**4**) with 1,4-benzoquinone (**5**) in water (three-phase system) and other organic solvents. It was found that water has a similar promotional effect on the reaction as observed by Breslow [10] (Figure 9.2).

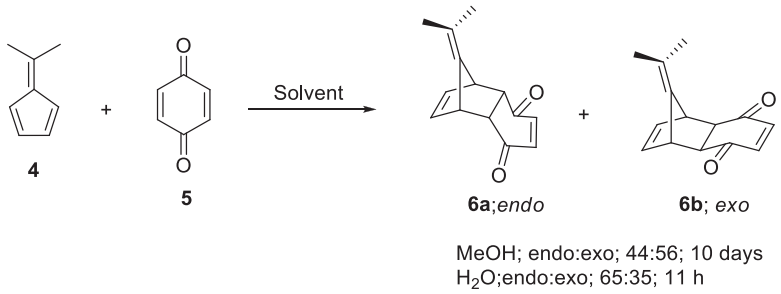

Figure 9.2: Diels–Alder cycloaddition reaction of dimethylfulvene and 1,4-benzoquione.

In addition, Sharpless et al. [7] have introduced the "on water" reactions using quadricyclane (**7**) and dimethylazodicarboxylate (**8**) as starting materials (Figure 9.3).

Fringuelli et al. [13] explored the inverse electron demand Diels–Alder reaction; diazenylbutene (**10**) reacted with electron-rich dienophile, that is, ethyl vinyl ether (**11**) in water as well as in organic solvents and a mixture of *endo* and *exo* adducts was obtained (Figure 9.4). The results confirmed that heterogeneous aqueous reaction provide better results than the homogenous reaction using dichloromethane.

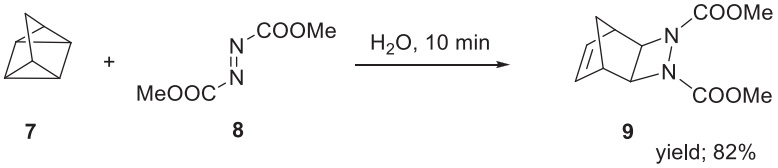

Figure 9.3: Reaction of quadricyclane and dimethyl azodicarboxylate in water.

However, nitroalkenes showed reverse trend. Intramolecular Diels–Alder reaction was performed in water using diene and iminium salt to obtain a tricyclic product (**14**) with 80% yield in 48 h (Figure 9.5), whereas in Et_2O only 13% of the product was formed after 66 h [14].

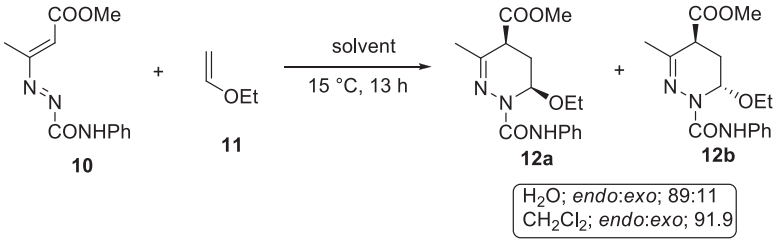

Figure 9.4: Inverse electron demand Diels–Alder reaction of diazabutene with ethyl vinyl ether.

Kobayashi [15] investigated the catalytic efficiency of AgOTf for aza-Diels–Alder reaction using Danishefsky's diene (**15**) with a variety of imines (**16**) in water and THF (Figure 9.6). The reaction provided better results in water.

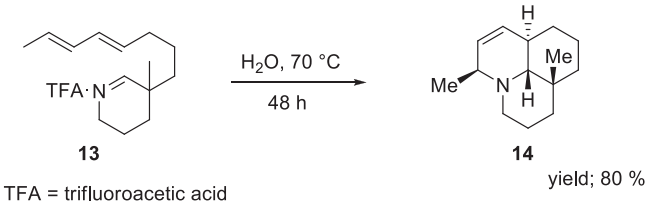

Figure 9.5: Intramolecular Diels–Alder reaction.

In 2013, Sugiyama et al. [16] used solid support DNA for asymmetric Diels–Alder reactions in water for the first time. Silica-immobilized DNA in combination with copper-dimethylbipyridine complex efficiently catalyzed the reaction of 2-azachalcone (**18**) with cyclopentadiene (**1**) and afforded a mixture of *endo* (**19**) and *exo* products with ratio of 99:1 and 94% *ee* (Figure 9.7); however, the reaction was sluggish and 99% conversions were achieved in 3 days.

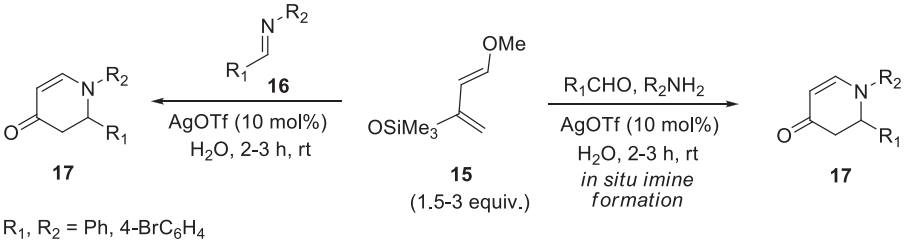

Figure 9.6: AgOTf-catalyzed aqueous aza-Diels–Alder reaction of Danishefsky's diene.

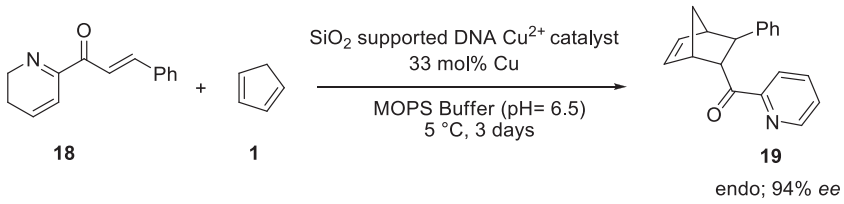

Figure 9.7: Silica-supported DNA for copper-catalyzed asymmetric Diels–Alder reactions.

Huisgen [3 + 2] cycloaddition reaction is one of the most versatile methods for the synthesis of five-membered heterocyclic ring systems [17]. Pandey and Pandey [18] studied the effect of water and benzene as reaction medium on the cycloaddition reaction by treating C,N-diphenylnitrone (**20**) with dipolarophiles such as acrylonitrile and methyl acrylate (Figure 9.8). The reaction proceeded faster in case of water and produced isoxazolidine derivatives **21** and **22** in excellent yields; however, no increase in the regio- or stereoselectivity was observed.

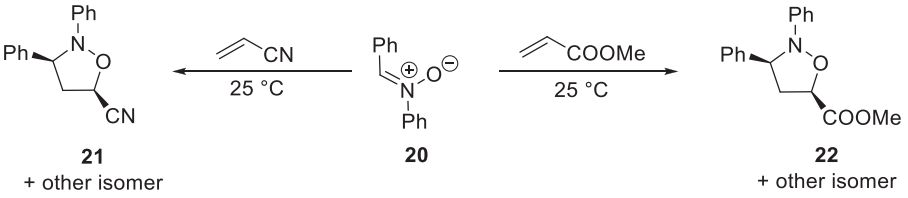

Figure 9.8: Aqueous nitrone [3 + 2] cycloaddition reaction with dipolarophiles.

Butler et al. [19] explored the reaction of phthalazinium-2-dicyanomethanide (**23**) with a range of vinyl ketones, and the yields and selectivity of the reaction in acetonitrile and water were compared. It was observed that the product yields were unaffected by the choice of reaction medium; on the other hand, a significant increase in the *endo* selectivity was observed when water was used as a reaction medium (Figure 9.9).

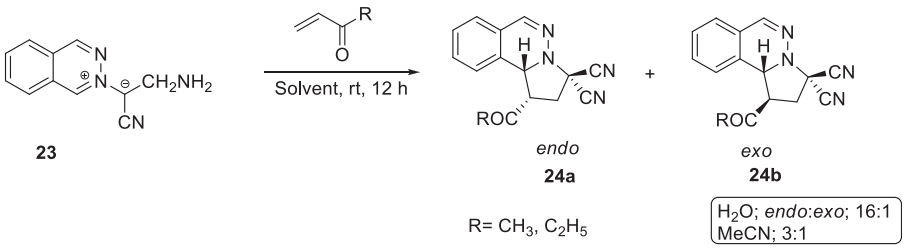

Figure 9.9: Huisgen cycloaddition of phthalazinium-2-dicyanomthanide with vinyl ketones.

Rees et al. [20] also reported that water as a reaction medium has a profound effect on regioselectivity of the Huisgen cycloaddition reaction of phenyl azide and substituted phenylacetylene. In toluene, two regioisomeric products were obtained in 1:1 ratio and exclusively one regioisomer was obtained in case of water. In an interesting aqueous azide Huisgen cycloaddition reaction [21], it was observed that the reaction of a substituted benzyl azide (**25**) with 2-chloroacrylonitrile (**26**) provided cyanotriazole derivative **27** in 46% and 98% yields in organic solvent and water, respectively (Figure 9.10). The disparity in yields was attributed to the in situ elimination of HCl, which leads to polymerization of 2-chloroacrylonitrile in organic solvent, whereas in biphasic reaction mixture the HCl was extracted in water phase; therefore, no polymerization was observed in aqueous medium.

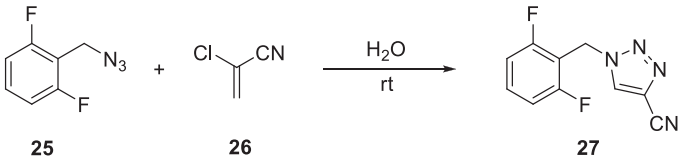

Figure 9.10: Huisgen cycloaddition reaction of benzyl azide with 2-chloroacrylonitrile.

Khalili et al. [22] described an oxozirconium chloride-catalyzed cycloaddition reaction of aryl cyanamides (**28**) and sodium azide in water, and 1-aryl tetrazoles (**29**) were obtained in high yields with remarkable selectivity (Figure 9.11). It was suggested that the Lewis acidic catalyst activates cyanamides to function as dipolarophiles.

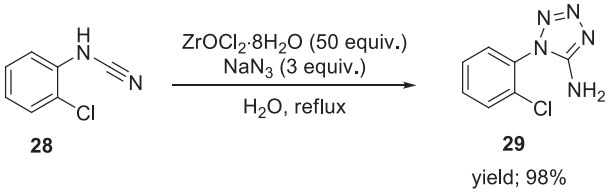

Figure 9.11: Oxozirconium chloride-catalyzed cycloaddition reaction.

Tsai et al. [23] reported $[Rh(cod)Cl]_2$/cationic 2,2′-bipyridyl catalyzed [2 + 2 + 2] cycloaddition reaction of α,ω-diynes with alkynes in water at 60 °C and provided access of tri- and tetra-substituted benzene derivatives in moderate to high yields (Figure 9.12).

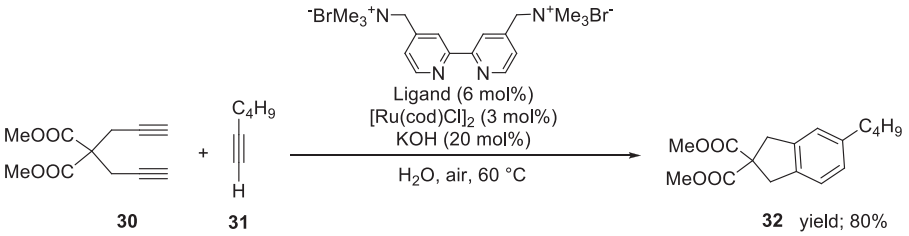

Figure 9.12: Rhodium-cationic 2,2′-bipyridyl complexes for the cyclotrimerization of alkynes.

Copper salts and copper complexes, due to their milder Lewis acidity, π-philic nature, and tendency to form acetylide complex with terminal alkynes, have been used as catalysts for Huisgen cycloaddition reaction in aqueous medium. CuBr-methyl phenyl sulfide [24], tris(triazoyl)methanol-copper(I) [25], CuI-hydroquinidine 1,4-phthalazinediyl diether ($(DHQD)_2PHAL$) [26], copper(II)-pyridinedicarboxyamide complex [27], [copper(II)-pyrrolide imine Schiff base complex [28], and $CuSO_4$ [29] are proved to be efficient and selective catalysts in water (Figure 9.13). It is worth mentioning that water-stable copper(I) species outperformed in cycloaddition reactions.

Xia et al. developed a solid-supported catalyst Cu-CPSIL (Cross-linked polymeric ionic liquid material-supported copper) by immobilizing copper(I) iodide on CPSIL (obtained from the reaction of cross-linked polystyrene with imidazolium salt) for substituted azide–alkyne cycloaddition reaction (Figure 9.14) [30]. The catalyst displayed best activity in water and the use of 1 mol% Cu-CPSIL afforded the expected product **37** in 98% yield; however, in case of organic solvents the product yields were comparatively low.

9.3 Coupling reactions

Transition metal-mediated coupling reactions, namely, Suzuki, Sonogashira, and Heck coupling are considered as one of the most widely used strategies for C–C bond formation. In the beginning, palladium was the key player in this area [31, 32]; recently, cost-effectiveness and Earth-abundant metals like copper and nickel have also been introduced [33, 34]. Herein, some of the representative reports demonstrating the role of water in coupling reactions have been compiled.

Handa et al. reported the use of nickel nanoparticles in combination with surfactant TPGS-750-M in Suzuki–Miyaura coupling reaction between various aryl–aryl/aryl–heteroaryl/hetero-heteroaryl systems [35]. The reaction was performed

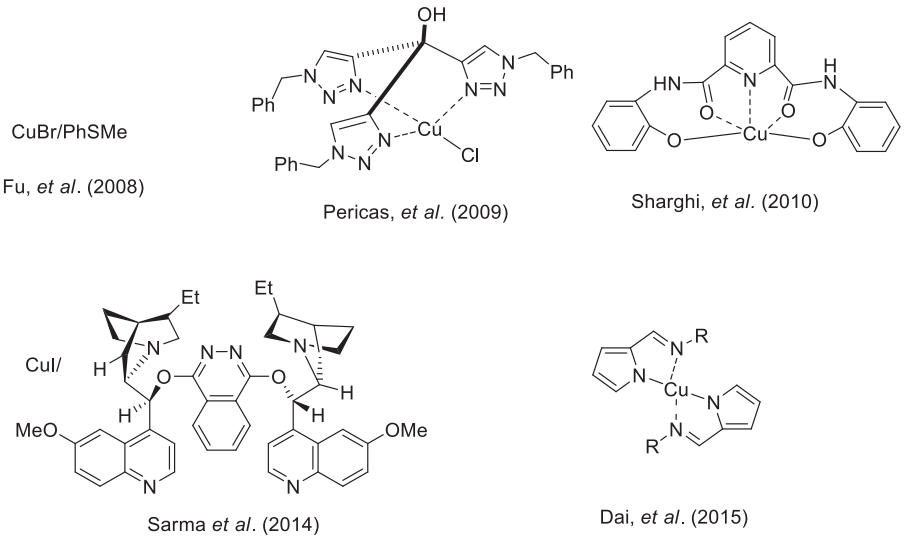

Figure 9.13: Different Cu-based catalysts for aqueous Huisgen cycloaddition reaction.

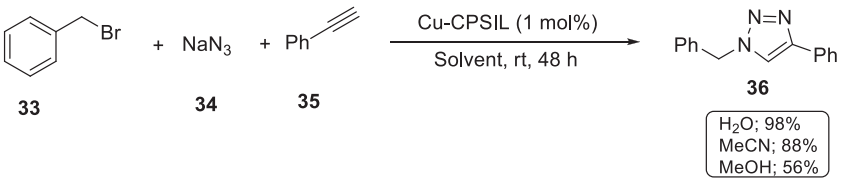

Figure 9.14: Cu-CPSIL-catalyzed azide–alkyne cycloaddition reaction.

at relatively low temperatures, with 0.35 equivalents of base, K_3PO_4, and almost stoichiometric ratio (1.05:1) of the aryl boron to aryl halide has been used (Figure 9.15). The Ni catalyst was reused for six runs with almost no change in its activity.

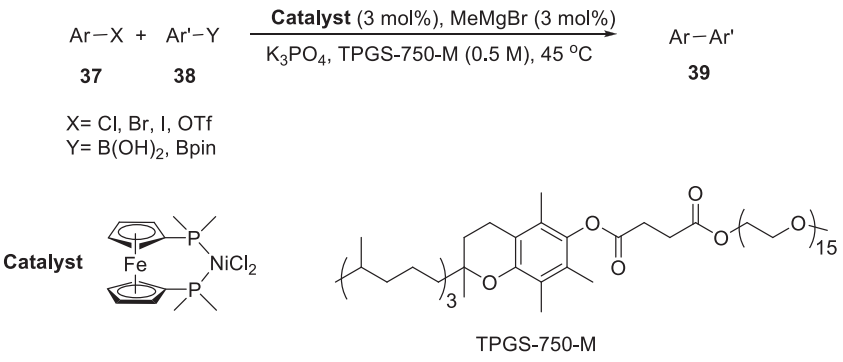

Figure 9.15: Ni-catalyzed Suzuki–Miyaura coupling reaction by Handa et al. [35].

Wu et al. [36] synthesized the phosphine dendrimer-stabilized nickel nanoparticles for Stille coupling reaction of aryl halides (**40**) with organotin compounds (**41**) in water at room temperature (Figure 9.16). Complete conversions were achieved within 2 h in water as solvent; on the other hand, only trace amounts of products were obtained in organic solvents. Ni catalyst was recovered from the reaction mixture using hexane. Further, the inductively coupled plasma and transmission electron microscopy analysis were performed to confirm that the reaction occurred heterogeneously on the surface of nanosized Ni catalyst encompassed by the nanoenvironment of dendrimers.

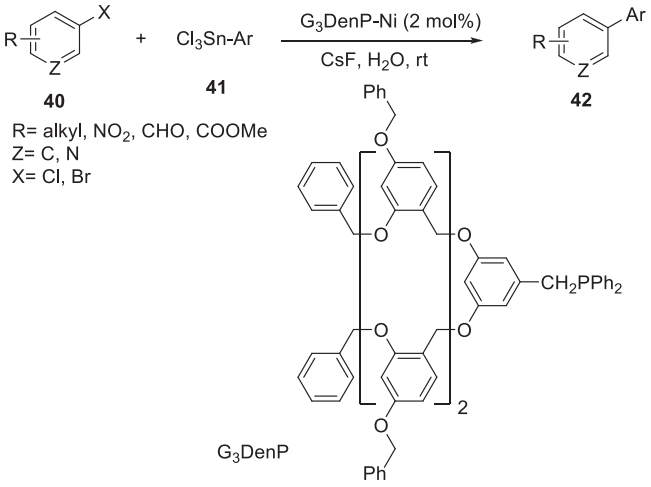

Figure 9.16: Ni nanoparticle-catalyzed Stille coupling reaction of aryl halides with organotin compounds.

Bimetallic nanomaterials constitute an important class of heterogeneous catalysts due to their enhanced catalytic activity, selectivity, and stability. Particularly, the nickel- and cobalt-ferrites are well known for catalyzing variety of organic reactions [37]. Moghaddam et al. [38] reported the $NiFe_2O_4$ nanoparticle-catalyzed copper-free Sonogashira coupling of various alkyl/aryl halides (**42**) with phenylacetylene (**43**) in water that produced the coupling products in excellent yields (Figure 9.17).

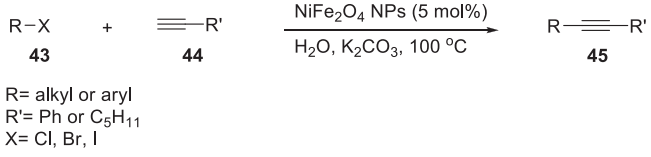

Figure 9.17: $NiFe_2O_4$-catalyzed copper-free Sonogashira coupling reaction in water.

Although the lesser reactivity of alkyl chlorides is often a matter of concern in such reactions, delightfully, this protocol was equally effective for aryl chlorides, bromides, and iodides. $NiFe_2O_4$ was recovered from the reaction mixture using an external magnetic field. Moreover, this method can be used in sensitive synthetic procedures due to the complete removal of the metal catalyst from the reaction mixture. Zhong et al. synthesized water-soluble PEPPSI-Pd-NHC complexes for Suzuki–Miyaura coupling reactions between aryl halides (**46**) and arylboronic acids (**47**) under aerobic conditions (Figure 9.18) [39]. The efficiency of the catalyst can be assessed from the fact that 99% yield has been obtained within 2 h with 0.1% catalyst loading.

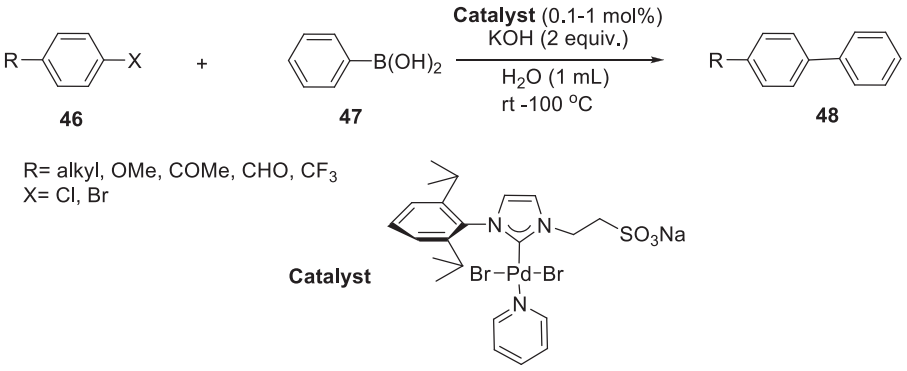

Figure 9.18: Water-soluble PEPPSI-Pd-NHC complex-mediated Suzuki coupling.

Uozumi and coworkers carried out the stereoselective Suzuki coupling reaction for the synthesis of biaryl motifs having axial chirality [40]. They have attempted this reaction in water using the heterogeneous palladium complex of PS–PEG-supported imidazoindoledicyclohexylphosphine ligand (PS–PEG–L*) in the presence of tetrabutylammonium fluoride (Figure 9.19). The heterogeneous variant also gave comparable yields and *ee*'s. Moreover, use of water offered extra advantages like better functional group tolerance and recovery of the catalyst from the reaction mixtures.

Lipshutz and Taft [41] presented the first example of the Heck reaction using water as solvent at room temperature and Triton X-100 or vitamin E-based phase transfer surfactant (PTS) (Figure 9.20). Good yields and remarkable *E*/*Z* selectivity were obtained by using Pd catalyst. It was proposed that on dissolution in water, PTS forms nanomicelles which lead to accommodation of organic substrates and the metal catalyst in the lipophilic core and to effective reactions between the lipophilic substrates.

In 2019, Mitrofanov and Beletskaya [42] reported copper-catalyzed "on water" Sonogashira coupling reaction of aryl iodides with terminal alkynes using CuI (5 mol%), diethoxyphosphoryl-1,10-phenanthroline ligand (5 mol%), PEG-400 (20 mol%) and

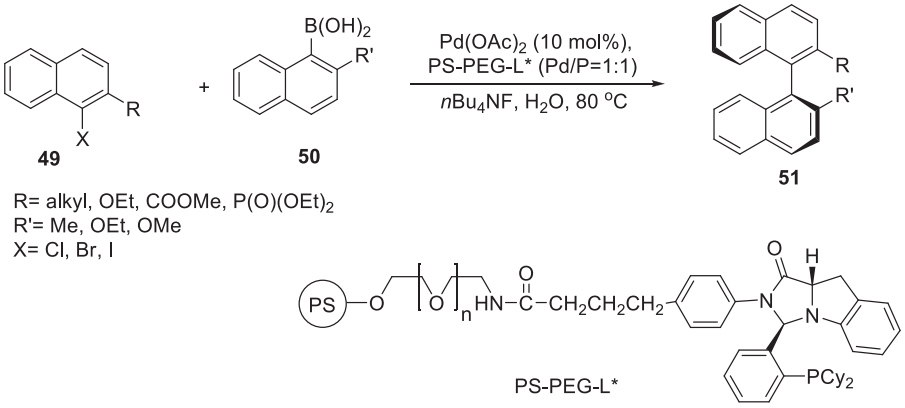

Figure 9.19: PS-PEG-supported Pd catalyst in asymmetric Suzuki coupling reaction.

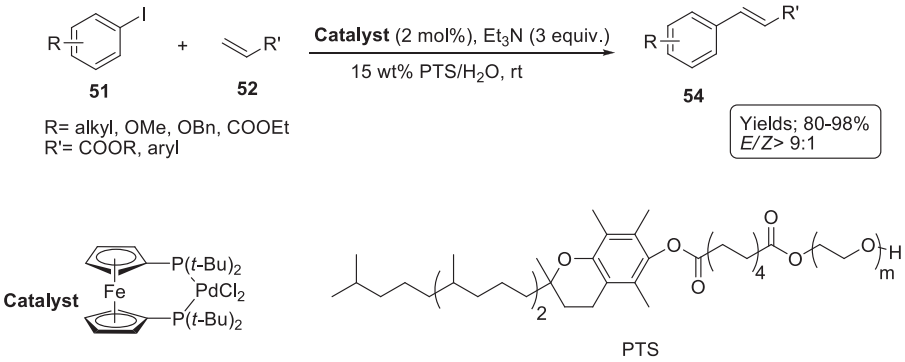

Figure 9.20: Pd/PTS-mediated Heck reaction in water.

K_2CO_3 (2 equiv.) in water and obtained 99% yield in 1 h (Figure 9.21). Authors confirmed that the catalytic system performed well under "on water" conditions, as the reactions performed in organic solvents were sluggish and low yields were obtained. The protocol did not work for aryl bromides.

Taillefer and coworkers reported the CuI/PPh_3-catalyzed Sonogashira coupling of aryl iodides with highly functionalized alkynes using water as the reaction medium (Figure 9.22) [43]. The reaction was effective on low catalyst loading, and complete conversion was observed. It was observed that the catalytic activity was pronounced in water as compared to the organic solvents.

Beller group [44] reported the first Ru-catalyzed carbonylative C–C bond formation by directed C–H activation of 2-phenylpyridine (Figure 9.23). Very low yields of the targeted products were obtained in the organic solvents, whereas yields were good when water was used as solvent. Authors proposed the mechanism in which the initial formation of cyclometalated Ru complex was followed by carbonylation and the

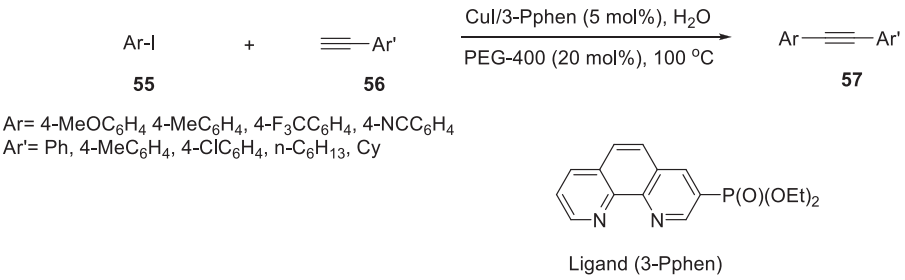

Figure 9.21: Cu-catalyzed Sonogashira coupling of aryl iodides with terminal alkynes.

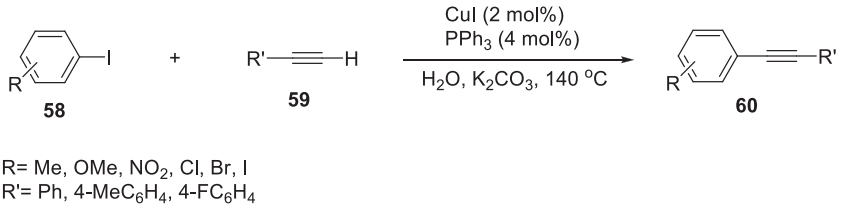

Figure 9.22: CuI/PPh_3-catalyzed Sonogashira coupling by Taillefer et al.

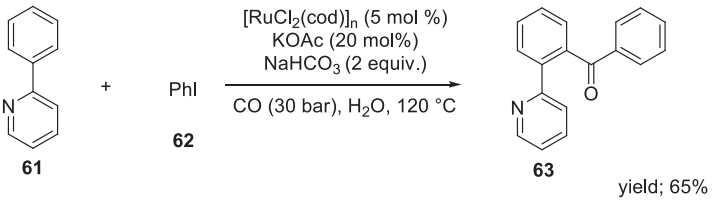

Figure 9.23: Ruthenium-catalyzed carbonylative C–C coupling reaction in water.

oxidative addition of the aryl halide. Finally, reductive elimination gives the product and the catalyst was regenerated.

9.4 Organometallic reactions

Carbon–carbon bond formation plays a pivotal role in synthetic organic chemistry [45]. For the formation of C–C bond, electrophiles and nucleophiles are required; in this regard, organometallic reagents serve as versatile nucleophiles. Classical organometallic nucleophile sources are Grignard, Gilman reagents, and so on. Although organometallic chemistry has made tremendous progress in the past decades, most of the reactions required dry organic solvents and inert atmosphere due to their moisture/oxygen intolerances [46]. Recently, great efforts have been made to develop the

sustainable chemical processes for highly reactive organometallic reaction, and reactions are performed in aqueous medium [47]. The protonation of the carbon–metal bond was prevented using different strategies such as reducing carbanion character of carbon–metal bond by using metals from groups 13 to 15 which increase the covalent character of the M–C bonds, "on water" or micellar catalysis conditions, and designing a radical pathway because neutral radical intermediates are stable toward water [48]. The research area over the past decade has seen remarkable developments. It has been realized that metal-mediated organic reactions can be performed in water under special circumstances.

Capriati group [49] has extensively explored air- and water-compatible organometallic chemistry, and their findings proved that water can serve as an alternative sustainable reaction medium for the organic transformation where organometallic reagents are the nucleophile precursors. They have designed a one-pot/two-step protocol by reacting aryl/alkyl γ-chloroketones and alkyl/aryl Grignard or organolithium at room temperature and in the presence of air using water as reaction medium: 2,2-disubstituted tetrahydrofurans (**66**) were obtained up to 85% yields (Figure 9.24) [50]. The authors postulated that the dangling H-bond interactions on organic/liquid water interface are responsible for activation of the carbonyl group and hydrophobicity of the reagents probably minimizing or preventing protonolysis of the organometallic reagent.

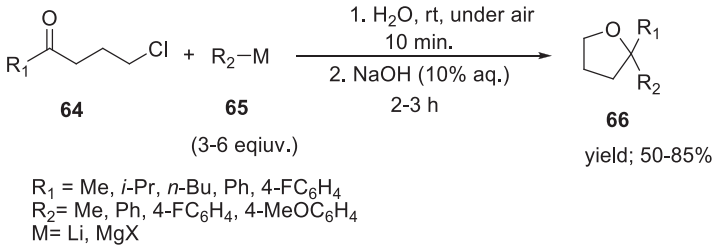

Figure 9.24: One-pot synthesis of 2,2-disubstituted tetrahydrofurans in aqueous solution.

In an interesting development, the same group developed a one-pot new methodology for the synthesis of substituted tertiary alcohols, where for the first time they combined organocatalysts AZADO (2-azaadamantane *N*-oxyl) and organolithium reagent in aqueous media to produce highly substituted tertiary alcohols (**70**) in excellent yields (up to 98%) (Figure 9.25) [51]. All the reactions were carried out at room temperature in the presence of air. The authors suggested that the reaction proceeds via organo-catalyzed oxidation of secondary alcohols followed by subsequent chemoselective addition of organolithium reagents, and the addition reaction took place within 3 s. It was observed that in case of water, greater selectivities were observed as compared to the organic solvents under inert atmosphere. Further, Capriati et al. have also demonstrated that water as a solvent promotes the

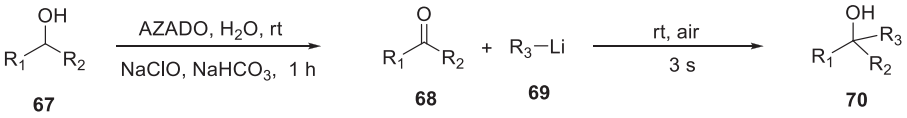

R_1= Ph, 4-MeC_6H_4, 2MeC_6H_4, 4-ClC_6H_4, 4-BrC_6H_4
R_2= Et; R_3= *n*-Bu, *sec*-Bu

Figure 9.25: Tandem protocol for the synthesis of tertiary alcohols in aqueous media.

fast and selective addition of organolithium reagents to imines or nitriles (**71**) at room temperature, under air, and gave corresponding secondary amines or tertiary carbinamines (**74**) up to 95% yield (Figure 9.26) [52]. Notably, under vigorous stirring conditions, the reaction was completed within 5 min and excellent yields were obtained, whereas gentle stirring produced lower yield that was attributed to decrease in the oil–water interfacial area. Isotope labeling experiments revealed that proton transfer at the oil–water interface was found to be the rate-determining step. However, in methanol, the product yield dropped considerably.

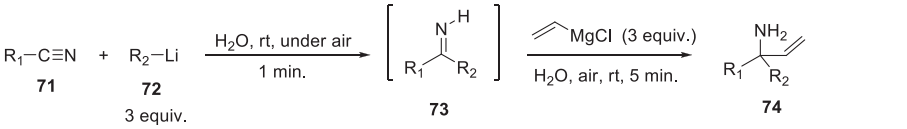

R_1= *n*-Pr, Ph, 4-ClC_6H_4, Bn
R_2= Et, *n*-Bu, *sec*-Bu, Ph

Figure 9.26: Synthesis of substituted amines in aqueous media by Capriati et al. [52].

Recently, the group developed a fast straightforward method for the synthesis of symmetric tertiary alcohols (**77**) (Figure 9.27) [53]. Tertiary alcohols have been synthesized via chemoselective double addition of RLi/RMgX from esters (organic electrophiles) at room temperature in the presence of air using bulk water and the reaction yields were up to 98%.

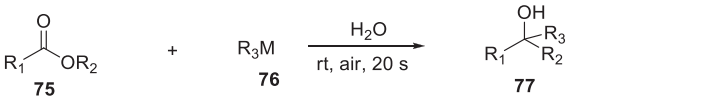

R_1= Ph, 4-MeC_6H_4, 2-MeOC_6H_4, 4-CNC_6H_4
R_2= Me, Et; R_3= Ph, Me, *n*-Bu, thienyl
M= Li, MgX

Figure 9.27: Synthesis of highly substituted tertiary alcohols in aqueous media by Capriati et al. [53].

9.5 C–H activation

C–H activation has emerged as a transformative tool in organic synthesis. The C–H functionalization relies on the controlled functionalization of specific C–H bonds, even in the presence of reactive functional groups [54]. Traditionally, the nonactivated C–H bonds were functionalized by free radical processes; however, the advancements in organometallic chemistry have opened new opportunities for site-selective C–H functionalization. The C–H functionalization has attracted attention of academia as well as industry, and in recent years the field has seen phenomenal progress [55]. In this section, we cover the recent advances in aqueous C–H functionalization reactions.

Dixneufet et al. [56] were the first to perform ruthenium-catalyzed C–H activation in water. They have used $[RuCl_2(p\text{-cymene})]_2$ complex in combination with potassium pivalate (KOPiv) and potassium carbonate to produce the pyridine-directed C–H functionalization of arenes (Figure 9.28). It was observed that C–H bond activation reactions proceeded more efficiently in water than in organic solvents. However, this catalytic system was not efficient at low temperatures.

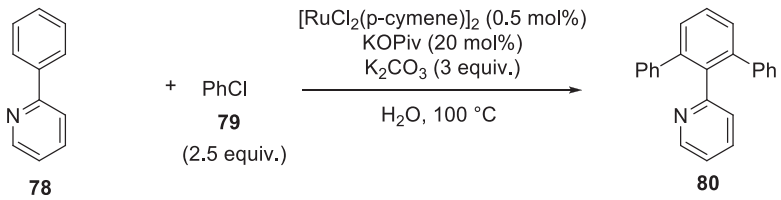

Figure 9.28: Ruthenium-catalyzed C–H activation in water.

Zhang et al. reported a nickel(II) sulfate-catalyzed C–H trifluoromethylation of *N*-phenylpicolinamide (**81**) using potassium persulfate ($K_2S_2O_8$) as initiator and Langlois' reagent (CF_3SO_2Na) (**82**) as CF_3 source, in water at 50 °C (Figure 9.29) [57]. Interestingly, due to catalyst miscibility with water, the catalyst was recovered and reused up to eight times without any significant loss in catalytic activity. It was believed that the catalytic cycle begins with the formation of a nickel intermediate covalently bound to picolinamide at the oil–water interface and the reaction proceeds via SET (Single Electron Transfer) mechanism.

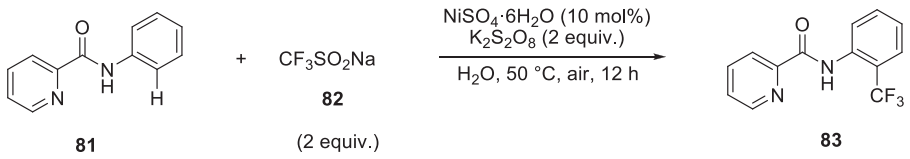

Figure 9.29: Nickel(II)-catalyzed C–H trifluoromethylation of *N*-phenylpicolinamide.

Zhu et al. have described a copper(II)-catalyzed direct azidation of anilines through C–H activation in aqueous solution and used $Cu(OAc)_2$ in combination H_2O_2 as an oxidant at room temperature (Figure 9.30) [58]. Among the solvents screened, water was found to be the best solvent and afforded 2-azidoaniline in 78% yield. Moreover, this protocol was equally effective for regioselective bromination/iodination on the *o*-position of aromatic amines. The mechanistic studies confirm the reaction proceed through a radical mechanism.

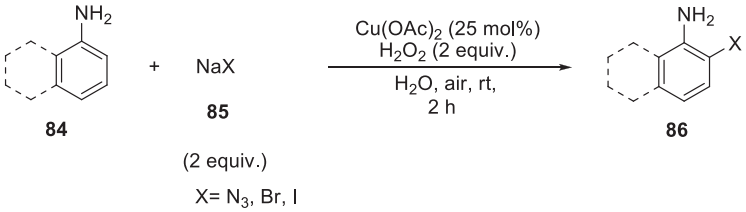

Figure 9.30: Copper(II)-catalyzed C–H azidation of anilines in aqueous medium.

Ackermann's group has made remarkable contribution in the development of aqueous transition-metal-catalyzed C–H activation [59]. For the first time, they have described ruthenium-catalyzed cross-dehydrogenative alkenylation of substituted benzoic acid and subsequent intramolecular oxa-Michael reaction in water, and phthalide (**89**) was obtained in excellent yields (Figure 9.31).

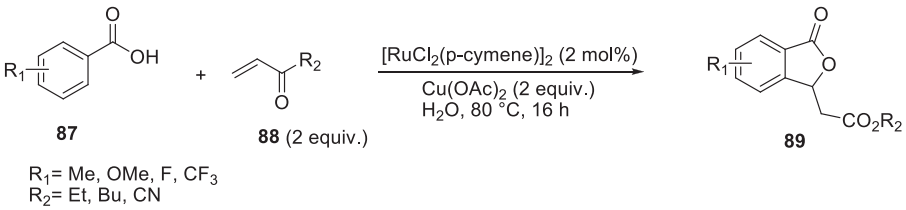

Figure 9.31: Ruthenium-catalyzed oxidative alkenylations in aqueous medium.

Based on isotope-labeling experiments, results suggested a kinetically relevant, irreversible C–H bond ruthenation through acetate assistance. Later, rhodium-catalyzed highly selective C–H monoamination was carried out by reacting pyridine derivatives with aryl azides in the presence of sodium tetrakis(3,5-trifluoromethyl)phenyl)borate (NaBArF) (Figure 9.32) [60]. In water at 110 °C, the catalytic system displayed excellent activity and provided quantitative yields; however, in case of organic solvents, the reaction yields were <10%. Moreover, deamination of pyridine derivatives was attributed to intermolecular H-bonding-assisted water-promoted roll-over mechanism. It was confirmed that water plays an important role in rhodacycle formation as well as in roll-over process which is vital for the second amination.

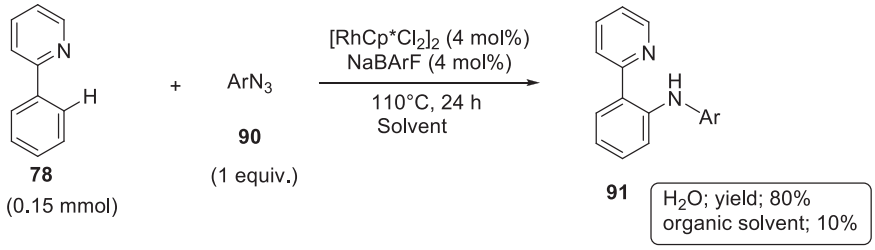

Figure 9.32: Rh-catalyzed highly selective C–H monoamination of 2-phenylpyridine.

In addition, Pd-catalyzed benzylic C–H amidation was described by Hikawa et al., and *o*-aminobenzamides (**92**) were treated with benzyl alcohols (**93**) in the presence of catalytic amount of $Pd(OAc)_2$ and sodium (diphenylphosphino)benzene-3-sulfonate in water at 120 °C to enable access to quinazolinone core (**94**) (Figure 9.33) [61]. It was revealed that water is essential for this transformation, as it activates the hydroxyl group of the benzyl alcohol by hydration and smoothly generates the (η^3-benzyl) palladium species which plays a key role in benzylic transfer and C–H activation and dehydrogenation processes.

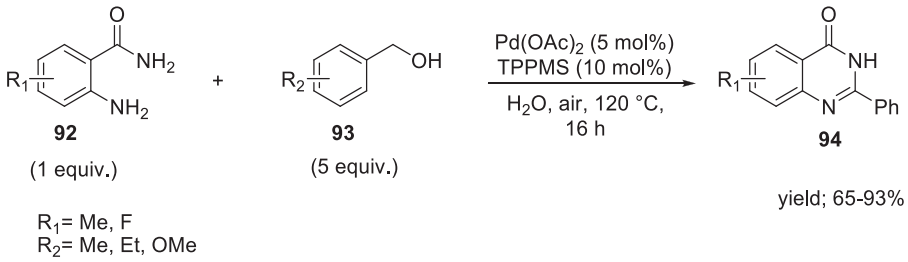

Figure 9.33: Pd-catalyzed benzylic C–H amidation with benzyl alcohol in water.

First, rhodium-catalyzed intermolecular C(sp^3)-H amination using water as solvent was reported in 2017 [62]. Hydrocarbons bearing different functional groups were reacted with trichloro-ethylsulfamate ($TcesNH_2$) and oxidant such as (diacetoxyiodo)benzene ($PhI(OAc)_2$) in the presence of bis[rhodium(α,α,α',α'-tetramethyl-1,3-benzenedipropionate) ($Rh_2(esp)_2$] catalyst and the corresponding aminated products were obtained in good to excellent yields (Figure 9.34).

The authors suggested that hydrophobic interactions were operative during the amination and provided additional acceleration to the intermolecular reaction.

Kim et al. [63] performed C(sp^3)–H activation reactions of 8-methylquinolines with a variety of allylic alcohols in the presence of $[RhCp^*Cl_2]_2$ as a catalyst and Cu $(OAc)_2$ and acetic acid as additives using water as the reaction medium at 100 °C (Figure 9.35). In the Rh(III)-catalyzed C–H alkylation, the formation of rhodacycle

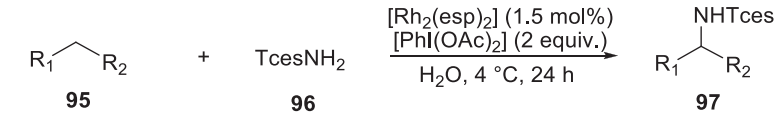

R_1= Ph, 2-MeC_6H_4, 4-MeOC_6H_4, 4-$NO_2C_6H_4$, 4-ClC_6H_4
R_2= Me, Et

Figure 9.34: Rh-catalyzed C(sp^3)-H amination of different hydrocarbons.

intermediates was confirmed on the basis of mechanistic studies, and the rhodacycle further reacted with allylic alcohols under oxidative conditions to give the resultant γ-quinoline-substituted carbonyl compounds.

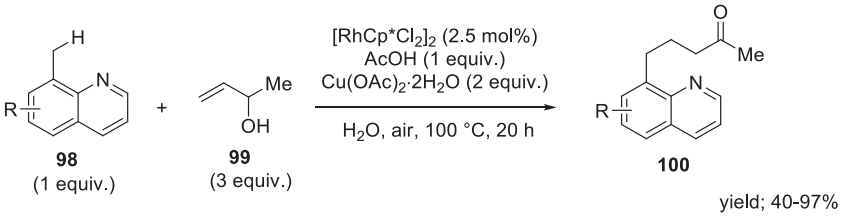

Figure 9.35: Cp*Rh(III)-catalyzed C(sp^3)-H alkylation of 8-methylquinolines.

9.6 Organocatalytic reactions

In the recent past, organocatalysts have established themselves as a promising alternative to metal-based catalysts in synthetic organic chemistry [64]. Organocatalysis is one of the fastest growing areas of research, due to their high stability to air and moisture, nontoxic nature, and ease in product separation [65]. Interestingly, noncovalent interactions promoted that organocatalysis was found to be compatible with aqueous conditions, and organocatalytic reactions in water have been extensively investigated recently [66]. In this section, we have discussed selective organocatalyzed reactions performed in aqueous media. Urea and thiourea-based catalysts have been widely explored in organocatalysis [67]. Xiao et al. [68] have developed a series of bifunctional pyrrolidine–thiourea organocatalysts and used in Michael addition reaction of cyclohexanone and nitro-olefins (Figure 9.36). The reaction was performed in aqueous medium at 35 °C and the corresponding nitro compounds (**103**) were obtained in excellent yields with remarkable

stereoselectivity: up to 99:1 dr and 99% *ee*. Hydrophobic 4-substituted acyloxyproline derivatives have been synthesized and used as organocatalysts for direct asymmetric aldol reaction; cyclic ketones and a variety of substituted benzaldehydes

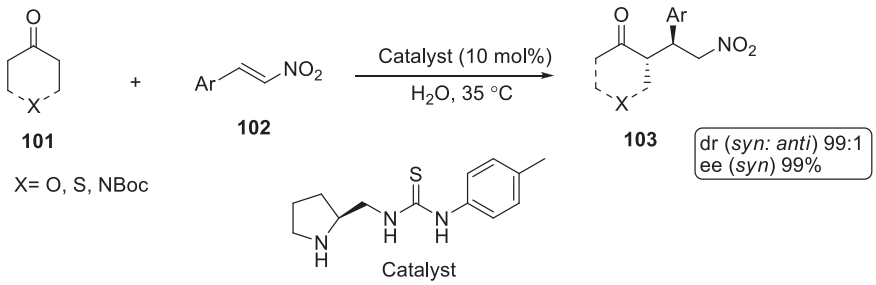

Figure 9.36: Aqueous pyrrolidine–thiourea-catalyzed Michael addition reaction.

were reacted in the presence of synthesized organocatalysts in water. Among all, [4-phenylbutanoate and 4-(pyren-1-yl)butanoate] outperformed and produced aldol products in quantitative yields and with excellent stereoselectivity (Figure 9.37) [69]. The enhanced stereoselectivity in aqueous medium was attributed to the generation of hydrophilic and hydrophobic regions between catalyst and water, and free –OH groups of interfacial water play a critical role in catalysis via the formation of hydrogen bonds. Moreover, these results established that other than proline, no additional chiral backbone is required for high stereoselectivities. Later, Pericás et al. mimicked aldolase by simple integration of proline and polystyrene through a 1,2,3-triazole linker, and further swelled it in water to form a hydrogen bonding network connecting the proline and 1,2,3-triazole fragments of the resin in water [70]. They investigated the catalytic efficiency of artificial aldolase for the direct aldol reactions of aldehydes and cyclic ketones in water. The catalyst displayed high activity, and the corresponding aldol products were obtained in moderate to excellent yields with enantioselectivity as high as 99% (Figure 9.38).

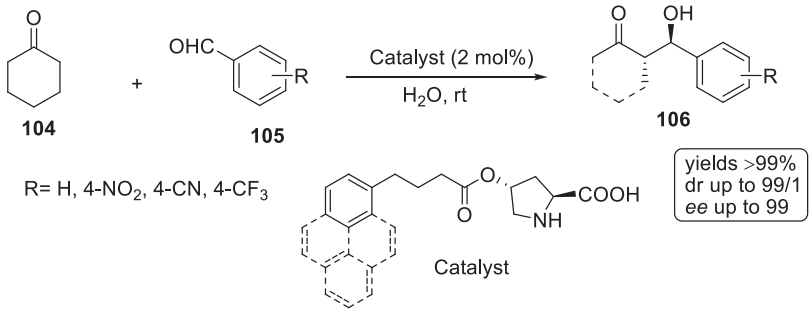

Figure 9.37: Catalytic aldol reactions of cyclohexanone and benzaldehydes.

Bifunctional squaramide in combination with inorganic base has been used as catalyst for the enantioselective conjugate addition of tritylthiol to in situ-generated aryl- and alkyl-substituted *o*-quinonemethides (Figure 9.39) [71]. High product

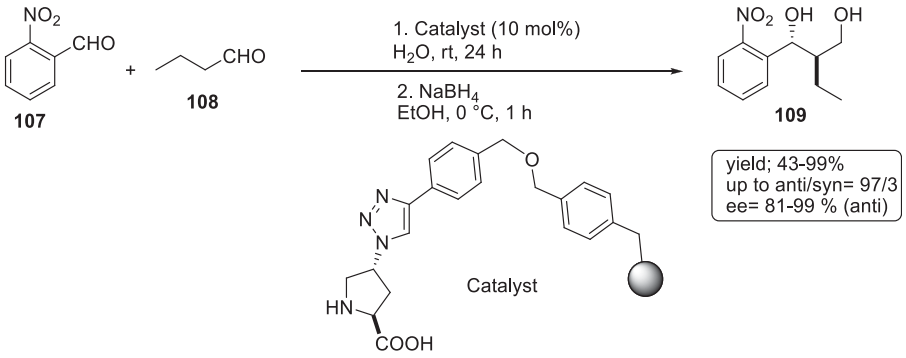

Figure 9.38: Asymmetric cross-aldol reactions in water with a polymer-supported proline-based catalyst.

yields (up to 99%) and good stereoselectivity (up to 94% *ee*) were achieved in aqueous medium. It was observed that water has a profound effect on rates and selectivities of the reaction, and the reaction mechanism relies on oil–water interface.

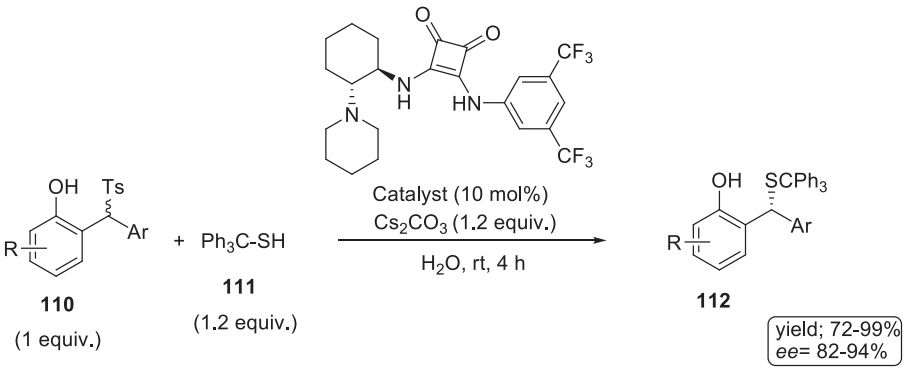

Figure 9.39: Enantioselective conjugate addition of tritylthiol in aqueous media.

In the recent past, organocatalysis has emerged as a promising alternative to metal-catalyzed reactions in organic synthesis. Hayashi et al. have investigated asymmetric Diels–Alder reaction of cyclopentadiene (**1**) and unsaturated aldehyde (**113**) using diarylprolinol silyl ether organocatalyst in the presence of perchloric acid as additive and water as the reaction medium (Figure 9.40) [72]. Both *exo* and *endo* isomers were obtained in excellent yields and enantioselectivity. However, the reaction was very slow in the absence of an additive.

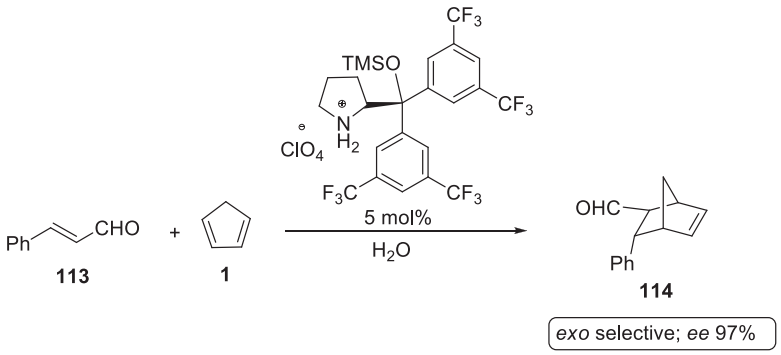

Figure 9.40: Organocatalyzed Diels–Alder reaction by Hayashi et al. [72].

Recently, Ghosh et al. [73] reported a hydroquinine-based primary amine–benzoic acid organocatalyst for enantioselective cycloaddition of enones with nitrodienes in water/other organic solvents and provided easy access to 3,4,5-trisubstituted cyclohexanones (**117**) (Figure 9.41). Water was found to have a promotional effect on the reaction rates and selectivity, that is, diastereoselectivity and enantioselectivity. The diastereomers were formed due to the epimerization at the nitro-bearing center.

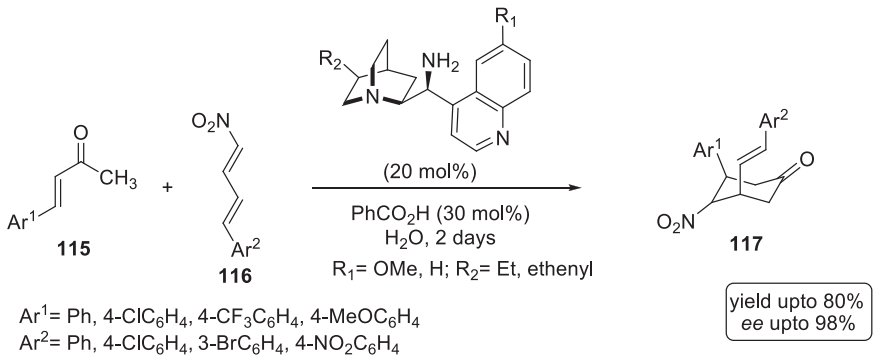

Figure 9.41: Organocatalyzed cycloaddition of enones and nitro dienes in water.

Later, De et al. demonstrated that two-dimensional graphene oxide (GO) is an efficient heterogeneous carbocatalyst for Diels–Alder reaction of 9-hydroxymethylanthracene (**118**) and *N*-substituted maleimides (**119**) in water at room temperature (Figure 9.42) [74]. High yields, easy workup, and catalyst reusability are the main features of this method. Combining experimental and

theoretical studies suggested that π-interactions between reactants and GO surface were responsible for decrease in the activation energy of reaction. Multicomponent reactions have become a synthetic tool which enables access to complex organic systems. Zhu et al. have described a simple and efficient chemoselective five-

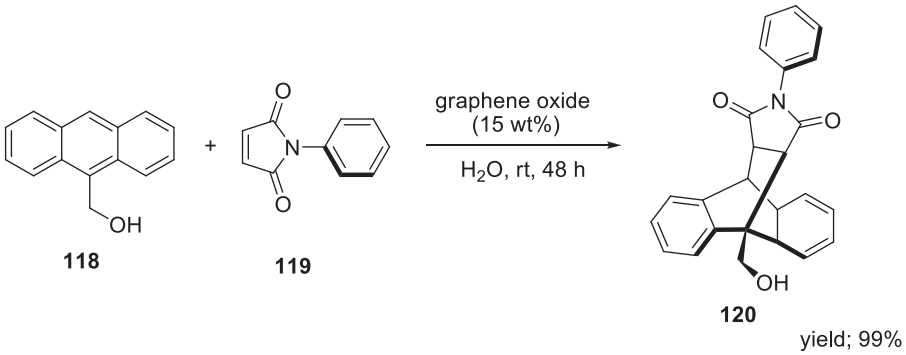

Figure 9.42: Two-dimensional graphene oxide carbocatalyzed Diels–Alder reaction.

component reaction using urea as catalyst in water and produced octahydroquinazoline-5-one derivatives in 60–85% yields (Figure 9.43) [75]. The reaction proceeded smoothly in water as compared with organic solvents.

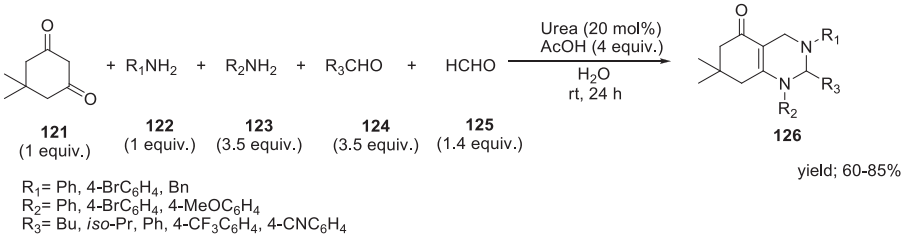

Figure 9.43: Urea-catalyzed five-component reaction in water.

In addition, Chaskar et al. [76] have reported iodoxy benzoic acid (IBX) organocatalyzed Biginelli reaction in aqueous medium (Figure 9.44). They reacted aldehyde, urea/thiourea, and β-keto esters in the presence of IBX in water to obtain 3,4-dihydropyrimidine -2(1*H*)-ones (**130**) in good yields; however, in organic solvents, the reaction was sluggish

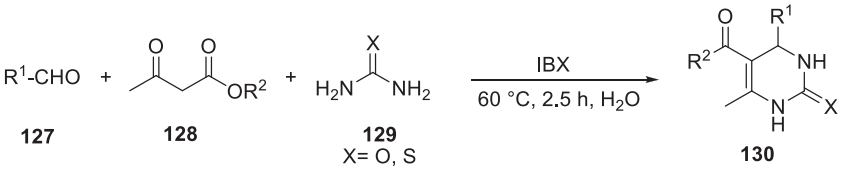

Figure 9.44: IBX-catalyzed synthesis of 3,4-dihydropyrimidine-2-(1*H*)-one in water.

and afforded poor product yields. Mechanistic investigations revealed that the IBX activates the carbonyl group to accelerate the formation of iminium.

9.7 Conclusions and future perspectives

The recent developments in aqueous heterogeneous catalysis changed the notion that water is not a suitable "solvent" for synthetic organic chemistry. Its inappropriate dissolution capabilities are no more a limitation and it has outperformed traditional organic solvents due to its unique properties. It has been established that water is more than just a reaction medium, and can play varying roles in organic reactions to impact reaction outcomes. Water can facilitate air-sensitive transition metal catalysis in open air due to its inherently low solubility of oxygen gas. Traditionally, Grignard, organozinc, and organolithium reagents are considered very sensitive toward water; the recent developments disapproved this parochial thinking. Although the field has made significant progress in the past few decades, the organic synthesis in aqueous medium is still in its infancy and further research is needed to fully understand the role of water. As the interest grows in aqueous heterogeneous catalysis, new and exciting phenomena will emerge which will help in designing new systems for aqueous chemistry in near future.

References

[1] Lindstrom, WM. Organic Reactions in Water: Principles, Strategies and Applications, 1st, Blackwell Publishing: Oxford, 2007.
[2] Sheldon, RA. Green solvents for sustainable organic synthesis: State of the art. Green Chem, 2005, 7, 267–278.
[3] Butler, RN, Coyne, AG. Water: Nature's reaction enforcers comparative effects for organic synthesis "In-Water" and "On-Water". Chem Rev, 2010, 110, 6302–6337.
[4] Breslow, R. Hydrophobic effects on simple organic reactions in water. Acc Chem Res, 1991, 24, 159–164.
[5] Breslow, R. Determining the geometries of transition states by use of antihydrophobic additives in water. Acc Chem Res, 2004, 37, 471–478.
[6] Kitanosono, T, Kobayashi, S. Reactions in water through "On-Water" mechanism. Chem Eur J, 2020, 26, 9408–9429.
[7] Narayan, S, Muldoon, J, Finn, MG, Fokin, VV, Kolb, HC, Sharpless, KB. "On Water": Unique reactivity of organic compounds in aqueous suspension. Angew Chem Int Ed, 2005, 44, 3275–3279.
[8] Chanda, A, Fokin, VV. Organic synthesis "On Water". Chem Rev, 2009, 109, 725–748.
[9] Cortes-Clerget, M, Yu, J, Kincaid, JRA, Walde, P, Gallou, F, Lipshutz, BH. Water as the reaction medium in organic chemistry: From our worst enemy to our best friend. Chem Sci, 2021, 12, 4237–4266.

[10] Rideout, DC, Breslow, R. Hydrophobic acceleration of Diels-Alder reactions. J Am Chem Soc, 1980, 102, 7816–7817.
[11] Li, G, Wang, B, Resasco, DE. Water-mediated heterogeneously catalyzed reactions. ACS Catal, 2020, 10, 2, 1294–1309.
[12] Griesbeck, AG. Fulvene cycloaddition reactions in water: Influence on rate and selectivity. Tetrahedron Lett, 1988, 29, 3477–3480.
[13] Attanasi, OA, De Crescentini, L, Filippone, P, Fringuelli, F, Mantellini, F, Matteucci, M, Piermatti, O, Pizzo, F. Inverse-electron-demand Diels-Alder reactions of (E)-3-diazenylbut-2-enes in water. Helv Chim Acta, 2001, 84, 513–525.
[14] Grieco, PA, Kaufman, MD. Construction of carbocyclic arrays containing nitrogen via intramolecular imino Diels–Alder reactions in polar media. a comparative study: 5.0 M lithium perchlorate–diethyl ether versus water. J Org Chem, 1999, 64, 6041–6048.
[15] Loncaric, C, Manabe, K, Kobayashi, S. AgOTf-catalyzed aza-Diels–Alder reactions of Danishefsky's diene with imines in water. Adv Synth Catal, 2003, 345, 475–477.
[16] Park, S, Ikehata, K, Sugiyama, H. Solid-supported DNA for asymmetric synthesis: A stepping-stone toward practical applications. Biomater Sci, 2013, 1, 1034–1036.
[17] Breugst, M, Reissig, HU. The Huisgen reaction: Milestones of the 1, 3-dipolar cycloaddition. Angew Chem Int Ed, 2020, 59, 12293–12307.
[18] Pandey, PS, Pandey, IK. Hydrophobic effect on 1, 3-dipolar cycloaddition reactions. Tetrahedron Lett, 1997, 41, 7237–7240.
[19] Butler, RN, Coyne, AG, Cunningham, WJ, Burke, LA. Kinetic and synthetic influences of water and solvent-free conditions on 1, 3-dipolar cycloaddition reactions: The phthalazinium and pyridaziniumdicyanomethanide 1, 3-dipoles: Surprisingly successful synthetic methods. J Chem Soc Perkin Trans, 2002, 2, 1807–1815.
[20] Gilchrist, TL, Rees, CW, Thomas, C. Reactive intermediates. Part XXV. Investigation of the pyrolysis of 1, 4-and 1, 5-diphenyl-1, 2, 3-triazoles by use of ^{13}C-labelled compounds. J Chem Soc Perkin Trans, 1975, 1, 8–11.
[21] Portmann, R, WO Patent 9802423, 1998.
[22] Khalili, B, Darabi, FS, Eftekhari-Sis, B, Rimaz, M. Green Chemistry: $ZrOCl_2{\cdot}8H2O$ catalyzed regioselective synthesis of 5-amino-1-aryl-1H-tetrazoles from secondary arylcyanamides in water. Monatsh Chem, 2013, 144, 1569–1572.
[23] Wang, Y-H, Huang, S-H, Lin, T-C, Tsai, F-Y. Rhodium(I)/cationic 2,2′-bipyridyl-catalyzed [2+2+2] cycloaddition of α,ω-diynes with alkynes in water under air. Tetrahedron, 2010, 66, 7136–7141.
[24] Wang, F, Fu, H, Jiang, Y, Zhao, Y. Catalyzed cycloaddition of sulfonyl azides with alkynes to synthesize N-sulfonyltriazoles "on Water" at room temperature. Adv Synth Catal, 2008, 350, 1830–1834.
[25] Ozçubukçu, S, Ozkal, E, Jimeno, C, Pericas, MA. A highly active catalyst for Huisgen 1,3-dipolar cycloadditions based on the tris-(triazolyl) methanol-Cu(I) structure. Org Lett, 2009, 11, 4680–4683.
[26] Sharghi, H, Hosseini-Sarvari, M, Moeini, F, Khalifeh, R, Beni, AS. One-pot, three-component synthesis of 1-(2-hydroxyethyl)-1H–1,2,3-triazole derivatives by copper-catalyzed 1,3-dipolar cycloaddition of 2-azido alcohols and terminal alkynes under mild conditions in water. Helv Chim Acta, 2010, 93, 435–449.
[27] Ali, AA, Chetia, M, Saikia, PJ, Sarma, D. $(DHQD)_2$PHAL ligand-accelerated Cu-catalyzed azide-alkyne cycloaddition reactions in water at room temperature. RSC Adv, 2014, 4, 64388–64392.

[28] Zhou, C, Zhang, J, Liu, P, Xie, J, Dai, B. 2-pyrrolecarbaldiminato-Cu(II) complex catalyzed three-component 1,3-dipolar cycloaddition for 1,4-disubstituted 1,2,3-triazoles synthesis in water at room temperature. RSC Adv, 2015, 5, 6661–6665.
[29] Shin, J-A, Oh, S-J, Lee, H-Y, Lim, Y-G. An efficient Cu-catalyzed azide–alkyne cycloaddition (CuAAC) reaction in aqueous medium with a zwitterionic ligand, betaine. Catal Sci Technol, 2017, 7, 2450–2456.
[30] Wang, Y, Liu, J, Xia, C. Insights into supported copper(II)-catalyzed azide-alkyne cycloaddition in water. Adv Synth Catal, 2011, 353, 1534–1542.
[31] Kambe, N, Iwasaki, T, Terao, J. Pd-catalyzed cross-coupling reactions of alkyl halides. Chem Soc Rev, 2011, 40, 10, 4937–4947.
[32] Torborg, C, Beller, M. Recent applications of palladium-catalyzed coupling reactions in the pharmaceutical, agrochemical, and fine chemical industries. Adv Synth Catal, 2009, 351, 3027–3043.
[33] Han, FS. Transition-metal-catalyzed Suzuki–Miyaura cross-coupling reactions: A remarkable advance from palladium to nickel catalysts. Chem Soc Rev, 2013, 42, 5270–5298.
[34] Thomas, AM, Sujatha, A, Anilkumar, G. Recent advances and perspectives in copper-catalyzed Sonogashira coupling reactions. RSC Adv, 2014, 4, 21688–21698.
[35] Handa, S, Slack, ED, Lipshutz, BH. Nanonickel-catalyzed Suzuki–Miyaura cross-couplings in water. Angew Chem Int Ed, 2015, 127, 12162–12166.
[36] Wu, L, Zhang, X, Tao, Z. A mild and recyclable nano-sized nickel catalyst for the Stille reaction in water. Catal Sci Technol, 2012, 2, 707–710.
[37] Kharisov, BI, Dias, HR, Kharissova, OV. Mini-review: Ferrite nanoparticles in the catalysis. Arab J Chem, 2019, 12, 1234–1246.
[38] Moghaddam, FM, Tavakoli, G, Rezvani, HR. A copper-free Sonogashira reaction using nickel ferrite as catalyst in water. Catal Commun, 2015, 60, 82–87.
[39] Zhong, R, Pöthig, A, Feng, Y, Riener, K, Herrmann, WA, Kühn, FE. Facile-prepared sulfonated water-soluble PEPPSI-Pd-NHC catalysts for aerobic aqueous Suzuki–Miyaura cross-coupling reactions. Green Chem, 2014, 16, 4955–4962.
[40] Uozumi, Y, Matsuura, Y, Arakawa, T, Yamada, YM. Asymmetric Suzuki–Miyaura coupling in water with a chiral palladium catalyst supported on an amphiphilic resin. Angew Chem Int Ed, 2009, 48, 2708–2710.
[41] Lipshutz, BH, Taft, BR. Heck couplings at room temperature in nanometer aqueous micelles. Org Lett, 2008, 10, 1329–1332.
[42] Mitrofanov, AY, Beletskaya, IP. Enhanced catalytic activity of CuI/diethoxyphosphoryl-1, 10-phenanthrolines in 'on water' Cu-catalyzed Sonogashira reaction. Mendeleev Commun, 2019, 29, 378–379.
[43] Liu, Y, Blanchard, V, Danoun, G, Zhang, Z, Tlili, A, Zhang, W, Monnier, F, Van Der Lee, A, Mao, J, Taillefer, M. Copper-Catalyzed Sonogashira Reaction in Water. Chem Select, 2017, 2, 11599–11602.
[44] Tlili, A, Schranck, J, Pospech, J, Neumann, H, Beller, M. Ruthenium-catalyzed carbonylative C-C coupling in water by directed C-H bond activation. Angew Chem Int Ed, 2013, 52, 6293–6297.
[45] Brahmachari, G. Design for carbon–carbon bond forming reactions under ambient conditions. RSC Adv, 2016, 6, 64676–64725.
[46] MingosD, MP, Crabtree, RH. Comprehensive Organometallic Chemistry III, Elsevier, Amsterdam, Boston, 2007.
[47] Zhou, F, Li, C-J. En route to metal-mediated and metal-catalysed reactions in water. Chem Sci, 2019, 10, 34–46.

[48] Perna, FM, Vitale, P, Capriati, V. Synthetic applications of polar organometallic and alkali-metal reagents under air and moisture. Curr Opin Green Sustain Chem, 2021, 100487.
[49] Joaquín, GA, Hevia, E, Capriati, V. The future of polar organometallic chemistry written in bio-based solvents and water. Chem Eur J, 2018, 24, 14854–14863.
[50] Cicco, L, Sblendorio, S, Mansueto, R, Perna, FM, Salomone, A, Florio, S, Capriati, V. Water opens the door to organolithiums and Grignard reagents: Exploring and comparing the reactivity of highly polar organometallic compounds in unconventional reaction media towards the synthesis of tetrahydrofurans. Chem Sci, 2016, 7, 1192–1199.
[51] Elorriaga, D, Rodríguez-Álvarez, MJ, Ríos-Lombardía, N, Morís, F, Soto, AP, González-Sabín, J, Hevia, E, García-Álvarez, J. Combination of organocatalytic oxidation of alcohols and organolithium chemistry (RLi) in aqueous media, at room temperature and under aerobic conditions. Chem Commun, 2020, 56, 8932–8935.
[52] Dilauro, G, Dell'Aera, M, Vitale, P, Capriati, V, Perna, FM. Unprecedented nucleophilic additions of highly polar organometallic compounds to imines and nitriles using water as a non-innocent reaction medium. Angew Chem Int Ed, 2017, 56, 10200–10203.
[53] Quivelli, AF, D'Addato, G, Vitale, P, García-Álvarez, J, Perna, FM, Capriati, V. Expeditious and practical synthesis of tertiary alcohols from esters enabled by highly polarized organometallic compounds under aerobic conditions in Deep Eutectic Solvents or bulk water. Tetrahedron, 2021, 81, 131898.
[54] Bergman, RG. C–H activation. Nature, 2007, 446, 391–393.
[55] Rej, S, Das, A, Chatani, N. Strategic evolution in transition metal-catalyzed directed C–H bond activation and future directions. Coord Chem Rev, 2020, 431, 213683.
[56] Percia, BA, Fischmeister, C, Bruneau, C, Dixneuf, PH. C-H bond functionalization in water catalyzed by carboxylato ruthenium(II) systems. Angew Chem Int Ed, 2010, 49, 6629–6632.
[57] Xu, J, Qiao, L, Shen, J, Chai, K, Shen, C, Zhang, P. Nickel (II)-catalyzed site-selective C–H bond trifluoromethylation of arylamine in water through a coordinating activation strategy. Org Lett, 2017, 19, 5661–5664.
[58] Wang, H, Dou, Y, Ge, J, Chhabra, M, Sun, H, Zhang, P, Zheng, Y, Zhu, Q. Regioselective and direct azidation of anilines via Cu(II)-catalyzed C–H functionalization in water. J Org Chem, 2017, 82, 11212–11217.
[59] Ackermann, L. Pospech, Ruthenium-catalyzed oxidative C–H bond alkenylations in water: Expedient synthesis of annulated lactones. Org Lett, 2011, 13, 4153–4155.
[60] Ali, MA, Yao, X, Li, G, Lu, H. Rhodium-catalyzed selective mono-and diamination of arenes with single directing site "on water". Org Lett, 2016, 18, 1386–1389.
[61] Hikawa, H, Ino, Y, Suzuki, H, Yokoyama, Y. Pd-catalyzed benzylic C–H amidation with benzyl alcohols in water: A strategy to construct quinazolinones. J Org Chem, 2012, 77, 7046–7051.
[62] Lu, X, Shi, Y, Zhong, F. Rhodium-catalyzed intermolecular C(sp^3)–H amination in a purely aqueous system. Green Chem, 2018, 20, 113–117.
[63] Kim, S, Han, S, Park, J, Sharma, S, Mishra, NK, Kwak, JH, Kim, IS. Cp*Rh(III)-catalyzed C(sp^3) –H alkylation of 8-methylquinolines in aqueous media. Chem Commun, 2017, 53, 3006–3009.
[64] Bertelsen, S, Jørgensen, KA. Organocatalysis – after the gold rush. Chem Soc Rev, 2009, 38, 2178–2189.
[65] Enders, D, Niemeier, O, Henseler, A. Organocatalysis by N-heterocyclic carbenes. Chem Rev, 2007, 107, 5606–5655.
[66] van Der Helm, MP, Klemm, B, Eelkema, R. Organocatalysis in aqueous media. Nature Rev Chem, 2019, 3, 491–508.

[67] Takemoto, Y. Recognition and activation by ureas and thioureas: Stereoselective reactions using ureas and thioureas as hydrogen-bonding donors. Org Biomol Chem, 2005, 3, 4299–4306.
[68] Cao, Y-J, Lai, -Y-Y, Wang, X, Li, Y-J, Xiao, W-J. Michael additions in water of ketones to nitroolefins catalyzed by readily tunable and bifunctional pyrrolidine–thiourea organocatalysts. Tetrahedron Lett, 2007, 48, 21–24.
[69] Gruttadauria, F, Lo Meo, M, Riela, P, Noto, S, Giacalone, R. New simple hydrophobic proline derivatives as highly active and stereoselective catalysts for the direct asymmetric Aldol reaction in aqueous medium. Adv Synth Catal, 2008, 350, 2747–2760.
[70] Font, D, Sayalero, S, Bastero, A, Jimeno, M, Pericás, A. Toward an artificial Aldolase. Org Lett, 2008, 10, 340–337.
[71] Guo, W, Wu, B, Zhou, X, Chen, P, Wang, X, Zhou, Y-G, Liu, Y, Li, C. Formal asymmetric catalytic thiolation with a bifunctional catalyst at a water-oil interface: Synthesis of benzyl thiols. Angew Chem Int Ed, 2015, 54, 4522–4526.
[72] Hayashi, Y, Samanta, S, Gotoh, H, Ishikawa, H. Asymmetric Diels–Alder reactions of α,β-unsaturated aldehydes catalyzed by a diarylprolinol silyl ether salt in the presence of water. Angew Chem Int Ed, 2008, 47, 6634–6637.
[73] Vamisetti, GB, Chowdhury, R, Kumar, M, Ghosh, SK. “On Water” organocatalyzed [4 + 2] cycloaddition of enones and nitro dienes for the enantioselective synthesis of densely substituted cyclohexanones. Org Lett, 2016, 18, 1964–1967.
[74] Girish, YR, Pandit, S, Pandit, S, De, M. Graphene oxide as a carbocatalyst for a Diels–Alder reaction in an aqueous medium. Chem Asian J, 2017, 12, 2393–2398.
[75] Zheng, S, Zhong, S, Chen, Z, Chen, W, Zhu, Q. Efficient synthesis of a series of novel octahydroquinazoline-5-ones via a simple on-water urea-catalyzed chemoselective five-component reaction. ACS Comb Sci, 2016, 18475–18481.
[76] Takale, S, Parab, S, Phatangare, K, Pisal, R, Chaskar, A. IBX in aqueous medium: A green protocol for the Biginelli reaction. Catal Sci Technol, 2011, 1, 1128–1132.

Ashu Gupta, Yukti Monga, Radhika Gupta,
Rakesh Kumar Sharma*

10 Design, development, and application of organic–inorganic hybrid nanocatalysts for organic reactions in aqueous medium

10.1 Introduction

Solvents play an indispensable role in every industrial process. In pharmaceutical industries, they are being utilized in every step, from a reaction medium during drug synthesis till its final delivery in the highest purified state and hence account for nearly 80–90% of the total mass utilization [1]. Besides pharma, they are equally fundamental in other significant sectors including food and flavors, materials such as paints, textiles, plastics and also in analytical laboratories. Hence, the overall toxicity profile of any given process relies heavily on choosing the right solvent. Thanks to the green chemists for offering a wide array of solvents which are promising alternatives to conventionally used volatile organic compounds and for making the processes green and sustainable [2]. Among all such alternatives, much emphasis has been given to water. Earlier water was considered as a *no-go* solvent by most organic chemists due to the historic paradigm that *like dissolves like* [3]. In fact, many reaction conditions, catalysts, and reagents demand *ultradry* organic solvents. However, growing needs toward sustainable development stimulated the chemical community to mimic the Mother Nature and explore the possibility of conducting organic reactions in aqueous medium across both academic and industrial fields [4]. Figure 10.1 summarizes few potential incentives of utilizing water as a medium for conducting reactions.

Once the utility of water was explored in organic synthesis, many water-compatible catalysts were developed. Special emphasis was given to heterogeneous catalysts which possess some inherent advantages over their homogeneous counterparts such as facile catalytic recycling using simple centrifugation and filtration techniques [5]. However, limited accessible active sites and propensity toward leaching of catalytic species from the support material decreases the overall activity of the heterogenized system. Hence, to preserve the desirable attributes of both the homogeneous

*Corresponding author: **Rakesh Kumar Sharma,** Green Chemistry Network Centre, Department of Chemistry, University of Delhi, New Delhi, India, e-mail: rksharmagreenchem@hotmail.com
Ashu Gupta, Department of Chemistry, Shyam Lal College, University of Delhi, New Delhi, India
Yukti Monga, Radhika Gupta, Department of Chemistry, Shyam Lal College, University of Delhi, New Delhi, India; Green Chemistry Network Centre, Department of Chemistry, University of Delhi, New Delhi, India

https://doi.org/10.1515/9783110733846-010

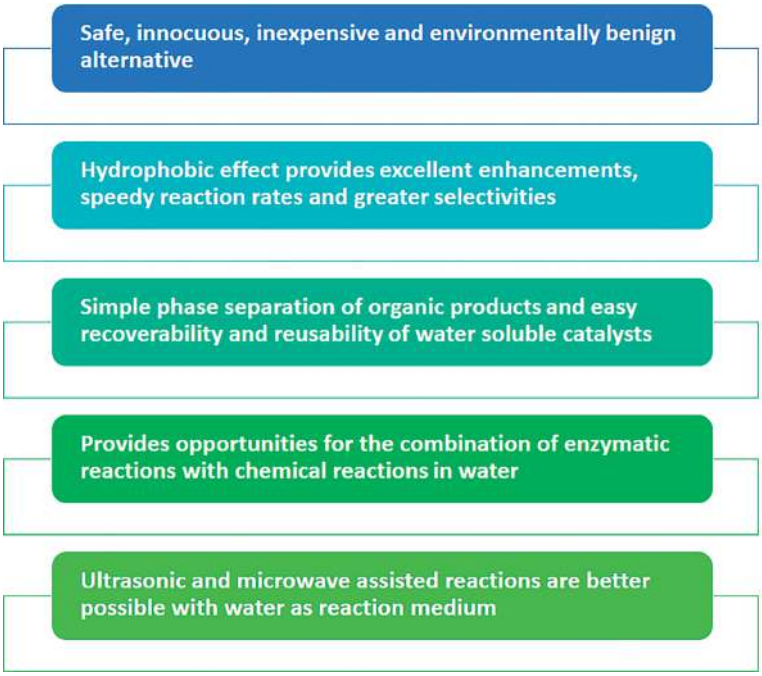

Figure 10.1: Some of the significant advantages of using water as a solvent in organic reactions.

and heterogeneous systems, organic–inorganic hybrid nanocatalysts have been developed. They have emerged as outstanding and sustainable alternatives to classical catalytic systems by acting as a bridge between the two. Numerous support materials have been designed and fabricated which have provided substantial enhancements in terms of catalytic activity, selectivity and loading due to their large surface area-to-volume ratio. Other useful features include enhanced contact between catalytic active sites and reagents, easy catalyst separability, and hence cost-effectiveness.

Owing to the phenomenal properties of organic–inorganic hybrid nanocatalysts, they have been utilized in diversified organic reactions including those in aqueous phase. The present chapter is a selection of some representative examples which provides an overview of design and fabrication of various organic–inorganic hybrid nanocatalysts and their applications in a variety of organic reactions in aqueous medium including coupling, oxidation, reduction, multicomponent, among others.

10.2 Types of organic–inorganic hybrid nanomaterials

Organic–inorganic hybrid nanomaterials represent a class of materials that are composed of inorganic materials (metal ions, metal clusters/nanoparticles, salts, nonmetallic elements/their derivatives, etc.) and organic moieties (molecules, ligands, polymers, biomolecules, etc.) that exhibit superior performance when compared with their individual components [6, 7]. These two entities are bound together by a hierarchy of interactions ranging from covalent bonds, π-complexation to self-assembly interactions such as electrostatic and H-bonding. Some of the most extensively used heterogenization approaches include covalent binding (attachment of catalytic species onto solid support via covalently anchored functional groups), adsorption (wherein catalytic species are adsorbed onto the surface of support via physisorption), and entrapment (in which catalytically active species is entrapped inside the cage-like pores of porous materials) (Figure 10.2) [8]. Among all, covalent anchoring is the superior because it minimizes the possibility of leaching problem. The benefits of such advanced hybrid nanoarchitectures are quite enormous as they result in the synergistic enhancement of functional properties of their individual constituents. They are powerful mimics of natural structures, very much tunable at the atomic level, extremely modifiable in terms of variety of building blocks, and provide scope for diverse methodologies by which they can be synthesized. This opens a plethora of opportunities for ensuring dynamic activity and selectivity toward particular reactants in organic reactions. Mentioned below are some widely used organic–inorganic hybrid nanosystems that have been developed for organic transformations.

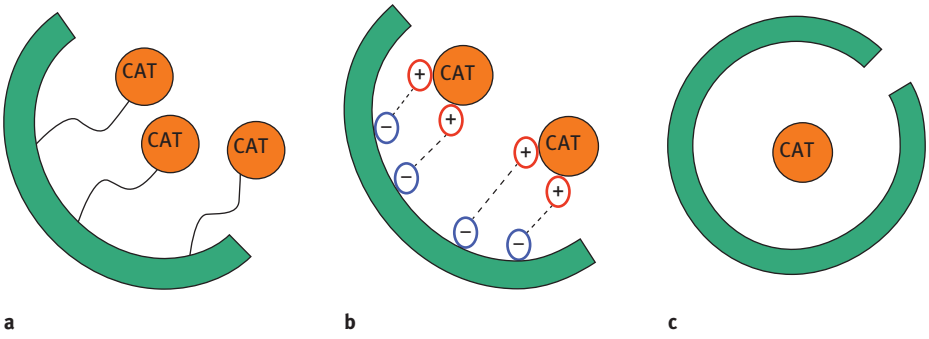

Figure 10.2: Most commonly used anchoring methodologies (a) covalent binding, (b) adsorption, and (c) entrapment. Obtained with permissions from ref. [8].

10.2.1 Silica nanosphere-based organic–inorganic hybrid nanomaterials

Silica (SiO_2) is one of the most plenteous materials found on earth which usually occur either in crystalline or amorphous form. It has a three-dimensional network structure containing [SiO_4] units which terminate at the surface through siloxane (≡Si–O–Si≡) or silanol (≡Si–OH) groups. Since past few decades, silica-based nanomaterials have garnered considerable attention, specially by chemists working in the domain of catalyst fabrication and organic synthesis [9]. This is attributed to the exceptionally favorable features which silica nanomaterials offer (Figure 10.3a).

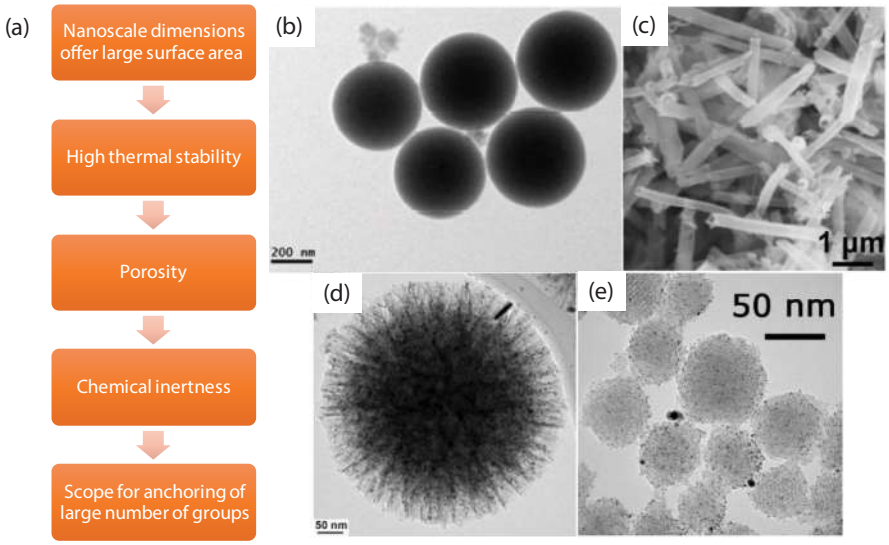

Figure 10.3: (a) Advantages offered by silica-nanomaterials when used as catalytic support and TEM images of (b) silica nanospheres supported palladium catalyst, (c) palladium anchored silica nanotubes, (d) KCC-1 supported palladium nanoparticles, and (e) MCM-41 supported gold nanoparticles. Obtained with permissions from ref. [10–13].

Hence, numerous nanostructured configurations have been developed to utilize them as catalytic support materials. For instance, Sharma et al. [10] synthesized silica nanospheres-supported palladium catalyst by immobilization of a palladium complex onto furfural modified and 3-aminopropyltriethoxysilane (APTES) functionalized silica nanospheres. Similarly, Liu et al. anchored palladium nanoparticles on amine functionalized silica nanotubes [11]. Other groups exploited the high surface area of fibrous nanosilica (KCC-1) to support palladium nanoparticles [12] and mesoporous silica (MCM-41) to support gold nanoparticles (Figure 3b–3e) [13].

10.2.2 Fe_3O_4 (iron oxide)-supported organic–inorganic hybrid nanomaterials

In recent years, magnetic nanoparticles (MNPs), especially Fe_3O_4, supported catalytic systems have been extensively utilized by the catalytic fraternity as a phenomenal support for the immobilization of homogeneous catalytic moieties [14, 15]. They possess several admirable characteristics such as high surface area to volume ratio, easy to control size and morphology, chemical inertness, excellent thermal stability, and ease of accessibility. Additionally, they provide outstanding magnetic separability which saves time and energy required during classical separation procedures by filtration and centrifugation (Figure 10.4) [16]. This also prevents unnecessary loss of catalyst during catalyst separation. However, these MNPs have an intrinsic tendency toward aggregation due to strong magnetic interactions. Also, if not kept under inert environments, these MNPs can be oxidized in atmospheric conditions which may lead to alterations in magnetic properties. Hence, a variety of protecting agents have been coated over these MNPs such as polymers [17], carbon [18], inert metals [19], silica [20], and many others. These protected MNPs can be further modified using suitable functional groups on which catalytic species can be easily anchored. All of the abovementioned features attribute toward clean and sustainable heterogeneous organic synthesis by virtue of which several kinds of catalytically active species such as metal complexes [21], metal nanoparticles [22], acidic/basic entities [23], ionic liquids [24, 25], and many others have been efficiently supported.

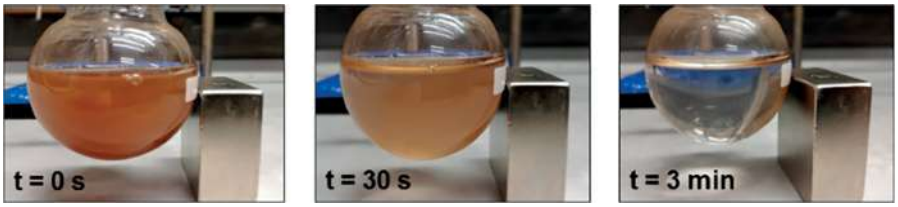

Figure 10.4: Facile magnetic separation of silica-coated magnetic nanoparticles supported ionic liquid catalyst after an organic transformation using simple external magnetic forces. Obtained with permissions from ref. [16].

10.2.3 Nanometal-organic frameworks

Lately, metal-organic frameworks (MOFs) have emerged as a unique type of catalysts with several fascinating features such as high surface area, structural diversity and tailorability [26–28]. They represent a new class of crystalline porous organic–inorganic hybrid materials. They are formed by self-assembly of inorganic metal ions/clusters and organic linkers, mostly based on carboxylates, N-donor groups, and

phosphonates. Although the porosity of MOFs is highly profitable for catalysis, the accessibility of active sites and mass transfers remain challenging and thus offers a room for improvement. The above issue becomes more questionable when large substrates are involved which face difficulty in diffusing toward the internal catalytic sites. In this regard, nano-MOFs have been designed and developed to decrease the diffusion length in comparison to its bulk partner and thus to improve the catalytic performance [29, 30]. For instance, Qi and co-workers synthesized nanosized $[Cu_3(BTC)_2]$ MOF[BTC = 1,3,5-benzenetricarboxylate], by employing different mediators that strongly influenced the sizes and morphologies [31]. Figure 10.5 depicts the SEM images of two nanosized MOFs; Cu-MOF-1 and Cu-MOF-2 of 90 nm diameter with spherical nanomorphology and 400 nm with octahedral morphology, respectively. However, in the absence of any mediator, the size of the obtained $[Cu_3(BTC)_2]$ was several μm.

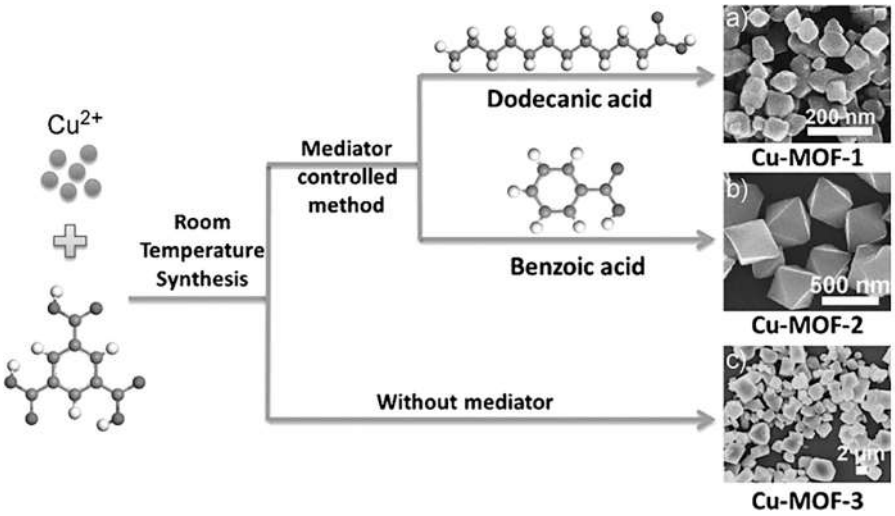

Figure 10.5: Synthesis of different nanosized $[Cu_3(BTC)_2]$ MOFs. Obtained with permissions from ref. 31.

The nano-MOFs have also been explored as efficient hosts for active catalytic species [32]. Recently, Yang et al. fabricated Pd nanocubes@ZIF-8 [ZIF (zeolitic imidazolate framework) is an MOF made by coordinating four imidazolate rings with zinc ions] by encapsulation of Pd nanocubes in ZIF-8 for the efficient and selective catalytic hydrogenation of olefins under light irradiation (Figure 10.6) [33].

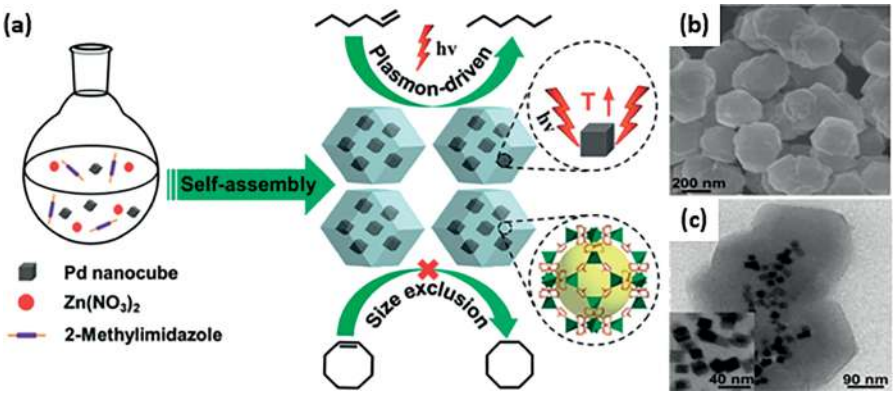

Figure 10.6: (a) Synthesis, (b) SEM, and (c) TEM image of Pd nanocubes@ZIF-8. Obtained with permissions from ref. 33.

10.2.4 Carbon-based organic–inorganic hybrid nanomaterials

Over the past few decades, carbon-based nanomaterials, especially carbon nanotubes (CNT), carbon nanofibers (CNF), and graphene oxide nanosheets (GON) have been extensively studied in various catalytic organic transformations. They possess several remarkable properties: carbon is a light element, in tubular form it is found to be the strongest material synthesized till date, variable thermal conductivity, highly functionalizable surface, to name a few [34, 35]. Figure 10.7a depicts the synthetic methodology for the formation of polyallylamine-functionalized Rh nanosheet assemblies-CNT (PAH@Rh-NSNSs/CNT) nanohybrids using polyallylamine hydrochloride (PAH) as a complexant and morphology directing, linker, and chemical functionalization agent [36]. The CNTs are defined as seamless cylinders of rolled up graphene sheets of carbon atoms. In addition to CNTs, GON offers some impressive structural benefits such as high thermal and chemical stability, high specific surface area, and porosity. Figure 10.7b exemplifies how GON are formed using graphite powder [37]. Recently, Sharma et al. synthesized GONs based cobalt nanocatalytic system (Co@BA@APTES@GO) for ester-amide exchange reaction (Figure 10.7c) [38]. Other emerging carbon material include CNFs which are described as cylindrical nanostructures with graphene layers arranged as stacked cones, cups, or plates. Figure 10.7d illustrates the TEM image of electrospun Co-CNF nanocatalyst which has been synthesized by carbonization of cobalt containing polyacrylonitrile nanofibers, a precursor of carbon nanofibers [39]. All of these offer immense opportunities to be utilized as excellent nanocatalyst materials for industrial scale organic transformations.

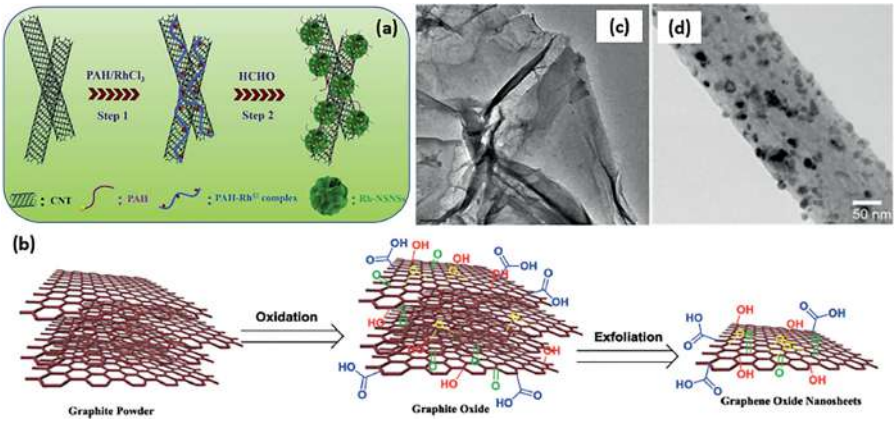

Figure 10.7: Illustration of various carbon-based nanocatalysts. Synthesis of (a) PAH@Rh-NSNSs/CNT nanohybrid and (b) GON. TEM images of (c) Co@BA@APTES@GO and (d) electrospun Co–carbon nanofiber. Obtained with permissions from ref. [36–39].

10.3 Applications of organic–inorganic hybrid nanocatalysts for organic reactions in aqueous medium

In the present scenario, green chemistry is the utmost need for a sustainable society. Principles of green chemistry also demands use of catalysts along with safer solvents and auxiliaries. Heterogeneous catalysis using water as a solvent is considered as a highly green and sustainable approach to reduce the environmental factor (E-factor) value for a reaction. In the above sections, numerous organic–inorganic hybrid nanomaterials have been discussed thoroughly. Mentioned below are some of the examples where these nanomaterials have been utilized in various important catalytic applications, typically in aqueous media because of its low cost and toxicity, ready availability, and above all its environmentally benign nature.

10.3.1 Silica nanospheres catalyzed reactions

The remarkable properties of silica nanospheres have led to their wide applicability in a variety of organic reactions. Coupling reactions are one of the most extensively explored categories. These reactions help to make industrially important moieties in a facile manner with the aid of a catalyst. Hence, designing of a suitable catalyst becomes highly important. It should be green, recoverable, and reusable. With this objective, He et al. developed a heterogeneous silica based Pd(II) organometallic

catalyst for water-mediated C–C coupling reactions including Barbier, Sonogashira, and Ullmann reactions [40]. The catalyst was made by coordinating Pd(II) ions to PPh_2-functionalized silica nanospheres containing an ordered mesoporous structure (MSN). Efficacy of the nanocatalyst was also compared with homogeneous catalyst Pd-$(PPh_3)_2Cl_2$. The results were found to be comparable with the traditional catalyst in terms of activity and selectivity. It could be attributed to high surface area, ordered mesoporous structure, and short pore channels, which facilitated the diffusion and adsorption of reactant molecules. Also, it could be used repeatedly, showing good potential for industrial applications.

Mondal et al. [41] also followed this sustainable practice by synthesizing the biaryl products using a MSN-supported Pd(II) 2-aminopyridine (AMP) complex in water as a solvent. The catalyst was prepared in situ by the cocondensation reaction between TEOS and [(chloromethyl)-phenylethyl]trimethoxysilane using cetyltrimethylammonium bromide as the structure-directing agent (Figure 10.8). The efficacy of the catalyst (Pd-AMP-MSN catalyst) was tested for various aromatic and heterocyclic halides (Figure 10.9). It is important to mention here that both electron-donating and electron-withdrawing substituents gave corresponding biphenyls in good to excellent yields under the optimized reaction conditions. The catalyst also reported to have excellent stability and reusability.

Following the similar trend of reactions in green solvent, Zhu et al. reported amine bridged periodic mesoporous organosilica catalyst (NH-PMO-NS) which was further used for Knoevenagel condensation in aqueous reaction medium (Figures 10.10 and 10.11) [42]. The formation of the catalyst was performed using surfactant supported amine-bridged silane and tetraethyl orthosilicate via condensation process, which is attributed to the presence of ample amine groups attached over short and straight mesoporous channels in silica nanospheres. Further, the ability of the catalyst was also tested in comparison to the homogeneous base catalyst (diethylamine) and the results were quite encouraging. Besides, the reported silica-based catalyst could be recycled and reused repetitively and easily. These basic catalytic sites are active, accessible, and facilitate diffusion, which ultimately encouraged the adsorption of organic reactants and led to enhanced activity and selectivity.

Another group designed a porous nanoweb catalyst by incorporating Co(II) ions onto modified silica NPs for decolorizing methylene blue dye in aqueous conditions [43]. For the fabrication, amine functionalized silica NPs were reacted with 2-acetylpyridine followed by addition of Co(II) ions (Si@NPCo). These NPs were further reacted with 1,3,5-benzenetricarboxylic acid forming the nanomaterials with hole nanoweb structure (SiO_2@NPCoCOOH) (Figure 10.12). The so-formed nanocatalyst was used for the oxidation-assisted degradation of methylene blue using water as a solvent and as an oxygen source under white LED light irradiation for 2 h. The results illustrate that the two methylene blue absorption peaks near 615 nm and 665 nm are diminished to nearly 30%, indicating that the catalyst has enough potential toward water remediation as well. It was reported that the hydroxyl radicals were generated during the reaction which were responsible for the degradation of the dye.

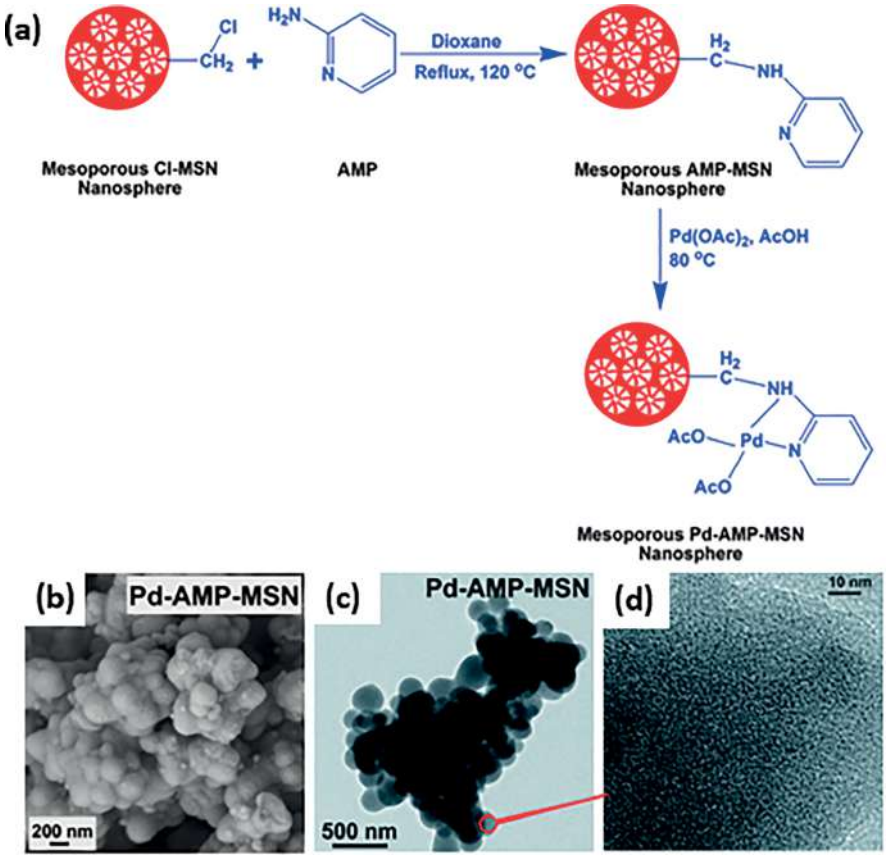

Figure 10.8: (a) Systematic formation, (b) FESEM, and (c)–(d) TEM image of Pd-AMP-MSN catalyst. Obtained with permissions from ref. 41.

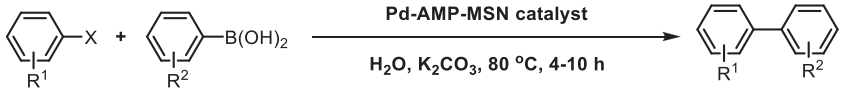

Figure 10.9: Suzuki–Miyaura coupling reaction in water medium catalyzed by Pd(II)-AMP-MSN catalyst.

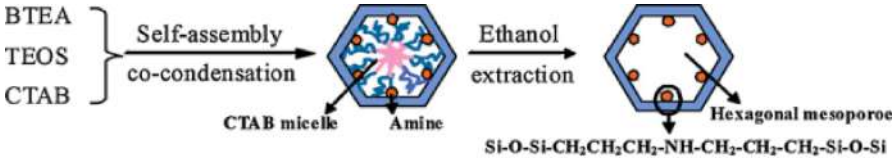

Figure 10.10: Showing the preparation of NH-PMO-NS by cocondensation method. Obtained with permissions from ref. 42.

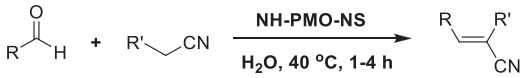

Figure 10.11: NH-PMO-NS catalyzed Knoevenagel reaction.

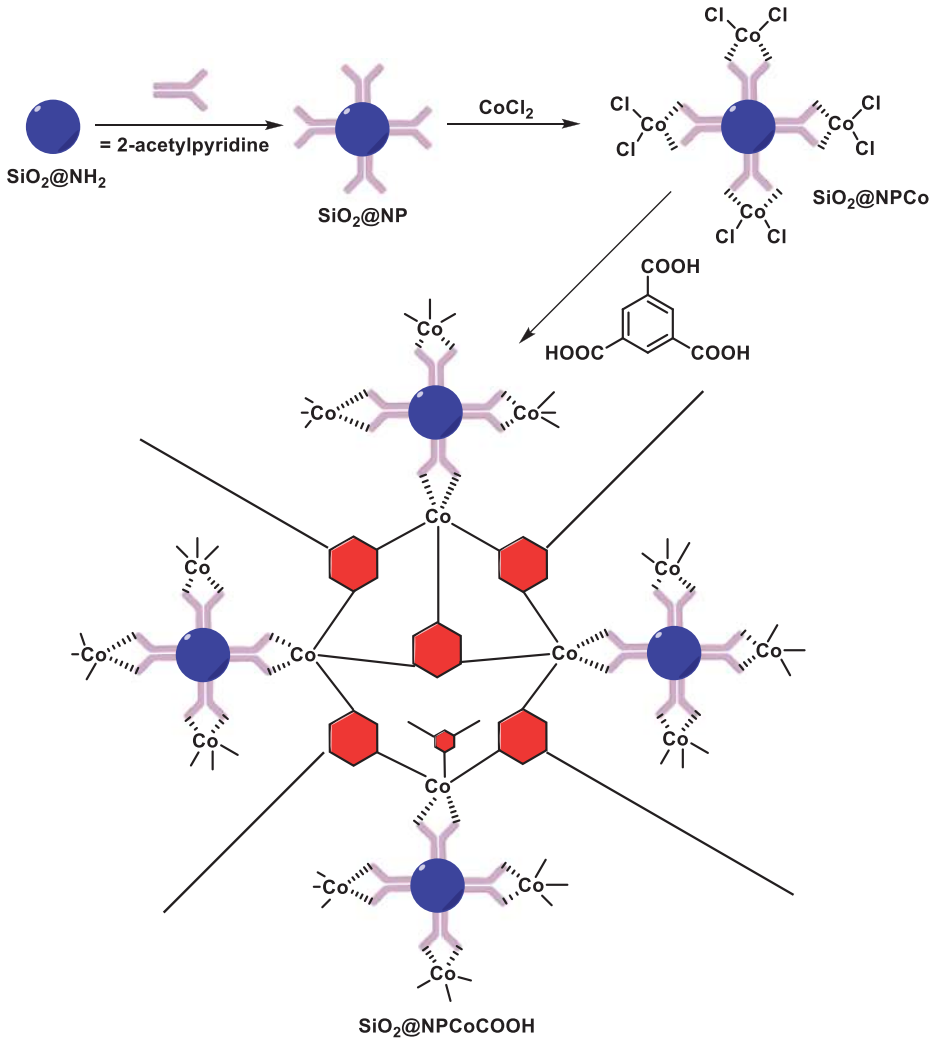

Figure 10.12: Fabrication of SiO_2@NPCoCOOH.

10.3.2 Fe_3O_4 (iron oxide)-based nanocatalyzed reactions

Among all kinds of organic–inorganic hybrid nanocatalysts, iron oxide supported catalytic systems have been widely explored and utilized [44]. It is due to the facile magnetic recovery that such kind of catalysts offer distinct advantage. They have been developed for nearly every kind of organic transformations ranging from coupling, oxidation, reduction, and multicomponent. In recent times, considering the biological importance of 3,3-di(indolyl)indolin-2-ones, Sharma and co-workers designed silica-protected magnetite nanoparticles supported DABCO-derived and acid-functionalized ionic liquid (DABCO-3@FSMNPs) [20]. The pseudo-three-component reaction was performed using indoles and isatins as reactants under aqueous medium using mild conditions. A variety of 3,3-di-(indolyl)indolin-2-ones were obtained in excellent yields under short reaction times (Figure 10.13). Besides, reported catalyst was magnetically recovered and again used for successive runs without appreciable loss in catalytic activity. The hybrid catalyst offered many additional advantages by anchoring viscous ionic liquids over magnetic support which not only helped in easy substrate diffusion but also made the reaction pathway more economical because of facile and efficient recovery of expensive ionic liquids.

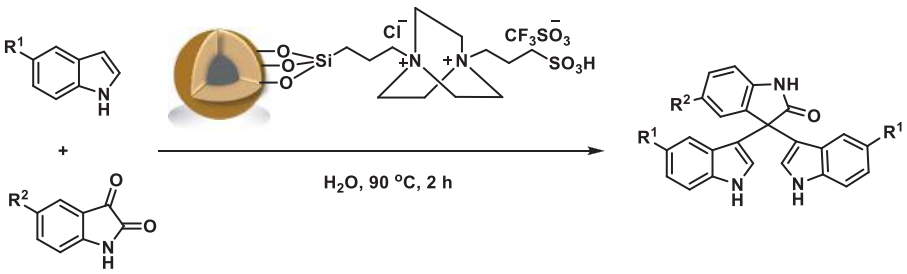

Figure 10.13: Synthesis of 3,3-di(indolyl)indolin-2-ones using DABCO-3@FSMNPs in aqueous medium.

Magnetic nanocatalysts have been widely explored in several coupling reactions. As an example, herein a heterogeneous magnetite-supported biguanide/$Pd(OAc)_2$ catalyst used for the Suzuki reaction in presence of water as media has been described [45]. The attachment of Pd(II) ions on magnetite support was performed by surface modification of MNPs with biguanide. The magnetic supported biguanide/$Pd(OAc)_2$ nanocatalyst (size ~ 40–45 nm confirmed using TEM) showed excellent catalytic activity for the abovementioned reaction in aqueous media. The reported catalyst was easily separated magnetically and could be recycled for many runs (Figure 10.14).

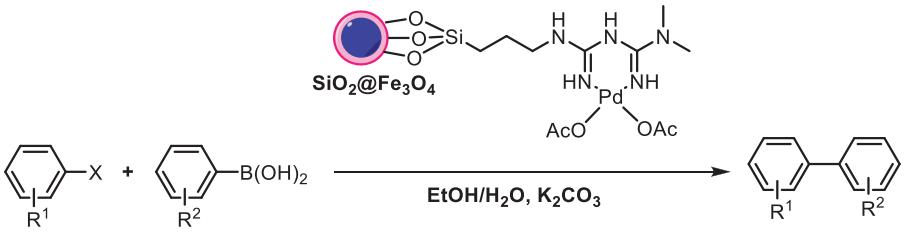

Figure 10.14: Magnetite-supported biguanide/$Pd(OAc)_2$ catalyzed Suzuki reaction in aqueous medium.

The previously mentioned research group designed another kind of environmentally benign nanocatalyst, this time a magnetically recoverable metal loaded nanoreactor for C–S coupling reaction(Figure 10.15) [46]. They fabricated a double shelled hollow nanoreactor using a template-free approach; inner Fe_3O_4 shell that imparts magnetic character and outer carbon shell that offers ample sites for metal decoration. The inner space of the material also contains large catalytic sites and provides space for conduction of the organic reaction. The reaction substrates can easily penetrate the cavity using porous double shells. They immobilized Ni(II) species and utilized the so-formed hybrid nanocatalyst in the oxidative coupling of aromatic thiols with arylhydrazines to form unsymmetrical diaryl sulfides using water as a green reaction medium. Some salient features of the work include oxidant- and ligand-free conditions, room temperature synthesis and formation of non-toxic by-products (nitrogen and water) (Figure 10.16). Wide-ranging functional groups were tested, applied, and provided the corresponding diaryl sulfide products in good to excellent yields. Besides, catalyst showed excellent reusability for consecutive seven runs, which made the protocol highly suitable from green chemistry viewpoints.

In order to develop other efficient nanocatalytic systems to promote organic reactions in aqueous media, Yeo et al. fabricated a core-satellite Fe_3O_4-Pd nanocomposite heterostructure for catalyzing decarboxylative coupling reaction using water as reaction media [47]. Figure 10.17 illustrates the synthetic approach for the formation of the nanocomposite. Initially, oleic acid stabilized Fe_3O_4 nanoparticles were prepared, followed by surface coating with pluronic copolymer (P123, PEO_{19}-PPO_{69}-PEO_{19}). Thereafter, Na_2PdCl_4 was added to introduce Pd nanoparticles. Surface coating with pluronic polymer provided better water dispersity to the MNPs and allowed the development of Pd nanoparticles at the surface only. In this, it also mentioned that pluronic copolymer stabilized nanoparticles surface act as nanoreactors to induce the solubilization of organic reactants and allowed the reactants to relate more closely to the Pd nanoparticles. The activity and selectivity of prepared Fe_3O_4-Pd MNPs were then tested for the decarboxylative coupling reaction of allyl alkynoate in presence of aqueous media (Table 10.1).

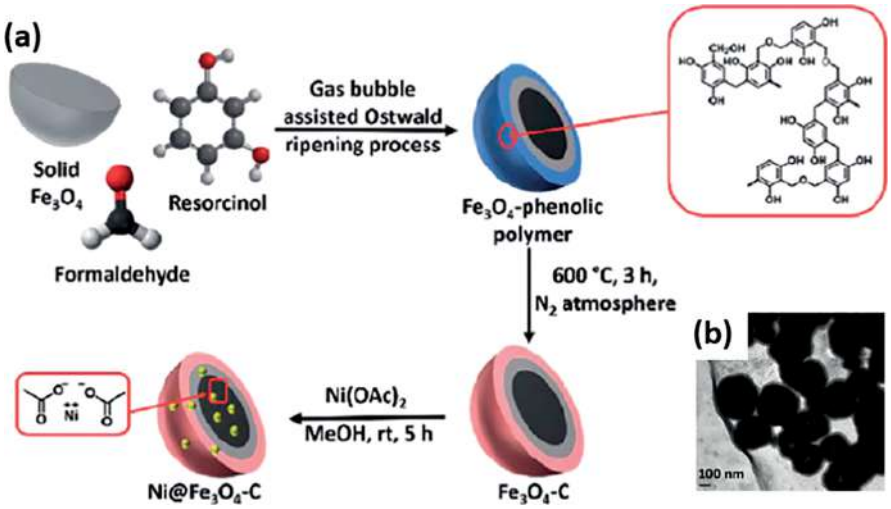

Figure 10.15: (a) Synthetic protocol and (b) TEM image of Ni-loaded double shelled nanoreactor. Obtained with permissions from ref. 46.

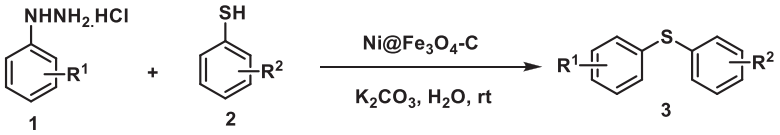

Figure 10.16: Synthesis of unsymmetrical diaryl sulfides using Ni-loaded double shelled nanoreactor.

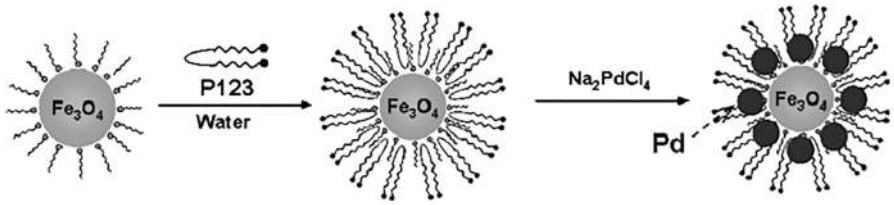

Figure 10.17: Synthesis of Fe_3O_4-Pd nanocomposite. Obtained with permissions from ref. 47.

Other type of organic reactions that performed significant role for the preparation of significant compounds are through oxidation reactions. Rajabi et al. [48] presented iron oxide nanoparticles supported over mesoporous silica which was used as catalyst for the oxidation of alkenes using hydrogen peroxide in aqueous medium. Styrene and its other substituted derivatives were efficaciously transformed to the respective aldehydes in excellent yields. Also, the formation of by-products and subsequent oxidations of aldehydes was absent in the reaction. The described procedure was found to

Table 10.1: Showing the results for catalytic decarboxylative coupling reaction of allyl alkynoate. Obtained with permissions from ref. 47.

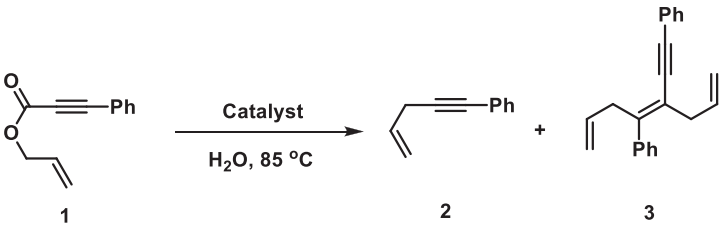

1 2 3

Entry	Catalyst	T (oC)	t (h)	Isolated Yield (%)[a]
1	5 mol% Fe_3O_4–Pd	85	2	25(**3**) (70)[b]
2	5 mol% Fe_3O_4–Pd	85	12	95(**3**)
3	Recovered from entry 2	85	12	88(**3**)
4	5 mol% Pd/C	85	12	20(4(**2**):1(**3**))[c]
5	5 mol% $Pd(PPh_3)_4$	85	6	92(4(**2**):1(**3**))[c]

[a]Isolated yield.
[b]Yield in parenthesis mentioned for recovered reactant.
[c]The ratio calculated by ^{1}H NMR.

be suitable for an array of different types of substituents (both electron donating and electron withdrawing) present at different positions of the aromatic ring. Other group, Karimi and Farhangi [49] developed a nitroxyl radical 2,2,6,6-tetramethylpiperidine-1-oxyl (TEMPO) anchored catalytic system for an aerobic oxidation of 1° and 2° alcohols in the absence of any transition metal and halide cocatalyst. In the reaction, molecular oxygen was utilized as an oxidant in the presence of non-halogenated and aqueous conditions. Magnetite-supported TEMPO nanocatalyst worked well for range of alcohols (1°, 2°, air sensitive, and sterically hindered alcohols) and changed to the desired carbonyl product with the outstanding results (Figure 10.18). The methodology offered effective retrieval of expensive TEMPO which is highly required for making it a successful candidate in many practical applications as well.

Another group reported multistep synthesis for MNPs-supported (*S*)-diphenyl prolinol trimethyl silylether (MNP-JHC), an asymmetric organocatalyst and also named as Jørgensen–Hayashi catalyst or α,α-diarylprolinol ethers based catalysts [50]. Asymmetric Michael addition reaction was performed using above-mentioned catalyst. Different enolizable aldehydes were used as reactants in water to give chiral products (Figure 10.19). Although other solvents such as acetonitrile, toluene, dichloromethane, chloroform and ethanol, were also screened during optimizations it was the aqueous conditions under which highest yield and enantiomeric excess was obtained. Hence, under the tested and improved conditions, 13 different reactants were used to

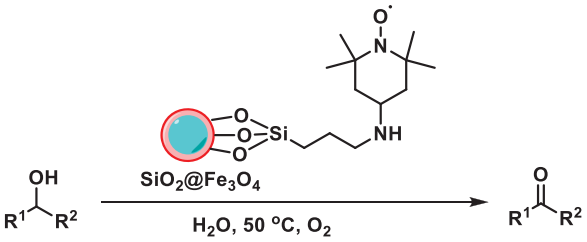

Figure 10.18: Magnetite-supported TEMPO catalyzed aerobic oxidation of alcohols.

obtain their corresponding products with moderate to excellent yields (up to 96%) as well as with good enantioselectivity (up to 90% *ee*). After the reaction, the catalyst was separated and reused for four times without losing stereoselectivity.

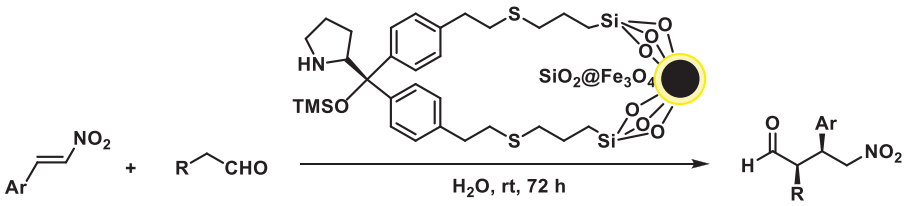

Figure 10.19: Asymmetric Michael addition of aldehydes to nitroalkenes in aqueous media using MNP-JHC.

10.3.3 Nanometal-organic frameworks-based catalyzed reactions

As described previously, nano-MOFs represent an exclusive class of solids with excellent catalytic, mass transport, and adsorption properties. Recently, Iqbal et al. developed a simple and innovative technique through in-situ self-assembly and solvothermal method for synthesizing hybrid Cu-NMOF/Ce-doped-Mg-Al-LDH nanocatalyst by supporting 2D Cu-NMOF, $[Cu_2(\mu\text{-OH})(\mu_4\text{-btc})(phen)_2]_n \cdot 5nH_2O$ on a cerium-doped Mg–Al layered double hydroxide (Ce-doped-Mg–Al–LDH) matrix [51]. The synthesized Cu-NMOF nanocrystals (10–20 nm) were attached on Ce-doped-Mg–Al–LDH's surface (100 cm nanosurface). The catalytic activity of above-mentioned catalyst in contrast to simple Cu-NMOF was also evaluated for reductive degradation of 4-nitrophenol (4-NP) and a series of organic dyes by using sodium borohydride as a reducing agent. The prepared nanocatalyst showed brilliant results in terms of catalytic activity toward degradation of 4-NP with 0.03 rate constant and up to $7.1 \times 103\ h^{-1}$ turnover frequency. A variety of other commonly used organic dyes were also decolorized with high TOF values. The reason for superior catalytic activity of hybrid catalyst over simple Cu–NMOF was also mentioned, it

is due to the synergic effect among Cu-NMOF and Ce-doped-Mg–Al–LDH components, while the Ce-doped-Mg–Al–LDH carrier acting as a co-catalyst. The prepared nanocatalyst was recovered and reused successfully for the five consecutive reaction runs without compromising the performance. Figure 10.20 depicts the UV-vis spectra of the reaction mixture for the reduction of 4-NP to 4-aminophenol using hybrid nanocatalyst.

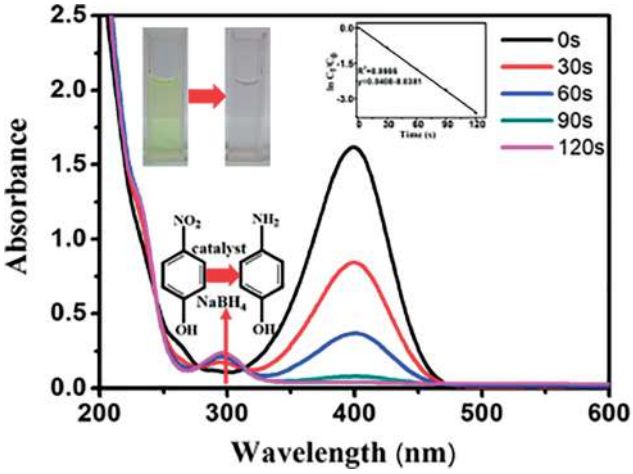

Figure 10.20: UV-vis absorption spectra of the reaction mixture at different time intervals catalyzed by Cu-NMOF/Ce-doped-MgAl-LDH. Inset: plot of $\ln(C_t/C_o)$ versus reaction time. Obtained with permissions from ref. 51.

10.3.4 Carbon-based nanocatalyst in organic reactions

Amongst various carbon-based nanomaterials, metal decorated GONs have been largely utilized in heterogeneous catalysis. Bahuguna et al. used GONs supported zinc oxide nanoparticles (ZnO-RGO) which was synthesized using hydrothermal method (Figure 10.21). The prepared ZnO-RGO catalyst was used for synthesis of symmetrical bisindolemethanes using green reaction medium, that is, water [52]. The ability of prepared nanocomposite was also tested for synthesis of three substituted derivatives of indole with chalcone. Only water or water–ethanol mixture was used as a solvent. Later, the same group also developed, another heterogeneous molybdenum based MoS_2-RGO nanocatalyst for the synthesis of both symmetrical and unsymmetrical bisindolemethane compounds under sustainable reaction conditions [53]. The developed MoS_2-RGO nanocomposite was also used for the synthesis of ketone derived bisindolemethanes. Green chemistry-based matrices calculations were also mentioned for such reactions. Results showed high atom economy (A.E. = 94.7%) and small E-factor (0.089). Industrial efficiency of the above-mentioned nanocomposite

was also reported and evaluated by performing two-gram scale reactions for the synthesis of vibrindole A and arundine (indole alkaloids). The synthesis of various bisindole methanes using MoS_2-RGO is presented in Figure 10.22.

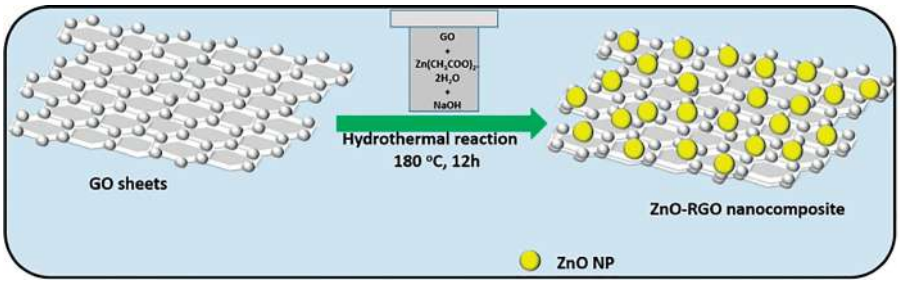

Figure 10.21: Synthesis of ZnO-RGO nanocomposite. Obtained with permissions from ref. 52.

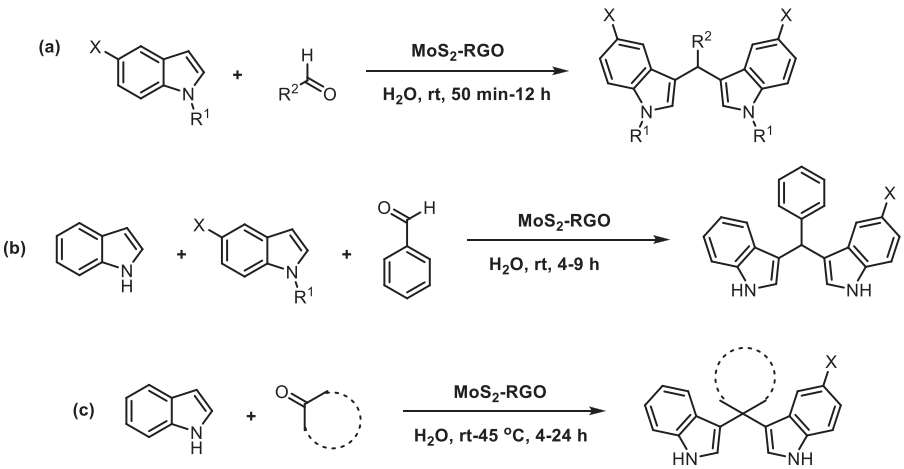

Figure 10.22: MoS_2-RGO catalyzed synthesis of (a) symmetrical bisindolemethanes, (b) unsymmetrical bisindolemethanes, and (c) ketone-derived bisindolemethanes.

Recently, such reduced GON were also used by Patil et al. [54] for the on-water aerobic oxidation of alcohols using supramolecule-based ruthenium catalyst. Ruthenium nanoparticles were supported on cyclodextrin-modified graphene oxides (rGO@Ru-RMβ-CD) by simultaneous one-pot reduction of ruthenium precursor and graphite oxide in aqueous medium. The RMβ-CD was reported to be used as capping agent, which controlled the growth of ruthenium nanoparticles. After this, the Ru NPs inserted between the graphene oxide layers, which functionalizes the surface of reduced graphene oxide through hydrogen bonding. Hence, RMβ-CD acted as a

phase transfer catalyst in water medium. The authors also mentioned the good selectivity for a wide range of substrates and even with sensitive functionalities. Not only this, but authors also efficaciously used the catalyst for total synthesis of a natural product "Brittonin A"using Wittig olefination and reduction in aqueous solvent (Figure 10.23). This work offered exceptional capability of the catalyst to switch between oxidation and reduction tendencies by simply exchanging the oxygen and hydrogen atmospheres.

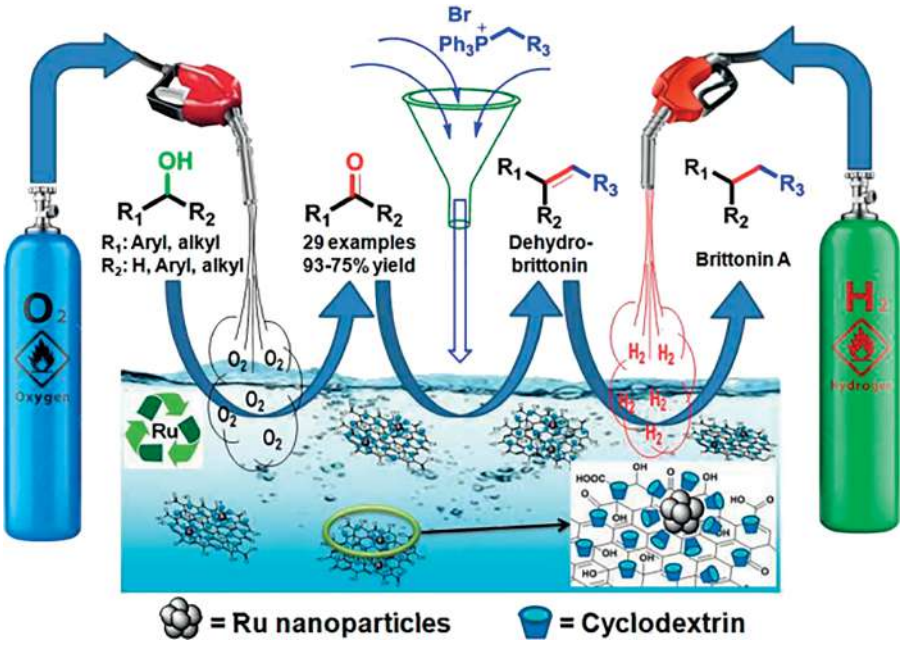

Figure 10.23: Catalytic activity of rGO@Ru-RMβ-CD in oxidation of alcohols and its further conversion into Brittonin A. Obtained with permissions from ref. 54.

10.4 Conclusion and future perspectives

Green chemistry has reformulated the definition of catalysis in many aspects. This is the one of the important reasons for the paradigm shift of the technology toward cleaner manufacturing process development. Water has emerged as powerful medium for various chemical transformations. In this chapter, we have included a variety of literature reports where water as reaction medium has shown distinct advantages. It has also worked well with different organic–inorganic hybrid nanocatalytic systems which constitute a new and advanced class of materials. This green combination of catalysts with water has provided numerous economic and

environmental benefits. This chapter highlighted and discussed the synthesis, catalytic performance, and other salient features of various supported catalysts such as silica nanospheres based magnetic supported, nano-MOF and reduced graphene oxide. Besides, they have also shown exceptional stability, recoverability, and reusability even for consecutive runs without affecting in catalytic performances. Therefore, the chapter opens large opportunities for their industrial scale utilization and represents an important step toward the sustainable advancement of chemical protocols.

References

[1] Constable, DJC, Jimenez-Gonzalez, C, Henderson, RK. Perspective on Solvent Use in the Pharmaceutical Industry. Org Process Res Dev, 2007, 11, 1, 133–137.
[2] Radhika Gupta, RJ, Sharma, RK. Alternative Reaction Media. In: Green Chemistry for Beginners: With a Foreword by Paul Anastas, Rakesh, K, Sharma, AS Ed. Jenny Stanford Publishing: New York, 2021.
[3] Cortes-Clerget, M, Yu, J, Kincaid, JRA, Walde, P, Gallou, F, Lipshutz, BH. Water as the reaction medium in organic chemistry: From our worst enemy to our best friend. Chem Sci, 2021, 12, 12, 4237–4266.
[4] Kitanosono, T, Masuda, K, Xu, P, Kobayashi, S. Catalytic Organic Reactions in Water toward Sustainable Society. Chem Rev, 2018, 118, 2, 679–746.
[5] Sudarsanam, P, Zhong, R, Van den Bosch, S, Coman, SM, Parvulescu, VI, Sels, BF. Functionalised heterogeneous catalysts for sustainable biomass valorisation. Chem Soc Rev, 2018, 47, 22, 8349–8402.
[6] Ananikov, VP. Organic-Inorganic Hybrid Nanomaterials. Nanomaterials (Basel), 2019, 9, 9, 1197.
[7] Kalia, S, Haldorai, Y. Organic-inorganic hybrid nanomaterials, Springer: New York, 2015, Vol. 267.
[8] Piscopo, CG. Supported Sulfonic Acids: Solid Catalysts for Batch and Continuous-Flow Synthetic Processes. ChemistryOpen, 2015, 4, 3, 383–388.
[9] Sharma, RK, Sharma, S, Dutta, S, Zboril, R, Gawande, MB. Silica-nanosphere-based organic–inorganic hybrid nanomaterials: Synthesis, functionalization and applications in catalysis. Green Chem, 2015, 17, 6, 3207–3230.
[10] Sharma, RK, Sharma, S. Silica nanosphere-supported palladium(II) furfural complex as a highly efficient and recyclable catalyst for oxidative amination of aldehydes. Dalton Trans, 2014, 43, 3, 1292–1304.
[11] Liu, J, Hao, J, Hu, C, He, B, Xi, J, Xiao, J, Wang, S, Bai, Z. Palladium Nanoparticles Anchored on Amine-Functionalized Silica Nanotubes as a Highly Effective Catalyst. J Phys Chem C, 2018, 122, 5, 2696–2703.
[12] Fihri, A, Cha, D, Bouhrara, M, Almana, N, Polshettiwar, V. Fibrous Nano-Silica (KCC-1)-Supported Palladium Catalyst: Suzuki Coupling Reactions Under Sustainable Conditions. ChemSusChem, 2012, 5, 1, 85–89.
[13] Ortega-Liebana, MC, Bonet-Aleta, J, Hueso, JL, Santamaria, JJC. Gold-based nanoparticles on amino-functionalized mesoporous silica supports as nanozymes for glucose oxidation. Catalysts, 2020, 10, 3, 333.

[14] Gawande, MB, Monga, Y, Zboril, R, Sharma, RK. Silica-decorated magnetic nanocomposites for catalytic applications. Coord Chem Rev, 2015, 288, 118–143.
[15] Sharma, RK, Dutta, S, Sharma, S, Zboril, R, Varma, RS, Gawande, MB. Fe3O4 (iron oxide)-supported nanocatalysts: Synthesis, characterization and applications in coupling reactions. Green Chem, 2016, 18, 11, 3184–3209.
[16] Cano, I, Martin, C, Fernandes, JA, Lodge, RW, Dupont, J, Casado-Carmona, FA, Lucena, R, Cardenas, S, Sans, V, de Pedro, I. Paramagnetic ionic liquid-coated SiO2@Fe3O4 nanoparticles – The next generation of magnetically recoverable nanocatalysts applied in the glycolysis of PET. Appl Catal B, 2020, 260, 118110.
[17] Ditsch, A, Laibinis, PE, Wang, DIC, Hatton, TA. Controlled Clustering and Enhanced Stability of Polymer-Coated Magnetic Nanoparticles. Langmuir, 2005, 21, 13, 6006–6018.
[18] Arora, G, Yadav, M, Gaur, R, Gupta, R, Sharma, RK, Novel, A. Template-Free Synthesis of Multifunctional Double-Shelled Fe3O4-C Nanoreactor as an Ideal Support for Confined Catalytic Reactions. ChemistrySelect, 2017, 2, 33, 10871–10879.
[19] Mandal, M, Kundu, S, Ghosh, SK, Panigrahi, S, Sau, TK, Yusuf, SM, Pal, T. Magnetite nanoparticles with tunable gold or silver shell. J Colloid Interface Sci, 2005, 286, 1, 187–194.
[20] Gupta, R, Yadav, M, Gaur, R, Arora, G, Rana, P, Yadav, P, Adholeya, A, Sharma, RK. Silica-Coated Magnetic-Nanoparticle-Supported DABCO-Derived Acidic Ionic Liquid for the Efficient Synthesis of Bioactive 3,3-Di(indolyl)indolin-2-ones. ACS Omega, 2019, 4, 25, 21529–21539.
[21] Sharma, RK, Monga, Y, Puri, A, Gaba, G. Magnetite (Fe3O4) silica based organic–inorganic hybrid copper(ii) nanocatalyst: A platform for aerobic N-alkylation of amines. Green Chem, 2013, 15, 10, 2800–2809.
[22] Rossi, LM, Costa, NJS, Silva, FP, Gonçalves, RV. Magnetic nanocatalysts: Supported metal nanoparticles for catalytic applications. Nanotechnol Rev, 2013, 2, 5, 597–614.
[23] Sobhani, S, Mesbah Falatooni, Z, Honarmand, M. Synthesis of phosphoric acid supported on magnetic core–shell nanoparticles: A novel recyclable heterogeneous catalyst for Kabachnik–Fields reaction in water. RSC Adv, 2014, 4, 30, 15797–15806.
[24] Gupta, R, Yadav, M, Gaur, R, Arora, G, Yadav, P, Sharma, RK. Magnetically supported ionic liquids: A sustainable catalytic route for organic transformations. Mater Horiz, 2020, 7, 12, 3097–3130.
[25] Gupta, R, Yadav, M, Gaur, R, Arora, G, Sharma, RK. A straightforward one-pot synthesis of bioactive N-aryl oxazolidin-2-ones via a highly efficient Fe3O4@SiO2-supported acetate-based butylimidazolium ionic liquid nanocatalyst under metal- and solvent-free conditions. Green Chem, 2017, 19, 16, 3801–3812.
[26] Cui, Y, Li, B, He, H, Zhou, W, Chen, B, Qian, G. Metal–Organic Frameworks as Platforms for Functional Materials. Acc Chem Res, 2016, 49, 3, 483–493.
[27] Liang, Z, Zhao, R, Qiu, T, Zou, R, Xu, Q. Metal-organic framework-derived materials for electrochemical energy applications. EnergyChem, 2019, 1, 1, 100001.
[28] Yadav, S, Dixit, R, Sharma, S, Dutta, S, Solanki, K, Sharma, RK. Magnetic metal–organic framework composites: Structurally advanced catalytic materials for organic transformations. Mater Adv, 2021, 2, 7, 2153–2187.
[29] Cai, X, Xie, Z, Li, D, Kassymova, M, Zang, S-Q, Jiang, H-L. Nano-sized metal-organic frameworks: Synthesis and applications. Coord Chem Rev, 2020, 417, 213366.
[30] Mai, HD, Rafiq, K, Yoo, H. Nano Metal-Organic Framework-Derived Inorganic Hybrid Nanomaterials: Synthetic Strategies and Applications. Chem – A Eur Jl, 2017, 23, 24, 5631–5651.
[31] Qi, Y, Luan, Y, Yu, J, Peng, X, Wang, G. Nanoscaled Copper Metal–Organic Framework (MOF) Based on Carboxylate Ligands as an Efficient Heterogeneous Catalyst for Aerobic Epoxidation

of Olefins and Oxidation of Benzylic and Allylic Alcohols. Chem – A Eur Jl, 2015, 21, 4, 1589–1597.
[32] Yang, Q, Xu, Q, Jiang, H-L. Metal–organic frameworks meet metal nanoparticles: Synergistic effect for enhanced catalysis. Chem Soc Rev, 2017, 46, 15, 4774–4808.
[33] Yang, Q, Xu, Q, Yu, SH, Jiang, HLJAC. Pd Nanocubes@ ZIF-8: Integration of Plasmon-Driven Photothermal Conversion with a Metal–Organic Framework for Efficient and Selective Catalysis. Angewandte Chemie, 2016, 128, 11, 3749–3753.
[34] Coville Neil, J, Mhlanga Sabelo, D, Nxumalo Edward, N, Shaikjee, A. A review of shaped carbon nanomaterials: Review article. S Afr J Sci, 2011, 107, 3, 1–15.
[35] Zhu, J, Holmen, A, Chen, D. Carbon Nanomaterials in Catalysis: Proton Affinity, Chemical and Electronic Properties, and their Catalytic Consequences. ChemCatChem, 2013, 5, 2, 378–401.
[36] Bai, J, Xing, S-H, Zhu, -Y-Y, Jiang, J-X, Zeng, J-H, Chen, Y. Polyallylamine-Rh nanosheet nanoassemblies–carbon nanotubes organic-inorganic nanohybrids: A electrocatalyst superior to Pt for the hydrogen evolution reaction. J Power Sources, 2018, 385, 32–38.
[37] Mohammadi, O, Golestanzadeh, M, Abdouss, M. Recent advances in organic reactions catalyzed by graphene oxide and sulfonated graphene as heterogeneous nanocatalysts: A review. New J Chem, 2017, 41, 20, 11471–11497.
[38] Sharma, RK, Sharma, A, Sharma, S, Dutta, S. Unprecedented Ester–Amide Exchange Reaction Using Highly Versatile Two-Dimensional Graphene Oxide Supported Base Metal Nanocatalyst. Ind Eng Chem Res, 2018, 57, 10, 3617–3627.
[39] Kim, M, Nam, D-H, Park, H-Y, Kwon, C, Eom, K, Yoo, S, Jang, J, Kim, H-J, Cho, E, Kwon, H. Cobalt-carbon nanofibers as an efficient support-free catalyst for oxygen reduction reaction with a systematic study of active site formation. J Mater Chem A, 2015, 3, 27, 14284–14290.
[40] He, W, Zhang, F, Li, H. Active and reusable Pd(ii) organometallic catalyst covalently bonded to mesoporous silica nanospheres for water-medium organic reactions. Chem Sci, 2011, 2, 5, 961–966.
[41] Mondal, P, Banerjee, S, Roy, AS, Mandal, TK, Islam, SM. In situ prepared mesoporous silica nanosphere supported palladium(ii) 2-aminopyridine complex catalyst for Suzuki–Miyaura cross-coupling reaction in water. J Mater Chem, 2012, 22, 38, 20434–20442.
[42] Zhu, F, Yang, D, Zhang, F, Li, H. Amine-bridged periodic mesoporous organosilica nanospheres as an active and reusable solid base-catalyst for water-medium and solvent-free organic reactions. J Mol Catal A Chem, 2012, 363–364, 387–397.
[43] Wang, L, Chen, Q, Li, C, Fang, FJ. J. O N ; Nanotechnology, Nano-Web Cobalt Modified Silica Nanoparticles Catalysts for Water Oxidation and MB Oxidative Degradation Journal of Nanoscience and Nanotechnology, 2016, 16, 5, 5364–5368.
[44] Gawande, MB, Rathi, AK, Branco, PS, Varma, RSJAS. Sustainable utility of magnetically recyclable nano-catalysts in water: Applications in organic synthesis. Applied Sci, 2013, 3, 4, 656–674.
[45] Beygzadeh, M, Alizadeh, A, Khodaei, MM, Kordestani, D. Biguanide/Pd(OAc)2 immobilized on magnetic nanoparticle as a recyclable catalyst for the heterogeneous Suzuki reaction in aqueous media. Catal Commun, 2013, 32, 86–91.
[46] Arora, G, Yadav, M, Gaur, R, Gupta, R, Rana, P, Yadav, P, Sharma, RK. A template free protocol for fabrication of a Ni(ii)-loaded magnetically separable nanoreactor scaffold for confined synthesis of unsymmetrical diaryl sulfides in water. RSC Adv, 2020, 10, 33, 19390–19396.
[47] Yeo, KM, Lee, SI, Lee, YT, Chung, YK, Lee, ISJ. C. l., Core–satellite heterostruture of Fe3O4–Pd nanocomposite: Selective and magnetically recyclable catalyst for decarboxylative coupling reaction in aqueous media. Chem Lett, 2008, 37, 1, 116–117.

[48] Rajabi, F, Karimi, N, Saidi, MR, Primo, A, Varma, RS, Luque, R. Unprecedented Selective Oxidation of Styrene Derivatives using a Supported Iron Oxide Nanocatalyst in Aqueous Medium. Adv Synth Catal, 2012, 354, 9, 1707–1711.
[49] Karimi, B, Farhangi, E, Highly Recyclable, A. Magnetic Core-Shell Nanoparticle-Supported TEMPO catalyst for Efficient Metal- and Halogen-Free Aerobic Oxidation of Alcohols in Water. Chem – A Eur J, 2011, 17, 22, 6056–6060.
[50] Wang, BG, Ma, BC, Wang, Q, Wang, W. Superparamagnetic Nanoparticle-Supported (S)-Diphenyl- prolinol Trimethylsilyl Ether as a Recyclable Catalyst for Asymmetric Michael Addition in Water. Adv Synth Catal, 2010, 352, 17, 2923–2928.
[51] Iqbal, K, Iqbal, A, Kirillov, AM, Liu, W, Tang, Y. Hybrid Metal–Organic-Framework/Inorganic Nanocatalyst toward Highly Efficient Discoloration of Organic Dyes in Aqueous Medium. Inorg Chem, 2018, 57, 21, 13270–13278.
[52] Bahuguna, A, Kumar, S, Krishnan, V. Nanohybrid of ZnO-RGO as Heterogeneous Green Catalyst for the Synthesis of Medicinally Significant Indole Alkaloids and Their Derivatives. ChemistrySelect, 2018, 3, 1, 314–320.
[53] Bahuguna, A, Kumar, S, Sharma, V, Reddy, KL, Bhattacharyya, K, Ravikumar, PC, Krishnan, V. Nanocomposite of MoS2-RGO as Facile, Heterogeneous, Recyclable, and Highly Efficient Green Catalyst for One-Pot Synthesis of Indole Alkaloids. ACS Sustain Chem Eng, 2017, 5, 10, 8551–8567.
[54] Patil, MR, Kapdi, AR, Vijay Kumar, A. Recyclable Supramolecular Ruthenium Catalyst for the Selective Aerobic Oxidation of Alcohols on Water: Application to Total Synthesis of Brittonin A. ACS Sustain Chem Eng, 2018, 6, 3, 3264–3278.

Subject Index

https://doi.org/10.1515/9783110733846-011